

FUNCTION OF CSB AT TELOMERES AND DNA DOUBLE-STRAND BREAKS

FUNCTIONAL ANALYSIS OF CSB IN TELOMERE MAINTENANCE AND DNA
DOUBLE-STRAND BREAK REPAIR

By NICOLE BATENBURG, B. Sc. (Hon)

A Thesis Submitted to the School of Graduate Studies in Partial Fulfilment of the
Requirements of the Degree of Doctor of Philosophy

McMaster University © Copyright by Nicole Batenburg, September 2017

McMaster University DOCTOR OF PHILOSOPHY (2017) Hamilton, Ontario (Science)

TITLE: Functional analysis of CSB in telomere maintenance and DNA double-strand
break repair

AUTHOR: Nicole Batenburg, B. Sc. (Hon)

SUPERVISOR: Dr. Xu-Dong Zhu

NUMBER OF PAGES: xv; 298

Abstract

Cockayne syndrome (CS) is a rare, segmental premature aging disorder in which the majority of cases are caused by mutations in the Cockayne syndrome group B protein (CSB). CSB is a multifunctional protein implicated in DNA repair, transcription and chromatin remodeling. The results presented here demonstrate that CSB plays an important role in telomere maintenance and DSB repair. We find that CS cells accumulate telomere doublets, have increased telomere-bound TRF1, decreased TERRA levels and a defect in telomerase-dependent telomere lengthening. These results imply that CS patients may be defective in telomere maintenance. We also uncover a novel and important role of CSB in DNA DSB repair. We show that CSB facilitates HR and suppresses NHEJ during S and G2 phase. We find that CSB interacts with RIF1 and is recruited by RIF1 to DSBs in S phase. At DSBs, CSB remodels the chromatin extensively, which in turn limits RIF1 recruitment and promotes BRCA1 accumulation. The chromatin remodeling activity of CSB requires not only damage-induced phosphorylation on S10 by ATM but also cell cycle-dependent phosphorylation of S158 by cyclin A-CDK2. Both modifications are needed for the intramolecular interaction of CSB N-terminal domain with its ATPase domain. This intramolecular interaction has previously been reported to regulate the ATPase activity of CSB. Taken together, these results suggest that ATM and CDK2 control of CSB to promote chromatin remodeling, which in turn inhibits RIF1 in DNA DSB repair pathway choice.

Acknowledgements

I would like to start by thanking my supervisor, Dr. Xu-Dong Zhu, for the opportunity to work in her lab. I feel like I have learned so much during my graduate studies in the lab, and I appreciated your continued interest and excitement for your research. I would also like to thank my committee members Dr. Bhagwati Gupta and Dr. Peter Whyte for all of the help over these past few years.

I would also like to express my appreciation to all members of the Zhu lab, both past and present. I am very grateful for the opportunity to learn from and work with each of them. The support from the students in the lab has been great over the past years.

Finally, I would like to thank all my friends from university and beyond. I would also like to thank my sisters Katie, Jackie and Rachel, and my parents Richard and Linda. Thank you for supporting me in all the choices that I have made in my life. I would not be where I am without you, I love you so much.

Table of Contents

Abstract	iii
Acknowledgements	iv
Table of Contents	v
List of Figures	viii
List of Abbreviations	xi
Preface	xv
Chapter 1	1
Introduction	1
1.1 Cockayne syndrome.....	2
1.2 Biochemical activity of Cockayne syndrome group B (CSB) protein	4
1.2.1 CSB exhibits ATPase activity	6
1.2.2 CSB binds to nucleic acids	6
1.2.3 CSB exhibits in vitro chromatin remodelling activity	7
1.2.4 ATP-independent functions of CSB	9
1.3 Role of Chromatin Remodelers in DNA repair	10
1.4 CSB and Nucleotide Excision Repair (NER)	11
1.4.1 NER – Global Genome Repair (GGR) vs. Transcription-Coupled repair (TCR)	11
1.4.2 Chromatin remodeling and NER.....	15
1.4.3 Role of CSB in NER.....	16
1.4.4 Regulation of CSB in NER	18
1.4.5 Relationship between CSB and p53 in UV response	20
1.5 CSB and Base Excision Repair (BER)	22
1.5.1 BER pathway	22
1.5.3 Chromatin remodeling and BER.....	24
1.5.3 Role of CSB in BER.....	25
1.5.4 Regulation of CSB in BER.....	29
1.6 Role of CSB in Transcription	31
1.7 Telomeres	35
1.7.1 Telomere structure and function	35
1.7.2 The Shelterin complex	37
1.7.3 Telomere lengthening and Telomerase	40
1.7.4 Telomere chromatin structure	42
1.7.5 Telomere transcription.....	44
1.7.6 Telomeres and aging	47
1.8 DNA Double-strand Break (DSB) Repair	48
1.8.1 Overview of the DNA damage response.....	48
1.8.2 Homologous recombination (HR)	51

1.8.3	<i>Non-homologous end joining (NHEJ)</i>	53
1.8.4	<i>Regulation in DNA DSB repair pathway choice</i>	55
1.8.6	<i>Chromatin remodeling and DSB repair</i>	56
1.9	Rationale and Objectives	58
1.10	References.....	60
Chapter 2		90
Cockayne Syndrome group B protein interacts with TRF2 and regulates telomere length and stability		90
2.1	Preface	91
2.2	Publication – Cockayne syndrome group B protein interacts with TRF2 and regulates telomere length and stability	92
2.2.1	<i>Abstract</i>	93
2.2.2	<i>Introduction</i>	94
2.2.3	<i>Materials and methods</i>	97
2.2.4	<i>Results</i>	103
2.2.5	<i>Discussion</i>	111
2.2.6	<i>Figures and figure legends</i>	115
2.2.7	<i>References</i>	132
Chapter 3		137
Cockayne syndrome group B protein regulates DNA double-strand break repair and checkpoint activation		137
3.1	Preface	138
3.2	Publication – Cockayne syndrome group B protein regulates DNA double-strand break repair and checkpoint activation	139
3.2.1	<i>Abstract</i>	140
3.2.2	<i>Introduction</i>	140
3.2.3	<i>Materials and methods</i>	144
3.2.4	<i>Results</i>	151
3.2.5	<i>Discussion</i>	166
3.2.6	<i>Figures and figure legends</i>	171
3.2.7	<i>References</i>	199
Chapter 4		206
ATM and CDK2 control chromatin remodeler CSB inhibit RIF1 in DSB repair pathway choice		206
4.1	Preface	207
4.2	Submitted Manuscript - ATM and CDK2 control chromatin remodeler CSB inhibit RIF1 in DSB repair pathway choice	208
4.2.1	<i>Abstract</i>	209
4.2.2	<i>Introduction</i>	209
4.2.3	<i>Materials and methods</i>	212

4.2.4	<i>Results</i>	222
4.2.5	<i>Discussion</i>	236
4.2.6	<i>Figure and figure legends</i>	240
4.2.7	<i>References</i>	278
Chapter 5	283
Discussion	283
5.1	Overview of findings	284
5.1.1	<i>Role of CSB at telomeres</i>	284
5.1.2	<i>Role of CSB in DSB repair</i>	285
5.2	Implications and Significance.....	288
5.3	Future Directions	291
5.4	References.....	293

List of Figures

Figure 1.1.	Schematic diagram of CSB	5
Figure 1.2.	Nucleotide excision repair (NER) pathway	13
Figure 1.3.	Base excision repair (BER) pathway	23
Figure 1.4.	Structure and composition of human telomeres	38
Figure 1.5.	Double-strand break repair pathways	52
Figure 2.1.	CSB interacts physically with TRF2	116
Figure 2.2.	CSB colocalizes as a small subset of human telomeres and prevents the formation of TIFs in CS cells	118
Figure 2.3.	CS primary fibroblasts carrying CSB mutations accumulate telomere doublets	120
Figure 2.4.	CSB is required to prevent the formation of telomere doublets	122
Figure 2.5.	CSB is required for telomere length maintenance	124
Figure 2.6.	CSB is required for maintaining the homeostatic level of TERRA	126
Figure 2.S.1.	Western analysis of CSB expression in normal and CS primary fibroblasts	128
Figure 2.S.2.	Characterization of hTERT expressing GM10905 cells	129
Figure 2.S.3.	Analysis of metaphase chromosomes from hTERT-GM10905	130
Figure 2.S.4.	Analysis of metaphase chromosomes from HeLa1.2.11 stably expressing either the vector alone or pRS-shCSB	131
Table 2.S.1	Summary of normal and CS primary fibroblast cell lines used	131
Figure 3.1.	Generation of CSB-KO cells	172
Figure 3.2.	Loss of CSB promotes NHEJ, impairs HR and renders cells sensitive to DSB-inducing agents	174
Figure 3.3.	Knockout of CSB impair HR-mediated DNA DSB repair in S and G2 cells	176
Figure 3.4.	Loss of CSB leads to an accumulation of NHEJ-promoting factors at sites of DNA DSBs in S and G2 cells	179
Figure 3.5.	Loss of CSB impairs ATM- and CHK2-dependent DNA damage checkpoint	181

Figure 3.6.	CSB is associated with chromatin following induction of DNA DSBs	183
Figure 3.7.	CSB carrying a W851R mutation is unable to suppress the recruitment of NHEJ-promoting factors to sites of DNA-DSBs in S and G2 cells	185
Figure 3.8.	The ATPase activity of CSB is needed for maintaining the ATM- and CHK2-mediated DNA damage checkpoint	187
Figure 3.S.1.	Treatment of DNA-PKcs inhibitor impairs the frequency of random integration in both parental (WT) and CSB-KO (KO) cells	189
Figure 3.S.2.	Normal cell cycle analysis of asynchronous parental (WT) and CSB-KO (KO) cells.	190
Figure 3.S.3	Knockout of CSB impairs the repair of DNA DSBs	191
Figure 3.S.4.	Knockout of CSB leads to an accumulation of NHEJ-promoting factors at site of DNA DSBs in S and G2 cells	193
Figure 3.S.5.	Knockout of CSB impairs the maintenance of the ATM- and CHK2-mediated DNA damage checkpoint	195
Figure 3.S.6.	Introduction of CSB but not CSB:PGBD3 alone suppress the defect in the recruitment of HR factors to sites of DNA DSBs	196
Figure 3.S.7.	Recruitment of DSB repair factors to sites of DNA damage is misregulated in cells derived from CS patients.	198
Figure 3.S.8.	The W851R mutations abrogates UV-induced chromatin association of CSB and its function in UV repair	200
Figure 4.1.	CSB interacts with RIF1 and is recruited by RIF1 to the site of FokI-induced DSBs	241
Figure 4.2.	RIF1 interacts with CSB and recruits CSB to DSBs via its CTD domain	243
Figure 4.3.	CSB interacts with RIF1 via its newly-identified winged helix domain (WHD) and inhibits RIF1 at DSBs	245
Figure 4.4.	RIF1 recruits CSB to FokI-induced DSBs in S phase, which in turn inhibits RIF1	248
Figure 4.5.	CSB is a chromatin remodeler and evicts histones from the chromatin surrounding I-PpoI-induced DSBs <i>in vivo</i>	251
Figure 4.6.	The N-terminus of CSB mediates its chromatin remodeling activity to repress RIF1 accumulation at sites of DSBs	253

Figure 4.7.	ATM controls the chromatin remodeling activity of CSB through S10 phosphorylation	256
Figure 4.8.	Cyclin A-CDK2 controls the chromatin remodeling activity of CSB through S158 phosphorylation.	258
Figure 4.9.	CSB phosphorylations on S10 and S158 modulate its intramolecular interaction between the N-terminus and the ATPase domain	260
Figure 4.S.1	RIF1-C interacts with CSB-C	262
Figure 4.S.2	RIF1 interacts with CSB and recruits CSB to sites of DSBs through its CTD	263
Figure 4.S.3	The WHD of CSB is necessary for its interaction with RIF1 and its recruitment to the site of FokI-induced DSBs	264
Figure 4.S.4	CSB contains a winged helix domain (WHD)	266
Figure 4.S.5	Loss of 53BP1 has little effect on cycle progression	268
Figure 4.S.6	Knockout of CSB does not affect the production of I-PpoI-induced DNA cleavage	269
Figure 4.S.7	Loss of CSB does not affect SMARCAD1 recruitment to sites of FokI-induced DSBs	271
Figure 4.S.8.	CSB phosphorylation on S10 is necessary to support cell survival in response to the PARP inhibitor Olaparib	272
Figure 4.S.9.	CSB phosphorylation on S158 is necessary for HR-mediated repair of DSBs	274
Table 4.S.1	Oligos for PCR ChIP assay	276
Table 4.S.2	Oligos for real-time PCR ChIP assay and real-time PCR DSB-induction assay	277

List of Abbreviations

53BP1	p53 binding protein 1
6-4 PP	6-4 pyrimidine-pyrimidone photoproducts
8-OH-dAdo	8-hydroxy-2'-deoxyadenosine
8-OH-dGuo	8-hydroxy-2'-deoxyguanosine
8-oxoA	8- hydroxyadenine
8-oxoG	8-hydroxyguanine
ACR	ATP-dependent chromatin remodeling
ALT	Alternative lengthening of telomeres
APE1	Apurinic/aprimidinic endonuclease
AP site	Apurinic/aprimidinic site
AT	Ataxia telangiectasia
ATM	Ataxia telangiectasia mutated
ATP	Adenine triphosphate
ATR	Ataxia telangiectasia Rad3-related
BER	Base excision repair
BRCA1	Breast cancer 1
BRCT	BRCA1 C terminus
CDK	Cyclin dependent kinase
CETN2	Centrin 2
CHD	Chromodomain, helicase, DNA binding
ChIP	Chromatin immunoprecipitation
CPD	Cyclobutene pyrimidine dimers
CPT	Camptothecin
Co-IP	Coimmunoprecipitation
CS	Cockayne syndrome
CSA	Cockayne syndrome group A protein
CSB	Cockayne syndrome group B protein
CST	CTC1-STN1-TEN1
CTC1	CST telomere replication complex component 1
CtIP	CtBP-interacting protein
Cul4A	Culin 4A complex
DAPI	4',6-Diamidine-2'-phenylindole dihydrochloride
DDB1	DNA damage binding protein 1
DDB2	DNA damage binding protein 2
DKC	Dyskeratosis congenita
DMSO	Dimethyl sulfoxide
DNA	Deoxyribonucleic acid
DNA-PK	DNA-dependent protein kinase
DSB	Double strand break
dsDNA	Double-stranded DNA
D-loop	Displacement loop

ELISA	Enzyme-linking immunosorbent assay
ERCC1	ERCC excision repair 1
EXO1	Exonuclease 1
FACS	Fluorescence activated cell sorting
Fapy-A	4,6-diamino-5-formamidopyrimidine
Fapy-G	2,6-diamino-4-hydroxy-5-formamidopyrimidine
FEN-1	Flap endonuclease 1
FISH	Fluorescent <i>in situ</i> hybridization
FITC	Fluorescent isothiocyanate
GFP	Green fluorescent protein
GG-NER	Global genome NER
HDAC	Histone deacetylase
HGPS	Hutchinson-Gilford progeria syndrome
HMGN1	High mobility group nucleosome-binding domain-containing protein 1
HMT	Histone methyltransferase
HP1	Heterochromatin protein 1
HR	Homologous recombination
hTERT	Human telomerase reverse transcriptase
hTR	Human telomerase RNA
IF	Immunofluorescence
INO80	Inositol requiring 80
IP	Immunoprecipitation
IR	Ionizing radiation
ISWI	Imitation switch
MDC1	Mediator of DNA damage checkpoint protein 1
MNase	Micrococcal nuclease
MRE11	Meiotic recombination 11
MRN	MRE11-RAD50-NBS1
NAP1L1/4	Nucleosome assembly protein 1-like 1
NBS1	Nijmegen breakage syndrome 1
NCPs	Nucleosome core particles
NEIL1/2	Nei endonuclease VIII-like 1
NER	Nucleotide excision repair
NHEJ	Non-homologous end-joining
NLS	Nuclear localization signal
NoRC	Nucleolar remodeling complex
NuRD	Nucleosome remodeling and deacetylation complex
OGG1	8-oxoguanine DNA glycosylase
ORC	Origin recognition complex
PAGE	Polyacrylamide gel electrophoresis
PAR	Poly (ADP-ribose)
PARP1	Poly (ADP-ribose) polymerase 1

PCNA	Proliferating nuclear antigen
PIP1	POT1 interacting protein 1
PNA	Peptide nucleic acid
POT1	Protection of telomeres 1
PTIP	Pax transactivation-domain interacting protein
PTM	Posttranslational modification
PTOP	POT1 and TIN2 organizing protein
RAP1	Human ortholog of the yeast repressor/activation protein 1
rDNA	ribosomal DNA
RFC	Replication factor C
RIF1	Rap1 interacting factor 1
RNA	Ribonucleic acid
RNAPI	RNA polymerase I
RNAPII	RNA polymerase II
Ros	Roscovitine
RPA	Replication protein A
RRS	Recovery of RNA synthesis
SDS	Sodium dodecyl sulfate
shRNA	Short hairpin RNA
siRNA	Short interfering RNA
SSB	Single strand break
ssDNA	Single-stranded DNA
SWI/SNF	Switching defective/sucrose nonfermenting
T-loop	Telomeric loop
TC-NER	Transcription-coupled nucleotide excision repair
TD	Telomere doublets
TERRA	Telomeric repeat containing RNA
TFIIE	Transcription initiation factor IIE
TFIIH	Transcription initiation factor IIH
TFE	Telomere free ends
TIN2	TRF1 interacting protein nuclear protein 2
TINT1	TIN2 interacting protein
TPP1	TINT1/PTOP/PIP1
TRF1	Telomere repeat binding factor 1
TRF2	Telomere repeat binding factor 2
TRFH	TRF homology
TRITC	Tetramethyl rhodamine isothiocyanate
UBD	Ubiquitin binding domain
USP7	Ubiquitin-specific-processing protease 7
UV	Ultraviolet
UVSSA	UV-stimulated scaffold protein V
WCE	Whole cell extract
WHD	Winged helix domain

WRN	Werner
WS	Werner syndrome
WT	Wild type
XBA2	XPA-binding protein 2
XP	Xeroderma pigmentosum
XPA/B/C/D/F/G	XP group A/B/C/D/F/G-complementing protein
XRCC	X-ray repair cross complementing

Preface

The work presented in the thesis is focused on the Cockayne syndrome group B (CSB) protein and the characterization of its novel roles in telomere maintenance and DNA double-strand break (DSB) repair. The work has been divided into three chapters. Chapters 2 and 3 have been published in peer reviewed journals and Chapter 4 has been submitted for publication. Each publication contains its own materials and methods section and an introduction reviewing the relevant literature for each chapter. A more comprehensive literature overview is provided in Chapter 1. The style of each of these publications has a referencing style that conforms to the journal in which they were submitted, and so each chapter has been prepared with a separate list of references. Lastly, Chapter 5 will discuss the findings and bring forth future direction.

All of the experiments included in this thesis were done by me except where indicated in the prefaces that preclude each individual chapter. The results discussed in each of these chapters contribute to the overall understanding of how CSB functions in the cell to regulate telomere maintenance and DNA DSB repair.

Chapter 1

Introduction

1.1 Cockayne syndrome

Cockayne syndrome (CS) is a rare autosomal recessive premature aging disorder which affects multiple systems in the body. It is a progressive disorder that is characterized by impaired physical and neurological development (Nance & Berry, 1992). The first case was reported in 1936 by Sir Edward A. Cockayne (Cockayne, 1936). CS occurs in 1 out of every 250,000 live births and has a prevalence of about 2.5 per million (Kleijer *et al*, 2008; Kubota *et al*, 2015; Wilson *et al*, 2016). The average life expectancy is about 12 years (Nance & Berry, 1992). Unfortunately, there is currently no cure for CS and most efforts are spent to treat symptoms of the disorder and to maximize quality of life.

Most CS patients show similar phenotypes, however the time of onset and the rate of progression can vary from patient to patient. Most symptoms start in early childhood. Several major criteria are used for diagnosis of CS, including growth failure, neurological developmental delay and progressive microcephaly. Other common symptoms include dental caries, loss of subcutaneous fat, hearing loss, pigmentary degeneration and cutaneous photosensitivity (Nance & Berry, 1992). There has been no reported predisposition of CS patients towards infection complications and immune deficiencies are not a feature of CS. The age of onset typically determines the life expectancy of the patient and as CS is a progressive disease it can take several months to years to develop symptoms sufficient for diagnosis.

CS has traditionally been thought of as a disorder defective in transcription and transcription-coupled nucleotide excision repair (TC-NER) (Mayne & Lehmann, 1982;

Troelstra *et al*, 1992a). NER is important for repair of damage induced by ultraviolet (UV) light, and it has previously been reported that the repair of such damage occurs faster in regions that are actively transcribed due to TC-NER (Bohr *et al*, 1985; Mellon *et al*, 1986). Reduced recovery of RNA synthesis (RRS) in CS fibroblasts after UV-irradiation remains the gold standard to confirm clinical suspicion of CS. While CS has been considered a disorder of TC-NER, transcriptional defects, defects in repair of other types of DNA damage and mitochondrial dysfunction may explain some of the clinical manifestations of CS (Karikkineth *et al*, 2016).

Due to the defect in DNA repair after UV-irradiation, CS has been grouped with other disorders with defective NER such as xeroderma pigmentosum (XP) and trichothiodystrophy (TTD). While XP patients often develop skin cancer, CS is not associated with an increased incidence of skin cancer (Kraemer *et al*, 1987, 1994; Lehmann, 2003). This may be in part due to an increase in apoptosis observed in CS cells after DNA damage (Balajee *et al*, 2000; Laposa *et al*, 2007; Latini *et al*, 2011). Using duplex sequencing for high-sensitivity of mutation detection, it was reported that CS cells do not accumulate UV-induced mutations whereas XP cells show a substantial increase in UV-induced mutations compared to normal cells (Reid-Bayliss *et al*, 2016). The lack of elevated UV-induced mutagenesis in CS suggests that while the TC-NER deficiency results in decreased cellular survival, it is not mutagenic. Therefore, the absence of skin cancer in CS patients is likely due to the absence of UV-induced mutations.

Mutations in a total of five genes have been shown to cause CS. The majority of CS cases are the result of mutations in two different genes that have been cloned and

identified. Between 70 and 80 percent of CS cases are caused by mutations in the gene *ERCC6* (CSB) (Troelstra *et al*, 1992a, 1993) while most of the remaining cases are caused by mutations in the gene *ERCC8* (CSA) (Henning *et al*, 1995). Mutations in XPB, XPD and XPG genes have also been seen in CS cases at very low frequency. In the *ERCC6* gene, all types of mutations have been found in CS patients including missense, frameshift, splicing mutants as well as deletions. The majority of missense mutations and in-frame deletions are found within the central ATPase domain. Nonsense and frameshift mutations occur at the N-terminus and C-terminus of the protein, often resulting in a truncated protein. There is no clear genotype-phenotype correlation in CS patients that carry mutations in the CSB gene.

1.2 Biochemical activity of Cockayne syndrome group B (CSB) protein

The human *ERCC6* gene is located on chromosome 10q11-q21 and encodes for the Cockayne syndrome group B protein (CSB) (Troelstra *et al*, 1992a, 1992b). The CSB protein is 1493 amino acids and has a predicted molecular weight of 168 kDa (**Figure 1.1**). It contains a central ATPase domain, which includes seven helicase-like motifs, similar to other members of this family. Domains I, II and VI are likely important for coordinating the binding and hydrolysis of the triphosphate. Domain III is likely important for coordinating ATP and nucleic acid binding while domains Ia, IV and V are likely important for making contact with nucleic acids. (Fairman-Williams *et al*, 2010). CSB also contains an acidic region, a glycine rich region, two putative nuclear

localization signals, a nucleotide binding domain and a ubiquitin binding domain (UBD) (Troelstra *et al*, 1992a; Anindya *et al*, 2010).

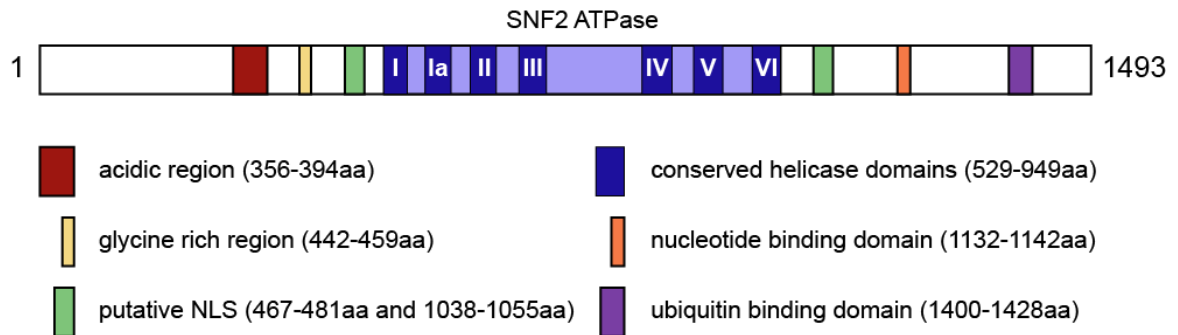


Figure 1.1. Schematic diagram of CSB. CSB contains an acidic stretch of residues, a glycine rich region, a nucleotide binding domain and a ubiquitin binding domain (UBD). CSB also contains two putative nuclear localization signals (NLS) on each side of the central, conserved SNF2 ATPase domain. The ATPase domain includes seven helicase-like motifs.

CSB belongs to the SNF2/SWI2 family of ATPases, which is a subfamily of the broader helicase superfamily (SF2). Unlike other SNF2 remodelers, CSB does not assemble into multisubunit complexes. No members of this family have been shown to exhibit helicase activity but they are instead thought to regulate chromatin structure by using the energy from ATP hydrolysis to disrupt protein-DNA interactions. Similar to other members of its protein family, CSB also does not exhibit any helicase activity (Berquist & Wilson, 2009; Citterio *et al*, 1998; Selby & Sancar, 1997). In most cases these proteins use the energy from ATP hydrolysis to disrupt the interaction between DNA and histones, therefore they are referred to as ATP-dependent chromatin remodelers (Clapier & Cairns, 2009).

1.2.1 CSB exhibits ATPase activity

CSB demonstrates ATP hydrolysis activity in the presence of DNA, showing that the ATPase activity is DNA-dependent. The ATP hydrolysis activity can be stimulated by several different DNA substrates which include double-stranded DNA fragments, stem-looped DNA, forked DNA fragments, plasmid DNA and nucleosomal DNA. The common feature in these different substrates is that they all contain double-stranded DNA. This seems to be essential as single-stranded DNA oligonucleotides, DNA/RNA hybrids or RNA/RNA duplexes fail to stimulate ATP hydrolysis (Berquist & Wilson, 2009; Citterio *et al*, 1998; Selby & Sancar, 1997). CSB is also capable of binding to different DNA substrates. CSB can bind to 34-bp and 90-bp duplex DNA in the absence of ATP (Berquist & Wilson, 2009; Selby & Sancar, 1997). CSB can also form a stable complex with double-stranded DNA containing a bubble structure and forked duplexes of DNA/DNA, DNA/RNA and RNA/RNA (Berquist & Wilson, 2009). In agreement with the notion that CSB binds to DNA in the absence of ATP, mutations in the conserved ATPase domain do not impact the interaction between CSB and DNA (Citterio *et al*, 2000).

1.2.2 CSB binds to nucleic acids

When incubated with nicked plasmid DNA, CSB induces a change in the DNA conformation detected as negative supercoiling (Citterio *et al*, 2000). This is independent of its ATPase activity as CSB carrying a mutation in the ATPase domain also induces this change. Analysis of scanning force microscopy suggests that CSB can wrap DNA when

incubated with singly nicked plasmid DNA and ATP (Beerens *et al*, 2005). Upon addition of CSB and ATP to the DNA molecules, the contour length of the DNA molecules decreases, likely due to DNA wrapping around the protein surface of CSB. Through single-molecule fluorescence approaches, CSB is found to induce distortion in the DNA, and ATP hydrolysis by CSB decreases this distortion in DNA. This agrees with the idea that ATP hydrolysis by CSB results in the unwrapping of DNA and decreased distortion (Lee *et al*, 2017).

1.2.3 CSB exhibits in vitro chromatin remodelling activity

Several studies have suggested that CSB can remodel chromatin *in vitro*. When incubated with *in vitro* assembled mononucleosomes, CSB alters the DNaseI accessibility to the DNA (Citterio *et al*, 2000). This change was only seen in the presence of ATP and was not observed when a CSB ATPase mutant was tested. To test if CSB can affect the nucleosome spacing/structure in an array, chromatin was reconstituted on plasmid DNA *in vitro*. When CSB is incubated with this substrate, there is a detectable change in the structure using micrococcal nuclease (MNase) digestion. In the presence of ATP, addition of CSB alters the digestion pattern, seen as a loss in the periodic spacing between nucleosomes. Addition of CSB that carries a mutation in the ATPase domain does not result in this alteration in digestion pattern. This supports the idea that CSB is an ATP-dependent chromatin remodeler (Citterio *et al*, 2000). Using coimmunoprecipitation (Co-IP) experiments, CSB can be seen to interact with all four of the core histone components *in vivo* (Citterio *et al*, 2000). Purified CSB is also capable of interacting with

each of the histone components separately. This interaction is dependent on the presence of the histone tails (Citterio *et al*, 2000). Given that histone tails are extensively modified, it is possible that histone modifications may play a role in modulating the recruitment and chromatin remodeling activity of CSB.

Compared to other well characterized chromatin remodelers, the remodeling activity of CSB seems to be relatively weak (Cho *et al*, 2013; Citterio *et al*, 2000). ATP-dependent chromatin remodelers are often part of large multisubunit complexes, and non-catalytic subunits often enhance the specific activity of the ATPase motor. Recently it has been shown that CSB interacts with the NAP1-like histone chaperones NAP1L1 and NAP1L4 (Cho *et al*, 2013). NAP1L1 or NAP1L4 greatly enhance the chromatin remodeling activity of CSB while they do not remodel nucleosomes on their own. These results suggests that CSB cooperates with these two histone chaperones to achieve robust and more efficient ATP-dependent chromatin remodelling activity (Cho *et al*, 2013; Lee *et al*, 2017). In an *in vitro* assay, NAP1L1 decreases the binding of CSB to DNA and promotes the dissociation of DNA-bound CSB (Lee *et al*, 2017), suggesting that NAP1L1 may regulate CSB to help maintain dynamic CSB-DNA interactions within the cell and decrease non-productive chromatin associations.

The oligomeric state of a chromatin remodeler can strongly influence the activity of the protein. The SWI/SNF remodeler, a complex of multiple subunits, functions as a monomer (Saha *et al*, 2002; Smith *et al*, 2003). In contrast, the ACT remodeling complex functions as a dimer (Racki *et al*, 2009). Scanning force microscopy size measurements of CSB bound to DNA indicate that CSB binds to DNA as a dimer as there is a 1.6-fold

increase in CSB volume when incubated with DNA (Beerens *et al*, 2005). Co-IP experiments using FLAG-tagged and GFP-tagged CSB in the CSB deficient cell line CS1AN demonstrate that CSB dimerizes *in vivo*. Gel filtration chromatography experiments using *in vivo* cross-linked cells were also conducted to address the oligomeric state of CSB (Christiansen *et al*, 2005). CSB co-migrates with a peak corresponding to a molecular weight of 360 kDa in addition to a second peak with a much large molecular mass. The dimerization of CSB is independent of DNA or ATP, and homodimerization occurs through the central ATPase domain. Interestingly, CSB only seems to be active as an ATPase when it is a dimer (Christiansen *et al*, 2005).

1.2.4 ATP-independent functions of CSB

In addition to chromatin remodelling, CSB has also been reported to have other biochemical functions *in vitro*. While the chromatin remodelling activity of CSB is dependent upon ATP, CSB has ATP-independent roles in promoting ssDNA annealing and strand exchange. *In vitro* biochemical studies have revealed that CSB promotes the annealing of homologous single-stranded DNA (ssDNA) 25-fold faster than that of spontaneous annealing (Muftuoglu *et al*, 2006). CSB also promotes strand exchange (Muftuoglu *et al*, 2006). Neither of these processes require ATP, in fact addition of ATP inhibits strand annealing. ATP binding may induce a conformational change in CSB that inhibits its strand annealing activity. Interestingly, phosphorylation of CSB by CKII inhibits ssDNA annealing while dephosphorylation by PP1 increases the ssDNA annealing activity. These findings suggest that post-translation modification of CSB

regulates its ssDNA annealing activity (Muftuoglu *et al*, 2006). The importance of this activity in the cell has not been shown yet, however it is possible that CSB may play a role in the re-annealing of DNA to promote the repair of transcription-stalling lesions.

1.3 Role of Chromatin Remodelers in DNA repair

The genetic information of all living organisms is stored with DNA, which is organized into a dynamic nucleoprotein complex called chromatin. Chromatin exists in a highly condensed form and is made up of nucleosomes each containing an octamer of histones H2A, H2B, H3, and H4 wrapped by 146 bp of DNA, a linker DNA of ~80 bp and histone H1. The integrity of DNA is constantly threatened by both endogenous and exogenous sources of damage. If not repaired, DNA damage interferes with essential processes in the cell such as transcription and replication, leading to genome instability, hallmarks of cancer and aging.

The highly-compacted chromatin structure limits the ability of other proteins to interact with DNA, therefore the chromatin structure needs to be remodeled to facilitate the access of damage detection and repair proteins to DNA. Chromatin remodeling includes post-translational modification of histones through the action of histone-modifying enzymes, the displacement, exchange and reposition of histones through the action of ATP-dependent chromatin remodeling complexes and histone chaperones.

ATP-dependent chromatin remodeling (ACR) complexes use the energy from ATP hydrolysis to catalyze disruption of DNA-histone contacts and as a result, they can slide and evict nucleosomes (Clapier & Cairns, 2009). There are four different

structurally related families of these complexes: SWI/SNF (switching defective/sucrose nonfermenting), INO80 (inositol requiring 80), CHD (chromodomain, helicase, DNA binding) and ISWI (imitation switch). Each family is defined by its characteristic core ATPase domain from the SWI2/SNF2 superfamily. Although there is some redundancy between these complexes, most remodelers are essential for cellular growth, development, or differentiation.

1.4 CSB and Nucleotide Excision Repair (NER)

1.4.1 NER – Global Genome Repair (GGR) vs. Transcription-Coupled repair (TCR)

Nucleotide excision repair (NER) is the sole DNA repair pathway responsible for the removal of DNA lesions induced by ultraviolet (UV) radiation. The major lesions induced by UV are cyclobutene-pyrimidine dimers (CPD) and 6-4 pyrimidine-pyrimidone photoproducts (6-4PP). There are two subpathways of NER, global genome NER (GG-NER) and transcription-coupled NER (TC-NER) (**Figure 1.2**) (Marteijn *et al*, 2014). In the GG-NER subpathway, the whole genome is scanned for distortions in the DNA helix associated with structural changes to nucleotides, while TC-NER is activated when RNA polymerase II (RNAPII) stalls during transcriptional elongation on a DNA lesion in the template strand of actively transcribed genes.

In the GG-NER subpathway, the protein XPC is the main damage sensor and is stabilized by its association with RAD23B and centrin 2 (CETN2) (Masutani *et al*, 1994; Nishi *et al*, 2005). To promote CPD repair, the UV-DDB (ultraviolet radiation-DNA damage-binding protein) complex comprised of the two proteins DDB1 and DDB2,

directly binds to the UV-induced lesions and functions as an auxiliary damage-recognition factor by promoting subsequent binding of XPC (Scrima *et al*, 2008; Wakasugi *et al*, 2002). Once XPC is bound to the DNA lesion, the TFIIH (transcription initiation factor IIH) complex is recruited by interaction with XPC-RAD23B (Araujo *et al*, 2001; Evans *et al*, 1997a; Riedl *et al*, 2003; Volker *et al*, 2001; Yokoi, 2000). This complex consists of ten protein subunits including two helicase subunits, XPB and XPD. XPB and XPD have opposite polarities and extend the open DNA configuration around the lesion (Compe & Egly, 2012; Evans *et al*, 1997b; Tapias *et al*, 2004). The TFIIH is thought to unwind the damaged DNA. Subsequently, the protein XPA is recruited and plays a role in verification of DNA damage as it can detect nucleotides with altered chemical structures in ssDNA (Camenisch *et al*, 2006).

The next step in the repair process is strand incision and removal of the lesions. Lesion excision is catalyzed by the structure-specific endonucleases XPF-ERCC1 and XPG, which incise the damaged strand at short distances 5' and 3' from the lesion respectively (Fagbemi *et al*, 2011). This excision leaves a gap of 22-30 nucleotides, which can trigger a DNA damage signaling reaction. The single-strand-binding protein RPA binds to and protects the non-damaged strand of DNA from endonucleases and ensures that XPF-ERCC1 and XPG specifically incise only the damaged strand (De Laat *et al*, 1998). The 5' incision is sufficient to initiate gap-filling DNA synthesis, even before the 3' incision is made. This may be to prevent the accumulation of ssDNA gaps that induce DNA damage signaling. The DNA gap-filling synthesis and ligation are executed by the replication proteins proliferating nuclear antigen (PCNA), replication

factor C (RFC), DNA Pol δ , DNA Pol ϵ , or DNA Pol κ , and DNA ligase 1 or XRCC1-DNA ligase 3 (Moser *et al*, 2007; Ogi *et al*, 2010).

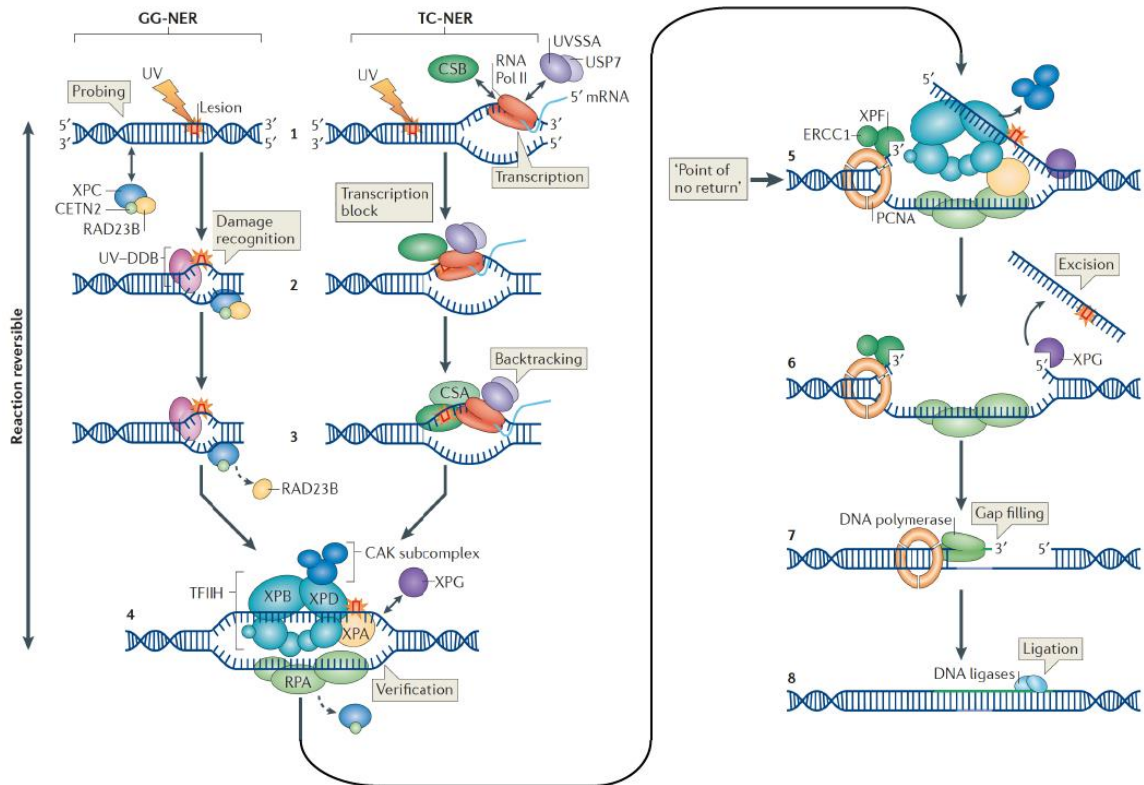


Figure 1.2. Nucleotide excision repair (NER) pathway. This repair pathway is discussed in the text. Reproduced from (Marteijn *et al*, 2014) with the permission from Nature Publishing Group (License: 4143640542678).

The removal of UV-induced lesions such as CPDs can be slow and ineffective, and the persistence of CPDs interferes with replication and transcription elongation. Long-term stalling of RNA polymerase and transcriptional arrest can trigger cell death (Ljungman & Zhang, 1996). The repair of UV-induced DNA damage occurs faster in regions that are actively transcribed due to the specialized subpathway TC-NER (Bohr *et*

al, 1985; Mellon *et al*, 1986). In TC-NER, RNA polymerase stalled on the DNA lesion acts as an indirect signal to initiate and carry out NER.

Arrested RNAPII recruits the proteins CSA and CSB which are important for the recruitment of the TC-NER machinery to the transcription-blocking DNA lesion (Fousteri *et al*, 2006). This includes the core NER factors and several TC-NER specific factors, such as UV-stimulated scaffold protein A (UVSSA), ubiquitin-specific-processing protease 7 (USP7), XPA-binding protein 2 (XBA2) and high mobility group nucleosome-binding domain-containing protein 1 (HMGN1) (Fousteri *et al*, 2006; Schwertman *et al*, 2012). When RNAPII stalls, it covers an area of the transcribed strand which prevents the NER incision machinery from accessing the lesion. Several models have been proposed for the fate of stalled RNAPII including translocation, displacement or degradation of RNAPII stalled at UV-induced lesions to allow access to repair proteins.

After treatment with UV-radiation or cisplatin, there is detectable ubiquitylation of RNAPII while little ubiquitylation is observed after treatment with hydrogen peroxide or ionizing radiation (IR) (Bregman *et al*, 1996). Ubiquitination reaches maximal levels several hours post UV and is no longer detectable 12 to 16 hours later. While RNAPII undergoes ubiquitination after UV (Bregman *et al*, 1996), degradation of RNAPII seems to only occur as a last resort when TC-NER is not functional (Anindya *et al*, 2007). The UV-arrested RNAPII is still in a complex with TC-NER factors, suggesting that it is not removed/degraded but remains at the UV damage site during the early steps in repair (Fousteri *et al*, 2006; Schwertman *et al*, 2012). This suggests it is likely that RNAPII backtracks upon encountering UV-induced DNA lesions. This backtracking would also

provide transcriptional proofreading where any mismatches would induce further backtracking and repair (Sigurdsson *et al*, 2010). The mechanism underlying the backtracking of RNAPII and assembly of the TC-NER complex is poorly understood.

1.4.2 Chromatin remodeling and NER

UV light is one of the most common environmental DNA damaging agents and most DNA lesions induced by UV are repaired by NER. The importance of chromatin remodeling for NER is clear from many experiments revealing that NER is more efficient on naked DNA than in chromatin. The chromatin structure, if not remodeled, limits the access of NER factors to DNA (Araki *et al*, 2000; Gong *et al*, 2005; Osley *et al*, 2007; Sugawara *et al*, 1993). For example, the recognition of CPDs by XPC-RAD23B is inhibited when the lesion is present in a nucleosome *in vitro* (Hara *et al*, 2000). In addition, human NER complexes need a nucleosome-free region of DNA of about 80-100 bp to access and to efficiently excise UV photoproducts, highlighting the requirement for transient disruption of one or more nucleosomes (Huang & Sancar, 1994). UV damage itself affects the chromatin and enhances unwrapping of nucleosomes (Duan & Smerdon, 2010). This enhanced ‘DNA breathing’ may allow for efficient recognition of DNA damage by the repair factors, which once bound might further unwrap the DNA. In mammals, several ATP-dependent chromatin remodeling complexes have been implicated in the repair of damage induced by UV-radiation including SWI/SNF, INO80 and ACF (Hara & Sancar, 2002, 2003; Jiang *et al*, 2010; Lan *et al*, 2010; Sánchez-Molina *et al*, 2011). One of them is CSB, which contains a SWI2/SNF2 ATPase domain. CSB is

able to remodel chromatin *in vitro* in an ATP-dependent manner (Citterio *et al*, 2000).

Whether and how CSB remodels chromatin to promote TC-NER *in vivo* has not yet been demonstrated.

1.4.3 Role of CSB in NER

CSB transiently interacts with elongating RNAPII and this interaction is stabilized after induction of DNA damage by exposure to UV-radiation (Van Den Boom *et al*, 2004).

This finding suggests that CSB plays an early role in damage sensing during TC-NER.

Using CSB-deficient cells, CSB is found to be one of the initial sensors of damage and is essential for the recruitment of NER core factors TFIIH, XPA, XPG, XPF/ERCC1 and RPA as well as CSA (Fousteri *et al*, 2006).

A key characteristic of CS is cellular sensitivity to UV-radiation as well as a defect in the recovery of transcription after exposure to UV-radiation. Cells derived from CS patients are defective in TC-NER while they have no defect in GG-NER (Venema *et al*, 1990; Van Hoffen *et al*, 1993). An assay used to measure defects in TC-NER is “a recovery of RNA synthesis” after UV irradiation, also known as RRS assays. RRS after exposure to UV-irradiation can be assayed by pulse labeling the cells at different timepoints after UV treatment with marked (radioactive or fluorescent) nucleotides (Mayne & Lehmann, 1982). When RNAPII stalls at UV-radiation induced lesions, there is an overall decline in transcription. In normal cells transcription recovers over time, however in TC-NER deficient cells, there is no transcriptional recovery.

CS cells are also deficient in the selective removal of UV-induced CPDs from the transcribed strand of active genes compared to the non-transcribed strand (Van Hoffen *et al*, 1993). In addition to strand preference, CSB also plays a role in the removal of UV-induced DNA damage in specific regions of a gene. In CS cells, repair of UV-induced DNA damage is inefficient at the promoter as well as the transcribed strand starting at nt position +20 and extending downstream. Repair of UV-induced damage at sequences surrounding the transcription initiation site is not defective in CS cells, suggesting that CSB is dispensable for the repair of damage surrounding the transcription initiation site (Tu *et al*, 1997).

CSB is a DNA-dependent ATPase, and its central ATPase domain is necessary for its chromatin remodeling activity (Citterio *et al*, 2000). Point mutations of conserved residues within the CSB ATPase domain impair the function of CSB in TC-NER, sensitizing cells to UV radiation and reducing the ability of CSB to promote transcriptional recovery (Brosh *et al*, 1999; Citterio *et al*, 1998, 2000; Muftuoglu *et al*, 2002). The ATPase activity of CSB is also important for the removal of UV-induced CPDs from the actively transcribed *DHFR* gene (Brosh *et al*, 1999). These results demonstrate that the chromatin remodeling activity of CSB is required for efficient TC-NER.

The importance of other regions of CSB in TC-NER has also been demonstrated. Within the N-terminus of CSB, there is an acidic stretch of residues. This region of CSB is dispensable for the repair of UV-induced damage (Brosh *et al*, 1999). Within the very C-terminus of CSB, a ubiquitin binding domain (UBD) has recently been identified. The

UBD domain in CSB is important for repair of UV-induced damage as deletion of this domain (Δ UBD) sensitizes cells to UV radiation (Anindya *et al*, 2010). Deletion of the CSB UBD affects neither the association of CSB to sites of arrested RNAPII nor TC-NER complex assembly after UV irradiation. Cells expressing CSB Δ UBD show a reduced rate of UV-induced DNA lesion excision, suggesting that the binding of CSB to an unknown ubiquitylated partner may promote the excision of transcription blocking lesions induced by UV radiation (Anindya *et al*, 2010).

1.4.4 Regulation of CSB in NER

As CSB is essential for TC-NER, it is important that the level and the activity of CSB are regulated within the cell. In untreated cells, CSB is localized to the nucleus of the cell but is loosely bound to DNA and mostly soluble. After exposure to UV-radiation, CSB becomes stably associated with the chromatin (Fousteri *et al*, 2006; Lake *et al*, 2010). Point mutations of conserved residues within the central ATPase domain compromise the UV-induced chromatin association of CSB, suggesting that UV-induced chromatin association of CSB is dependent upon its ATPase activity. Deletion of the N-terminus of CSB results in binding to chromatin in the absence of damage, while deletion of the C-terminus of CSB abrogates its UV-induced chromatin association. This finding suggests that the N-terminus of CSB negatively regulates its association with chromatin, perhaps by sequestering the DNA-binding domain within the C-terminus in untreated cells (Lake *et al*, 2010). After damage, this inhibition is relieved and CSB then stably binds to the chromatin at the expense of ATP hydrolysis.

CSB is reported to undergo ubiquitylation after UV and later be degraded. CSB interacts with CSA, which is a subunit of the Cullin 4A (Cul4A) complex, an E3 ubiquitin ligase complex. Addition of CSA can stimulate the *in vitro* DNA-dependent ATPase activity of CSB (Tantin *et al*, 1997). Mass spectrometry analysis of CSA purified by tandem affinity purification revealed an interaction with CSB (Fei & Chen, 2012). CSB binds to CSA at early stages of DNA repair following exposure to UV-radiation. The ligase activity of the CSA complex is upregulated after UV irradiation (Groisman *et al*, 2003), and CSB is later removed from the CSA complex by proteasome-dependent degradation at later stages (Groisman *et al*, 2006). Consistent with this finding, CSB degradation at later timepoints after exposure to UV is dependent upon CSA, suggesting that the main role of CSA is to remove CSB from DNA by degradation. CSB has also been reported to be polyubiquitinated and degraded by BRCA1 after UV (Wei *et al*, 2011), suggesting that multiple pathways may regulate CSB stability after UV irradiation.

The ubiquitin-specific protease 7 (USP7) and the recently identified TC-NER factor UVSSA (UV-stimulated scaffold protein A) form a complex together and play a role in the early steps of TC-NER. The UVSSA/USP7 complex travels along with RNAPII, accumulates at damage-stalled RNAPII and stabilizes the interaction between RNAPII and CSB by counteracting the polyubiquitination of CSB and RNAPII (Fei & Chen, 2012; Schwertman *et al*, 2012; Zhang *et al*, 2012). These findings suggest that TC-NER involves a very extensive network of highly-regulated ubiquitylation and deubiquitylation events.

In addition to ubiquitination, CSB also undergoes UV-induced SUMOylation (Sin *et al*, 2016). This SUMOylation is mediated by SUMO-conjugating enzyme (E2), Ubc9. The very C-terminus of CSB is important for this modification, however the modification itself does not occur there. Instead SUMOylation occurs at lysine 205 (K205), which is important for functional TC-NER (Sin *et al*, 2016). How SUMOylation of CSB regulates its function in TC-NER remains uncharacterized.

1.4.5 Relationship between CSB and p53 in UV response

Lack of CSB leads to an increase in apoptosis after UV treatment, which is dependent upon its ATPase activity (Balajee *et al*, 2000). The tumor suppressor p53 is a master regulator of the transcriptional response to stress and plays a key role in triggering senescence and apoptosis. CSB interacts with p53 (Wang *et al*, 1995) and this interaction is mediated through the C-terminus of p53 and the central ATPase domain of CSB (Lake *et al*, 2011). This interaction suggests that CSB and p53 function together in the response to DNA damage.

p53 functions as a transcription factor and binds to DNA in both a sequence-dependent and sequence-independent manner. When CSB interacts with p53, it sequesters the C-terminus of p53, exposing the core domain and enhancing the sequence-independent DNA binding of p53 (Lake *et al*, 2011). Reintroduction of CSB into CS cells leads to increased p53-chromatin association, implying that CSB promotes chromatin association of p53 (Lake *et al*, 2011). These results suggest that CSB promotes

the sequence-independent binding of p53 to chromatin to help p53 in scanning the genome for damaged DNA or finding its target genes.

CSB competes for p53 binding with the co-activator p300 (Filippi *et al*, 2008). CSB shows a higher affinity than p300 for interaction with p53, suggesting that CSB negatively regulates the transcriptional activity of p53. In the absence of CSB, there is increased binding between p53 and p300, resulting in the stabilization of p53 and activation of its target genes. This would then titrate away essential transcription factors such as p300, indicating that CSB may regulate p53 interaction with other transcriptional factors.

In undamaged cells, the p53 level is kept low by constant polyubiquitylation by the E3 ubiquitin ligase Mdm2, and subsequent proteasome-mediated degradation (Fuchs *et al*, 1998; Haupt *et al*, 1997; Honda *et al*, 1997; Kubbutat *et al*, 1997). Upon DNA damage, p53 is phosphorylated on multiple residues. Phosphorylation of serine 15 by the kinases ATM/ATR/DNA-PK inhibits the interaction between p53 and Mdm2 and results in stabilization (Shieh *et al*, 1997; Siliciano *et al*, 1997). Stabilized p53 then undergoes other post-translational modifications (PTM) and binds to the promoters of a variety of genes. This results in the induction of different transcriptional programs involved in cycle arrest, DNA repair or apoptosis (Beckerman & Prives, 2010; Rodier *et al*, 2007). CS cells show elevated and persistent levels of p53 before and after exposure to UV damage and undergo high levels of apoptosis after DNA damage (Balajee *et al*, 2000; Laposa *et al*, 2007; Latini *et al*, 2011). This increase in p53 is due to insufficient Mdm2-mediated ubiquitylation and degradation of p53 (Latini *et al*, 2011). It has been suggested

that CSB and CSA proteins may enhance the polyubiquitination and degradation of p53 *in vitro* and *in vivo* (Latini *et al*, 2011).

Together these results show that CSB and p53 function together in the cell where CSB regulates both the chromatin association of p53 as well as the protein stability before and after damage. How this interaction between CSB and p53 might affect DNA repair is not known, but it has been suggested that this interaction plays an important role in keeping the balance between cellular aging and cancer susceptibility (Frontini & Proietti-De-Santis, 2012). Therefore, CS cells, which have elevated levels of p53, are unable to maintain this balance and undergo high levels of apoptosis.

1.5 CSB and Base Excision Repair (BER)

1.5.1 BER pathway

Base excision repair (BER) is the repair pathway responsible for removal and correction of small base lesions that do not significantly distort the DNA helix structure. This damage usually results from deamination, oxidation, or methylation and can be caused by endogenous sources as well as environmental chemicals, radiation, or treatment with cytostatic drugs. The BER pathway requires four different types of enzymes: DNA glycosylase, AP endonuclease (APE1), DNA polymerase and DNA ligases (**Figure 1.3**).

The BER pathway is initiated by one of at least 11 distinct DNA glycosylases which each recognize different types of base damage (Robertson *et al*, 2009). The DNA glycosylase recognizes its specific damaged DNA base and causes a distortion of the DNA helix resulting in the flipping out of the damaged base from the DNA helix. It then

catalyzes cleavage of the N-glycosidic bond between the damaged base and the deoxyribose sugar, removing the damaged base and creating an apurinic/aprimidinic site (AP site). The AP site is then bound by APE1, which cleaves the DNA backbone on the 5' side of the abasic deoxyribose phosphate, creating a single-strand break or nick in the DNA (Hegde *et al*, 2008). The synthesis step can then proceed in two separate ways, short patch repair or long patch repair. In short patch repair, the repair polymerase Pol β can bind to the abasic site and use the intact, undamaged strand as a template for DNA

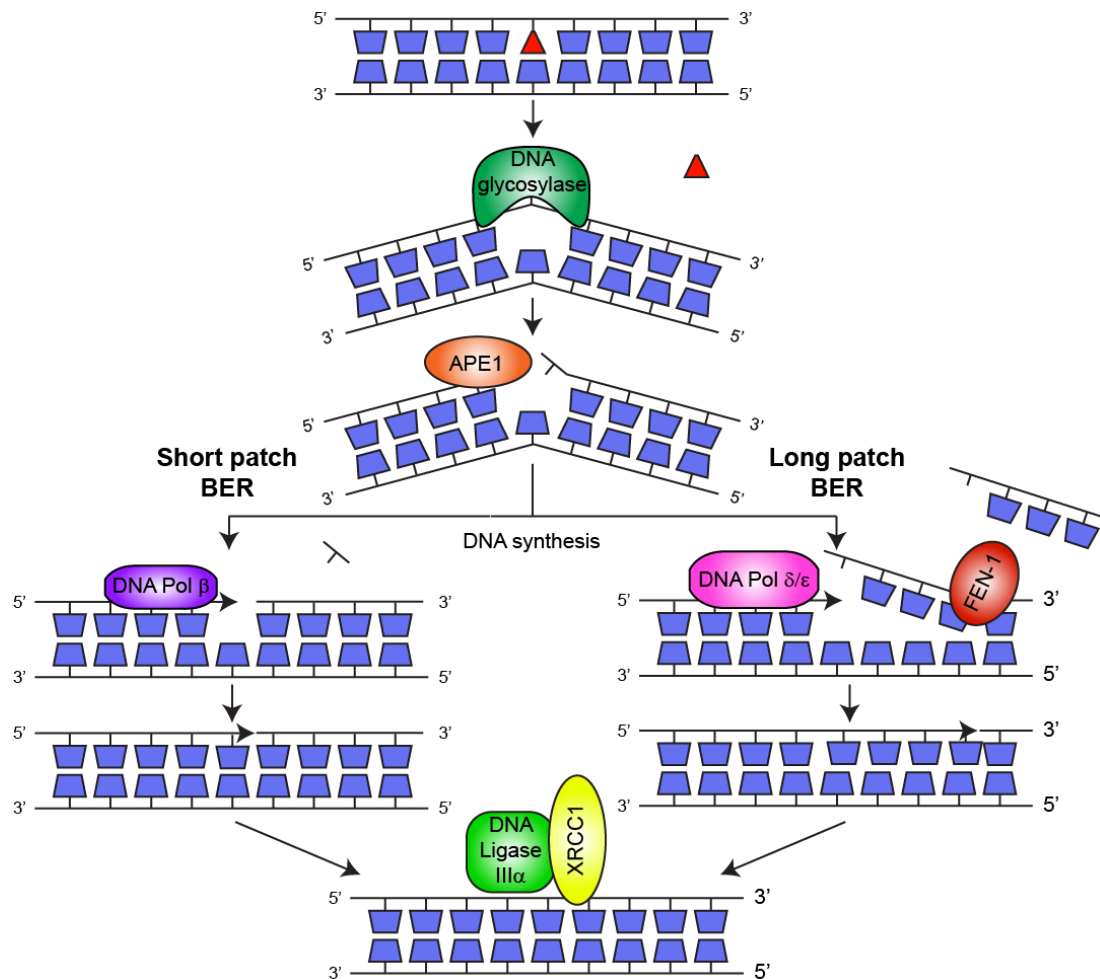


Figure 1.3. Base excision repair pathway. This repair pathway is described within the text.

synthesis, adding a single nucleotide. The remaining deoxyribose phosphate is cleaved and removed by the 5'-deoxyribosephosphatase activity of Pol β (Matsumoto & Kim, 1995; Singhal & Wilson, 1993; Sobol *et al*, 1996). In long patch repair, one of the processive polymerases, Pol δ or Pol ϵ adds up to 13 nucleotides to the 3' hydroxyl group of the nucleotide 5' of the nick (Dogliotti *et al*, 2001; Fortini *et al*, 1998; Stucki *et al*, 1998). The 5' stretch of displaced nucleotides is cleaved by the flap endonuclease FEN-1 (Kim *et al*, 1998; Klungland & Lindahl, 1997). The final step of BER is ligation of the nicked strand by DNA ligase III α in complex with XRCC1 (Caldecott *et al*, 1994; Kubota *et al*, 2015; Wei *et al*, 1995). The protein PARP-1 (Poly (ADP-ribose) polymerase-1) also promotes repair by binding to the single-strand break intermediate and enhances the recruitment of Pol β and XRCC1-DNA ligase III α (El-Khamisy *et al*, 2003; Leppard *et al*, 2003; Prasad *et al*, 2001).

1.5.3 Chromatin remodeling and BER

Similar to NER, repair of base damage by BER is facilitated by chromatin remodeling. Using *in vitro* assembled nucleosome core particles (NCPs) with different base lesions as templates for repair, each step of BER is negatively impacted by the presence of histones (Beard *et al*, 2003; Cole *et al*, 2010; Hinz *et al*, 2010; Odell *et al*, 2010, 2013; Rodriguez & Smerdon, 2013). This inhibition is mainly due to decreased access of the repair proteins to their respective lesions. As BER occurs efficiently in cells, the results from the *in vitro* experiments confirm that chromatin rearrangement occurs at DNA damage sites *in vivo*. Addition of ATP-dependent chromatin remodeling (ACR) complexes can

facilitate the removal of lesions in nucleosomes *in vitro* (Menoni *et al*, 2007, 2012b; Nakanishi *et al*, 2007). These findings show that ACR complexes can remodel nucleosomes in the presence of recombinant BER proteins, which then have increased activity on their otherwise difficult access to substrates. The bulky DNA adducts repaired by NER are helix-distorting and enhance the unwrapping of the nucleosome, initiating the process of DNA accessibility (Duan & Smerdon, 2010). This means that NER factors can bind without significant intervention of other factors. This is contrary to the base modifications recognized by BER, which generally cause minimal disruption to the DNA helix or the nucleosome structure (Rodriguez & Smerdon, 2013), suggesting that any increase in exposure of the lesions to repair proteins would require the help of nucleosome-disrupting activity. Contrary to NER, there have been no reported interactions between BER proteins and ACR complexes. While ACR complexes clearly promote BER activity, it is unclear if this is due to activity of ACR complexes directly at the DNA lesions or if this is simply a combination of promoting expression of BER genes and increased opportunities for binding in open chromatin. Any process that regulates BER plays a role in genomic maintenance, mutagenesis and aging.

1.5.3 Role of CSB in BER

Accumulation of unrepaired oxidative damage in either nuclear or mitochondrial DNA observed in CS cells (Balaban *et al*, 2005; Fukui & Moraes, 2008; Gredilla, 2010), could in part account for the prominent degeneration symptoms seen in CS patients. CSB has been reported to interact physically and functionally with several different proteins that

are known to be involved in the BER pathway (Aamann *et al*, 2013; Fan & Lake, 2013; Khobta & Epe, 2013), suggesting that CSB participates in BER.

Nuclear OGG1 was the first BER protein which was found in complex with CSB. OGG1 is the main DNA glycosylase that is responsible for the excision of the DNA base damage 8-oxoG (8-hydroxyguanine) (Klungland & Bjelland, 2007). Extracts from CS cells are defective in the excision of 8-oxoG (Dianov *et al*, 1999). There is no defect of uracil or thymidine glycol excision activity in CS cells, suggesting that CSB plays a role in the removal of only certain types of base damage. Indeed, this defect in the excision of 8-oxoG has been reported by several other groups as well (Selzer *et al*, 2002; Tuo *et al*, 2001, 2002a). The level of hOGG1 mRNA is decreased in CS cells compared to normal cells, suggesting that CSB promotes repair of 8-oxoG at least in part by regulating the expression of OGG1 (Dianov *et al*, 1999; Tuo *et al*, 2002a). The ATPase activity of CSB is not required for removal of 8-oxoG as CSB ATPase mutants defective in ATPase activity are still capable of processing 8-oxoG (Selzer *et al*, 2002; Tuo *et al*, 2001). Following γ -radiation, there is a significant increase in the levels of 8-OH-dGuo (8-hydroxy-2'-deoxyguanosine) and 8-OH-dAdo (8-hydroxy-2'-deoxyadenosine) in the genome of CS cells compared to normal cells (Tuo *et al*, 2001, 2002b, 2003), suggesting that the role of CSB in BER extends beyond affecting the expression of OGG1 as this enzyme does not excise 8-oxoA (8-hydroxyadenine). The mechanism by which CSB participates in the removal of 8-oxoG in nuclear DNA remains unknown. CSB may promote 8-oxoG removal by directly contributing to the activity of OGG1 as when cells

are depleted of CSB with a specific antibody against CSB, there was a decrease in excision of 8-oxoG (Tuo *et al*, 2002a).

CSB also interacts with other DNA glycosylases. NEIL1 is responsible for the excision of formamidopyrimidines (Fapy-G and Fapy-A) which are another class of base modification induced by oxidative damage (Hu *et al*, 2005). CSB and NEIL1 interact with each other and colocalize in the cell. CSB promotes excision activity of NEIL1 towards Fapy-G and Fapy-A lesions (Muftuoglu *et al*, 2009). CSB also interacts with NEIL2 (Aamann *et al*, 2014), which is a DNA glycosylase responsible for the excision of oxidation products of cytosine including 5-hydroxyuracil (5-OH-U) (Dou *et al*, 2003). CSB promotes the *in vitro* incision activity of NEIL2 against FapyA lesions as well as its more classical substrate 5-OH-U when present in a bubble structure (Aamann *et al*, 2014). After oxidative stress, CSB and NEIL2 colocalize in the cell.

CSB also interacts with the apurinic/aprimidinic (AP) endodeoxyribonuclease APE1, which is responsible for the repair of AP sites by incision at the 5'-side of the lesion. ELISA and Co-IP experiments demonstrate that CSB interacts with APE1 (Wong *et al*, 2007). CSB promotes the incision activity of APE1 in an ATP-independent manner, and this is more pronounced when the AP site was present in a DNA bubble, which mimics a DNA transcription intermediate, than in the fully paired AP duplex which is the classical BER substrate. These results suggest that CSB may preferentially stimulate APE1 activity in transcriptionally active regions. There is no significant accumulation of AP sites in the genome of CS cells compared to normal cells and the incision activity of whole cell extracts from CS cells towards AP sites is also normal

(Wong *et al*, 2007). These results suggest that CSB does not play a key role in global genome repair of abasic lesions. On the other hand, the importance of CSB interaction with APE1 is underscored by the sensitivity of CS cells to methyl methanesulfonate (MMS), which is known to generate high levels of AP sites (Wong *et al*, 2007; Wyatt & Pittman, 2006).

CSB also interacts with the poly(ADP-ribose) polymerase-1 (PARP1) (Thorslund *et al*, 2005). PARP1 is an enzyme that immediately binds to free single-strand breaks (SSB) in DNA, which can be generated as an intermediate during BER. After binding to the SSB, PARP1 modifies various proteins by poly(ADP-ribosyl)ation as well as itself and promotes DNA synthesis and ligation. PARP1 interacts with and poly(ADP-ribosyl)ates several key factors of the BER pathway including OGG1, XRCC1, Pol β , DNA ligase III α and PCNA, suggesting that it regulates BER (Dantzer *et al*, 2000; Frouin *et al*, 2003; Leppard *et al*, 2003; Masson *et al*, 1998; Noren Hooten *et al*, 2011). CSB binds to both inactive (unmodified) and active (modified) PARP1 and its interaction with PARP1 not affected by oxidative stress (Thorslund *et al*, 2005). CSB interacts with PARP1 via its N-terminus (amino acids 2-341), which is also poly(ADP-ribosyl)ated PARP1 after oxidative stress. The poly(ADP-ribosyl)ation of CSB inhibits its *in vitro* DNA-dependent ATPase activity (Thorslund *et al*, 2005). The CSB/PARP1 complex relocates to sites of DNA damage in the cell after oxidative stress (Thorslund *et al*, 2005). How the poly(ADP-ribosyl)ation of CSB affects its own activity and function in the cells remains unclear. However, as both proteins are involved in DNA repair, chromatin

remodeling and transcription (De Vos *et al*, 2012; Stevnsner *et al*, 2008), it is possible that CSB and PARP1 may function together to regulate repair of DNA damage.

In addition to interacting with proteins involved in BER, CSB is also recruited to sites of oxidative damage (Menoni *et al*, 2012a). Using a laser-assisted procedure to locally inflict oxidative DNA lesions, CSB is found to accumulate at the sites of damage. CSB is recruited quickly after induction of oxidative damage, which precedes the recruitment of OGG1. Knockdown of OGG1 did not affect the recruitment of CSB, suggesting the CSB is recruited by 8-oxoG and not by repair intermediates. CSB remains at the sites of oxidative damage for several hours, which is in agreement with the reported BER kinetics of oxidative damage (Amouroux *et al*, 2010; Will *et al*, 1999). These findings suggest that CSB binds to 8-oxoG and not other types of damage induced by the laser. Though CSB accumulates on oxidative damage, none of the core NER factors downstream of CSB show significant accumulation. This further suggests that CSB plays a role in BER outside of its role in NER.

1.5.4 Regulation of CSB in BER

The function of CSB in BER is regulated by post-translational modification. Mass spectrometry analysis of CSB identified that CSB is ubiquitylated on lysine 991 (K991) in untreated cells (Ranes *et al*, 2016). K991 is located just outside of the core ATPase domain and is highly conserved in CSB orthologues. Mutating this site (K991R) does not affect the DNA-dependent ATPase activity of CSB or its function in TC-NER. On the other hand, cells expressing the K991R mutant are sensitive to oxidative damage. A

similar sensitivity to oxidative damage was seen in cells expressing CSB Δ UBD (Ranes *et al*, 2016) which is deficient in TC-NER (Anindya *et al*, 2010). Ubiquitylation of K991 is unaffected after exposure to UV-radiation but induced after oxidative damage. The K991R and CSB Δ UBD mutants are both capable of accumulating at sites of oxidative damage comparable to WT, however they both fail to dissociate in a timely manner. These results suggest that ubiquitylation of K991 and the UBD of CSB are not required for its recruitment to oxidative damage but are necessary dissociation from the site of oxidative damage. The mutation K991R is the first separation-of-function mutation of CSB as it is not important for UV, but is important for oxidative damage repair.

CSB is reported to interact with the non-receptor protein tyrosine kinase c-Abl (Imam *et al*, 2007). The kinase c-Abl is activated upon genotoxic and oxidative stress. Similar to PARP1, this interaction is mediated through the N-terminus of CSB. CSB is phosphorylated by c-Abl at tyrosine 932 after treatment with hydrogen peroxide to induce oxidative damage, and this phosphorylation alters the localization of CSB in the nucleus and nucleolus. These results suggest that phosphorylation of CSB by c-Abl may regulate the recruitment of CSB in response to oxidative stress. As this phosphorylation site is within the ATPase domain of CSB, it is reasonable to speculate that c-Abl mediated phosphorylation of CSB may regulate its ATPase activity, however this has not been addressed.

Together, CSB interacts with and promotes the function of several different proteins known to have important roles in the BER pathway. Based on the multiple interactions, it is likely that at least part of the phenotype observed in CS patients is due to

the lack of these interactions. It remains to be seen if CSB plays a role in BER on the whole genome scale or just a subtype.

1.6 Role of CSB in Transcription

In addition to its role in transcription-coupled repair, CSB also plays a role in general transcription. CSB deficient cells have reduced RNA synthesis (Balajee *et al*, 1997; van Gool *et al*, 1997) and CSB can stimulate transcription elongation *in vitro* (Selby & Sancar, 1997; Van der Horst *et al*, 1997; Proietti-De-Santis *et al*, 2006). CSB is reported to interact with several different factors which are known to be involved in transcription.

Using Co-IP, CSB is found in a complex with RNA polymerase I (RNAPI) (Bradsher *et al*, 2002; Yuan *et al*, 2007). Using anion exchange chromatography, CSB and RNAPI are found in the same fraction. Using immunofluorescence (IF), CSB is enriched in the nucleolus along with RNAPI, TFIIH, XPG and TIF-1B, supporting the notion that these are in a complex together (Bradsher *et al*, 2002). A direct interaction between RNAPI and CSB has yet to be demonstrated. CSB along with TFIIH promotes the transcription of rDNA by RNAPI *in vitro* (Bradsher *et al*, 2002). The rate of rDNA synthesis is significantly lower in CS cells as well as in cells depleted for CSB by using shRNA or siRNA (Yuan *et al*, 2007). An ATPase-deficient mutant of CSB is unable to promote rRNA transcription, suggesting that the ATPase activity of CSB is required for the activation of RNAPI transcription.

The transcription of rRNA is regulated largely by chromatin remodeling and epigenetic modifications, some of which are controlled by CSB (McStay & Grummt,

2008). CSB interacts with the histone methyl transferase (HMT) G9a, which methylates lysine 9 of histone H3 (H3K9me). This modification along with the binding of heterochromatin protein 1 gamma (HP1 γ) are required for rRNA synthesis initiation and elongation (Yuan *et al*, 2007). CSB promotes H3K9me by G9a in an ATPase dependent manner, suggesting that CSB may remodel the chromatin to promote histone methylation (Yuan *et al*, 2007). Another important epigenetic mark that regulates rRNA synthesis is DNA methylation of the rDNA promoter, however no association between CSB and DNA methylation has been reported (Schmitz *et al*, 2009).

CSB is associated with activating and repressing complexes in the nucleolus. The rDNA genes can be separated into three different categories: silenced, active and poised genes (Xie *et al*, 2012). Silent genes contain methylated CpGs in the promoters and heterochromatic histone marks that are mediated by the nucleolar remodeling complex (NoRC). The heterochromatic nature of these silent genes restricts the access of transcriptional machinery. Active genes contain euchromatic structure with unmethylated promoters where CSB, RNAPI and G9a are recruited and are actively transcribed (Xie *et al*, 2012). Poised genes are silent genes but are ready to be activated. These poised genes are regulated by the nucleosome remodeling and deacetylation (NuRD) complex, and these genes contain both euchromatic and heterochromatic marks. Components of the preinitiation complex UBF and SL1 are also found at these genes, but not RNAPI (Xie *et al*, 2012). CSB interacts with the NuRD complex to remodel the chromatin and activate these poised genes allowing for recruitment of RNAPI and transcription (Xie *et al*, 2012).

Several reports have shown that CSB also interacts with RNA polymerase II (RNAPII). One study shows that RNAPII interacts with CSB at high concentrations of salt, and the interaction is DNA-independent as it is not affected by the presence of ethidium bromide (van Gool *et al*, 1997). In contrast, a separate study using Co-IP showed that CSB only interacts with RNAPII at a lower concentration of salt (Bradsher *et al*, 2002). This shows that the interaction between CSB and RNAPII may be sensitive to experimental differences in immunoprecipitation protocol. Immunoprecipitated CSB and its associated proteins are capable of supporting transcription in an *in vitro* assay when RNAPII is omitted, further demonstrating that CSB is associated with active RNAPII (Van Den Boom *et al*, 2004). In addition to RNAPII, CSB is found in a complex with XPB and XPD, both of which are subunits of TFIIH (Bradsher *et al*, 2002). CSB is also important for the recruitment of RNAPII and XPB to chromatin after UV (Fousteri *et al*, 2006). EMSA experiments with purified CSB demonstrate that CSB and TFIIH bind to stalled RNAPII. The binding of TFIIH to RNAPII is dependent upon CSB, suggesting that CSB mediates this interaction (Tantin *et al*, 1997). One study has suggested that CSB also interacts with TFIIIE and XPA (Selby & Sancar, 1997). TFIIIE promotes initiation of RNA synthesis together with TFIIH, and CSB is pulled down with p34, a subunit of TFIIIE.

Given that CSB interacts with several components of the transcriptional machinery, researchers have addressed if CSB regulates transcription on a genomic level. Using microarray analysis, it was observed that CSB significantly regulates the expression of 112 genes out of the 6912 genes analyzed after oxidative stress, suggesting

that CSB regulates the expression of certain genes (Kyng *et al*, 2003). After UV-radiation, loss of CSB leads to a decrease in recruitment of RNAPII and its associated transcription factors, even to the promoters of some undamaged genes (Proietti-De-Santis *et al*, 2006). Each of these studies look at the effect of CSB after damage, however they did not clearly address if CSB regulates transcription in undamaged cells. Microarray analysis of CSB deficient and complemented cells revealed that that loss of CSB results in significant changes in gene expression in the absence of external stress (Newman *et al*, 2006). Genes down regulated by CSB include a number of tumor suppressors, growth inhibitors and inflammatory mediators, while genes upregulated by CSB vary more so in function and include oxidative metabolism, proliferation, cell cycle progression, neuronal survival, the immune response, DNA repair, RNA processing and drug resistance (Newman *et al*, 2006). Many of the genes regulated by CSB overlap with genes that are regulated by histone deacetylase (HDAC) inhibitors, suggesting that loss of CSB phenocopies treatment with a chromatin-disrupting agent. There was also significantly overlap between genes suppressed by CSB and PARP1, promoting the idea that CSB and PARP1 function outside of BER to regulate transcription. CSB did not seem to affect the expression of any acetyltransferases or methyltransferases, suggesting that CSB has a direct role in regulating chromatin modification. Finally, many genes regulated by CSB are also regulated in models of human aging, implying that CS is a true progeria as the clinical symptoms of CS suggest.

1.7 Telomeres

1.7.1 *Telomere structure and function*

Telomeres are nucleoprotein complexes found at the ends of linear eukaryotic chromosomes. Telomeric DNA consists of short, double-stranded and G-rich tandem repeats (Palm & de Lange, 2008). The sequence of the repeats varies among species (Louis & Vershinin, 2005), with mammalian telomere repeats being TTAGGG (Meyne *et al*, 1989; Moyzis *et al*, 1988). The TTAGGG repeat containing strand is known as the “G-rich strand”, and the complementary CCCTAA containing strand is known as the “C-rich strand”. The average telomere length varies among different species. In humans, the average length at birth is about 10-15 kilobase (kb) pairs, and the length decreases with age (de Lange *et al*, 1990; Harley *et al*, 1990).

The end of the telomere is not blunt-ended, but consists of a single-stranded protrusion of the G-rich strand which is referred to as the 3' overhang (**Figure 1.4a**) (Greider & Blackburn, 1985; Makarov *et al*, 1997; McElligott & Wellinger, 1997). This overhang is the result of Apollo nuclease activity at the leading strand end (Sfeir *et al*, 2005; Wu *et al*, 2010, 2012). Both strands are then further processed by the resection activity of EXO1 (Sfeir *et al*, 2005; Wu *et al*, 2012). The 3' overhang of mammalian telomeres can vary between 50-500 nucleotides (Palm & de Lange, 2008). Electron microscopy analysis has shown that mouse and human telomeres are organized into a large duplex lariat structure called the t-loop (Palm & de Lange, 2008; Griffith *et al*, 1999; Greider, 1999). T-loops are thought to be formed by the invasion of the 3' overhang into the double-stranded telomeric DNA where it forms complementary base

pairing with the C-rich strand (Griffith *et al*, 1999; Greider, 1999). The point of invasion in the double stranded DNA is called the D-loop (**Figure 1.4a**). T-loops are thought to help protect chromosome ends and have been proposed to be the solution to the problem of telomere protection. The size of the t-loop is variable but this does not seem to have any relevance towards its function (Palm & de Lange, 2008).

Each time a cell replicates, they make a copy of the genome, ensuring that each daughter cell has one complete copy of the genome. The genomes of eukaryotes are organized in linear chromosomes and this poses a problem for DNA replication at chromosomes ends. This is referred to as the end-replication problem (Olovnikov, 1973; Watson, 1972). DNA polymerases synthesize DNA from the template only in the 5'-3' direction, so the lagging strand DNA must be synthesized in many small fragments called Okazaki fragments. DNA polymerase requires a 3'-OH group as a start for the addition of nucleotides, so during lagging strand synthesis they use a short RNA primer for each Okazaki fragment. These RNA primers are eventually removed, degraded and replaced by DNA. The last RNA primer of the lagging strand cannot be replaced by DNA polymerase after it is removed as there is no 3'-OH available. This results in the gradual shortening of chromosome ends with each cell division in the absence of any telomere extension mechanisms. An additional cause for progressive telomere shortening is exonucleolytic degradation which generates the 3' overhang (Huffman *et al*, 2000). This produces an overhang that results in a lack of template during the next leading strand synthesis (Lingner *et al*, 1995; Palm & de Lange, 2008). After every round of replication, there is loss at the ends of the chromosome, resulting in progressive shortening of the

chromosome. The presence of telomeres at the chromosome ends acts as a buffer so that no vital coding DNA is lost with this shortening, but instead the telomeres shorten with each cell division.

1.7.2 The Shelterin complex

The shelterin complex is a six-subunit protein complex that binds to the TTAGGG repeats found in mammalian telomeric DNA (de Lange, 2005; Liu *et al*, 2004a) (**Figure 1.4b**). Shelterin plays an important role not only protecting chromosome ends from being recognized as DNA breaks but also regulating telomerase-mediated telomere length maintenance as well as alternative lengthening of telomeres (ALT) (de Lange, 2005; Palm & de Lange, 2008). The components of the shelterin complex are as follows: TRF1 (telomeric repeat binding factor 1), TRF2 (telomeric repeat binding factor 2), POT1 (protection of telomeres 1), TIN2 (TRF2- and TRF1-Interacting Nuclear protein 2), RAP1 (human ortholog of the yeast Repressor/Activator Protein 1), and TPP1 (formerly known as TINT1/PTOP/PIP1) (Palm & de Lange, 2008). The whole shelterin complex is localized to the telomeres via TRF1, TRF2 and POT1, which each bind to telomeric DNA repeats.

TRF1 and TRF2 both bind to double-stranded telomeric DNA. They share a common domain structure consisting of the TRF homology (TRFH) domain and a C-terminal SANT/Myb DNA-binding domain (Broccoli *et al*, 1997; Chong *et al*, 1995). They differ in their N-termini, where TRF1 contains an acidic domain and TRF2 contains a basic domain. TRF1 and TRF2 each homodimerize through their respective TRFH

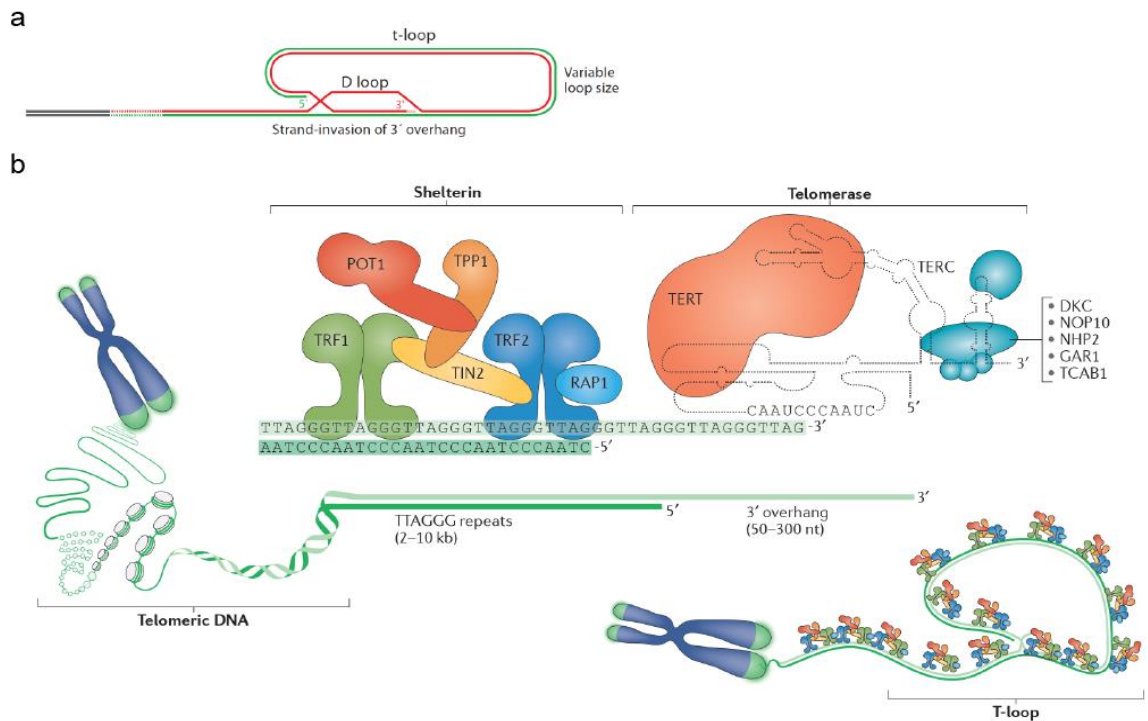


Figure 1.4. Structure and composition of human telomeres. (a) The higher order t-loop and D-loop structure of telomeres described further in text. Reproduced from (Palm & de Lange, 2008). (b) Human telomeres are made of up three components: telomeric DNA, the shelterin complex and the telomerase complex. Reproduced from (Maciejowski & de Lange, 2017) with permission from Nature Publishing Group (Licence: 4147361431463).

domain and bind DNA as homodimers (Bianchi *et al*, 1997; Court *et al*, 2005; Fairall *et al*, 2001; Hanaoka & Nagadoi, 2005; Nishikawa *et al*, 2001). TRF1 and TRF2 can act as architectural factors, changing the higher-order structure of telomeric DNA. The two Myb domains of a TRF1 dimer can bind at a distance or on two different molecules and in different orientations (Bianchi *et al*, 1999; Griffith *et al*, 1998). TRF1 is found to form loops and pair stretches of telomeric DNA whereas TRF2 can promote T-loop formation when provided with the appropriate telomeric substrate (Griffith *et al*, 1999; Stansel *et al*, 2001). The TRFH domain also contains a peptide docking site through which TRF1 and

TRF2 recruit other proteins to telomeres. The motif F/YxLxP on target proteins is critical for the recognition by the TRFH domain (Chen *et al*, 2008c). Although TRF1 and TRF2 share a highly homologous TRFH domain, they cannot form heterodimers and recognize different target proteins (Palm & de Lange, 2008; Chen *et al*, 2008c). Both TRF1 and TRF2 undergo various post-translational modification (Walker & Zhu, 2012), which in turn regulate their telomeric DNA binding activity, cellular localization and stability.

Overexpression of TRF1 leads to telomere shortening, while depletion of TRF1 results in telomerase-mediated telomere elongation (Ancelin *et al*, 2002; McKerlie & Zhu, 2011; McKerlie *et al*, 2013; Smogorzewska *et al*, 2000; van Steensel & de Lange, 1997). These findings suggest that TRF1 acts as a negative regulator of telomerase-dependent telomere length maintenance. TRF2 is best known for its role in telomere protection which is dependent upon the ATM- and p53-mediated DNA damage response (Ancelin *et al*, 2002; Karlseder *et al*, 1999; van Steensel & de Lange, 1997; Zhu *et al*, 2000). Loss of TRF2 or overexpression of a TRF2 mutant that cannot be recruited to telomeres promotes telomere end-to-end fusions which is dependent upon non-homologous end-joining (NHEJ) (Celli & de Lange, 2005; Van Steensel *et al*, 1998; Smogorzewska *et al*, 2002). Overexpression of TRF2 lacking the N-terminal basic domain results in telomere loss that is dependent on homologous recombination (Wang *et al*, 2004). These findings reveal that TRF2 functions to protect telomere ends from being recognized as DNA double strand breaks.

RAP1 is an important but poorly understood component of the shelterin complex. RAP1 binds TRF2 and is dependent on TRF2 for its localization to the telomeres as

RAP1 lacks DNA-binding activity (Li *et al*, 2000a; Li & de Lange, 2003). TIN2 is found in the center of the shelterin complex and can bind TRF1, TRF2 and TPP1, serving as a bridge to bring the different shelterin components together (Kim *et al*, 1999b, 2004; Ye *et al*, 2004a). TIN2 recruits TPP1 and POT1 to the shelterin complex. TPP1 connects POT1 with TIN2 which is thought to be the main pathway to recruit POT1 to telomeres (Hockemeyer *et al*, 2007; Liu *et al*, 2004b; Ye *et al*, 2004b). POT1 contains two OB folds that recognize and bind to single-stranded telomeric DNA (Baumann & Cech, 2001; Lei *et al*, 2004; Loayza *et al*, 2004). The binding of POT1 to the single-stranded telomeric DNA promotes the protection of the telomere ends from nucleolytic degradation (Hockemeyer *et al*, 2005; Lei *et al*, 2004; Yang *et al*, 2005).

1.7.3 Telomere lengthening and Telomerase

Telomerase is a ribonucleoprotein composed of two components, a RNA component called hTR or hTERC in humans and a reverse transcriptase protein component called hTERT in humans (**Figure 1.4b**) (Feng *et al*, 1995; Greider & Blackburn, 1989; Lingner *et al*, 1997; Nakamura *et al*, 1997; Shippen-Lentz & Blackburn, 1990). Telomerase is active in cells with extended proliferative potential such as germ cells or committed progenitor cells. Telomerase synthesizes one strand of the telomeric DNA by using its RNA component as a template to extend the 3' G-rich overhang (Greider & Blackburn, 1989; Shippen-Lentz & Blackburn, 1990; Kelleher *et al*, 2002; Autexier & Lue, 2006). Synthesis of the complementary C-strand occurs through lagging strand synthesis by DNA polymerase α and the CST (CTC1-STN1-TEN1) complex (Dai *et al*, 2010; Huang

et al, 2012; Kasbek *et al*, 2013; Miyake *et al*, 2009; Surovtseva *et al*, 2009; Wang *et al*, 2012; Wu *et al*, 2012). The addition of telomeric DNA by telomerase helps with the end-replication problem and nuclease action (Wellinger *et al*, 1996) and helps prevent the chromosome ends from being recognized as DNA damage (Fagagna *et al*, 2003; Takai *et al*, 2003; Zou *et al*, 2004).

The average telomere length of telomerase-positive cells is kept within a narrow, species-specific range (Lejnine *et al*, 1995), indicating that telomere length maintenance is highly regulated. The maintenance of telomere length is a balancing act between telomerase and proteins that bind telomeric DNA (Chan & Blackburn, 2004; Marcand *et al*, 1997). Components of the shelterin complex are found to regulate the access of telomerase to the ends of the telomere both positively and negatively. TPP1 interacts with the hTERT subunit and recruits it to the telomeres during S phase when replication occurs (Abreu *et al*, 2010; Latrick & Cech, 2010; Nandakumar *et al*, 2012; Wang *et al*, 2007b; Zhong *et al*, 2012). On the other hand, TRF1 along with TIN2 restricts telomerase access to the ends of telomeres, resulting in an inhibition of telomerase-dependent telomere elongation (Ancelin *et al*, 2002; Broccoli *et al*, 1997; de Lange, 2005; Loayza & de Lange, 2003; Okamoto *et al*, 2008; Smogorzewska *et al*, 2000; Takai *et al*, 2010; van Steensel & de Lange, 1997). Telomere length and the abundance of telomere bound shelterin complexes may work as a feedback loop in preventing excessive elongation of the telomeres. The ‘protein counting model’ has been proposed to explain this observation, suggesting that the more TRF1 and POT1 are bound to telomeres, the

stronger telomerase-mediated telomere elongation is inhibited (Loayza & de Lange, 2003; Marcand *et al*, 1997; van Steensel & de Lange, 1997).

1.7.4 Telomere chromatin structure

Similar to the rest of the genome, mammalian telomeres are organized in nucleosomal chromatin (Pisano *et al*, 2008; Tommerup *et al*, 1994). Long telomeres are organized into closely spaced nucleosomal arrays where the nucleosomes are separated by DNA linkers about 40 bp shorter than in bulk DNA (Fajkus *et al*, 1995; Lejnine *et al*, 1995; Makarov *et al*, 1993; Tommerup *et al*, 1994). Short telomeres are organized into an unusual chromatin structure as evidenced by a more diffuse micrococcal nuclease (MNase) digestion pattern than that of long telomeres (Tommerup *et al*, 1994). Intrinsic features such as DNA flexibility and stiffness can influence the wrapping of DNA around the histone octamer (Anselmi *et al*, 2000; Filesi *et al*, 2000). It has been suggested that telomeric DNAs may require more energy than genomic DNA to wind around the histone octamer (Fajkus *et al*, 1995; Pisano *et al*, 2008). In agreement with this, *in vitro* reconstitution studies show that telomeric DNAs form the least stable nucleosomes compared to all DNA sequences studied so far (Cacchione *et al*, 1997; Filesi *et al*, 2000; Rossetti *et al*, 1998). Components of the shelterin complex are reported to affect telomere nucleosome structure. TRF1 can promote the sliding of the nucleosome toward adjacent sequences (Pisano *et al*, 2010), while TRF2 can induce compaction of an *in vitro* assembled nucleosome array (Baker *et al*, 2011). When ATP-dependent chromatin remodelers are added, TRF2 causes an increase in telomeric nucleosomal spacing (Galati

et al, 2006). The differing roles of TRF1 and TRF2 are due to the differences in their N-termini (Poulet *et al*, 2012).

Histone post-translational modifications play a key role in influencing most cellular processes. Different modifications have been found associated with telomeric regions, and various factors influence the organization of telomeric chromatin. Telomere chromatin is generally considered to be “heterochromatic,” based on studies conducted in yeast and *Drosophila* telomeres. These studies have shown that establishment of a heterochromatic state at the telomere and subtelomere is essential for the protection of chromosome ends (Shore, 2001; Raffa *et al*, 2011). Yeast Rap1 recruits the Sir complex to telomeres, which is essential for the formation of a heterochromatic state that spreads to the subtelomere region, repressing genes next to the telomere (Ottaviani *et al*, 2008). *Drosophila* telomeres are enriched in trimethylation of lysine 9 of histone H3 (H3K9me3), which is recognized by heterochromatin protein 1 (HP1) (Fanti *et al*, 1998). HP1 is an essential factor for the protection of *Drosophila* telomeres and for the spreading of heterochromatin (Schotta *et al*, 2002).

In mouse cells, chromatin immunoprecipitation (ChIP) analysis reveals that both telomeres and subtelomeres are enriched in heterochromatic marks including H3K9me3 and H4K20me3, and hypoacetylation of H3 and H4 (Blasco, 2007). The epigenetic state of telomeres is regulated by telomere length. In telomerase deficient mice with short telomeres, levels of H3K9me3 and H4K20me3 are decreased whereas levels of H3 and H4 acetylation are increased (Benetti *et al*, 2007). These findings suggest that as telomeres shorten, there is a loss of heterochromatic marks leading to a more open

chromatin state. Establishment of a heterochromatic region is important for the structural integrity of mouse telomeres as deletion of HMTases result in telomere instability and altered telomere length (García-Cao *et al*, 2003; Blasco *et al*, 2005; Gonzalo *et al*, 2006).

The epigenetic state of telomeres in human cells is less clear. ChIP analysis suggest that the levels of heterochromatic marks such as H3K9me3, H4K20me3, and H3K27me3 are low at telomeres in human fibroblasts (O’Sullivan *et al*, 2010). In another study, H3K9me3 was underrepresented at telomeres but enriched at subtelomeres (Rosenfeld *et al*, 2009). A genome-wide analysis of several different human cell lines reveals that H3K9me3 is enriched at telomeric DNA as well as other repetitive sequences (Ernst *et al*, 2011). Evidence for the establishment of a heterochromatin state at telomeres in humans comes from studies analyzing the effect of SIRT6 depletion. SIRT6 is a NAD⁺-dependent histone deacetylase that specifically removes acetyl residues from H3K9 (Michishita *et al*, 2008) and H3K56 (Michishita *et al*, 2009). SIRT6 associates with telomeres in S-phase where it deacetylates histone H3. Depletion of SIRT6 leads to hyperacetylation of H3K9 and H3K56, telomere fusions and premature senescence (Michishita *et al*, 2008). These data suggest that heterochromatic marks such as histone hypoacetylation are important for the integrity of telomeres in human cells.

1.7.5 Telomere transcription

Although telomeric DNA does not contain any genes and telomere chromatin is enriched in heterochromatic histone marks, the telomeres are transcribed into telomeric repeat-containing RNA (TERRA) (Azzalin *et al*, 2007). This large non-coding RNA forms an

integral component of telomeric heterochromatin (Luke & Lingner, 2009; Blasco & Schoeftner, 2008). TERRA is transcribed in the centromere to telomere direction, indicating that the transcriptional start site lies in the subtelomeric region (Luke & Lingner, 2009; Nergadze *et al*, 2009). TERRA is transcribed primarily by RNA polymerase II (RNAPII) and transcripts range in length from approximately 0.1 to 9 kb (Azzalin *et al*, 2007; Blasco & Schoeftner, 2008). TERRA expression is cell-cycle regulated, peaking at the G1-S transition and declines from S phase to G2 in telomerase positive cells. This may be to avoid collision between RNAPII-mediated transcription and replication forks during S-phase (Flynn *et al*, 2015).

In vitro studies indicate that TERRA can directly inhibit telomerase as evidenced by the fact that a TERRA-mimicking RNA oligonucleotides can inhibit telomerase activity (Blasco & Schoeftner, 2008). *In vivo* studies in yeast suggest that a stable RNA/DNA hybrid forms between TERRA and telomeric DNA, which inhibits the access of telomerase to the chromosome end (Blasco & Schoeftner, 2008). In human cells, TERRA levels are decreased when telomeres are elongated (Arnoult *et al*, 2012). Although TERRA can inhibit telomerase activity *in vitro*, in human cells the overexpression of TERRA does not prevent telomerase-mediated telomere elongation (Farnung *et al*, 2012).

TERRA levels are regulated either transcriptionally at TERRA's subtelomeric CpG-rich promoter (Blasco & Schoeftner, 2008; Episkopou *et al*, 2014; Ng *et al*, 2009; Yehezkel *et al*, 2008), post-transcriptionally by regulating the stability of nontelomere-associated TERRA in the nucleoplasm (Deng *et al*, 2012) or TERRA RNA:DNA hybrids.

During transcription, RNA molecules can anneal to their genomic template during or after transcription to generate RNA:DNA hybrids. Strand displacement by the RNA:DNA hybrids forms a special structure called a R-loop (Costantino & Koshland, 2015).

TERRA can form R-loops at the telomeres, which may act as a barrier to the progression of the replication fork (Rippe & Luke, 2015). In telomerase-expressing cells, TERRA transcription is decreased in S-phase, which is thought to minimize the interference with the replication fork. The major enzyme involved in the resolution of RNA:DNA hybrids is the RNA endonuclease H (RNase H), which degrades the RNA component of the hybrid (Arudchandran *et al*, 2000). RNase H is reported to resolve TERRA R-loops in human ALT (Alternative Lengthening of Telomeres) cells, however RNase H does not function in telomerase-positive cells (Arora *et al*, 2014). This may be due to the fact that TERRA levels and TERRA R-loops are higher in ALT cells compared to telomerase-positive cells (Arora *et al*, 2014; Azzalin *et al*, 2007; Blasco & Schoeftner, 2008; Lovejoy *et al*, 2012; Episkopou *et al*, 2014).

TERRA plays an important role in regulating telomere maintenance. When TERRA transcript levels are reduced using short interfering RNA (siRNA) against TERRA, the telomeres become unstable (Deng *et al.*, 2009). TERRA localizes at telomeres and interacts with both TRF1 and TRF2. Knockdown of TRF1 results in a decrease in TERRA levels, while knockdown of TRF2 results in an increase in TERRA levels (Blasco & Schoeftner, 2008; Caslini *et al*, 2009). TERRA promotes the interaction between TRF2 and ORC1 that is important for the association of H3K9me3 and heterochromatin protein 1 (HP1) with telomeres (Deng *et al*, 2009). In human cells, there

is an inverse correlation between H3K9me3 density at telomere chromatin and TERRA levels (Arnoult *et al*, 2012; Episkopou *et al*, 2014). TERRA has also been reported to interact with the methyltransferase responsible for this mark, SUV39H1, as well as with the heterochromatin proteins HP1 α and HP1 β (Deng *et al*, 2009). These findings suggest that TERRA may be part of a negative feedback loop mechanism (Arnoult *et al*, 2012). At telomeres of normal length, TERRA inhibits its own expression by SUV39H1-mediated H3K9me3 at telomeres, decreasing further transcription. These results suggest that an initial round of transcription is necessary to prevent further TERRA transcription (Rippe & Luke, 2015).

1.7.6 Telomeres and aging

In most somatic cells, telomerase is absent. Therefore, telomeres will shorten after every round of replication. When telomeres reach a critically short length, they cannot maintain proper structure and their ends become unprotected (Ju & Rudolph, 2008). Senescence is usually activated once the telomere length reaches 2-3 kb (Britt-Compton *et al*, 2006). Once the chromosomes are no longer protected, they activate the DNA damage response which induces permanent cell cycle arrest called senescence or apoptosis (cell death) (Ju & Rudolph, 2008; Harley *et al*, 1990). This shortening of telomeres has led to the idea that telomeres function as a ‘molecular clock,’ meaning that the length of the telomeres determines the proliferative ability of a cell (Mitteldorf, 2013). This limit on uncontrolled proliferation imposed by telomere shortening is thought to function as a tumor suppressor mechanism.

Shortening of telomeres has been associated with human aging (Von Zglinicki & Martin-Ruiz, 2005), and a correlation is seen between long telomere length and increased life expectancy (Cawthon *et al*, 2003). Several premature aging disorders such as dyskeratosis congenita (DKC) (Mitchell *et al*, 1999), ataxia telangiectasia (AT) (Metcalf *et al*, 1996), Hutchinson-Gilford progeria (HG) (Benson *et al*, 2010; Cao *et al*, 2011) and Werner syndrome (WS) (Crabbe *et al*, 2004) have been shown to display an accelerated rate of telomere shortening and an increase in telomere instability. Telomere dysfunction is considered to be an underlying cause of premature aging (Kong *et al*, 2013). Therefore, it is of essence to understand the mechanism by which telomeres are maintained.

1.8 DNA Double-strand Break (DSB) Repair

1.8.1 Overview of the DNA damage response

DNA damage can result from endogenous sources such as reactive oxygen species or by-products of cellular metabolism, or from exogenous sources such as ultraviolet (UV) light, ionizing radiation (IR) or mutagenic chemicals and toxins. These agents cause various DNA lesions including mismatched bases, 8-oxoG lesions, pyrimidine dimers, single-strand breaks and double-strand breaks. DNA double-strand breaks (DSBs) are one of the most cytotoxic forms of DNA damage. The two main pathways that repair DNA DSBs in mammalian cells are non-homologous end-joining (NHEJ) and homologous recombination (HR) (**Figure 1.5**). Each of these pathways will be discussed

in a greater detail below. If these breaks are not quickly and accurately repaired, they can lead to genomic instability, hallmarks of cancer and aging.

The DNA damage response (DDR) is a signal transduction pathway that senses DNA damage and initiates a tightly controlled response to protect the cell and repair the damage. The DDR is mediated primarily by proteins of the phosphatidylinositol 3-kinase-like protein kinase (PIKKs) family: ATM (ataxia telangiectasia mutated protein), ATR (ATM and Rad-3 related protein) and DNA-PKcs (DNA-dependent protein kinase catalytic subunit). This family of kinases shows a strong preference for phosphorylating serine or threonine followed by a glutamine (S/T-Q) (Kim *et al*, 1999a). ATM is a main kinase that responds to DSBs whereas ATR responds to ssDNA generated during DSB repair or following replication fork collapse.

ATM interacts with the MRN (Mre11/Rad50/Nbs1) complex, which is one of the first protein complexes recruited to DSBs. MRN can tether the two ends of the DSB and prepare them for DNA repair (De Jager *et al*, 2001). MRN recruits ATM to the DSB site (Carson *et al*, 2003; Falck *et al*, 2005; Lee & Paull, 2004, 2005; Uziel *et al*, 2003). While ATM is later displaced from the break site, it remains associated with the chromatin flanking the DSB (Berkovich *et al*, 2007). ATM autophosphorylates itself on serine 1981 (S1981), leading to the dissociation from its inactive dimeric form to an active monomeric form (Bakkenist & Kastan, 2003). When ATM is in its active monomeric form it phosphorylates many different substrates that are important for DNA repair, checkpoint activation and cell cycle arrest (Bakkenist & Kastan, 2003; Lee & Paull, 2004, 2005; Matsuoka *et al*, 2007). MRN promotes the efficiency of ATM activation, as full

activation of ATM requires the presence of the MRN complex (Buscemi *et al*, 2001; Girard *et al*, 2002; Lim *et al*, 2000; Uziel *et al*, 2003; Yazdi *et al*, 2002; You *et al*, 2005)

One of the first phosphorylation events mediated by ATM is the phosphorylation of serine139 on the histone variant H2A.X, forming γ H2AX. This phosphorylation spreads away from the DSBs into megabase size domains (Rogakou *et al*, 1999). Once formed, γ H2AX then recruits MDC1 (mediator of DNA damage checkpoint protein 1), which recognizes the phosphorylated Ser139 on γ H2AX through its BRCT (breast cancer-associated protein 1 carboxy-terminal) domain (Stucki *et al*, 2005). MDC1 initiates DSB signaling by interacting with and recruiting the E3 ubiquitin ligase RNF8 (Huen *et al*, 2007; Kolas *et al*, 2007; Mailand *et al*, 2007). Once at DSBs, RNF8 along with its partner E2 enzyme UBC13 ubiquitylates γ H2AX and H2A (Huen *et al*, 2007; Mailand *et al*, 2007; Wang & Elledge, 2007). This promotes the recruitment of the E3 ubiquitin ligase RNF168 which furthers ubiquitylates γ H2AX and H2A lysine 13 and 15 (H2AK13/15). The ubiquitylated chromatin then serves as a platform for downstream factors crucial for downstream signaling and repair (Jackson & Durocher, 2013; Panier & Durocher, 2009).

The repair protein 53BP1 is recruited to damaged chromatin downstream of RNF168 activity (Doil *et al*, 2009; Stewart *et al*, 2009). 53BP1 is a bivalent chromatin reader that binds demethylated H4 Lys20 (H4K20me2) and ubiquitylated H2A Lys13/15 via its tandem Tudor and ubiquitination-dependent recruitment (UDR) domains (Botuyan *et al*, 2006; Fradet-Turcotte *et al*, 2013; Zgheib *et al*, 2009). Access of 53BP1 to

H4K20me2 is impaired by the acetylation of histone H4 Lys16 (H4K16) which is mediated by the acetyltransferase TIP60 (Hsiao & Mizzen, 2013; Tang *et al.*, 2013). TIP60 also acetylates H2AK15 that inhibits ubiquitylation and 53BP1 recruitment (Jacquet *et al.*, 2016).

Ubiquitylation of H2A by RNF8 and RNF168 also provides a platform for RAP80 which binds directly to Lys63 polyubiquitylation at DSBs (Hu *et al.*, 2012; Kim *et al.*, 2007a; Sobhian *et al.*, 2007; Wang *et al.*, 2007a; Yan *et al.*, 2007). RAP80 recruits its associated proteins including Abraxas which binds to BRCA1 (Feng *et al.*, 2009; Shao *et al.*, 2009; Wang *et al.*, 2007a). BRCA1 is recruited to IR-induced DSBs in a RAP80 dependent manner (Hu *et al.*, 2011; Kim *et al.*, 2007b). Analysis of BRCA1 recruitment to enzymatically generated DSBs reveals that RAP80 is responsible for the recruitment of BRCA1 to the chromatin flanking DSBs, while the MRN complex recruits BRCA1 close to the DSB (Goldstein & Kastan, 2015). These results suggest that two distinct fractions of BRCA1 are present at damaged chromatin.

1.8.2 Homologous recombination (HR)

Homologous recombination (**Figure 1.5a**) occurs during S or G2 phase of the cell cycle when the sister chromatid is in close proximity (Moynahan & Jasin, 2010; San Filippo *et al.*, 2008). A key step in the initiation of HR is 5' to 3' end resection of the break to generate 3' single-stranded DNA (ssDNA). The initial phase of resection is performed by the MRN complex along with CtIP (CtBP-interacting protein), processing about 20 bp from the DSB (Huertas & Jackson, 2009; Limbo *et al.*, 2007; Truong *et al.*, 2013). In the

second phase of end resection, the helicase BLM and exonucleases EXO1 and DNA2 generate long stretches of ssDNA, committing the cells to HR (Bolderson *et al*, 2010; Nimonkar *et al*, 2011; Sartori *et al*, 2007; Sun *et al*, 2012).

Once ssDNA is generated, replication protein A (RPA) binds to the ssDNA overhangs, which acts as a sensor of the accumulation of ssDNA and prevents the formation of secondary structures (Alani *et al*, 1992; Egger *et al*, 2002; Sugiyama *et al*,

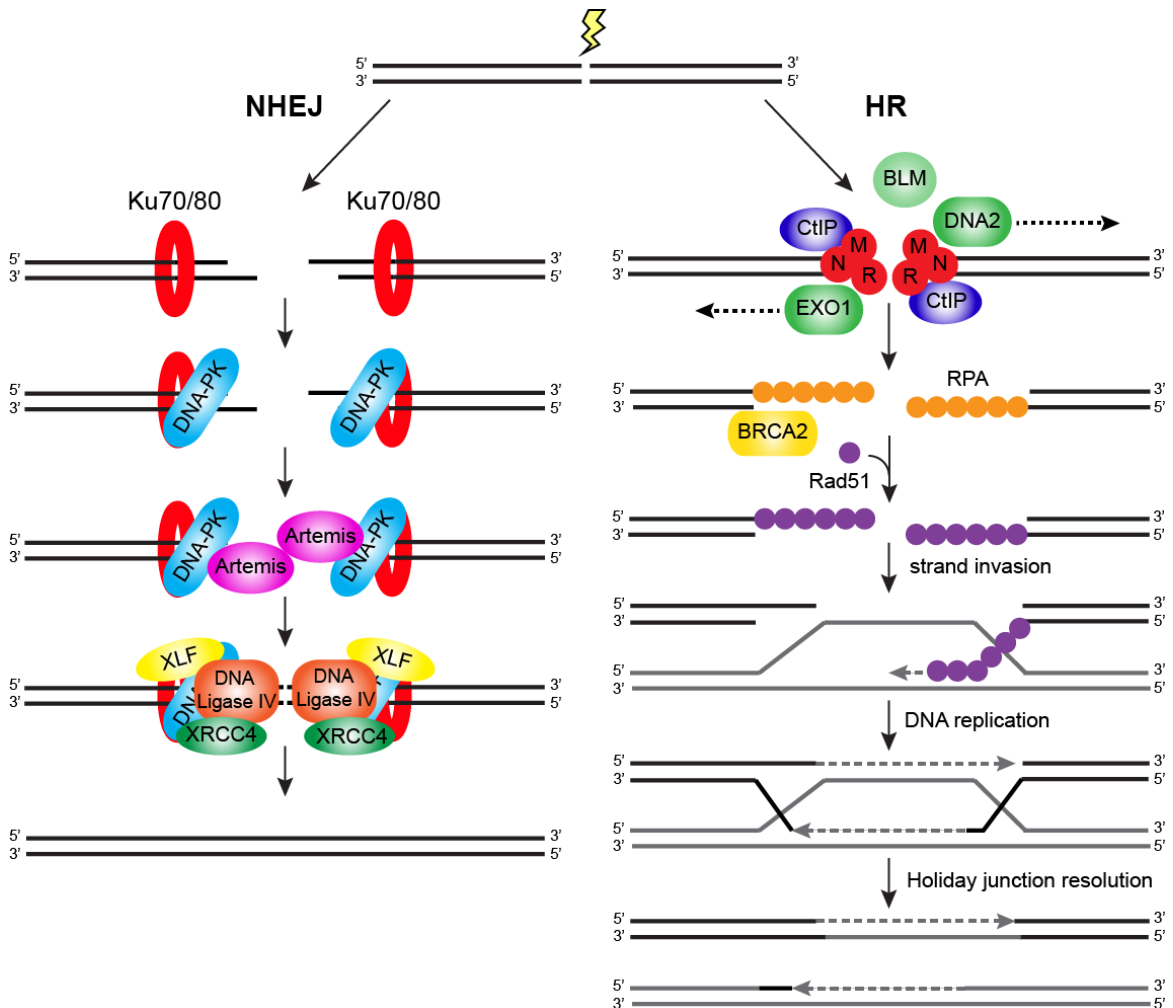


Figure 1.5. Double strand break repair pathways – Non-homologous end-joining (NHEJ) and homologous recombination (HR). The two main DSB repair pathways NHEJ and HR are described further within the text.

1997). RPA is then replaced with the RAD51 recombinase by the mediator protein BRCA2. Filament formation of RAD51 along the resected ssDNA mediates the search for a distant homologous sequence and subsequent strand invasion between the resected end of the break and the duplex homologous donor sequence (Renkawitz *et al*, 2013; Shinohara *et al*, 1992; Shinohara & Ogawa, 1998; Sugawara *et al*, 2003). This leads to the formation of a D-loop joint molecule composed of ssDNA and the target duplex. Using the homologous sequence as a template, synthesis occurs to replace the nucleotides lost due to resection through either Pol δ or Pol ϵ (Li *et al*, 2009; Prindle & Loeb, 2012; Sebesta *et al*, 2011). In DSB repair, the other end of the break is captured by the displaced strand of the donor duplex which is used to prime a second round of DNA synthesis, leading to the formation of a double Holiday junction (dHJ). The dHJ is cleaved and resolved by helicase and resolvase activity, and the ends are ligated to complete repair (Liu, 2004; Mimitou & Symington, 2009; Singh *et al*, 2008; Wu & Hickson, 2003; Xu *et al*, 2008; Cejka *et al*, 2010).

1.8.3 Non-homologous end joining (NHEJ)

NHEJ (**Figure 1.5b**), a second major pathway for the repair of DSBs, functions throughout the interphase and does not require a homologous template for repair (Moore & Haber, 1996; Sonoda *et al*, 2006). In NHEJ, DNA DSBs are rapidly bound by the Ku heterodimer (Ku70 and Ku80), which has a ring structure allowing itself to clamp onto the DSB ends (Cary *et al*, 1997; Falzon *et al*, 1993; Mahaney *et al*, 2009; Walker *et al*, 2001). Ku localizes to the DSB within seconds and independently of other NHEJ factors,

suggesting that it is an early sensor of DSBs (Kim *et al*, 2005; Mari *et al*, 2006). Ku interacts with DNA-PKcs and recruits it to DSBs where DNA-PKcs is activated (DeFazio *et al*, 2002; Gottlieb & Jackson, 1993; Uematsu *et al*, 2007). The DNA-PKcs-Ku complex serves to tether the ends of the DSBs and protect the ends from nuclease attack. Autophosphorylation of DNA-PKcs results in the destabilization of the DNA-PKcs interaction with the DNA ends (Chan & Lees-Miller, 1996; Merkle *et al*, 2002), paving the way for other NHEJ proteins.

The nature of DSBs induced by IR is complex and end processing may be required to prepare them for ligation. If processing occurs, there is potential for loss of nucleotides, making NHEJ an error-prone process. Indeed, NHEJ occurs with loss of sequence from DNA ends which is regulated in part by DNA-PKcs (Budman & Chu, 2005; Cui *et al*, 2005; Ding *et al*, 2003). Artemis, an end processing enzyme, is a 5' to 3' endonuclease that interacts with DNA-PKcs (Ma *et al*, 2002; Soubeyrand *et al*, 2006). The autophosphorylation and displacement of DNA-PKcs from the DSB is required for the activation of Artemis as it regulates the access of Artemis to its DNA substrate (Goodarzi *et al*, 2006; Yannone *et al*, 2008). Processing of the DNA ends can lead to DNA gaps which are filled by polymerase μ and λ , which interact with and are recruited by Ku through their N-terminal BRCT domains (Bertocci *et al*, 2006; Ma *et al*, 2004; Mahajan *et al*, 2002). Once the DNA ends have been processed and gaps have been filled in, they must be ligated to complete repair. Ligation is carried out by DNA ligase IV, which is in complex with XRCC4. XRCC4 interacts with DNA Ligase IV and stimulates its activity (Grawunder *et al*, 1997, 1998). XLF is also recruited to the DSB by Ku, is

stabilized at the break by interacting with the XRCC4-DNA ligase IV complex (Yano *et al*, 2008), and stimulates the activity of DNA ligase IV (Ahnesorg *et al*, 2006; Gu *et al*, 2007; Li *et al*, 2008; Lu *et al*, 2007; Tsai *et al*, 2007).

1.8.4 Regulation in DNA DSB repair pathway choice

When confronted with a DSB, the cell must commit to either NHEJ or HR to repair the break. This is commonly referred to as DNA DSB repair pathway choice, which is highly regulated. A key determinant of DSB repair pathway choice is DNA end resection, which is controlled in a cell cycle-dependent manner. In S/G2 phase, CDK-dependent phosphorylation of CtIP and EXO1 promote end resection (Bennardo *et al*, 2008; Tomimatsu *et al*, 2014; Yun & Hiom, 2009). In addition, ATM also promotes end resection by phosphorylating HR components including BRCA1 (Li *et al*, 2000b), CtIP, EXO1 and BLM (Peterson *et al*, 2013; Wang *et al*, 2013). On the other hand, in G1 phase, CDK activity is low and resection of DSBs is greatly reduced, thereby favoring NHEJ over HR (Aylon *et al*, 2004; Grzegorz *et al*, 2004).

The commitment to DNA end resection is controlled by two opposing proteins, 53BP1 and BRCA1. In G1 phase, 53BP1 promotes NHEJ by inhibiting DNA resection. This requires the ATM-mediated phosphorylation of the 53BP1 N-terminal region which promotes the recruitment of its effectors RIF1 and PTIP (Callen *et al*, 2013; Escribano-Díaz *et al*, 2013; Feng *et al*, 2013; Zimmermann *et al*, 2013). Both RIF1 and PTIP are independently involved in blocking DNA end resection (Callen *et al*, 2013; Chapman *et al*, 2013; Escribano-Díaz *et al*, 2013; Wang *et al*, 2014). In G1 phase, RIF1 inhibits the

recruitment of BRCA1 to DSBs, as in RIF1 depleted G1 cells, BRCA1 is recruited to DSBs (Escribano-Díaz *et al*, 2013). In addition, RIF1 has been reported to recruit the protein REV7 which inhibits DNA end resection (Boersma *et al*, 2015; Xu *et al*, 2015).

In S and G2 phase, CDK-mediated phosphorylation of CtIP promotes initiation of resection in S-phase by formation of a CtIP/MRN/BRCA1 complex that triggers the removal of 53BP1/RIF1, relieving the inhibition of end resection (Chen *et al*, 2008b; Escribano-Díaz *et al*, 2013; Sartori *et al*, 2007; Wang *et al*, 2013). In BRCA1 depleted S and G2 phase cells, RIF1 is recruited to DSBs and resection inhibited. As a result, in S phase, NHEJ occurs at replication-associated DSBs, leading to chromosome rearrangements. Deletion of 53BP1 in BRCA1 deficient cells prevents chromosome rearrangements, demonstrating the importance of BRCA1-dependent inhibition of 53BP1 to enable the transition from NHEJ to HR (Bouwman *et al*, 2010; Bunting *et al*, 2010, 2012; Cao *et al*, 2009). Therefore, correct choice in DSB repair pathway is essential to the maintenance of genome integrity.

1.8.6 Chromatin remodeling and DSB repair

Chromatin structure plays a key role in regulating DSB repair and signaling. The compaction of chromatin influences cellular sensitivity to DSBs and the efficiency of the DDR (Murga *et al*, 2007). Breaks that occur in heterochromatin are repaired slower than those that occur in euchromatin (Goodarzi *et al*, 2008, 2011). Similar to NER and BER, DSB repair also requires the function of several ATP-dependent chromatin remodeling complexes to promote efficient repair.

Several chromatin remodeling complexes including the SWI/SNF, INO80, CHD and ISWI complexes are reported to be recruited to DSBs, regulating the activation of the DDR and recruitment of DSB repair factors (Jeggo & Downs, 2014; Lans *et al*, 2012). Depletion of and of these remodelers is reported to lead to cellular sensitivity to DSBs.

Complete nucleosome disassembly has been reported at an HO-induced DSB in budding yeast (Tsukuda *et al*, 2005). Upon induction of the DSB, histone loss is seen up to several kilobases flanking the break site (Chen *et al*, 2008a; Osley *et al*, 2007). The yeast INO80 ATP-dependent nucleosome remodeler promotes nucleosome eviction surrounding a DSB and is required for efficient end processing (Chen *et al*, 2008a; Morrison *et al*, 2004; Van Attikum *et al*, 2004). In addition INO80, SWR-C, NuA4, SWI-SNF and RSC are recruited to DSBs in asynchronous yeast cells (Bennett *et al*, 2013). During G1 phase, recruitment of these remodelers is inhibited by the Ku70/80 complex, while in G2 phase, their recruitment is promoted and is dependent upon the early stages of end resection (Bennett *et al*, 2013). These enzymes also promote the recruitment of RPA and Rad51 to DSBs (Chen *et al*, 2012; Costelloe *et al*, 2012; Gospodinov *et al*, 2011; Toiber *et al*, 2013).

Chromatin disassembly also occurs in mammalian cells during DSB repair. ChIP studies show that histones H2A/B, H3 and H4 are displaced from chromatin surrounding a DSB induced by the homing nuclease I-PpoI in mammalian cells (Berkovich *et al*, 2007; Goldstein *et al*, 2013; Li & Tyler, 2016). This displacement can be seen over 7kb away from the break site (Goldstein *et al*, 2013), and is dependent upon ATM and NBS1 (Berkovich *et al*, 2007). As in yeast, in mammalian cells the remodeler INO80 is

important for HR and regulates remodeling at DSBs (Gospodinov *et al*, 2011; Li & Tyler, 2016; Wu *et al*, 2007). The level of nucleosome disruption is also affected by cell cycle (Goldstein *et al*, 2013). In G1 arrested cells, H2A/B is displaced from chromatin surrounding a DSB. In cycling cells, H3 and H4 are displaced in addition to H2A/H2B. These results show that NHEJ involves only partial disruption, while complete nucleosome disruption occurs during S/G2 phase and is associated with end resection and HR (Goldstein *et al*, 2013). On the other hand, a separate study suggests that NHEJ can also be associated with complete disassembly of nucleosomes (Li & Tyler, 2016). The location of DSBs differ in these two studies. Perhaps the chromatin context of the break may influence the disassembly of nucleosomes at breaks.

1.9 Rationale and Objectives

Cockayne syndrome is a complex disease which displays several different phenotypes and affects multiple systems within the body. CS has been well described as a premature aging syndrome, however the cause of CS is still not well understood. As described in this chapter, many premature aging syndromes have been associated with defects in telomere maintenance, however there has been no report of telomere defects in CS. This link between premature aging and telomere defects suggests that CS patients may also have telomere defects and that the CSB protein may play a role in telomere maintenance. This hypothesis forms the basis of the experiments described in Chapter 2.

CSB-deficient cells known to be sensitive to DNA damage induced by UV radiation and agents that induce oxidative damage. In addition, CSB-deficient cells are

also sensitive to ionizing radiation (IR) (Leadon & Cooper, 1993; Tuo *et al*, 2002b, 2003), camptothecin (CPT) (Squires *et al*, 2012) and etoposide (Elli *et al*, 1996), all of which are known to induce DNA DSBs. These findings suggest that CSB may play a role in DSB repair. This hypothesis forms the basis of the work described in Chapter 3 and 4.

Proper maintenance of telomeres and genome integrity is essential for cell survival and proliferation. Disruption of telomere maintenance and DNA DSB repair can lead to cancer and aging. This thesis provides invaluable knowledge on the role of CSB in telomere maintenance and DSB repair.

1.10 References

- Aamann MD, Hvitby C, Popuri V, Muftuoglu M, Lemming L, Skeby CK, Keijzers G, Ahn B, Bjørås M, Bohr VA & Stevensner T (2014) Cockayne Syndrome group B protein stimulates NEIL2 DNA glycosylase activity. *Mech. Ageing Dev.* **135**: 1–14
- Aamann MD, Muftuoglu M, Bohr VA & Stevensner T (2013) Multiple interaction partners for Cockayne syndrome proteins: Implications for genome and transcriptome maintenance. *Mech. Ageing Dev.* **134**: 212–224
- Abreu E, Aritonovska E, Reichenbach P, Cristofari G, Culp B, Terns RM, Lingner J & Terns MP (2010) TIN2-Tethered TPP1 Recruits Human Telomerase to Telomeres In Vivo. *Mol. Cell. Biol.* **30**: 2971–2982
- Ahnesorg P, Smith P & Jackson SP (2006) XLF interacts with the XRCC4-DNA Ligase IV complex to promote DNA nonhomologous end-joining. *Cell* **124**: 301–313
- Alani E, Thresher R, Griffith JD & Kolodner RD (1992) Characterization of DNA-binding and strand-exchange stimulation properties of γ -RPA, a yeast single-strand-DNA-binding protein. *J. Mol. Biol.* **227**: 54–71
- Amouroux R, Campalans A, Epe B & Radicella JP (2010) Oxidative stress triggers the preferential assembly of base excision repair complexes on open chromatin regions. *Nucleic Acids Res.* **38**: 2878–2890
- Ancelin K, Brunori M, Bauwens S, Koering C-E, Brun C, Ricoul M, Pommier J-P, Sabatier L & Gilson E (2002) Targeting Assay To Study the cis Functions of Human Telomeric Proteins: Evidence for Inhibition of Telomerase by TRF1 and for Activation of Telomere Degradation by TRF2. *Mol. Cell. Biol.* **22**: 3474–3487
- Anindya R, Aygün O & Svejstrup JQ (2007) Damage-Induced Ubiquitylation of Human RNA Polymerase II by the Ubiquitin Ligase Nedd4, but Not Cockayne Syndrome Proteins or BRCA1. *Mol. Cell* **28**: 386–397
- Anindya R, Mari PO, Kristensen U, Kool H, Giglia-Mari G, Mullenders LH, Fousteri M, Vermeulen W, Egly JM & Svejstrup JQ (2010) A Ubiquitin-Binding Domain in Cockayne Syndrome B Required for Transcription-Coupled Nucleotide Excision Repair. *Mol. Cell* **38**: 637–648
- Anselmi C, Bocchinfuso G, Santis P De, Savino M & Scipioni A (2000) A theoretical model for the prediction of sequence-dependent nucleosome thermodynamic stability. *Biophys J* **79**: 601–613
- Araki M, Masutani C, Maekawa T, Watanabe Y, Yamada A, Kusumoto R, Sakai D, Sugawara K, Ohkuma Y & Hanaoka F (2000) Reconstitution of damage DNA excision reaction from SV40 minichromosomes with purified nucleotide excision repair proteins. *Mutat. Res. Repair* **459**: 147–160
- Araujo SJ, Nigg EA & Wood RD (2001) Strong Functional Interactions of TFIIH with XPC and XPG in Human DNA Nucleotide Excision Repair, without a Preassembled Repairosome. *Mol. Cell. Biol.* **21**: 2281–2291
- Arnoult N, Van Beneden A & Decottignies A (2012) Telomere length regulates TERRA levels through increased trimethylation of telomeric H3K9 and HP1 α . *Nat. Struct. Mol. Biol.* **19**: 948–956

- Arora R, Lee Y, Wischnewski H, Brun CM, Schwarz T & Azzalin CM (2014) RNaseH1 regulates TERRA-telomeric DNA hybrids and telomere maintenance in ALT tumour cells. *Nat. Commun.* **5**: 5220
- Arudchandran A, Cerritelli SM, Narimatsu SK, Itaya M, Shin DY, Shimada Y & Crouch RJ (2000) The absence of ribonuclease H1 or H2 alters the sensitivity of *Saccharomyces cerevisiae* to hydroxyurea, caffeine and ethyl methanesulphonate: Implications for roles of RNases H in DNA replication and repair. *Genes to Cells* **5**: 789–802
- Van Attikum H, Fritsch O, Hohn B & Gasser SM (2004) Recruitment of the INO80 complex by H2A phosphorylation links ATP-dependent chromatin remodeling with DNA double-strand break repair. *Cell* **119**: 777–788
- Autexier C & Lue NF (2006) The structure and function of telomerase reverse transcriptase. *Annu. Rev. Biochem.* **75**: 493–517
- Aylon Y, Liefshitz B & Kupiec M (2004) The CDK regulates repair of double-strand breaks by homologous recombination during the cell cycle. *EMBO J.* **23**: 4868–4875
- Azzalin CM, Reichenbach P, Khoriantz L, Giulotto E & Lingner J (2007) Telomeric repeat containing RNA and RNA surveillance factors at mammalian chromosome ends. *Science* **318**: 798–801
- Baker AM, Fu Q, Hayward W, Victoria S, Pedroso IM, Lindsay SM & Fletcher TM (2011) The telomere binding protein trf2 induces chromatin compaction. *PLoS One* **6**: e19124
- Bakkenist CJ & Kastan MB (2003) DNA damage activates ATM through intermolecular autophosphorylation and dimer dissociation. *Nature* **421**: 499–506
- Balaban RS, Nemoto S & Finkel T (2005) Mitochondria, oxidants, and aging. *Cell* **120**: 483–495
- Balajee a S, Proietti De Santis L, Brosh RM, Selzer R & Bohr V a (2000) Role of the ATPase domain of the Cockayne syndrome group B protein in UV induced apoptosis. *Oncogene* **19**: 477–89
- Balajee AS, May A, Dianov GL, Friedberg EC & Bohr VA (1997) Reduced RNA polymerase II transcription in intact and permeabilized Cockayne syndrome group B cells. *Proc. Natl. Acad. Sci. U. S. A.* **94**: 4306–11
- Baumann P & Cech TR (2001) Pot1, the putative telomere end-binding protein in fission yeast and humans. *Science* **292**: 1171–5
- Beard BC, Wilson SH & Smerdon MJ (2003) Suppressed catalytic activity of base excision repair enzymes on rotationally positioned uracil in nucleosomes. *Proc. Natl. Acad. Sci. U. S. A.* **100**: 7465–7470
- Beckerman R & Prives C (2010) Transcriptional regulation by p53. *Cold Spring Harb. Perspect. Biol.* **2**:
- Beerens N, Hoeijmakers JHJ, Kanaar R, Vermeulen W & Wyman C (2005) The CSB protein actively wraps DNA. *J. Biol. Chem.* **280**: 4722–4729
- Benetti R, Blasco MA, García-Cao M & Blasco M (2007) Telomere length regulates the epigenetic status of mammalian telomeres and subtelomeres. *Nat. Genet.* **39**: 243–50
- Bennardo N, Cheng A, Huang N & Stark JM (2008) Alternative-NHEJ is a

- mechanistically distinct pathway of mammalian chromosome break repair. *PLoS Genet.* **4**: e1000110
- Bennett G, Papamichos-Chronakis M & Peterson CL (2013) DNA repair choice defines a common pathway for recruitment of chromatin regulators. *Nat. Commun.* **4**: 1–10
- Benson EK, Lee SW & Aaronson S a (2010) Role of progerin-induced telomere dysfunction in HGPS premature cellular senescence. *J. Cell Sci.* **123**: 2605–2612
- Berkovich E, Monnat RJ & Kastan MB (2007) Roles of ATM and NBS1 in chromatin structure modulation and DNA double-strand break repair. *Nat. Cell Biol.* **9**: 683–690
- Berquist BR & Wilson DM (2009) Nucleic Acid Binding Activity of Human Cockayne Syndrome B Protein and Identification of Ca²⁺ as a Novel Metal Cofactor. *J. Mol. Biol.* **391**: 820–832
- Bertocci B, De Smet A, Weill JC & Reynaud CA (2006) Nonoverlapping Functions of DNA Polymerases Mu, Lambda, and Terminal Deoxynucleotidyltransferase during Immunoglobulin V(D)J Recombination In Vivo. *Immunity* **25**: 31–41
- Bianchi A, Smith S, Chong L, Elias P & De Lange T (1997) TRF1 is a dimer and bends telomeric DNA. *EMBO J.* **16**: 1785–1794
- Bianchi A, Stansel RM, Fairall L, Griffith JD, Rhodes D & De Lange T (1999) TRF1 binds a bipartite telomeric site with extreme spatial flexibility. *EMBO J.* **18**: 5735–5744
- Blasco MA (2007) The epigenetic regulation of mammalian telomeres. *Nat Rev Genet* **8**: 299–309
- Blasco MA, Gonzalo S, García-Cao M, Fraga MF, Schotta G, Peters AHFM, Cotter SE, Eguía R, Dean DC, Esteller M, Jenuwein T & Blasco M (2005) Role of the RB1 family in stabilizing histone methylation at constitutive heterochromatin. *Nat. Cell Biol.* **7**: 420–8
- Blasco M & Schoeftner S (2008) Developmentally regulated transcription of mammalian telomeres by DNA-dependent RNA polymerase II. *Nat. Cell Biol.* **10**: 228–36
- Boersma V, Moatti N, Segura-Bayona S, Peuscher MH, van der Torre J, Wevers B a, Orthwein A, Durocher D & Jacobs JLL (2015) MAD2L2 controls DNA repair at telomeres and DNA breaks by inhibiting 5' end resection. *Nature* **521**: 537–40
- Bohr VA, Smith CA, Okumoto DS & Hanawalt PC (1985) DNA repair in an active gene: Removal of pyrimidine dimers from the DHFR gene of CHO cells is much more efficient than in the genome overall. *Cell* **40**: 359–369
- Bolderson E, Tomimatsu N, Richard DJ, Boucher D, Kumar R, Pandita TK, Burma S & Khanna KK (2010) Phosphorylation of Exo1 modulates homologous recombination repair of DNA double-strand breaks. *Nucleic Acids Res.* **38**: 1821–1831
- Van Den Boom V, Citterio E, Hoogstraten D, Zotter A, Egly JM, Van Cappellen WA, Hoeijmakers JHJ, Houtsmuller AB & Vermeulen W (2004) DNA damage stabilizes interaction of CSB with the transcription elongation machinery. *J. Cell Biol.* **166**: 27–36
- Botuyan MV, Lee J, Ward IM, Kim JE, Thompson JR, Chen J & Mer G (2006) Structural Basis for the Methylation State-Specific Recognition of Histone H4-K20 by 53BP1

- and Crb2 in DNA Repair. *Cell* **127**: 1361–1373
- Bouwman P, Aly A, Escandell JM, Pieterse M, Bartkova J, van der Gulden H, Hiddingh S, Thanasoula M, Kulkarni A, Yang Q, Haffty BG, Tommiska J, Blomqvist C, Drapkin R, Adams DJ, Nevanlinna H, Bartek J, Tarsounas M, Ganesan S & Jonkers J (2010) 53BP1 loss rescues BRCA1 deficiency and is associated with triple-negative and BRCA-mutated breast cancers. *Nat. Struct. Mol. Biol.* **17**: 688–695
- Bradsher J, Auriol J, De Santis LP, Iben S, Vonesch JL, Grummt I & Egly JM (2002) CSB is a component of RNA pol I transcription. *Mol. Cell* **10**: 819–829
- Bregman DB, Halaban R, van Gool AJ, Henning KA, Friedberg EC & Warren SL (1996) UV-induced ubiquitination of RNA polymerase II: a novel modification deficient in Cockayne syndrome cells. *Proc. Natl. Acad. Sci. U. S. A.* **93**: 11586–90
- Britt-Compton B, Rowson J, Locke M, Mackenzie I, Kipling D & Baird DM (2006) Structural stability and chromosome-specific telomere length is governed by cis-acting determinants in humans. *Hum. Mol. Genet.* **15**: 725–733
- Broccoli D, Smogorzewska A, Chong L & de Lange T (1997) Human telomeres contain two distinct Myb-related proteins, TRF1 and TRF2. *Nat. Genet.* **17**: 231–5
- Brosh RM, Balajee S, Selzer RR, Sunesen M, Proietti De Santis L & Bohr V a (1999) The ATPase domain but not the acidic region of Cockayne syndrome group B gene product is essential for DNA repair. *Mol. Biol. Cell* **10**: 3583–94
- Budman J & Chu G (2005) Processing of DNA for nonhomologous end-joining by cell-free extract. *EMBO J.* **24**: 849–860
- Bunting SF, Callén E, Kozak ML, Kim JM, Wong N, López-Contreras AJ, Ludwig T, Baer R, Faryabi RB, Malhowski A, Chen HT, Fernandez-Capetillo O, D’Andrea A & Nussenzweig A (2012) BRCA1 Functions Independently of Homologous Recombination in DNA Interstrand Crosslink Repair. *Mol. Cell* **46**: 125–135
- Bunting SF, Callén E, Wong N, Chen HT, Polato F, Gunn A, Bothmer A, Feldhahn N, Fernandez-Capetillo O, Cao L, Xu X, Deng CX, Finkel T, Nussenzweig M, Stark JM & Nussenzweig A (2010) 53BP1 inhibits homologous recombination in brca1-deficient cells by blocking resection of DNA breaks. *Cell* **141**: 243–254
- Buscemi G, Savio C, Zannini L, Miccichè F, Masnada D, Nakanishi M, Tauchi H, Komatsu K, Mizutani S, Khanna K, Chen P, Concannon P, Chessa L & Delia D (2001) Chk2 activation dependence on Nbs1 after DNA damage. *Mol. Cell. Biol.* **21**: 5214–5222
- Cacchione S, Cerone MA & Savino M (1997) In vitro low propensity to form nucleosomes of four telomeric sequences. *FEBS Lett.* **400**: 37–41
- Caldecott KW, McKeown CK, Tucker JD, Ljungquist S & Thompson LH (1994) An interaction between the mammalian DNA repair protein XRCC1 and DNA ligase III. *Mol. Cell. Biol.* **14**: 68–76
- Callen E, Di Virgilio M, Kruhlak MJ, Nieto-Soler M, Wong N, Chen HT, Faryabi RB, Polato F, Santos M, Starnes LM, Wesemann DR, Lee JE, Tubbs A, Sleckman BP, Daniel JA, Ge K, Alt FW, Fernandez-Capetillo O, Nussenzweig MC & Nussenzweig A (2013) 53BP1 mediates productive and mutagenic DNA repair through distinct phosphoprotein interactions. *Cell* **153**: 1266–1280

- Camenisch U, Dip R, Schumacher SB, Schuler B & Naegeli H (2006) Recognition of helical kinks by xeroderma pigmentosum group A protein triggers DNA excision repair. *Nat. Struct. Mol. Biol.* **13**: 278–284
- Cao K, Blair CD, Faddah DA, Kieckhaefer JE, Olive M, Erdos MR, Nabel EG & Collins FS (2011) Progerin and telomere dysfunction collaborate to trigger cellular senescence in normal human fibroblasts. *J. Clin. Invest.* **121**: 2833–2844
- Cao L, Xu X, Bunting SF, Liu J, Wang RH, Cao LL, Wu JJ, Peng TN, Chen J, Nussenzweig A, Deng CX & Finkel T (2009) A Selective Requirement for 53BP1 in the Biological Response to Genomic Instability Induced by Brca1 Deficiency. *Mol. Cell* **35**: 534–541
- Carson CT, Schwartz RA, Stracker TH, Lilley CE, Lee D V. & Weitzman MD (2003) The Mre11 complex is required for ATM activation and the G₂ / M checkpoint. *EMBO J.* **22**: 6610–6620
- Cary RB, Peterson SR, Wang J, Bear DG, Bradbury EM & Chen DJ (1997) DNA looping by Ku and the DNA-dependent protein kinase. *Proc. Natl. Acad. Sci. U. S. A.* **94**: 4267–72
- Caslini C, Connelly J a, Serna A, Broccoli D & Hess JL (2009) MLL associates with telomeres and regulates telomeric repeat-containing RNA transcription. *Mol. Cell. Biol.* **29**: 4519–4526
- Cawthon RM, Smith KR, O'Brien E, Sivatchenko A & Kerber RA (2003) Association between telomere length in blood and mortality in people aged 60 years or older. *Lancet* **361**: 393–395
- Cejka P, Plank JL, Bachrati CZ, Hickson ID & Kowalczykowski SC (2010) Rmi1 stimulates decatenation of double Holliday junctions during dissolution by Sgs1–Top3. *Nat. Struct. Mol. Biol.* **17**: 1377–1382
- Celli GB & de Lange T (2005) DNA processing is not required for ATM-mediated telomere damage response after TRF2 deletion. *Nat. Cell Biol.* **7**: 712–8
- Chan DW & Lees-Miller SP (1996) The DNA-dependent protein kinase is inactivated by autophosphorylation of the catalytic subunit. *J. Biol. Chem.* **271**: 8936–8941
- Chan SRWL & Blackburn EH (2004) Telomeres and telomerase. *Philos. Trans. R. Soc. Lond. B. Biol. Sci.* **359**: 109–21
- Chapman JR, Barral P, Vannier JB, Borel V, Steger M, Tomas-Loba A, Sartori AA, Adams IR, Batista FD & Boulton SJ (2013) RIF1 Is Essential for 53BP1-Dependent Nonhomologous End Joining and Suppression of DNA Double-Strand Break Resection. *Mol. Cell* **49**: 858–871
- Chen CC, Carson JJ, Feser J, Tamburini B, Zabaronick S, Linger J & Tyler JK (2008a) Acetylated Lysine 56 on Histone H3 Drives Chromatin Assembly after Repair and Signals for the Completion of Repair. *Cell* **134**: 231–243
- Chen L, Nievera CJ, Lee AY-L & Wu X (2008b) Cell cycle-dependent complex formation of BRCA1.CtIP.MRN is important for DNA double-strand break repair. *J. Biol. Chem.* **283**: 7713–7720
- Chen X, Cui D, Papusha A, Zhang X, Chu C-D, Tang J, Chen K, Pan X & Ira G (2012) The Fun30 nucleosome remodeller promotes resection of DNA double-strand break

- ends. *Nature* **489**: 576–580
- Chen Y, Yang Y, van Overbeek M, Donigian JR, Baciú P, de Lange T & Lei M (2008c) A shared docking motif in TRF1 and TRF2 used for differential recruitment of telomeric proteins. *Science* **319**: 1092–6
- Cho I, Tsai PF, Lake RJ, Basheer A & Fan HY (2013) ATP-Dependent Chromatin Remodeling by Cockayne Syndrome Protein B and NAP1-Like Histone Chaperones Is Required for Efficient Transcription-Coupled DNA Repair. *PLoS Genet.* **9**: e1003407
- Chong L, van Steensel B, Broccoli D, Erdjument-Bromage H, Hanish J, Tempst P & de Lange T (1995) A human telomeric protein. *Science* **270**: 1663–7
- Christiansen M, Thorslund T, Jochimsen B, Bohr VA & Stevnsner T (2005) The Cockayne syndrome group B protein is a functional dimer. *FEBS J.* **272**: 4306–4314
- Citterio E, Van Den Boom V, Schnitzler G, Kanaar R, Bonte E, Kingston RE, Hoeijmakers JH & Vermeulen W (2000) ATP-dependent chromatin remodeling by the Cockayne syndrome B DNA repair-transcription-coupling factor. *Mol. Cell. Biol.* **20**: 7643–7653
- Citterio E, Rademakers S, van der Horst GT, van Gool a J, Hoeijmakers JH & Vermeulen W (1998) Biochemical and biological characterization of wild-type and ATPase-deficient Cockayne syndrome B repair protein. *J. Biol. Chem.* **273**: 11844–51
- Clapier CR & Cairns BR (2009) The Biology of Chromatin Remodeling Complexes. *Annu. Rev. Biochem.* **78**: 273–304
- Cockayne EA (1936) Dwarfism with retinal atrophy and deafness. *Arch. Dis. Child.* **11**: 1 LP-8
- Cole HA, Tabor-Godwin JM & Hayes JJ (2010) Uracil DNA glycosylase activity on nucleosomal DNA depends on rotational orientation of targets. *J. Biol. Chem.* **285**: 2876–2885
- Compe E & Egly J-M (2012) TFIIH: when transcription met DNA repair. *Nat. Rev. Mol. Cell Biol.* **13**: 476–476
- Costantino L & Koshland D (2015) The Yin and Yang of R-loop biology. *Curr. Opin. Cell Biol.* **34**: 39–45
- Costelloe T, Louge R, Tomimatsu N, Mukherjee B, Martini E, Khadaroo B, Dubois K, Wiegant WW, Thierry A, Burma S, van Attikum H & Llorente B (2012) The yeast Fun30 and human SMARCAD1 chromatin remodellers promote DNA end resection. *Nature* **489**: 581–584
- Court R, Chapman L, Fairall L & Rhodes D (2005) How the human telomeric proteins TRF1 and TRF2 recognize telomeric DNA: a view from high-resolution crystal structures. *EMBO Rep.* **6**: 39–45
- Crabbe L, Verdun RE, Haggblom CI & Karlseder J (2004) Defective telomere lagging strand synthesis in cells lacking WRN helicase activity. *Science* **306**: 1951–3
- Cui X, Yu Y, Gupta S, Cho YM, Lees-Miller SP & Meek K (2005) Autophosphorylation of DNA-dependent protein kinase regulates DNA end processing and may also alter double-strand break repair pathway choice. *Mol Cell Biol* **25**: 10842–10852

- Dai X, Huang C, Bhusari A, Sampathi S, Schubert K & Chai W (2010) Molecular steps of G-overhang generation at human telomeres and its function in chromosome end protection. *EMBO J.* **29**: 2788–2801
- Dantzer F, de La Rubia G, Ménissier-De Murcia J, Hostomsky Z, de Murcia G & Schreiber V (2000) Base excision repair is impaired in mammalian cells lacking Poly(ADP-ribose) polymerase-1. *Biochemistry* **39**: 7559–7569
- DeFazio LG, Stansel RM, Griffith JD & Chu G (2002) Synapsis of DNA ends by DNA-dependent protein kinase. *EMBO J.* **21**: 3192–3200
- Deng Z, Norseen J, Wiedmer A, Riethman H & Lieberman PM (2009) TERRA RNA Binding to TRF2 Facilitates Heterochromatin Formation and ORC Recruitment at Telomeres. *Mol. Cell* **35**: 403–413
- Deng Z, Wang Z, Stong N, Plasschaert R, Moczan A, Chen HS, Hu S, Wikramasinghe P, Davuluri R V, Bartolomei MS, Riethman H & Lieberman PM (2012) A role for CTCF and cohesin in subtelomere chromatin organization, TERRA transcription, and telomere end protection. *Embo J* **31**: 4165–4178
- Dianov G, Bischoff C, Sunesen M & Bohr VA (1999) Repair of 8-oxoguanine in DNA is deficient in Cockayne syndrome group B cells. *Nucleic Acids Res.* **27**: 1365–1368
- Ding Q, Reddy Y V, Wang W, Woods T, Douglas P, Ramsden DA, Lees-Miller SP & Meek K (2003) Autophosphorylation of the catalytic subunit of the DNA-dependent protein kinase is required for efficient end processing during DNA double-strand break repair. *Mol. Cell. Biol.* **23**: 5836–5848
- Dogliotti E, Fortini P, Pascucci B & Parlanti E (2001) The mechanism of switching among multiple BER pathways. *Prog. Nucleic Acid Res. Mol. Biol.* **68**: 3–27
- Doil C, Mailand N, Bekker-Jensen S, Menard P, Larsen DH, Pepperkok R, Ellenberg J, Panier S, Durocher D, Bartek J, Lukas J & Lukas C (2009) RNF168 Binds and Amplifies Ubiquitin Conjugates on Damaged Chromosomes to Allow Accumulation of Repair Proteins. *Cell* **136**: 435–446
- Dou H, Mitra S & Hazra TK (2003) Repair of Oxidized Bases in DNA Bubble Structures by Human DNA Glycosylases NEIL1 and NEIL2. *J. Biol. Chem.* **278**: 49679–49684
- Duan MR & Smerdon MJ (2010) UV damage in DNA promotes nucleosome unwrapping. *J. Biol. Chem.* **285**: 26295–26303
- Eggler AL, Inman RB & Cox MM (2002) The Rad51-dependent pairing of long DNA substrates is stabilized by replication protein A. *J. Biol. Chem.* **277**: 39280–39288
- El-Khamisy SF, Masutani M, Suzuki H & Caldecott KW (2003) A requirement for PARP-1 for the assembly or stability of XRCC1 nuclear foci at sites of oxidative DNA damage. *Nucleic Acids Res.* **31**: 5526–5533
- Elli R, Chessa L, Antonelli A, Petrinelli P, Ambra R & Marcucci L (1996) Effects of topoisomerase II inhibition in lymphoblasts from patients with progeroid and ‘chromosome instability’ syndromes. *Cancer Genet. Cytogenet.* **87**: 112–116
- Episkopou H, Draskovic I, Van Beneden A, Tilman G, Mattiussi M, Gobin M, Arnoult N, Londoño-Vallejo A & Decottignies A (2014) Alternative Lengthening of Telomeres is characterized by reduced compaction of telomeric chromatin. *Nucleic Acids Res.* **42**: 4391–4405

- Ernst J, Kheradpour P, Mikkelsen TS, Shores N, Ward LD, Epstein CB, Zhang X, Wang L, Issner R, Coyne M, Ku M, Durham T, Kellis M & Bernstein BE (2011) Mapping and analysis of chromatin state dynamics in nine human cell types. *Nature* **473**: 43–9
- Escribano-Díaz C, Orthwein A, Fradet-Turcotte A, Xing M, Young JTF, Tkáč J, Cook MA, Rosebrock AP, Munro M, Canny MD, Xu D & Durocher D (2013) A Cell Cycle-Dependent Regulatory Circuit Composed of 53BP1-RIF1 and BRCA1-CtIP Controls DNA Repair Pathway Choice. *Mol. Cell* **49**: 872–883
- Evans E, Fellows J, Coffey A & Wood RD (1997a) Open complex formation around a lesion during nucleotide excision repair provides a structure for cleavage by human XPG protein. *EMBO J.* **16**: 625–638
- Evans E, Moggs JG, Hwang JR, Egly JM & Wood RD (1997b) Mechanism of open complex and dual incision formation by human nucleotide excision repair factors. *EMBO J.* **16**: 6559–6573
- Fagagna F d'Adda di, Reaper PM, Clay-Farrace L, Fiegler H, Carr P, von Zglinicki T, Saretzki G, Carter NP & Jackson SP (2003) A DNA damage checkpoint response in telomere-initiated senescence. *Nature* **426**: 194–198
- Fagbemi AF, Orelli B & Schärer OD (2011) Regulation of endonuclease activity in human nucleotide excision repair. *DNA Repair (Amst)*. **10**: 722–729
- Fairall L, Chapman L, Moss H, De Lange T & Rhodes D (2001) Structure of the TRFH dimerization domain of the human telomeric proteins TRF1 and TRF2. *Mol. Cell* **8**: 351–361
- Fairman-Williams ME, Guenther UP & Jankowsky E (2010) SF1 and SF2 helicases: Family matters. *Curr. Opin. Struct. Biol.* **20**: 313–324
- Fajkus J, Kovařík A, mKrálovics R & Bezděk M (1995) Organization of telomeric and subtelomeric chromatin in the higher plant *Nicotiana tabacum*. *MGG Mol. Gen. Genet.* **247**: 633–638
- Falck J, Coates J & Jackson SP (2005) Conserved modes of recruitment of ATM, ATR and DNA-PKcs to sites of DNA damage. *Nature* **434**: 605–611
- Falzon M, Fewell JW & Kuff EL (1993) EBP-80, a transcription factor closely resembling the human autoantigen Ku, recognizes single- to double-strand transitions in DNA. *J. Biol. Chem.* **268**: 10546–10552
- Fan YH & Lake RJ (2013) Structure, function and regulation of CSB: A multi-talented gymnast. *Mech. Ageing Dev.* **134**: 202–211
- Fanti L, Giovinazzo G, Berloco M & Pimpinelli S (1998) The heterochromatin protein 1 prevents telomere fusions in *Drosophila*. *Mol Cell* **2**: 527–538
- Farnung BO, Brun CM, Arora R, Lorenzi LE & Azzalin CM (2012) Telomerase efficiently elongates highly transcribing telomeres in human cancer cells. *PLoS One* **7**: e35714
- Fei J & Chen J (2012) KIAA1530 protein is recruited by cockayne syndrome complementation group protein A (CSA) to participate in transcription-coupled repair (TCR). *J. Biol. Chem.* **287**: 35118–35126
- Feng J, Funk WD, Wang SS, Weinrich SL, Avilion AA, Chiu CP, Adams RR, Chang E, Allsopp RC, Yu J & al. et (1995) The RNA component of human telomerase.

- Science* **269**: 1236–41
- Feng L, Fong KW, Wang J, Wang W & Chen J (2013) RIF1 counteracts BRCA1-mediated end resection during DNA repair. *J. Biol. Chem.* **288**: 11135–11143
- Feng L, Huang T & Chen J (2009) MERIT40 facilitates BRCA1 localization and DNA damage repair. *Genes Dev.* **23**: 719–728
- Filesi I, Cacchione S, De Santis P, Rossetti L & Savino M (2000) The main role of the sequence-dependent DNA elasticity in determining the free energy of nucleosome formation on telomeric DNAs. *Biophys. Chem.* **83**: 223–237
- Filippi S, Latini P, Frontini M, Palitti F, Egly J-M & Proietti-De-Santis L (2008) CSB protein is (a direct target of HIF-1 and) a critical mediator of the hypoxic response. *EMBO J.* **27**: 2545–2556
- Flynn RL, Cox KE, Jeitany M, Wakimoto H, Bryll AR, Ganem NJ, Bersani F, Pineda JR, Suva ML, Benes CH, Haber DA, Boussin FD & Zou L (2015) Alternative lengthening of telomeres renders cancer cells hypersensitive to ATR inhibitors. *Science (80-.).* **347**: 273–277
- Fortini P, Pascucci B, Parlanti E, Sobol RW, Wilson SH & Dogliotti E (1998) Different DNA polymerases are involved in the short- and long-patch base excision repair in mammalian cells. *Biochemistry* **37**: 3575–3580
- Fousteri M, Vermeulen W, van Zeeland AA & Mullenders LHF (2006) Cockayne Syndrome A and B Proteins Differentially Regulate Recruitment of Chromatin Remodeling and Repair Factors to Stalled RNA Polymerase II In Vivo. *Mol. Cell* **23**: 471–482
- Fradet-Turcotte A, Canny MD, Escribano-Díaz C, Orthwein A, Leung CCY, Huang H, Landry M-C, Kitevski-LeBlanc J, Noordermeer SM, Sicheri F & Durocher D (2013) 53BP1 is a reader of the DNA-damage-induced H2A Lys 15 ubiquitin mark. *Nature* **499**: 50–54
- Frontini M & Proietti-De-Santis L (2012) Interaction between the Cockayne syndrome B and p53 proteins: Implications for aging. *Aging (Albany. NY).* **4**: 89–97
- Frouin I, Maga G, Denegri M, Riva F, Savio M, Spadari S, Prosperi E & Scovassi AI (2003) Human proliferating cell nuclear antigen, poly(ADP-ribose) polymerase-1, and p21waf1/cip1. A dynamic exchange of partners. *J. Biol. Chem.* **278**: 39265–39268
- Fuchs SY, Adler V, Buschmann T, Wu X & Ronai Z (1998) Mdm2 association with p53 targets its ubiquitination. *Oncogene* **17**: 2543–7
- Fukui H & Moraes CT (2008) The mitochondrial impairment, oxidative stress and neurodegeneration connection: reality or just an attractive hypothesis? *Trends Neurosci.* **31**: 251–256
- Galati A, Rossetti L, Pisano S, Chapman L, Rhodes D, Savino M & Cacchione S (2006) The Human Telomeric Protein TRF1 Specifically Recognizes Nucleosomal Binding Sites and Alters Nucleosome Structure. *J. Mol. Biol.* **360**: 377–385
- García-Cao M, O’Sullivan R, Peters AHFM, Jenuwein T & Blasco MA (2003) Epigenetic regulation of telomere length in mammalian cells by the Suv39h1 and Suv39h2 histone methyltransferases. *Nat. Genet.* **36**: 94–99

- Girard P-M, Riballo E, Begg AC, Waugh A & Jeggo P a (2002) Nbs1 promotes ATM dependent phosphorylation events including those required for G1/S arrest. *Oncogene* **21**: 4191–9
- Goldstein M, Derheimer FA, Tait-Mulder J & Kastan MB (2013) Nucleolin mediates nucleosome disruption critical for DNA double-strand break repair. *Proc. Natl. Acad. Sci.* **110**: 16874–16879
- Goldstein M & Kastan MB (2015) Repair versus checkpoint functions of BRCA1 are differentially regulated by site of chromatin binding. *Cancer Res.* **75**: 2699–2707
- Gong F, Kwon Y & Smerdon MJ (2005) Nucleotide excision repair in chromatin and the right of entry. *DNA Repair (Amst)*. **4**: 884–896
- Gonzalo S, Jaco I, Fraga MF, Chen T, Li E, Esteller M & Blasco MA (2006) DNA methyltransferases control telomere length and telomere recombination in mammalian cells. *Nat Cell Biol* **8**: 416–424
- Goodarzi AA, Kurka T & Jeggo PA (2011) KAP-1 phosphorylation regulates CHD3 nucleosome remodeling during the DNA double-strand break response. *Nat. Struct. Mol. Biol.* **18**: 831–839
- Goodarzi AA, Noon AT, Deckbar D, Ziv Y, Shiloh Y, Löbrich M & Jeggo PA (2008) ATM Signaling Facilitates Repair of DNA Double-Strand Breaks Associated with Heterochromatin. *Mol. Cell* **31**: 167–177
- Goodarzi AA, Yu Y, Riballo E, Douglas P, Walker SA, Ye R, Härer C, Marchetti C, Morrice N, Jeggo PA & Lees-Miller SP (2006) DNA-PK autophosphorylation facilitates Artemis endonuclease activity. *EMBO J.* **25**: 3880–3889
- van Gool AJ, Citterio E, Rademakers S, van Os R, Vermeulen W, Constantinou A, Egly JM, Bootsma D & Hoeijmakers JH (1997) The Cockayne syndrome B protein, involved in transcription- coupled DNA repair, resides in an RNA polymerase II-containing complex. *EMBO J.* **16**: 5955–5965
- Gospodinov A, Vaissiere T, Krastev DB, Legube G, Anachkova B & Herceg Z (2011) Mammalian Ino80 Mediates Double-Strand Break Repair through Its Role in DNA End Strand Resection. *Mol. Cell. Biol.* **31**: 4735–4745
- Gottlieb TM & Jackson SP (1993) The DNA-dependent protein kinase: Requirement for DNA ends and association with Ku antigen. *Cell* **72**: 131–142
- Grawunder U, Wilm M, Wu X, Kulesza P, Wilson TE, Mann M & Lieber MR (1997) Activity of DNA ligase IV stimulated by complex formation with XRCC4 protein in mammalian cells. *Nature* **388**: 492–5
- Grawunder U, Zimmer D & Lieber MR (1998) DNA ligase IV binds to XRCC4 via a motif located between rather than within its BRCT domains. *Curr. Biol.* **8**: 873–879
- Gredilla R (2010) DNA damage and base excision repair in mitochondria and their role in aging. *J. Aging Res.* **2011**: 257093
- Greider CW (1999) Telomeres do D-loop-T-loop. *Cell* **97**: 419–422
- Greider CW & Blackburn EH (1985) Identification of a specific telomere terminal transferase activity in tetrahymena extracts. *Cell* **43**: 405–413
- Greider CW & Blackburn EH (1989) A telomeric sequence in the RNA of Tetrahymena telomerase required for telomere repeat synthesis. *Nature* **337**: 331–337

- Griffith J, Bianchi A & de Lange T (1998) TRF1 promotes parallel pairing of telomeric tracts in vitro. *J. Mol. Biol.* **278**: 79–88
- Griffith JD, Comeau L, Rosenfield S, Stansel RM, Bianchi A, Moss H & De Lange T (1999) Mammalian telomeres end in a large duplex loop. *Cell* **97**: 503–514
- Groisman R, Kuraoka I, Chevallier O, Gaye N, Magnaldo T, Tanaka K, Kisselev AF, Harel-Bellan A & Nakatani Y (2006) CSA-dependent degradation of CSB by the ubiquitin-proteasome pathway establishes a link between complementation factors of the Cockayne syndrome. *Genes Dev.* **20**: 1429–1434
- Groisman R, Polanowska J, Kuraoka I, Sawada JI, Saijo M, Drapkin R, Kisselev AF, Tanaka K & Nakatani Y (2003) The ubiquitin ligase activity in the DDB2 and CSA complexes is differentially regulated by the COP9 signalosome in response to DNA damage. *Cell* **113**: 357–367
- Grzegorz I, Pellicoli A, Balijja A, Wang X, Fiorani S, Carotenuto W, Liberi G, Bressan D, Wan L, Hollingsworth NM, Haber JE & Foiani M (2004) DNA end resection, homologous recombination and DNA damage checkpoint activation require CDK1. *Nature* **431**: 1011–1017
- Gu J, Lu H, Tsai AG, Schwarz K & Lieber MR (2007) Single-stranded DNA ligation and XLF-stimulated incompatible DNA end ligation by the XRCC4-DNA ligase IV complex: Influence of terminal DNA sequence. *Nucleic Acids Res.* **35**: 5755–5762
- Hanaoka S, Nagadoi A & Nishimura Y (2005) Comparison between TRF2 and TRF1 of their telomeric DNA-bound structures and DNA-binding activities. *Protein Sci.* **14**: 119–130
- Hara R, Mo J & Sancar A (2000) DNA Damage in the Nucleosome Core Is Refractory to Repair by Human Excision Nuclease. *Mol. Cell. Biol.* **20**: 9173–9181
- Hara R & Sancar A (2002) The SWI/SNF Chromatin-Remodeling Factor Stimulates Repair by Human Excision Nuclease in the Mononucleosome Core Particle. *Mol. Cell. Biol.* **22**: 6779–6787
- Hara R & Sancar A (2003) Effect of damage type on stimulation of human excision nuclease by SWI/SNF chromatin remodeling factor. *Mol. Cell. Biol.* **23**: 4121–5
- Harley CB, Futcher AB & Greider CW (1990) Telomeres shorten during ageing of human fibroblasts. *Nature* **345**: 458–60
- Haupt Y, Maya R, Kazaz A & Oren M (1997) Mdm2 promotes the rapid degradation of p53. *Nature* **387**: 296–299
- Hegde ML, Hazra TK & Mitra S (2008) Early steps in the DNA base excision/single-strand interruption repair pathway in mammalian cells. *Cell Res.* **18**: 27–47
- Henning KA, Li L, Iyer N, McDaniel LD, Reagan MS, Legerski R, Schultz RA, Stefanini M, Lehmann AR, Mayne L V. & Friedberg EC (1995) The Cockayne syndrome group A gene encodes a WD repeat protein that interacts with CSB protein and a subunit of RNA polymerase II TFIIH. *Cell* **82**: 555–564
- Hinz JM, Rodriguez Y & Smerdon MJ (2010) Rotational dynamics of DNA on the nucleosome surface markedly impact accessibility to a DNA repair enzyme. *Proc. Natl. Acad. Sci.* **107**: 4646–4651
- Hockemeyer D, Palm W, Else T, Daniels J-P, Takai KK, Ye JZ-S, Keegan CE, de Lange

- T & Hammer GD (2007) Telomere protection by mammalian Pot1 requires interaction with Tpp1. *Nat. Struct. Mol. Biol.* **14**: 754–61
- Hockemeyer D, Sfeir AJ, Shay JW, Wright WE & de Lange T (2005) POT1 protects telomeres from a transient DNA damage response and determines how human chromosomes end. *EMBO J.* **24**: 2667–78
- Van Hoffen A, Natarajan AT, Mayne L V., Zeeland AA van, Mullenders LHF & Venema J (1993) Deficient repair of the transcribed strand of active genes in cockayne's syndrome cells. *Nucleic Acids Res.* **21**: 5890–5895
- Honda R, Tanaka H & Yasuda H (1997) Oncoprotein MDM2 is a ubiquitin ligase E3 for tumor suppressor p53. *FEBS Lett.* **420**: 25–27
- Van der Horst GTJ, Van Steeg H, Berg RJW, Van Gool AJ, De Wit J, Weeda G, Morreau H, Beems RB, Van Kreijl CF, De Gruijl FR, Bootsma D & Hoeijmakers JHJ (1997) Defective transcription-coupled repair in Cockayne syndrome B mice is associated with skin cancer predisposition. *Cell* **89**: 425–435
- Hsiao KY & Mizzen CA (2013) Histone H4 deacetylation facilitates 53BP1 DNA damage signaling and double-strand break repair. *J. Mol. Cell Biol.* **5**: 157–165
- Hu J, De Souza-Pinto NC, Haraguchi K, Hogue BA, Jaruga P, Greenberg MM, Dizdaroglu M & Bohr VA (2005) Repair of formamidopyrimidines in DNA involves different glycosylases: Role of the OGG1, NTH1, and NEIL1 enzymes. *J. Biol. Chem.* **280**: 40544–40551
- Hu X, Paul A & Wang B (2012) Rap80 protein recruitment to DNA double-strand breaks requires binding to both small ubiquitin-like modifier (SUMO) and ubiquitin conjugates. *J. Biol. Chem.* **287**: 25510–25519
- Hu Y, Scully R, Sobhian B, Xie A, Shestakova E & Livingston DM (2011) RAP80-directed tuning of BRCA1 homologous recombination function at ionizing radiation-induced nuclear foci. *Genes Dev.* **25**: 685–700
- Huang C, Dai X & Chai W (2012) Human Stn1 protects telomere integrity by promoting efficient lagging-strand synthesis at telomeres and mediating C-strand fill-in. *Cell Res.* **22**: 1681–1695
- Huang JC & Sancar A (1994) Determination of minimum substrate size for human excinuclease. *J. Biol. Chem.* **269**: 19034–19040
- Huen MSY, Grant R, Manke I, Minn K, Yu X, Yaffe MB & Chen J (2007) RNF8 Transduces the DNA-Damage Signal via Histone Ubiquitylation and Checkpoint Protein Assembly. *Cell* **131**: 901–914
- Huertas P & Jackson SP (2009) Human CtIP mediates cell cycle control of DNA end resection and double strand break repair. *J. Biol. Chem.* **284**: 9558–65
- Huffman KE, Levene SD, Tesmer VM, Shay JW & Wright WE (2000) Telomere shortening is proportional to the size of the G-rich telomeric 3'-overhang. *J. Biol. Chem.* **275**: 19719–19722
- Imam SZ, Indig FE, Cheng WH, Saxena SP, Stevnsner T, Kufe D & Bohr VA (2007) Cockayne syndrome protein B interacts with and is phosphorylated by c-Abl tyrosine kinase. *Nucleic Acids Res.* **35**: 4941–4951
- Jackson SP & Durocher D (2013) Regulation of DNA Damage Responses by Ubiquitin

- and SUMO. *Mol. Cell* **49**: 795–807
- Jacquet K, Fradet-Turcotte A, Avvakumov N, Lambert JP, Roques C, Pandita RK, Paquet E, Herst P, Gingras AC, Pandita TK, Legube G, Doyon Y, Durocher D & Côté J (2016) The TIP60 Complex Regulates Bivalent Chromatin Recognition by 53BP1 through Direct H4K20me Binding and H2AK15 Acetylation. *Mol. Cell* **62**: 409–421
- De Jager M, Van Noort J, Van Gent DC, Dekker C, Kanaar R & Wyman C (2001) Human Rad50/Mre11 is a flexible complex that can tether DNA ends. *Mol. Cell* **8**: 1129–1135
- Jeggo PA & Downs JA (2014) Roles of chromatin remodellers in DNA double strand break repair. *Exp. Cell Res.* **329**: 69–77
- Jiang Y, Wang X, Bao S, Guo R, Johnson DG, Shen X & Li L (2010) INO80 chromatin remodeling complex promotes the removal of UV lesions by the nucleotide excision repair pathway. *Proc. Natl. Acad. Sci. U. S. A.* **107**: 17274–17279
- Ju Z & Rudolph L (2008) Telomere dysfunction and stem cell ageing. *Biochimie* **90**: 24–32
- Karikkineth AC, Scheibye-Knudsen M, Fivenson E, Croteau DL & Bohr VA (2016) Cockayne syndrome: Clinical features, model systems and pathways. *Ageing Res. Rev.* **33**: 3–17
- Karlseder J, Broccoli D, Dai Y, Hardy S & de Lange T (1999) p53- and ATM-dependent apoptosis induced by telomeres lacking TRF2. *Science* **283**: 1321–1325
- Kasbek C, Wang F & Price CM (2013) Human TEN1 maintains telomere integrity and functions in genome-wide replication restart. *J. Biol. Chem.* **288**: 30139–30150
- Kelleher C, Teixeira MT, Förstemann K & Lingner J (2002) Telomerase: Biochemical considerations for enzyme and substrate. *Trends Biochem. Sci.* **27**: 572–579
- Khobta A & Epe B (2013) Repair of oxidatively generated DNA damage in Cockayne syndrome. *Mech. Ageing Dev.* **134**: 253–260
- Kim H, Chen J & Yu X (2007a) Ubiquitin-Binding Protein RAP80 Mediates BRCA1-Dependent DNA Damage Response. *Science (80-.)*. **316**: 1202–1205
- Kim H, Huang J & Chen J (2007b) CCDC98 is a BRCA1-BRCT domain-binding protein involved in the DNA damage response. *Nat. Struct. Mol. Biol.* **14**: 710–715
- Kim JS, Krasieva TB, Kurumizaka H, Chen DJ, Taylor AMR & Yokomori K (2005) Independent and sequential recruitment of NHEJ and HR factors to DNA damage sites in mammalian cells. *J. Cell Biol.* **170**: 341–347
- Kim K, Biade S & Matsumoto Y (1998) Involvement of flap endonuclease 1 in base excision DNA repair. *J. Biol. Chem.* **273**: 8842–8848
- Kim S, Lim D, Christine E, Kastan MB & Canman CE (1999a) Substrate Specificities and Identification of Putative Substrates of ATM Kinase Family Members Substrate Specificities and Identification of Putative Substrates of ATM Kinase Family Members. *J. Biol. Chem.* **274**: 37538–37543
- Kim SH, Beausejour C, Davalos AR, Kaminker P, Heo SJ & Campisi J (2004) TIN2 mediates functions of TRF2 at human telomeres. *J. Biol. Chem.* **279**: 43799–43804
- Kim SH, Kaminker P, Campisi J, Kim SH, Kaminker P & Campisi J (1999b) TIN2, a new regulator of telomere length in human cells. *Nat. Genet.* **23**: 405–412

- Kleijer WJ, Laugel V, Berneburg M, Nardo T, Fawcett H, Gratchev A, Jaspers NGJ, Sarasin A, Stefanini M & Lehmann AR (2008) Incidence of DNA repair deficiency disorders in western Europe: Xeroderma pigmentosum, Cockayne syndrome and trichothiodystrophy. *DNA Repair (Amst)*. **7**: 744–750
- Klungland A & Bjelland S (2007) Oxidative damage to purines in DNA: Role of mammalian Ogg1. *DNA Repair (Amst)*. **6**: 481–488
- Klungland A & Lindahl T (1997) Second pathway for completion of human DNA base excision-repair: Reconstitution with purified proteins and requirement for DNase IV (FEN1). *EMBO J*. **16**: 3341–3348
- Kolas NK, Chapman JR, Nakada S, Ylanko J, Chahwan R, Sweeney FD, Panier S, Mendez M, Wildenhain J, Thomson TM, Pelletier L, Jackson SP & Durocher D (2007) Orchestration of the DNA-Damage Response by the RNF8 Ubiquitin Ligase. *Science (80-.)*. **318**: 1637–1640
- Kong CM, Lee XW & Wang X (2013) Telomere shortening in human diseases. *FEBS J*. **280**: 3180–3193
- Kraemer KH, Lee MM, Andrews AD & Lambert WC (1994) The role of sunlight and DNA repair in melanoma and nonmelanoma skin cancer. The xeroderma pigmentosum paradigm. *Arch. Dermatol*. **130**: 1018–21
- Kraemer KH, Lee MM & Scotto J (1987) Xeroderma pigmentosum. Cutaneous, ocular, and neurologic abnormalities in 830 published cases. *Arch. Dermatol*. **123**: 241–50
- Kubbutat MHG, Jones SN & Vousden KH (1997) Regulation of p53 stability by Mdm2. *Nature* **387**: 299–303
- Kubota M, Ohta S, Ando A, Koyama A, Terashima H, Kashii H, Hoshino H, Sugita K & Hayashi M (2015) Nationwide survey of Cockayne syndrome in Japan: Incidence, clinical course and prognosis. *Pediatr. Int*. **57**: 339–47
- Kyng KJ, May A, Brosh RM, Cheng W-H, Chen C, Becker KG & Bohr V a (2003) The transcriptional response after oxidative stress is defective in Cockayne syndrome group B cells. *Oncogene* **22**: 1135–49
- De Laat WL, Appeldoorn E, Sugasawa K, Weterings E, Jaspers NGJ & Hoeijmakers JHJ (1998) DNA-binding polarity of human replication protein A positions nucleases in nucleotide excision repair. *Genes Dev*. **12**: 2598–2609
- Lake RJ, Basheer A & Fan HY (2011) Reciprocally regulated chromatin association of Cockayne syndrome protein B and p53 protein. *J. Biol. Chem*. **286**: 34951–34958
- Lake RJ, Geyko A, Hemashettar G, Zhao Y & Fan HY (2010) UV-Induced Association of the CSB Remodeling Protein with Chromatin Requires ATP-Dependent Relief of N-Terminal Autorepression. *Mol. Cell* **37**: 235–246
- Lan L, Ui A, Nakajima S, Hatakeyama K, Hoshi M, Watanabe R, Janicki SM, Ogiwara H, Kohno T, Kanno S ichiro & Yasui A (2010) The ACF1 Complex Is Required for DNA Double-Strand Break Repair in Human Cells. *Mol. Cell* **40**: 976–987
- de Lange T (2005) Shelterin: The protein complex that shapes and safeguards human telomeres. *Genes Dev*. **19**: 2100–2110
- de Lange T, Shiue L, Myers RM, Cox DR, Naylor SL, Killery a M & Varmus HE (1990) Structure and variability of human chromosome ends. *Mol. Cell. Biol*. **10**: 518–527

- Lans H, Marteiijn JA & Vermeulen W (2012) ATP-dependent chromatin remodeling in the DNA-damage response. *Epigenetics Chromatin* **5**:
- Laposa R, Huang E & Cleaver J (2007) Increased apoptosis, p53 up-regulation, and cerebellar neuronal degeneration in repair-deficient Cockayne syndrome mice. *Proc. Natl. Acad. Sci. U. S. A.* **104**: 1389–1394
- Latini P, Frontini M, Caputo M, Gregan J, Cipak L, Filippi S, Kumar V, Vélez-cruz R, Stefanini M, Palitti F & Proietti-de-santis L (2011) CSA and CSB proteins interact with p53 and regulate its Mdm2-dependent ubiquitination. *Cell Cycle* **10**: 3719–3730
- Lattrick CM & Cech TR (2010) POT1–TPP1 enhances telomerase processivity by slowing primer dissociation and aiding translocation. *EMBO J.* **29**: 924–933
- Leadon S a & Cooper PK (1993) Preferential repair of ionizing radiation-induced damage in the transcribed strand of an active human gene is defective in Cockayne syndrome. *Proc. Natl. Acad. Sci. U. S. A.* **90**: 10499–10503
- Lee J-H & Paull TT (2004) Direct activation of the ATM protein kinase by the Mre11/Rad50/Nbs1 complex. *Science* **304**: 93–96
- Lee J-H & Paull TT (2005) ATM Activation by DNA Double-Strand Breaks Through the Mre11-Rad50-Nbs1 Complex. *Science (80-.)*. **308**: 551–554
- Lee JY, Lake RJ, Kirk J, Bohr VA, Fan H-Y & Hohng S (2017) NAP1L1 accelerates activation and decreases pausing to enhance nucleosome remodeling by CSB. *Nucleic Acids Res.* **45**: 4696–4707
- Lehmann AR (2003) DNA repair-deficient diseases, xeroderma pigmentosum, Cockayne syndrome and trichothiodystrophy. *Biochimie* **85**: 1101–1111
- Lei M, Podell ER & Cech TR (2004) Structure of human POT1 bound to telomeric single-stranded DNA provides a model for chromosome end-protection. *Nat. Struct. Mol. Biol.* **11**: 1223–1229
- Lejnine S, Makarov VL & Langmore JP (1995) Conserved nucleoprotein structure at the ends of vertebrate and invertebrate chromosomes. *Proc. Natl. Acad. Sci. U. S. A.* **92**: 2393–7
- Leppard JB, Dong Z, Mackey ZB & Tomkinson AE (2003) Physical and functional interaction between DNA ligase IIIalpha and poly(ADP-Ribose) polymerase 1 in DNA single-strand break repair. *Mol. Cell. Biol.* **23**: 5919–5927
- Li B & de Lange T (2003) Rap1 affects the length and heterogeneity of human telomeres. *Mol. Biol. Cell* **14**: 5060–8
- Li B, Oestreich S & de Lange T (2000a) Identification of Human Rap1: Implications for Telomere Evolution. *Cell* **101**: 471–483
- Li S, Ting NS, Zheng L, Chen PL, Ziv Y, Shiloh Y, Lee EY & Lee WH (2000b) Functional link of BRCA1 and ataxia telangiectasia gene product in DNA damage response. *Nature* **406**: 210–215
- Li X, Stith CM, Burgers PM & Heyer WD (2009) PCNA Is Required for Initiation of Recombination-Associated DNA Synthesis by DNA Polymerase. *Mol. Cell* **36**: 704–713
- Li X & Tyler JK (2016) Nucleosome disassembly during human non-homologous end

- joining followed by concerted HIRA- and CAF-1-dependent reassembly. *Elife* **5**: 1–18
- Li Y, Chirgadze DY, Bolanos-Garcia VM, Sibanda BL, Davies OR, Ahnesorg P, Jackson SP & Blundell TL (2008) Crystal structure of human XLF/Cernunnos reveals unexpected differences from XRCC4 with implications for NHEJ. *EMBO J.* **27**: 290–300
- Lim D, Kim S, Xu B & Maser RS (2000) ATM phosphorylates p95/nbs1 in an S-phase checkpoint pathway. *Nature* **404**: 613–617
- Limbo O, Chahwan C, Yamada Y, de Bruin RAM, Wittenberg C & Russell P (2007) Ctp1 Is a Cell-Cycle-Regulated Protein that Functions with Mre11 Complex to Control Double-Strand Break Repair by Homologous Recombination. *Mol. Cell* **28**: 134–146
- Lingner J, Cooper JP & Cech TR (1995) Telomerase and DNA end replication: No longer a lagging strand problem? *Science* (80-.). **269**: 1533
- Lingner J, Hughes TR, Shevchenko A, Mann M, Lundblad V & Cech TR (1997) Reverse transcriptase motifs in the catalytic subunit of telomerase. *Science* **276**: 561–7
- Liu D, O'Connor MS, Qin J & Songyang Z (2004a) Telosome, a mammalian telomere-associated complex formed by multiple telomeric proteins. *J. Biol. Chem.* **279**: 51338–51342
- Liu D, Safari A, O'Connor MS, Chan DW, Laegerler A, Qin J & Songyang Z (2004b) POT1 interacts with POT1 and regulates its localization to telomeres. *Nat. Cell Biol.* **6**: 673–680
- Liu Y (2004) RAD51C Is Required for Holliday Junction Processing in Mammalian Cells. *Science* (80-.). **303**: 243–246
- Ljungman M & Zhang F (1996) Blockage of RNA polymerase as a possible trigger for u.v. light-induced apoptosis. *Oncogene* **13**: 823–31
- Loayza D & de Lange T (2003) POT1 as a terminal transducer of TRF1 telomere length control. *Nature* **423**: 1013–1018
- Loayza D, Parsons H, Donigian J, Hoke K & De Lange T (2004) DNA binding features of human POT1: A nonamer 5'-TAGGGTTAG-3' minimal binding site, sequence specificity, and internal binding to multimeric sites. *J. Biol. Chem.* **279**: 13241–13248
- Louis EJ & Vershinin A V. (2005) Chromosome ends: Different sequences may provide conserved functions. *BioEssays* **27**: 685–697
- Lovejoy CA, Li W, Reisenweber S, Thongthip S, Bruno J, de Lange T, De S, Petrini JHJ, Sung PA, Jasin M, Rosenbluh J, Zwang Y, Weir BA, Hatton C, Ivanova E, Macconail L, Hanna M, Hahn WC, Lue NF, Reddel RR, et al (2012) Loss of ATRX, genome instability, and an altered DNA damage response are hallmarks of the alternative lengthening of Telomeres pathway. *PLoS Genet.* **8**: e1002772
- Lu H, Pannicke U, Schwarz K & Lieber MR (2007) Length-dependent binding of human XLF to DNA and stimulation of XRCC4-DNA ligase IV activity. *J. Biol. Chem.* **282**: 11155–11162
- Luke B & Lingner J (2009) TERRA: telomeric repeat-containing RNA. *EMBO J.* **28**:

2503–2510

- Ma Y, Lu H, Tippin B, Goodman MF, Shimazaki N, Koiwai O, Hsieh CL, Schwarz K & Lieber MR (2004) A biochemically defined system for mammalian nonhomologous DNA end joining. *Mol. Cell* **16**: 701–713
- Ma Y, Pannicke U, Schwarz K & Lieber MR (2002) Hairpin opening and overhang processing by an Artemis/DNA-dependent protein kinase complex in nonhomologous end joining and V(D)J recombination. *Cell* **108**: 781–794
- Maciejowski J & de Lange T (2017) Telomeres in cancer: tumour suppression and genome instability. *Nat. Rev. Mol. Cell Biol.* **18**: 175–186
- Mahajan KN, Nick McElhinny S a, Mitchell BS & Ramsden DA (2002) Association of DNA polymerase μ (pol μ) with Ku and ligase IV: role for pol μ in end-joining double-strand break repair. *Mol. Cell. Biol.* **22**: 5194–202
- Mahaney BL, Meek K & Lees-Miller SP (2009) Repair of ionizing radiation-induced DNA double-strand breaks by non-homologous end-joining. *Biochem. J.* **417**: 639–50
- Mailand N, Bekker-Jensen S, Fastrup H, Melander F, Bartek J, Lukas C & Lukas J (2007) RNF8 Ubiquitylates Histones at DNA Double-Strand Breaks and Promotes Assembly of Repair Proteins. *Cell* **131**: 887–900
- Makarov VL, Hirose Y & Langmore JP (1997) Long G tails at both ends of human chromosomes suggest a C strand degradation mechanism for telomere shortening. *Cell* **88**: 657–666
- Makarov VL, Lejnine S, Bedoyan J & Langmore JP (1993) Nucleosomal organization of telomere-specific chromatin in rat. *Cell* **73**: 775–787
- Marcand S, Gilson E & Shore D (1997) A protein-counting mechanism for telomere length regulation in yeast. *Science* **275**: 986–990
- Mari P-O, Florea BI, Persengiev SP, Verkaik NS, Bruggenwirth HT, Modesti M, Gigliamari G, Bezstarosti K, Demmers JAA, Luider TM, Houtsmuller AB & van Gent DC (2006) Dynamic assembly of end-joining complexes requires interaction between Ku70/80 and XRCC4. *Proc. Natl. Acad. Sci.* **103**: 18597–18602
- Marteijn J a, Lans H, Vermeulen W & Hoeijmakers JHJ (2014) Understanding nucleotide excision repair and its roles in cancer and ageing. *Nat. Rev. Mol. Cell Biol.* **15**: 465–81
- Masson M, Niedergang C, Schreiber V, Muller S, Menissier-de Murcia J & de Murcia G (1998) XRCC1 is specifically associated with poly(ADP-ribose) polymerase and negatively regulates its activity following DNA damage. *Mol. Cell. Biol.* **18**: 3563–71
- Masutani C, Sugasawa K, Yanagisawa J, Sonoyama T, Ui M, Enomoto T, Takio K, Tanaka K, van der Spek PJ & Bootsma D (1994) Purification and cloning of a nucleotide excision repair complex involving the xeroderma pigmentosum group C protein and a human homologue of yeast RAD23. *EMBO J.* **13**: 1831–1843
- Matsumoto Y & Kim K (1995) Excision of deoxyribose phosphate residues by DNA polymerase beta during DNA repair. *Science* **269**: 699–702
- Matsuoka S, Ballif BA, Smogorzewska A, McDonald ER, Hurov KE, Luo J, Bakalarski

- CE, Zhao Z, Solimini N, Lerenthal Y, Shiloh Y, Gygi SP & Elledge SJ (2007) ATM and ATR Substrate Analysis Reveals Extensive Protein Networks Responsive to DNA Damage. *Science* (80-.). **316**: 1160–1166
- Mayne L & Lehmann A (1982) Failure of RNA Synthesis to Recover after UV Irradiation : An Early Defect in Cells from Individuals with Cockayne’s Syndrome and Xeroderma Pigmentosum Failure of RNA Synthesis to Recover after UV Irradiation : An Early Defect in Cells from Individuals. *Cancer Res.* **42**: 1473–1478
- McElligott R & Wellinger RJ (1997) The terminal DNA structure of mammalian chromosomes. *EMBO J.* **16**: 3705–3714
- McKerlie M, Walker JR, Mitchell TRH, Wilson FR & Zhu XD (2013) Phosphorylated (pT371)TRF1 is recruited to sites of DNA damage to facilitate homologous recombination and checkpoint activation. *Nucleic Acids Res.* **41**: 10268–10282
- McKerlie M & Zhu X-D (2011) Cyclin B-dependent kinase 1 regulates human TRF1 to modulate the resolution of sister telomeres. *Nat. Commun.* **2**: 371
- McStay B & Grummt I (2008) The Epigenetics of rRNA Genes: From Molecular to Chromosome Biology. *Annu. Rev. Cell Dev. Biol.* **24**: 131–157
- Mellon I, Bohr VA, Smith CA & Hanawalt PC (1986) Preferential DNA repair of an active gene in human cells. *Proc. Natl. Acad. Sci. U. S. A.* **83**: 8878–8882
- Menoni H, Gasparutto D, Hamiche A, Cadet J, Dimitrov S, Bouvet P & Angelov D (2007) ATP-Dependent Chromatin Remodeling Is Required for Base Excision Repair in Conventional but Not in Variant H2A.Bbd Nucleosomes. *Mol. Cell. Biol.* **27**: 5949–5956
- Menoni H, Hoeijmakers JHJ & Vermeulen W (2012a) Nucleotide excision repair-initiating proteins bind to oxidative DNA lesions in vivo. *J. Cell Biol.* **199**: 1037–1046
- Menoni H, Shukla MS, Gerson V, Dimitrov S & Angelov D (2012b) Base excision repair of 8-oxoG in dinucleosomes. *Nucleic Acids Res.* **40**: 692–700
- Merkle D, Douglas P, Moorhead GBG, Leonenko Z, Yu Y, Cramb D, Bazett-Jones DP & Lees-Miller SP (2002) The DNA-dependent protein kinase interacts with DNA to form a protein - DNA complex that is disrupted by phosphorylation. *Biochemistry* **41**: 12706–12714
- Metcalf JA, Parkhill J, Campbell L, Stacey M, Biggs P, Byrd PJ & Taylor AM (1996) Accelerated telomere shortening in ataxia telangiectasia. *Nat. Genet.* **13**: 350–3
- Meyne J, Ratliff RL & Moyzis RK (1989) Conservation of the human telomere sequence (TTAGGG)_n among vertebrates. *Proc. Natl. Acad. Sci. U. S. A.* **86**: 7049–53
- Michishita E, McCord RA, Berber E, Kioi M, Padilla-Nash H, Damian M, Cheung P, Kusumoto R, Kawahara TLA, Barrett JC, Chang HY, Bohr VA, Ried T, Gozani O & Chua KF (2008) SIRT6 is a histone H3 lysine 9 deacetylase that modulates telomeric chromatin. *Nature* **452**: 492–6
- Michishita E, McCord RA, Boxer LD, Barber MF, Hong T, Gozani O & Chua KF (2009) Cell cycle-dependent deacetylation of telomeric histone H3 lysine K56 by human SIRT6. *Cell Cycle* **8**: 2664–2666
- Mimitou EP & Symington LS (2009) Nucleases and helicases take center stage in

- homologous recombination. *Trends Biochem. Sci.* **34**: 264–272
- Mitchell JR, Wood E & Collins K (1999) A telomerase component is defective in the human disease dyskeratosis congenita. *Nature* **402**: 551–5
- Mitteldorf JJ (2013) Telomere biology: cancer firewall or aging clock? *Biochem.* **78**: 1054–1060
- Miyake Y, Nakamura M, Nabetani A, Shimamura S, Tamura M, Yonehara S, Saito M & Ishikawa F (2009) RPA-like Mammalian Ctc1-Stn1-Ten1 Complex Binds to Single-Stranded DNA and Protects Telomeres Independently of the Pot1 Pathway. *Mol. Cell* **36**: 193–206
- Moore JK & Haber JE (1996) Cell cycle and genetic requirements of two pathways of nonhomologous end-joining repair of double-strand breaks in *Saccharomyces cerevisiae*. *Mol Cell Biol* **16**: 2164–2173
- Morrison AJ, Highland J, Krogan NJ, Arbel-Eden A, Greenblatt JF, Haber JE & Shen X (2004) INO80 and gamma-H2AX interaction links ATP-dependent chromatin remodeling to DNA damage repair. *Cell* **119**: 767–775
- Moser J, Kool H, Giakzidis I, Caldecott K, Mullenders LHF & Foustari MI (2007) Sealing of Chromosomal DNA Nicks during Nucleotide Excision Repair Requires XRCC1 and DNA Ligase IIIa in a Cell-Cycle-Specific Manner. *Mol. Cell* **27**: 311–323
- Moynahan ME & Jasin M (2010) Mitotic homologous recombination maintains genomic stability and suppresses tumorigenesis. *Nat. Rev. Mol. Cell Biol.* **11**: 196–207
- Moyzis RK, Buckingham JM, Cram LS, Dani M, Deaven LL, Jones MD, Meyne J, Ratliff RL & Wu JR (1988) A highly conserved repetitive DNA sequence, (TTAGGG)_n, present at the telomeres of human chromosomes. *Proc. Natl. Acad. Sci. U. S. A.* **85**: 6622–6
- Muftuoglu M, Selzer R, Tuo J, Brosh RM & Bohr VA (2002) Phenotypic consequences of mutations in the conserved motifs of the putative helicase domain of the human Cockayne syndrome group B gene. *Gene* **283**: 27–40
- Muftuoglu M, Sharma S, Thorslund T, Stevnsner T, Soerensen MM, Brosh RM & Bohr VA (2006) Cockayne syndrome group B protein has novel strand annealing and exchange activities. *Nucleic Acids Res.* **34**: 295–304
- Muftuoglu M, de Souza-Pinto NC, Dogan A, Aamann M, Stevnsner T, Rybanska I, Kirkali G, Dizdaroglu M & Bohr VA (2009) Cockayne syndrome group B protein stimulates repair of formamidopyrimidines by NEIL1 DNA glycosylase. *J. Biol. Chem.* **284**: 9270–9279
- Murga M, Jaco I, Fan Y, Soria R, Martinez-Pastor B, Cuadrado M, Yang SM, Blasco MA, Skoultchi AI & Fernandez-Capetillo O (2007) Global chromatin compaction limits the strength of the DNA damage response. *J. Cell Biol.* **178**: 1101–1108
- Nakamura TM, Morin GB, Chapman KB, Weinrich SL, Andrews WH, Lingner J, Harley CB & Cech TR (1997) Telomerase catalytic subunit homologs from fission yeast and human. *Science* **277**: 955–9
- Nakanishi S, Prasad R, Wilson SH & Smerdon M (2007) Different structural states in oligonucleosomes are required for early versus late steps of base excision repair.

- Nucleic Acids Res.* **35**: 4313–4321
- Nance MA & Berry SA (1992) Cockayne syndrome: review of 140 cases. *Am J Med Genet* **42**: 68–84
- Nandakumar J, Bell CF, Weidenfeld I, Zaug AJ, Leinwand LA & Cech TR (2012) The TEL patch of telomere protein TPP1 mediates telomerase recruitment and processivity. *Nature* **492**: 285–289
- Nergadze SG, Farnung BO, Wischniewski H, Khoriauli L, Vitelli V, Chawla R, Giulotto E & Azzalin CM (2009) CpG-island promoters drive transcription of human telomeres. *RNA* **15**: 2186–94
- Newman JC, Bailey AD & Weiner AM (2006) Cockayne syndrome group B protein (CSB) plays a general role in chromatin maintenance and remodeling. *Proc. Natl. Acad. Sci. U. S. A.* **103**: 9613–8
- Ng LJ, Croyley JE, Pickett HA, Reddel RR & Suter CM (2009) Telomerase activity is associated with an increase in DNA methylation at the proximal subtelomere and a reduction in telomeric transcription. *Nucleic Acids Res.* **37**: 1152–1159
- Nimonkar A V., Genschel J, Kinoshita E, Polaczek P, Campbell JL, Wyman C, Modrich P & Kowalczykowski SC (2011) BLM-DNA2-RPA-MRN and EXO1-BLM-RPA-MRN constitute two DNA end resection machineries for human DNA break repair. *Genes Dev.* **25**: 350–362
- Nishi R, Okuda Y, Watanabe E, Mori T, Iwai S, Masutani C, Sugasawa K & Hanaoka F (2005) Centrin 2 stimulates nucleotide excision repair by interacting with xeroderma pigmentosum group C protein. *Mol Cell Biol* **25**: 5664–5674
- Nishikawa T, Okamura H, Nagadoi a, König P, Rhodes D & Nishimura Y (2001) Solution structure of a telomeric DNA complex of human TRF1. *Structure* **9**: 1237–1251
- Noren Hooten N, Kompaniez K, Barnes J, Lohani A & Evans MK (2011) Poly(ADP-ribose) polymerase 1 (PARP-1) binds to 8-oxoguanine-DNA glycosylase (OGG1). *J. Biol. Chem.* **286**: 44679–44690
- O’Sullivan RJ, Kubicek S, Schreiber SL & Karlseder J (2010) Reduced histone biosynthesis and chromatin changes arising from a damage signal at telomeres. *Nat. Struct. Mol. Biol.* **17**: 1218–1225
- Odell ID, Newick K, Heintz NH, Wallace SS & Pederson DS (2010) Non-specific DNA binding interferes with the efficient excision of oxidative lesions from chromatin by the human DNA glycosylase, NEIL1. *DNA Repair (Amst)*. **9**: 134–143
- Odell ID, Wallace SS & Pederson DS (2013) Rules of engagement for base excision repair in chromatin. *J Cell Physiol* **228**: 258–266
- Ogi T, Limsirichaikul S, Overmeer RM, Volker M, Takenaka K, Cloney R, Nakazawa Y, Niimi A, Miki Y, Jaspers NG, Mullenders LHF, Yamashita S, Fousteri MI & Lehmann AR (2010) Three DNA Polymerases, Recruited by Different Mechanisms, Carry Out NER Repair Synthesis in Human Cells. *Mol. Cell* **37**: 714–727
- Okamoto K, Iwano T, Tachibana M & Shinkai Y (2008) Distinct roles of TRF1 in the regulation of telomere structure and lengthening. *J. Biol. Chem.* **283**: 23981–23988
- Olovnikov AM (1973) A theory of marginotomy. The incomplete copying of template

- margin in enzymic synthesis of polynucleotides and biological significance of the phenomenon. *J. Theor. Biol.* **41**: 181–190
- Osley MA, Tsukuda T & Nickoloff JA (2007) ATP-dependent chromatin remodeling factors and DNA damage repair. *Mutat. Res. - Fundam. Mol. Mech. Mutagen.* **618**: 65–80
- Ottaviani A, Gilson E & Magdinier F (2008) Telomeric position effect: From the yeast paradigm to human pathologies. *Biochimie* **90**: 93–107
- Palm W & de Lange T (2008) How Shelterin Protects Mammalian Telomeres. *Annu. Rev. Genet.* **42**: 301–334
- Panier S & Durocher D (2009) Regulatory ubiquitylation in response to DNA double-strand breaks. *DNA Repair (Amst).* **8**: 436–443
- Peterson SE, Li Y, Wu-Baer F, Chait BT, Baer R, Yan H, Gottesman ME & Gautier J (2013) Activation of DSB Processing Requires Phosphorylation of CtIP by ATR. *Mol. Cell* **49**: 657–667
- Pisano S, Galati A & Cacchione S (2008) Telomeric nucleosomes: Forgotten players at chromosome ends. *Cell. Mol. Life Sci.* **65**: 3553–3563
- Pisano S, Leoni D, Galati A, Rhodes D, Savino M & Cacchione S (2010) The human telomeric protein hTRF1 induces telomere-specific nucleosome mobility. *Nucleic Acids Res.* **38**: 2247–2255
- Poulet A, Pisano S, Faivre-Moskalenko C, Pei B, Tauran Y, Haftek-Terreau Z, Brunet F, Le Bihan YV, Ledu MH, Montel F, Hugo N, Amiard S, Argoul F, Chaboud A, Gilson E & Giraud-Panis MJ (2012) The N-terminal domains of TRF1 and TRF2 regulate their ability to condense telomeric DNA. *Nucleic Acids Res.* **40**: 2566–2576
- Prasad R, Lavrik OI, Kim SJ, Kedar P, Yang XP, Vande Berg BJ & Wilson SH (2001) DNA polymerase beta -mediated long patch base excision repair. Poly(ADP-ribose)polymerase-1 stimulates strand displacement DNA synthesis. *J. Biol. Chem.* **276**: 32411–4
- Prindle MJ & Loeb LA (2012) DNA polymerase delta in dna replication and genome maintenance. *Environ. Mol. Mutagen.* **53**: 666–682
- Proietti-De-Santis L, Drané P & Egly J-M (2006) Cockayne syndrome B protein regulates the transcriptional program after UV irradiation. *EMBO J.* **25**: 1915–23
- Racki LR, Yang JG, Naber N, Partensky PD, Acevedo A, Purcell TJ, Cooke R, Cheng Y & Narlikar GJ (2009) The chromatin remodeller ACF acts as a dimeric motor to space nucleosomes. *Nature* **462**: 1016–1021
- Raffa GD, Ciapponi L, Cenci G & Gatti M (2011) Terminin: A protein complex that mediates epigenetic maintenance of Drosophila telomeres. *Nucleus* **2**: 383–391
- Ranes M, Boeing S, Wang Y, Wienholz F, Menoni H, Walker J, Encheva V, Chakravarty P, Mari PO, Stewart A, Giglia-Mari G, Snijders AP, Vermeulen W & Svejstrup JQ (2016) A ubiquitylation site in Cockayne syndrome B required for repair of oxidative DNA damage, but not for transcription-coupled nucleotide excision repair. *Nucleic Acids Res.* **44**: 5246–5255
- Reid-Bayliss KS, Arron ST, Loeb LA, Bezrookove V & Cleaver JE (2016) Why Cockayne syndrome patients do not get cancer despite their DNA repair deficiency.

- Proc. Natl. Acad. Sci.* **113**: 201610020
- Renkawitz J, Lademann CA, Kalocsay M & Jentsch S (2013) Monitoring Homology Search during DNA Double-Strand Break Repair In Vivo. *Mol. Cell* **50**: 261–272
- Riedl T, Hanaoka F & Egly JM (2003) The comings and goings of nucleotide excision repair factors on damaged DNA. *EMBO J.* **22**: 5293–5303
- Rippe K & Luke B (2015) TERRA and the state of the telomere. *Nat. Struct. Mol. Biol.* **22**: 853–858
- Robertson AB, Klungland A, Rognes T & Leiros I (2009) Base excision repair: The long and short of it. *Cell. Mol. Life Sci.* **66**: 981–993
- Rodier F, Campisi J & Bhaumik D (2007) Two faces of p53: Aging and tumor suppression. *Nucleic Acids Res.* **35**: 7475–7484
- Rodriguez Y & Smerdon MJ (2013) The structural location of DNA lesions in nucleosome core particles determines accessibility by base excision repair enzymes. *J. Biol. Chem.* **288**: 13863–13875
- Rogakou EP, Boon C, Redon C & Bonner WM (1999) Megabase Chromatin Domains Involved in DNA Double-Strand Breaks In Vivo. *J. Cell Biol.* **146**: 905–915
- Rosenfeld JA, Wang Z, Schones DE, Zhao K, DeSalle R & Zhang MQ (2009) Determination of enriched histone modifications in non-genic portions of the human genome. *BMC Genomics* **10**: 143
- Rossetti L, Cacchione S, Fuà M & Savino M (1998) Nucleosome assembly on telomeric sequences. *Biochemistry* **37**: 6727–6737
- Saha A, Wittmeyer J & Cairns BR (2002) Chromatin remodeling by RSC involves ATP-dependent DNA translocation. *Genes Dev.* **16**: 2120–2134
- San Filippo J, Sung P & Klein H (2008) Mechanism of Eukaryotic Homologous Recombination. *Annu. Rev. Biochem.* **77**: 229–257
- Sánchez-Molina S, Mortusewicz O, Bieber B, Auer S, Eckey M, Leonhardt H, Friedl AA & Becker PB (2011) Role for hACF1 in the G2/M damage checkpoint. *Nucleic Acids Res.* **39**: 8445–8456
- Sartori AA, Lukas C, Coates J, Mistrik M, Fu S, Bartek J, Baer R, Lukas J & Jackson SP (2007) Human CtIP promotes DNA end resection. *Nature* **450**: 509–514
- Schmitz KM, Schmitt N, Hoffmann-Rohrer U, Schäfer A, Grummt I & Mayer C (2009) TAF12 Recruits Gadd45a and the Nucleotide Excision Repair Complex to the Promoter of rRNA Genes Leading to Active DNA Demethylation. *Mol. Cell* **33**: 344–353
- Schotta G, Ebert A, Krauss V, Fischer A, Hoffmann J, Rea S, Jenuwein T, Dorn R & Reuter G (2002) Central role of Drosophila SU(VAR)3-9 in histone H3-K9 methylation and heterochromatic gene silencing. *EMBO J.* **21**: 1121–1131
- Schwertman P, Lagarou A, Dekkers DHW, Raams A, van der Hoek AC, Laffeber C, Hoeijmakers JHJ, Demmers J a a, Fousteri M, Vermeulen W & Marteijn J a (2012) UV-sensitive syndrome protein UVSSA recruits USP7 to regulate transcription-coupled repair. *Nat. Genet.* **44**: 598–602
- Scrima A, Koničková R, Czyzewski BK, Kawasaki Y, Jeffrey PD, Groisman R, Nakatani Y, Iwai S, Pavletich NP & Thomä NH (2008) Structural Basis of UV DNA-Damage

- Recognition by the DDB1-DDB2 Complex. *Cell* **135**: 1213–1223
- Sebesta M, Burkovics P, Haracska L & Krejci L (2011) Reconstitution of DNA repair synthesis in vitro and the role of polymerase and helicase activities. *DNA Repair (Amst)*. **10**: 567–576
- Selby CP & Sancar A (1997) Cockayne syndrome group B protein enhances elongation by RNA polymerase II. *Proc. Natl. Acad. Sci. U. S. A.* **94**: 11205–9
- Selzer RR, Nyaga S, Tuo J, May A, Muftuoglu M, Christiansen M, Citterio E, Brosh Jr. RM & Bohr VA (2002) Differential requirement for the ATPase domain of the Cockayne syndrome group B gene in the processing of UV-induced DNA damage and 8-oxoguanine lesions in human cells. *Nucleic Acids Res.* **30**: 782–793
- Sfeir AJ, Chai W, Shay JW & Wright WE (2005) Telomere-end processing the terminal nucleotides of human chromosomes. *Mol. Cell* **18**: 131–8
- Shao G, Patterson-Fortin J, Messick TE, Feng D, Shanbhag N, Wang Y & Greenberg RA (2009) MERIT40 controls BRCA1-Rap80 complex integrity and recruitment to DNA double-strand breaks. *Genes Dev.* **23**: 740–754
- Shieh SY, Ikeda M, Taya Y & Prives C (1997) DNA damage-induced phosphorylation of p53 alleviates inhibition by MDM2. *Cell* **91**: 325–334
- Shinohara a & Ogawa T (1998) Stimulation by Rad52 of yeast Rad51-mediated recombination. *Nature* **391**: 404–407
- Shinohara A, Ogawa H & Ogawa T (1992) Rad51 protein involved in repair and recombination in *S. cerevisiae* is a RecA-like protein. *Cell* **69**: 457–470
- Shippen-Lentz D & Blackburn EH (1990) Functional evidence for an RNA template in telomerase. *Science* **247**: 546–52
- Shore D (2001) Telomeric chromatin: Replicating and wrapping up chromosome ends. *Curr. Opin. Genet. Dev.* **11**: 189–198
- Sigurdsson S, Dirac-Svejstrup AB & Svejstrup JQ (2010) Evidence that Transcript Cleavage Is Essential for RNA Polymerase II Transcription and Cell Viability. *Mol. Cell* **38**: 202–210
- Siliciano JD, Canman CE, Taya Y, Sakaguchi K, Appella E & Kastan MB (1997) DNA damage induces phosphorylation of the amino terminus of p53. *Genes Dev.* **11**: 3471–3481
- Sin Y, Tanaka K & Saijo M (2016) The C-terminal region and SUMOylation of cockayne syndrome group B protein play critical roles in transcription-coupled nucleotide excision repair. *J. Biol. Chem.* **291**: 1387–1397
- Singh TR, Ali AM, Busygina V, Raynard S, Fan Q, Du CH, Andreassen PR, Sung P & Meetei AR (2008) BLAP18/RMI2, a novel OB-fold-containing protein, is an essential component of the Bloom helicase-double Holliday junction dissolvasome. *Genes Dev.* **22**: 2856–2868
- Singhal RK & Wilson SH (1993) Short gap-filling synthesis by DNA polymerase beta is processive. *J. Biol. Chem.* **268**: 15906–11
- Smith CL, Horowitz-Scherer R, Flanagan JF, Woodcock CL & Peterson CL (2003) Structural analysis of the yeast SWI/SNF chromatin remodeling complex. *Nat Struct Biol* **10**: 141–145

- Smogorzewska A, Karlseder J, Holtgreve-Grez H, Jauch A & De Lange T (2002) DNA ligase IV-dependent NHEJ of deprotected mammalian telomeres in G1 and G2. *Curr. Biol.* **12**: 1635–1644
- Smogorzewska A, van Steensel B, Bianchi A, Oelmann S, Schaefer MR, Schnapp G & de Lange T (2000) Control of human telomere length by TRF1 and TRF2. *Mol Cell Biol* **20**: 1659–1668
- Sobhian B, Shao G, Lilli DR, Culhane AC, Moreau LA, Xia B, Livingston DM & Greenberg RA (2007) RAP80 Targets BRCA1 to Specific Ubiquitin Structures at DNA Damage Sites. *Science (80-)*. **316**: 1198–1202
- Sobol RW, Horton JK, Kühn R, Gu H, Singhal RK, Prasad R, Rajewsky K & Wilson SH (1996) Requirement of mammalian DNA polymerase-beta in base-excision repair. *Nature* **379**: 183–6
- Sonoda E, Hohegger H, Saberi A, Taniguchi Y & Takeda S (2006) Differential usage of non-homologous end-joining and homologous recombination in double strand break repair. *DNA Repair (Amst)*. **5**: 1021–1029
- Soubeyrand S, Pope L, De Chasseval R, Gosselin D, Dong F, de Villartay JP & Haché RJG (2006) Artemis Phosphorylated by DNA-dependent Protein Kinase Associates Preferentially with Discrete Regions of Chromatin. *J. Mol. Biol.* **358**: 1200–1211
- Squires S, Ryan AJ, Strutt HL & Johnson RT (2012) Hypersensitivity of Cockayne's Syndrome Cells to Camptothecin Is Associated with the Generation of Abnormally High Levels of Double Strand Breaks in Nascent. *DNA Repair (Amst)*. **53**: 2012–2019
- Stansel RM, De Lange T & Griffith JD (2001) T-loop assembly in vitro involves binding of TRF2 near the 3' telomeric overhang. *EMBO J.* **20**: 5532–5540
- van Steensel B & de Lange T (1997) Control of telomere length by the human telomeric protein TRF1. *Nature* **385**: 740–3
- Van Steensel B, Smogorzewska A & De Lange T (1998) TRF2 protects human telomeres from end-to-end fusions. *Cell* **92**: 401–413
- Stevnsner T, Muftuoglu M, Aamann MD & Bohr VA (2008) The role of Cockayne Syndrome group B (CSB) protein in base excision repair and aging. *Mech. Ageing Dev.* **129**: 441–448
- Stewart GS, Panier S, Townsend K, Al-Hakim AK, Kolas NK, Miller ES, Nakada S, Ylanko J, Olivarius S, Mendez M, Oldreive C, Wildenhain J, Tagliaferro A, Pelletier L, Taubenheim N, Durandy A, Byrd PJ, Stankovic T, Taylor AMR & Durocher D (2009) The RIDDLE Syndrome Protein Mediates a Ubiquitin-Dependent Signaling Cascade at Sites of DNA Damage. *Cell* **136**: 420–434
- Stucki M, Clapperton JA, Mohammad D, Yaffe MB, Smerdon SJ & Jackson SP (2005) MDC1 directly binds phosphorylated histone H2AX to regulate cellular responses to DNA double-strand breaks. *Cell* **123**: 1213–1226
- Stucki M, Pascucci B, Parlanti E, Fortini P, Wilson SH, Hübscher U & Dogliotti E (1998) Mammalian base excision repair by DNA polymerases delta and epsilon. *Oncogene* **17**: 835–843
- Sugasawa K, Masutani C & Hanaoka F (1993) Cell-free repair of UV-damaged simian

- virus 40 chromosomes in human cell extracts. I. Development of a cell-free system detecting excision repair of UV-irradiated SV40 chromosomes. *J. Biol. Chem.* **268**: 9098–9104
- Sugawara N, Wang X & Haber JE (2003) In vivo roles of Rad52, Rad54, and Rad55 proteins in Rad51-mediated recombination. *Mol. Cell* **12**: 209–219
- Sugiyama T, Zaitseva EM & Kowalczykowski SC (1997) A single-stranded DNA-binding protein is needed for efficient presynaptic complex formation by the *Saccharomyces cerevisiae* Rad51 protein. *J. Biol. Chem.* **272**: 7940–7945
- Sun J, Lee KJ, Davis AJ & Chen DJ (2012) Human Ku70/80 protein blocks exonuclease 1-mediated DNA resection in the presence of human Mre11 or Mre11/Rad50 protein complex. *J. Biol. Chem.* **287**: 4936–4945
- Surovtseva Y V., Churikov D, Boltz KA, Song X, Lamb JC, Warrington R, Leehy K, Heacock M, Price CM & Shippen DE (2009) Conserved Telomere Maintenance Component 1 Interacts with STN1 and Maintains Chromosome Ends in Higher Eukaryotes. *Mol. Cell* **36**: 207–218
- Takai H, Smogorzewska A & De Lange T (2003) DNA damage foci at dysfunctional telomeres. *Curr. Biol.* **13**: 1549–1556
- Takai KK, Hooper S, Blackwood S, Gandhi R & de Lange T (2010) In vivo stoichiometry of shelterin components. *J. Biol. Chem.* **285**: 1457–1467
- Tang J, Cho NW, Cui G, Manion EM, Shanbhag NM, Botuyan MV, Mer G & Greenberg RA (2013) Acetylation limits 53BP1 association with damaged chromatin to promote homologous recombination. *Nat. Struct. Mol. Biol.* **20**: 317–325
- Tantin D, Kansal a & Carey M (1997) Recruitment of the putative transcription-repair coupling factor CSB/ERCC6 to RNA polymerase II elongation complexes. *Mol. Cell. Biol.* **17**: 6803–14
- Tapias A, Auriol J, Forget D, Enzlin JH, Schärer OD, Coin F, Coulombe B & Egly JM (2004) Ordered Conformational Changes in Damaged DNA Induced by Nucleotide Excision Repair Factors. *J. Biol. Chem.* **279**: 19074–19083
- Thorslund T, Kobbe C Von, Harrigan JA, Indig FE, Christiansen M, Stevnsner T & Bohr VA (2005) Cooperation of the Cockayne Syndrome Group B Protein and Poly (ADP-Ribose) Polymerase 1 in the Response to Oxidative Stress. *Society* **25**: 7625–7636
- Toiber D, Erdel F, Bouazoune K, Silberman DM, Zhong L, Mulligan P, Sebastian C, Cosentino C, Martinez-Pastor B, Giacosa S, D’Urso A, Näär AM, Kingston R, Rippe K & Mostoslavsky R (2013) SIRT6 recruits SNF2H to DNA break sites, preventing genomic instability through chromatin remodeling. *Mol. Cell* **51**: 454–468
- Tomimatsu N, Mukherjee B, Catherine Hardebeck M, Ilcheva M, Vanessa Camacho C, Louise Harris J, Porteus M, Llorente B, Khanna KK & Burma S (2014) Phosphorylation of EXO1 by CDKs 1 and 2 regulates DNA end resection and repair pathway choice. *Nat. Commun.* **5**:
- Tommerup H, Dousmanis a & de Lange T (1994) Unusual chromatin in human telomeres. *Mol. Cell. Biol.* **14**: 5777–85
- Troelstra C, van Gool A, de Wit J, Vermeulen W, Bootsma D & Hoeijmakers JH (1992a)

- ERCC6, a member of a subfamily of putative helicases, is involved in Cockayne's syndrome and preferential repair of active genes. *Cell* **71**: 939–953
- Troelstra C, Heslen W, Bootsma D & Hoeijmakers JHJ (1993) Structure and expression of the excision repair gene ERCC6, involved in the human disorder cockayne's syndrome group B. *Nucleic Acids Res.* **21**: 419–426
- Troelstra C, Landsvater RM, Wiegant J, van der Ploeg M, Viel G, Buys CHCM & Hoeijmakers JHJ (1992b) Localization of the nucleotide excision repair gene ERCC6 to human chromosome 10q11-q21. *Genomics* **12**: 745–749
- Truong LN, Li Y, Shi LZ, Hwang PY-H, He J, Wang H, Razavian N, Berns MW & Wu X (2013) Microhomology-mediated End Joining and Homologous Recombination share the initial end resection step to repair DNA double-strand breaks in mammalian cells. *Proc. Natl. Acad. Sci.* **110**: 7720–7725
- Tsai CJ, Kim S a & Chu G (2007) Cernunnos/XLF promotes the ligation of mismatched and noncohesive DNA ends. *Proc. Natl. Acad. Sci. U. S. A.* **104**: 7851–6
- Tsukuda T, Fleming AB, Nickoloff JA & Osley MA (2005) Chromatin remodelling at a DNA double-strand break site in *Saccharomyces cerevisiae*. *Nature* **438**: 379–383
- Tu Y, Bates S & Pfeifer GP (1997) Sequence-specific and domain-specific DNA repair in xeroderma pigmentosum and Cockayne syndrome cells. *J. Biol. Chem.* **272**: 20747–20755
- Tuo J, Chen C, Zeng X, Christiansen M & Bohr VA (2002a) Functional crosstalk between hOgg1 and the helicase domain of Cockayne syndrome group B protein. *DNA Repair (Amst)*. **1**: 913–927
- Tuo J, Jaruga P, Rodriguez H, Bohr V & Dizdaroglu M (2003) Primary fibroblasts of Cockayne syndrome patients are defective in cellular repair of 8-hydroxyguanine and 8-hydroxyadenine resulting from oxidative stress. *FASEB J.* **17**: 668–674
- Tuo J, Jaruga P, Rodriguez H, Dizdaroglu M & Bohr VA (2002b) The cockayne syndrome group B gene product is involved in cellular repair of 8-hydroxyadenine in DNA. *J. Biol. Chem.* **277**: 30832–30837
- Tuo J, Müftüoglu M, Chen C, Jaruga P, Selzer RR, Brosh RM, Rodriguez H, Dizdaroglu M & Bohr VA (2001) The Cockayne Syndrome Group B Gene Product Is Involved in General Genome Base Excision Repair of 8-Hydroxyguanine in DNA. *J. Biol. Chem.* **276**: 45772–45779
- Uematsu N, Weterings E, Yano KI, Morotomi-Yano K, Jakob B, Taucher-Scholz G, Mari PO, Van Gent DC, Chen BPC & Chen DJ (2007) Autophosphorylation of DNA-PKCS regulates its dynamics at DNA double-strand breaks. *J. Cell Biol.* **177**: 219–229
- Uziel T, Lerenthal Y, Moyal L, Andegeko Y, Mittelman L & Shiloh Y (2003) Requirement of the MRN complex for ATM activation by DNA damage. *EMBO J.* **22**: 5612–5621
- Venema J, Mullenders LH, Natarajan AT, van Zeeland AA & Mayne L V (1990) The genetic defect in Cockayne syndrome is associated with a defect in repair of UV-induced DNA damage in transcriptionally active DNA. *Proc. Natl. Acad. Sci. U. S. A.* **87**: 4707–4711

- Volker M, Moné MJ, Karmakar P, Van Hoffen A, Schul W, Vermeulen W, Hoeijmakers JHJ, Van Driel R, Van Zeeland AA & Mullenders LHF (2001) Sequential assembly of the nucleotide excision repair factors in vivo. *Mol. Cell* **8**: 213–224
- De Vos M, Schreiber V & Dantzer F (2012) The diverse roles and clinical relevance of PARPs in DNA damage repair: Current state of the art. *Biochem. Pharmacol.* **84**: 137–146
- Wakasugi M, Kawashima A, Morioka H, Linn S, Sancar A, Mori T, Nikaido O & Matsunaga T (2002) DDB accumulates at DNA damage sites immediately after UV irradiation and directly stimulates nucleotide excision repair. *J. Biol. Chem.* **277**: 1637–1640
- Walker JR, Corpina RA & Goldberg J (2001) Structure of the Ku heterodimer bound to DNA and its implications for double-strand break repair. *Nature* **412**: 607–14
- Walker JR & Zhu XD (2012) Post-translational modifications of TRF1 and TRF2 and their roles in telomere maintenance. *Mech. Ageing Dev.* **133**: 421–434
- Wang B & Elledge SJ (2007) Ubc13/Rnf8 ubiquitin ligases control foci formation of the Rap80/Abraxas/Brc1/Brc36 complex in response to DNA damage. *Proc. Natl. Acad. Sci.* **104**: 20759–20763
- Wang B, Matsuoka S, Ballif BA, Zhang D, Smogorzewska A, Gygi SP & Elledge SJ (2007a) Abraxas and RAP80 form a BRCA1 protein complex required for the DNA damage response. *Science* **316**: 1194–8
- Wang F, Podell ER, Zaug AJ, Yang Y, Baciú P, Cech TR & Lei M (2007b) The POT1–TPP1 telomere complex is a telomerase processivity factor. *Nature* **445**: 506–510
- Wang F, Stewart JA, Kasbek C, Zhao Y, Wright WE & Price CM (2012) Human CST Has Independent Functions during Telomere Duplex Replication and C-Strand Fill-In. *Cell Rep.* **2**: 1096–1103
- Wang H, Shi LZ, Wong CCL, Han X, Hwang PYH, Truong LN, Zhu Q, Shao Z, Chen DJ, Berns MW, Yates JR, Chen L & Wu X (2013) The Interaction of CtIP and Nbs1 Connects CDK and ATM to Regulate HR-Mediated Double-Strand Break Repair. *PLoS Genet.* **9**:
- Wang J, Aroumougame A, Lohrich M, Li Y, Chen D, Chen J & Gong Z (2014) PTIP associates with artemis to dictate DNA repair pathway choice. *Genes Dev.* **28**: 2693–2698
- Wang RC, Smogorzewska A & De Lange T (2004) Homologous recombination generates t-loop-sized deletions at human telomeres. *Cell* **119**: 355–368
- Wang XW, Yeh H, Schaeffer L, Roy R, Moncollin V, Egly JM, Wang Z, Freidberg EC, Evans MK & Taffe BG (1995) p53 modulation of TFIIH-associated nucleotide excision repair activity. *Nat. Genet.* **10**: 188–195
- Watson JD (1972) Origin of concatemeric T7 DNA. *Nat. New Biol.* **239**: 197–201
- Wei L, Lan L, Yasui A, Tanaka K, Saijo M, Matsuzawa A, Kashiwagi R, Maseki E, Hu Y, Parvin JD, Ishioka C & Chiba N (2011) BRCA1 contributes to transcription-coupled repair of DNA damage through polyubiquitination and degradation of Cockayne syndrome B protein. *Cancer Sci.* **102**: 1840–1847
- Wei YF, Robins P, Carter K, Caldecott K, Pappin DJ, Yu GL, Wang RP, Shell BK, Nash

- RA & Schär P (1995) Molecular cloning and expression of human cDNAs encoding a novel DNA ligase IV and DNA ligase III, an enzyme active in DNA repair and recombination. *Mol. Cell. Biol.* **15**: 3206–3216
- Wellinger RJ, Ethier K, Labrecque P & Zakian VA (1996) Evidence for a new step in telomere maintenance. *Cell* **85**: 423–33
- Will O, Gocke E, Eckert I, Schulz I, Pflaum M, Mahler HC & Epe B (1999) Oxidative DNA damage and mutations induced by a polar photosensitizer, Ro19-8022. *Mutat. Res. - DNA Repair* **435**: 89–101
- Wilson BT, Stark Z, Sutton RE, Danda S, Ekbote A V, Elsayed SM, Gibson L, Goodship JA, Jackson AP, Keng WT, King MD, McCann E, Motojima T, Murray JE, Omata T, Pilz D, Pope K, Sugita K, White SM & Wilson IJ (2016) The Cockayne Syndrome Natural History (CoSyNH) study: clinical findings in 102 individuals and recommendations for care. *Genet. Med.* **18**: 483–93
- Wong HK, Muftuoglu M, Beck G, Imam SZ, Bohr VA & Wilson DM (2007) Cockayne syndrome B protein stimulates apurinic endonuclease 1 activity and protects against agents that introduce base excision repair intermediates. *Nucleic Acids Res.* **35**: 4103–4113
- Wu L & Hickson ID (2003) The Bloom's syndrome helicase suppresses crossing over during homologous recombination. *Nature* **426**: 870–874
- Wu P, van Overbeek M, Rooney S & de Lange T (2010) Apollo Contributes to G Overhang Maintenance and Protects Leading-End Telomeres. *Mol. Cell* **39**: 606–617
- Wu P, Takai H & De Lange T (2012) Telomeric 3' overhangs derive from resection by Exo1 and Apollo and fill-in by POT1b-associated CST. *Cell* **150**: 39–52
- Wu S, Shi Y, Mulligan P, Gay F, Landry J, Liu H, Lu J, Qi HH, Wang W, Nikoloff JA, Wu C & Shi Y (2007) A YY1–INO80 complex regulates genomic stability through homologous recombination–based repair. *Nat. Struct. Mol. Biol.* **14**: 1165–1172
- Wyatt MD & Pittman DL (2006) Methylating agents and DNA repair responses: Methylated bases and sources of strand breaks. *Chem. Res. Toxicol.* **19**: 1580–1594
- Xie W, Ling T, Zhou Y, Feng W, Zhu Q, Stunnenberg HG, Grummt I & Tao W (2012) The chromatin remodeling complex NuRD establishes the poised state of rRNA genes characterized by bivalent histone modifications and altered nucleosome positions. *Proc. Natl. Acad. Sci. U. S. A.* **109**: 8161–6
- Xu D, Guo R, Soback A, Bachrati CZ, Yang J, Enomoto T, Brown GW, Hoatlin ME, Hickson ID & Wang W (2008) RMI, a new OB-fold complex essential for Bloom syndrome protein to maintain genome stability. *Genes Dev.* **22**: 2843–2855
- Xu G, Chapman JR, Brandsma I, Yuan J, Mistrik M, Bouwman P, Bartkova J, Gogola E, Warmerdam D, Barazas M, Jaspers JE, Watanabe K, Pieterse M, Kersbergen A, Sol W, Celie PHN, Schouten PC, van den Broek B, Salman A, Nieuwland M, et al (2015) REV7 counteracts DNA double-strand break resection and affects PARP inhibition. *Nature* **521**: 541–544
- Yan J, Kim YS, Yang XP, Li LP, Liao G, Xia F & Jetten AM (2007) The ubiquitin-interacting motif-containing protein RAP80 interacts with BRCA1 and functions in DNA damage repair response. *Cancer Res.* **67**: 6647–6656

- Yang Q, Zheng Y-L & Harris CC (2005) POT1 and TRF2 cooperate to maintain telomeric integrity. *Mol. Cell. Biol.* **25**: 1070–80
- Yannone SM, Khan IS, Zhou RZ, Zhou T, Valerie K & Povirk LF (2008) Coordinate 5' and 3' endonucleolytic trimming of terminally blocked blunt DNA double-strand break ends by Artemis nuclease and DNA-dependent protein kinase. *Nucleic Acids Res.* **36**: 3354–3365
- Yano K, Morotomi-Yano K, Wang S-Y, Uematsu N, Lee K-J, Asaithamby A, Weterings E & Chen DJ (2008) Ku recruits XLF to DNA double-strand breaks. *EMBO Rep.* **9**: 91–96
- Yazdi PT, Wang Y, Zhao S, Patel N, Lee EYHP & Qin J (2002) SMC1 is a downstream effector in the ATM/NBS1 branch of the human S-phase checkpoint. *Genes Dev.* **16**: 571–582
- Ye JZS, Donigian JR, Van Overbeek M, Loayza D, Luo Y, Krutchinsky AN, Chait BT & De Lange T (2004a) TIN2 binds TRF1 and TRF2 simultaneously and stabilizes the TRF2 complex on telomeres. *J. Biol. Chem.* **279**: 47264–47271
- Ye JZS, Hockemeyer D, Krutchinsky AN, Loayza D, Hooper SM, Chait BT & De Lange T (2004b) POT1-interaction protein PIP1: A telomere length regulator that recruits POT1 to the TIN2/TRF1 complex. *Genes Dev.* **18**: 1649–1654
- Yehezkel S, Segev Y, Viegas-Péquignot E, Skorecki K & Selig S (2008) Hypomethylation of subtelomeric regions in ICF syndrome is associated with abnormally short telomeres and enhanced transcription from telomeric regions. *Hum. Mol. Genet.* **17**: 2776–2789
- Yokoi M (2000) The Xeroderma Pigmentosum Group C Protein Complex XPC-HR23B Plays an Important Role in the Recruitment of Transcription Factor IIIH to Damaged DNA. *J. Biol. Chem.* **275**: 9870–9875
- You Z, Chahwan C, Bailis J, Hunter T & Russell P (2005) ATM Activation and Its Recruitment to Damaged DNA Require Binding to the C Terminus of Nbs1. *Mol. Cell. Biol.* **25**: 5363–5379
- Yuan X, Feng W, Imhof A, Grummt I & Zhou Y (2007) Activation of RNA Polymerase I Transcription by Cockayne Syndrome Group B Protein and Histone Methyltransferase G9a. *Mol. Cell* **27**: 585–595
- Yun MH & Hiom K (2009) CtIP-BRCA1 modulates the choice of DNA double-strand-break repair pathway throughout the cell cycle. *Nature* **459**: 460–463
- Zgheib O, Pataky K, Brugger J & Halazonetis TD (2009) An Oligomerized 53BP1 Tudor Domain Suffices for Recognition of DNA Double-Strand Breaks. *Mol. Cell. Biol.* **29**: 1050–1058
- Von Zglinicki T & Martin-Ruiz C (2005) Telomeres as Biomarkers for Ageing and Age-Related Diseases. *Curr. Mol. Med.* **5**: 197–203
- Zhang X, Horibata K, Saijo M, Ishigami C, Ukai A, Kanno S, Tahara H, Neilan EG, Honma M, Nohmi T, Yasui A & Tanaka K (2012) Mutations in UVSSA cause UV-sensitive syndrome and destabilize ERCC6 in transcription-coupled DNA repair. *Nat. Genet.* **44**: 593–7
- Zhong FL, Batista LFZ, Freund A, Pech MF, Venteicher AS & Artandi SE (2012) TPP1

- OB-fold domain controls telomere maintenance by recruiting telomerase to chromosome ends. *Cell* **150**: 481–494
- Zhu XD, Küster B, Mann M, Petrini JH & de Lange T (2000) Cell-cycle-regulated association of RAD50/MRE11/NBS1 with TRF2 and human telomeres. *Nat. Genet.* **25**: 347–52
- Zimmermann M, Lottersberger F, Buonomo SB, Sfeir A & de Lange T (2013) 53BP1 Regulates DSB Repair Using Rif1 to Control 5' End Resection. *Science (80-.).* **339**: 700–704
- Zou Y, Sfeir A, Gryaznov SM, Shay JW & Wright (2004) Does a Sentinel or a Subset of Short Telomeres Determine Replicative Senescence? *Mol. Biol. Cell* **15**: 3709–3718

Chapter 2

Cockayne Syndrome group B protein interacts with TRF2 and regulates telomere length and stability

2.1 Preface

Several premature aging disorders including Werner's syndrome, Xeroderma Pigmentosum and Hutchinson Gilford Progeria are characterized to have defects in telomere maintenance. Cockayne syndrome (CS) is a segmental premature aging syndrome for which the state of telomeres has not been addressed. It has been suggested that CSB has many different functions in the cells, some of which are uncharacterized and may account for the premature aging phenotype associated with CS. The work presented in this chapter provides support for a role of CSB in telomere maintenance. This work contributes toward our understanding of how telomere dysfunction relates to aging and may be beneficial for determining treatment options of CS patients.

This work was published in *Nucleic Acids Research*, on August 13, 2012, in pages 9661-9674, volume 40, issue 19, DOI: <https://doi.org/10.1093/nar/gks745>. The original idea to investigate CS cells for a telomere defect and the finding that CSB and TRF2 interact *in vivo* was a collaborative effort between Taylor Mitchell and Derrik Leach. All figures in the paper are the work of either myself or Taylor Mitchell. I produced in its entirety figures 3, 4A-D, 5A-E, 6, and Supplementary figures S2B and S3. The paper was written as a collaborative effort between myself, Taylor Mitchell and Dr. Zhu with input from Derrik Leach and Dr. Andrew Rainbow.

2.2 Publication – Cockayne syndrome group B protein interacts with TRF2 and regulates telomere length and stability

Nucleic Acids Research, 2012, 1–14
doi:10.1093/nar/gks745

Cockayne Syndrome group B protein interacts with TRF2 and regulates telomere length and stability

Nicole L. Batenburg, Taylor R. H. Mitchell, Derrick M. Leach, Andrew J. Rainbow and Xu-Dong Zhu*

Department of Biology, McMaster University, 1280 Main St. West Hamilton, ON, Canada L8S4K1

Received April 17, 2012; Revised June 30, 2012; Accepted July 13, 2012

Corresponding author:

Xu-Dong Zhu
Department of Biology, LSB438
McMaster University
1280 Main St. West
Hamilton, Ontario
Canada L8S4K1
Phone: (905) 525-9140 ext. 27737
Fax: (905)522-6066
Email: zhuxu@mcmaster.ca

2.2.1 Abstract

The majority of Cockayne syndrome (CS) patients carry a mutation in CSB, a large nuclear protein implicated in DNA repair, transcription and chromatin remodeling. However, whether CSB may play a role in telomere metabolism has not yet been characterized. Here we report that CSB physically interacts with TRF2, a duplex telomeric DNA binding protein essential for telomere protection. We find that CSB localizes at a small subset of human telomeres and that it is required for preventing the formation of telomere dysfunction-induced foci (TIFs) in CS cells. We find that CS cells or CSB knockdown cells accumulate telomere doublets, the suppression of which requires CSB. We find that overexpression of CSB in CS cells promotes telomerase-dependent telomere lengthening, a phenotype that is associated with a decrease in the amount of telomere-bound TRF1, a negative mediator of telomere length maintenance. Furthermore, we show that CS cells or CSB knockdown cells exhibit misregulation of TERRA, a large non-coding telomere repeat-containing RNA important for telomere maintenance. Taken together, these results suggest that CSB is required for maintaining the homeostatic level of TERRA, telomere length and integrity. These results further imply that CS patients carrying CSB mutations may be defective in telomere maintenance.

2.2.2 Introduction

Telomeres are heterochromatic structures found at the ends of linear eukaryotic chromosomes. Mammalian telomeric DNA consists of tandem repeats of TTAGGG that are bound by a telomere-specific complex known as shelterin/telosome (1-3). Shelterin, composed of six protein subunits including TRF1, TRF2, TIN2, hRap1, TPP1 and POT1, functions not only to regulate telomere length maintenance but also to protect natural chromosome ends from being recognized as damaged DNA (1,2,4). Telomeric DNA has been shown to be transcribed into a large non-coding telomere repeat-containing RNA (5), referred to as TERRA, which is implicated in maintaining the integrity of telomere heterochromatin (5,6). Disruption of the shelterin complex or the telomere heterochromatic state can lead to induction of telomere abnormalities including telomere end-to-end fusions, telomere loss and telomere doublets/fragile telomeres (1,2,6). These dysfunctional telomeres have been shown to be associated with DNA damage response factors such as γ H2AX and 53BP1, resulting in the formation of nuclear structures that are referred to as telomere dysfunction-induced foci (TIFs) (7-10).

TRF2 is one of the two shelterin subunits that bind specifically to duplex telomeric DNA (11,12), the other being TRF1 (13). Overexpression of TRF1 leads to telomere shortening whereas removal of TRF1 from telomeres promotes telomerase-dependent telomere lengthening (14-16), implying that TRF1 may restrict the access of telomerase to the ends of telomeres.

While TRF1 has been implicated in telomere length maintenance, TRF2 is best known for its role in telomere protection. TRF2 contains a N-terminal basic domain, a

central TRF homology domain (TRFH) and a C-terminal Myb-like DNA binding domain (11,12). The N-terminal basic domain is rich in glycine and arginine residues, also referred to as a GAR domain. The TRFH domain of TRF2 not only mediates homo-dimerization but also acts as a protein-interaction platform at telomeres to recruit additional shelterin subunits and other accessory proteins (17,18). Removal of TRF2 from telomeres either by conditional knockout or overexpression of a dominant-negative allele of TRF2 lacking both the N-terminal basic/GAR domain and the C-terminal Myb-like DNA binding domain promotes telomere end-to-end fusions (19,20). Overexpression of TRF2 lacking its N-terminal basic/GAR domain promotes telomere loss (8) whereas overexpression of TRF2 carrying amino acid substitutions in the same basic/GAR domain induces the formation of telomere doublets (10).

Cockayne syndrome (CS) is a rare human hereditary disorder characterized by severe postnatal growth failure, progressive neurological degeneration and segmental premature aging including sensorineural hearing loss, retinal degeneration and loss of subcutaneous fat (21,22). CS patients show hypersensitivity to UV light and the average life span of CS patients is approximately 12 years (23-25). Although five genes have been identified to be responsible for the disease including CSA, CSB, XPB, XPD and XPG, the majority of CS patients carry a defect in the CSB gene (21,22,25).

Cockayne Syndrome group B protein (CSB), also known as ERCC6, is a nuclear protein of 1493 amino acids in length, containing several distinct domains including an acidic domain, a glycine rich domain, a SWI/SNF-like ATPase domain, a nucleotide binding domain (NTB) and a ubiquitin binding domain (UBD) (Fig. 1A) (21,26-28). CSB

has been shown to play a key role in transcription-coupled repair (TCR) (21,29), a sub-pathway of nucleotide excision repair (NER) responsible for removing bulky lesions such as UV-induced DNA damage (cyclobutane pyrimidine dimers and 6-pyrimidine-4-pyrimidone photoproducts). In addition to NER, CSB has also been implicated in base excision repair (BER) (30,31), transcription (32-35), chromatin maintenance and remodeling (36). However, whether CSB may play a role in telomere maintenance relevant to cancer and aging has not yet been characterized.

Here we report that CSB physically interacts with TRF2. While multiple domains of CSB are engaged in its interaction with TRF2, the TRFH domain of TRF2 is required and sufficient for binding CSB. We show that CS cells or CSB knockdown cells exhibit an accumulation of telomere doublets and an induction of TIF formation. Re-introduction of wild type CSB into CS cells suppresses the formation of telomere doublets and TIFs, indicative of its role in telomere protection. In addition, we find that CS cells undergo telomere shortening whereas overexpression of CSB into CS cells results in telomerase-dependent telomere lengthening. The latter is associated with a reduction in the amount of telomere-bound TRF1, a negative mediator of telomere length maintenance (14-16). Furthermore, we find that CS cells or CSB knockdown cells display misregulation of TERRA expression. Collectively, these results suggest that CSB is required for maintaining the homeostatic level of TERRA, telomere length and stability.

2.2.3 *Materials and methods*

DNA constructs and antibodies

The complementary (cDNA) for CSB purchased from mammalian gene collection (MGC) contained three missense mutations (C666, P1041 and P1294). The QuickChange site-directed mutagenesis kit (Stratagene) was used to revert these mutations to wild type. The corrected CSB cDNA was then subcloned into the retroviral vector pLPC-puro (37) or pLPC-N-Myc-puro (37). The pLPC-N-Myc-CSB plamid was used as a template for PCR to generate CSB truncation alleles CSB-N (aa 2-510), CSB-ATPase (aa 510-960) and CSB-C (aa 972-1493). The cDNA for TRF2 was a generous gift from Titia de Lange, Rockefeller University. The TRF2 truncation alleles TRF2^{ΔBAM} (aa 45-453), TRF2^{TRFH} (aa 45-245) and TRF2^{linker} (aa 246-453) were generated by PCR and cloned into pLPC-FH2 (38) (a kind gift from Titia de Lange, Rockefeller University). pBabe-neo-hTERT was kindly provided by Robert Weinberg, MIT.

The oligonucleotides encoding siRNA directed against CSB have been previously described (39). The annealed oligonucleotides were ligated into pRetroSuper vector (kindly provided by Titia de Lange, Rockefeller University), giving rise to pRetroSuper-shCSB.

Antibodies to TRF1 (13), TRF2 (40) and hRap1 (41) were kind gifts from Titia de Lange, Rockefeller University. Commercial antibodies used were rabbit anti-CSB (Bethyl A301-345A), mouse anti-CSB (Abcam Ab66598), anti-Myc (9E10, Calbiochem), anti- γ -H2AX (Upstate) and anti- γ -tubulin (GTU88, Sigma).

Cell Culture and retroviral infection

HeLaI.211 and HeLaII cells were a gift from Titia de Lange, Rockefeller University. HeLaI.2.11 and HeLaII are sublines of HeLa cells of different telomere length (59). Primary fibroblast cell lines GM38 (normal), GM9503 (normal), GM8399 (normal), GM10901 (heterozygote), GM10905 (CS), GM739 (CS), GM1428(CS) and a transformed CS cell line (GM16095) were obtained from the NIGMS Human Genetic Cell Repository (Coriell Institute for Medical Research, Camden, NJ). GM16095 is a SV40-transformed cell line derived from GM739 (27). Supplementary Table S1 lists the nature of CSB mutations and the age of individuals from whom biopsies were taken to establish the primary cell lines. Cells were grown in DMEM medium with 10% fetal bovine serum (FBS) for transformed cell lines GM16095, HeLa and Phoenix cells, and 15% FBS for all primary fibroblasts, supplemented with non-essential amino acids, glutamine, 100 U/ml penicillin and 0.1 mg/ml streptomycin. Retroviral gene delivery was carried out as described (42,43). Phoenix amphotropic retroviral packaging cells were transfected with the desired DNA constructs. For hTERT-mediated immortalization, three days after the last infection, neomycin (600 µg/ml) was added to the medium to select for hTERT-expressing cells. Otherwise, twelve hours after the last infection, puromycin (2 µg/ml) was added to the medium and the cells were maintained in the selection medium for the entirety of the experiments.

Immunoblotting and immunoprecipitation

Immunoblotting was carried out as previously described (10,40). Immunoprecipitation (IP) of endogenous TRF2 was performed essentially as described (10,40). For IP of endogenous CSB, HeLa cells were collected and resuspended in ice-cold NP-40 buffer (1% NP-40, 150 mM NaCl, 10 mM sodium phosphate, pH 7.2). Following incubation on ice for 20 min, the supernatant was recovered by micro-centrifugation at 13000 rpm for 10 min. Protein extracts of 1.5 mg was mixed with 2 μ l mouse anti-CSB antibody (Abcam) and the mixture was incubated overnight at 4°C. Protein G-beads (30 μ l) was added to the mixture on the next day and the IP pellet was washed five times each with 1 ml of ice-cold NP-40 buffer containing 1 mM DTT, 1 μ g/ml aprotinin, 1 μ g/ml leupeptin, 10 μ g/ml pepstatin and 1 mM PMSF.

Co-immunoprecipitation from 293T cells was carried out essentially as described (38) except for the method of transfection used. Human 293T cells grown on 6-cm plates with 95% confluency were transfected using Lipofectamine 2000 (Invitrogen) according to the manufacturer's protocol. For each co-transfection, a total of 8 μ g DNA mixture was used. The ratio of CSB constructs to TRF2 constructs in each DNA mixture was 3:1.

Chromatin Immunoprecipitations (ChIPs)

Chromatin immunoprecipitations (ChIPs) were carried out essentially as described (44-46). Cells were directly fixed with 1% formaldehyde in PBS for 1 h, followed by sonication (10 cycles of 20 s each, 50% duty and 5 output). For each ChIP, 200 μ l cell lysate (equivalent to 2×10^6 cells) was used. For the total telomeric DNA, 50 μ l supernatant (corresponding to one-quarter of the amount of lysate used for IP) were processed along with the IP samples

at the step of reversing the crosslinks. Four-fifths of immunoprecipitated DNA was loaded on the dot blots whereas two inputs each containing 5% of total DNA was included to assess the consistency of loading. The ratio of the signal from each ChIP relative to the signal from the input lane was multiplied by 5% (5% represents 5% of total DNA) and a factor of 1.25 (since four fifths of the precipitated DNA was loaded for each ChIP), giving rise to the percentage of total telomeric DNA recovered from each ChIP.

Immunofluorescence (IF) and fluorescence *in situ* hybridization (FISH)

Immunofluorescence was performed essentially as described (40,43). Briefly, cells grown on coverslips were rinsed with PBS, incubated in Triton X-100 buffer (0.5% Triton X-100, 20 mM HEPES-KOH [pH7.9], 50 mM NaCl, 3 mM MgCl₂, and 300 mM sucrose) at RT for 5 min and then fixed for 10 min in PBS-buffered 3% paraformaldehyde and 2% sucrose. Following permeabilization at RT for 10 min in Triton X-100 buffer, fixed cells were blocked with 0.5% bovine serum albumin (Sigma) and 0.2% gelatin (Sigma) in PBS and then incubated at RT for 2 hr with both rabbit anti-hRap1 and mouse anti- γ H2AX or mouse anti-CSB.

Immunofluorescence (IF)-fluorescence *in situ* hybridization (FISH) analysis was conducted as described (9). Briefly, cells grown on coverslips were fixed at RT for 10 min in PBS-buffered 2% paraformaldehyde, washed in PBS twice for 5 min each, followed by incubation at RT for 30 min in blocking buffer containing 1 mg/ml BSA, 3% goat serum, 0.1% Triton X-100 and 1 mM EDTA in PBS. Blocked coverslips were incubated with anti-Myc antibody in blocking buffer at RT for 1 hr. After three washes in PBS, coverslips were

incubated with TRITC-conjugated donkey anti-mouse (1:100, Jackson Laboratories) at RT for 30 min. Subsequently, cells on coverslips were fixed again in PBS-buffered 2% paraformaldehyde for 5 min and followed by dehydration in a series of 70, 85 and 100% ethanol. The air-dried coverslips were denatured at 80 °C for 10 min and hybridized with 0.5 µg/ml FITC-conjugated-(CCCTAA)₃ PNA probe (Biosynthesis Inc.) for 2 hr in dark at RT. Following incubation, cover slips were washed with 70% formamide and 10 mM Tris-HCl (pH 7.2) twice for 15 min. After 3 washes in PBS, DNA was counter-stained with 4,6-diamidino-2-phenylindole (DAPI; 0.2 µg/ml) and embedded in 90% glycerol/10% PBS containing 1 mg/ml *p*-phenylene diamine (Sigma). All cell images were recorded on a Zeiss Axioplan 2 microscope with a Hamamatsu C4742-95 camera and processed in Open Lab.

Metaphase chromosome spreads

Metaphase chromosome spreads were essentially prepared as described (19,43). Cells were arrested in nocodazole (0.1 µg/ml) for 90-120 min. Following arrest, cells were harvested by trypsinization, incubated for 7 min at 37°C in 75 mM KCl, and fixed in freshly-made methanol/glacial acetic acid (3:1). Cells were stored overnight at 4°C, dropped onto slides and air-dried overnight in a chemical hood.

FISH analysis on metaphase chromosome spreads was carried out essentially as described (43,47). Slides with chromosome spreads were incubated with 0.5 µg/ml FITC-conjugated-(CCCTAA)₃ PNA probe (Biosynthesis Inc.) for 2 hr at room temperature. Following incubation, slides were washed, counter-stained with 0.2 µg/ml DAPI, and embedded in 90% glycerol/10% PBS containing 1 mg/ml *p*-phenylene diamine (Sigma).

All cell images were recorded on a Zeiss Axioplan 2 microscope with a Hamamatsu C4742-95 camera and processed in Open Lab.

Northern analysis of TERRA

Total RNA was isolated from cells using TRIzol® Reagent (Invitrogen) according to the manufacture's instructions. Northern analysis was performed essentially as described with minor modifications (5). Briefly, 20 µg of RNA was loaded onto 1.3% formaldehyde agarose gels and run at 60 V for 7 hrs. The gel was then stained with ethidium bromide to inspect the presence of the 28S and 18S ribosomal RNA, both of which were indicators of RNA quality. RNA was then transferred to a Nylon membrane (Hybond-N, GE) and was blocked in Church mix (0.5 M Na₂PO₄ [pH 7.2], 1 mM EDTA, 7% SDS, and 1% bovine serum albumin) for 1 hour at 65°C. The membrane was then incubated overnight at 65°C with a radioactively-labeled 800-bp TTAGGG repeat-containing fragment as previously described (44). For the GAPDH control, the membrane was incubated with a radioactively-labeled DNA fragment containing the GAPDH gene. Following incubation, the membrane was washed once with 1X SSC, 0.1% SDS at room temperature, three times in 0.5X SSC at 65°C and then exposed to a PhosphorImager screen. The signals on the membrane were quantified by ImageQuant analysis.

Telomere length analysis and TRAP assays

Genomic DNA isolated from cells was digested with *RsaI* and *HinfI* and loaded onto a 0.7% agarose gel in 0.5xTBE. Blotting for telomeric fragments was carried out according to standard protocols (48,49). The average telomeric restriction fragment length was

determined by PhosphorImager analysis using ImageQuant and MS Excel as described (50).

The activity of telomerase in cells was determined using a Trapeze telomerase detection kit (Chemicon) according to the protocol provided by the manufacturer. PCR amplification was performed for 31 cycles. The products were separated on a 12.5% nondenaturing polyacrylamide gel in 0.5X TBE buffer and visualized using SYBR green (Invitrogen).

2.2.4 Results

Physical interaction between CSB and TRF2

To investigate the role of CSB in telomere biology, we decided to ask whether CSB might interact with components of the shelterin complex essential for telomere maintenance. Coimmunoprecipitation with anti-CSB antibody brought down endogenous TRF2 (Figure. 1B). CSB association with TRF2 was also detected in a reverse immunoprecipitation (IP) using anti-TRF2 antibody and HeLa nuclear extracts (Figure. 1C). The interaction of CSB with TRF2 was further confirmed when Flag-tagged TRF2 was co-expressed with Myc-CSB in 293T cells (Figure. 1D). Taken together, these results reveal that CSB interacts with TRF2 *in vivo*.

To gain further understanding of CSB interaction with TRF2, we examined the interaction between various CSB domains and TRF2. Flag-TRF2 was coexpressed with Myc-tagged CSB-N carrying the first 510 amino acids including the acidic and the glycine-rich domains, Myc-tagged CSB-ATPase containing the central 450 amino acids or Myc-

tagged CSB-C carrying the last 521 amino acids including the nucleotide binding domain (NTB) and ubiquitin binding domain (UBD) in 293T cells. Coimmunoprecipitation studies with anti-Myc antibody revealed that all three CSB truncation mutants were able to pull down Flag-TRF2 (Figure. 1D), suggesting that multiple domains of CSB may be engaged in its interaction with TRF2.

TRF2 contains an N-terminal basic/GAR domain, a central TRFH domain, a linker region and a C-terminal Myb-like DNA binding domain (Figure. 1E). To investigate the domain of TRF2 important for its interaction with CSB, we coexpressed Myc-CSB with Flag-tagged TRF2^{ΔBΔM} lacking both the basic domain and the Myb-like domain, Flag-tagged TRF2 carrying the TRFH dimerization domain alone (Flag-TRF2^{TRFH}) or Flag-tagged TRF2 carrying the linker region alone (Flag-TRF2^{linker}) in 293T cells. Coimmunoprecipitation with anti-Myc antibody showed that both Flag-tagged TRF2^{ΔBΔM} and Flag-tagged TRF2^{TRFH} were able to interact with Myc-CSB (Figure. 1F). In contrast no interaction between Myc-CSB and Flag-TRF2^{linker} was detected despite a high level of expression of Flag-TRF2^{linker} (Figure. 1F). These results suggest that the TRFH domain is required and sufficient for TRF2 interaction with CSB.

CSB localizes at a fraction of human telomeres and is required to suppress the formation telomere dysfunction-induced foci (TIFs) in CS cells.

To investigate whether CSB may be associated with human telomeres, we performed dual indirect immunofluorescence with anti-CSB antibody in conjunction with anti-hRap1 antibody, a marker for interphase telomeres (41). We observed an overlap between

several anti-hRap1 staining (green) and anti-CSB staining (red) foci in HeLa cells (Figure. 2A). The co-localization of CSB with several hRap1 foci was also detected in CSB-complemented immortalized CS cells hTERT-GM10905 (Figure. 2A). In addition, we also performed IF-FISH analysis with anti-Myc antibody in conjunction with a FITC-conjugated telomeric DNA-containing PNA probe in SV40-transformed CS cells GM16095 stably expressing Myc-tagged CSB. We again observed the presence of CSB (red) at several telomeres (green) (Figure. 2B). Taken together, these results suggest that CSB may be associated with a small subset of human telomeres although we cannot rule out the possibility that observed co-staining of CSB with telomeres may be coincidental.

Dysfunctional telomeres are known to attract DNA damage response factors including γ H2AX (7-10). To investigate whether CS cells may accumulate dysfunctional telomeres, dual indirect immunofluorescence was performed on hTERT-GM10905 expressing either CSB or the vector alone with anti-hRap1 antibody in conjunction with anti- γ H2AX antibody. We observed an induction of TIFs in vector-expressing hTERT-GM10905 cells when compared to CSB-complemented hTERT-GM10905 cells (Figure. 2C). While 18% of vector-expressing hTERT-GM10905 cells exhibited five or more TIFs, such TIFs were detected in only 1% of CSB-complemented hTERT-GM10905 cells (Figure. 2D). These results suggest that CSB is required for telomere protection.

Primary fibroblasts derived from CS patients carrying a CSB mutation show an accumulation of telomere doublets.

To investigate whether CSB may be required for maintaining telomere structure, we performed FISH analysis of metaphase spreads on two cell lines (GM10901 and GM10905) at various passages to inspect for the presence of any telomere abnormalities including telomere loss (chromatid ends without a detectable telomeric signal), telomere fusions, telomere-containing double minute chromosomes (TDM) and telomere doublets/fragile telomeres (more than one telomeric signal at a single chromatid end). GM10901 and GM10905 are two respective primary fibroblast cell lines derived from a mother heterozygote for a CSB mutation and her CS offspring. We did not observe any significant accumulation of TDM and telomere fusions in either GM10901 or GM10905 (Figure. 3A). While telomere loss was detected in both GM10901 and GM10905 (Figure. 3B), no significant difference in the formation of telomere loss was found when GM10901 and GM10905 cells of various passages were compared (Figure. 3B). In contrast, we found that various passages of GM10905 cells consistently exhibited an accumulation of telomere doublets when compared to the heterozygote GM10901 cells of similar passages (Figure. 3C).

We also examined the presence of telomere loss and telomere doublets in two other CS cell lines GM1428 and GM739 in comparison to three fibroblast cell lines (GM38, GM9503, GM8399) derived from normal individuals. We found that when compared to the normal control cells, both GM1428 and GM739 displayed an increase in the formation of telomere loss and telomere doublets (Figure. 3D and 3E), the latter

consistent with our earlier finding. No full length CSB was detected in any CS cells examined (Supplementary Figure. S1). Taken together, these results suggest that CSB is required for maintaining the integrity of telomere structure.

Introduction of wild type CSB into CS cells suppresses the formation of telomere doublets.

Formally it is possible that the increased formation of telomere doublets observed in CS primary fibroblasts might be due to the difference in the genetic background between CS cells and normal control cells. To address this question, we decided to examine telomere structures in several pairs of cell lines with isogenic background.

CS primary fibroblasts GM10905 was immortalized with exogenously expressed catalytic subunit of telomerase (hTERT) (Supplementary Figure. S2A) to overcome poor growth and premature senescence associated with CS cells. Subsequently, retrovirus expressing either wild type CSB or the vector alone was used to infect hTERT-GM10905 cells, generating two stable isogenic cell lines (hTERT-GM10905-vector and hTERT-GM10905-CSB). FISH analysis revealed that overexpression of hTERT drastically reduced telomere loss (Figure. 4A and Supplementary Figure. S2B), however, it had little effect on the accumulation of telomere doublets in GM10905 cells (Figure. 4B and Supplementary Figure. S2B). On the other hand, we found that introduction of wild type CSB into hTERT-GM10905 cells led to a reduction in the formation of telomere doublets (Figure. 4C and Supplementary Figure. S3). We observed a 40% decrease ($P = 0.009$) in

the formation of telomere doublets in CSB-complemented hTERT-GM10905 cells when compared to vector-expressing hTERT-GM10905 cells (Figure. 4C).

We also examined the formation of telomere doublets in a second pair of isogenic CS cell lines (GM16095) complemented with either the vector alone or wild type CSB. Introduction of wild type CSB also resulted in a reduction in the formation of telomere doublets in GM16095 (Figure. 4D). To further investigate the role of CSB in the formation of telomere doublets, we knocked down CSB in HeLaI.2.11 cells (Figure. 4E) and found that depletion of CSB led to an induction of telomere doublets (Figure. 4F and Supplementary Figure. S4). Taken together, these results suggest that CSB prevents the formation of telomere doublets.

Aphidicolin, an inhibitor of DNA replication, has been shown to induce telomere doublets (9,51). We found that treatment with aphidicolin resulted in a further increase in the formation of telomere doublets in CS cells (GM16095) (Figure. 4G), consistent with previous findings that the effect of aphidicolin was additive (9,46,48). We also observed an increase in the formation of telomere doublets in CSB-complemented GM16095 cells upon aphidicolin treatment although such increase was less than that observed in GM16095 cells expressing the vector alone (Figure. 4G). These results suggest that telomere doublets observed in CS cells may have arisen from a defect associated with telomere replication.

Introduction of wild type CSB into CS cells promotes telomerase-dependent telomere lengthening.

We observed that the median telomere length in hTERT-immortalized heterozygote mother GM10901 cells was longer than that in hTERT-immortalized CS offspring GM10905 cells (Figure. 5A). Therefore we decided to examine whether CSB might be involved in telomere length maintenance. To address this question, pools (not single cell clones) of hTERT-GM10905 cells stably expressing the vector alone or wild type CSB were continuously cultured for over 60 population doublings (PDs) and their telomere length dynamics was examined. Analysis of telomere restriction fragments revealed that the median telomere length in hTERT-GM10905 cells expressing the vector alone declined at a rate of about 11.6 bp/PD whereas the median telomere length increased at a rate of 21.5 bp/PD for the first 42 PDs and then plateaued in hTERT-GM10905 cells expressing wild type CSB (Figure. 5B and 5C). A decline in the level of CSB expression in hTERT-GM10905-CSB cells was noticed after PD60 (Figure. 5D), suggesting that the loss of CSB expression may in part contribute to the plateau of the median telomere length seen between PD42 and PD61 in these cells. We did not observe any significant difference in the growth rate between hTERT-GM10905-vector and hTERT-GM10905-CSB cells (Figure. 5E). Taken together, these results suggest that CSB is required for telomerase-dependent telomere elongation.

We also performed ChIP analysis with an antibody against TRF1 or TRF2, both of which are mediators of telomere length maintenance (14-16,42). We found that introduction of wild type CSB into hTERT-GM10905 cells had little effect on telomeric

association of TRF2 (Figure. 5F and 5G) but it led to a significant decrease in TRF1 association with telomeric DNA (Figure. 5F and 5G). When compared to CSB-complemented hTERT-GM10905 cells, we observed a 54% ($P = 0.006$) increase in the amount of telomere-bound TRF1 in hTERT-GM10905 cells expressing the vector alone (Figure. 5G). The level of TRF1 in the vector-expressing hTERT-GM10905 cells was indistinguishable from that in the CSB-complemented hTERT-GM10905 cells (Figure. 5H). These results suggest that association of TRF1 with telomeric DNA may be deregulated in CS cells carrying a CSB mutation.

CSB is required for maintaining the homeostatic level of TERRA.

CSB has been implicated in transcription (32-35) and therefore we decided to examine whether CSB may be involved in regulating the expression of TERRA, a large non-coding telomere repeat-containing RNA (5). Northern analysis on three pairs of isogenic cell lines revealed a misregulation of TERRA associated with CS cells or CSB knockdown cells. We observed a 35% increase ($P = 0.017$) in the level of TERRA in hTERT-GM10905 expressing the vector alone when compared to hTERT-GM10905 cells complemented with wild type CSB (Figure. 6A and 6B). On the other hand, the level of TERRA in GM16095 cells expressing the vector alone was about 45% ($P = 0.016$) less than that in GM16095 complemented with wild type CSB (Figure. 6C and 6D). Knockdown of CSB led to a 38% ($P = 0.038$) reduction in the level of TERRA in HeLaI.2.11 cells (Figure. 6E and 6F). These results suggest that CSB is required for the homeostatic level of TERRA and that the level

of TERRA may increase or decrease in CS cells depending upon the nature of CSB mutations.

2.2.5 Discussion

CSB, a multifunctional protein, plays an important role in DNA repair, transcription and chromatin remodeling. In this report, we have uncovered a role for CSB in telomere maintenance and protection. We have shown that CSB interacts physically with TRF2, a key component of the shelterin complex essential for telomere maintenance. We have demonstrated that CS cells or CSB knockdown cells exhibit an accumulation of telomere doublets and an induction of TIF formation. We have shown that CS cells carrying a CSB mutation are defective in telomerase-dependent telomere elongation whereas introduction of CSB into CS cells results in telomerase-dependent telomere elongation, suggesting that CSB is required for telomere length maintenance. Furthermore, we have shown that the level of TERRA is misregulated in CS cells or CSB knockdown cells. Taken together, these results reveal an important role of CSB in the maintenance of telomere length and integrity. These results further imply that CS patients lacking functional CSB are defective in telomere maintenance, which is associated with cancer and aging.

Our coimmunoprecipitation studies suggest that a small percentage of endogenous TRF2 (estimated to be about 1-5%) interacts with CSB and vice versa. This low level of interaction is similar to previously reported association between TRF2 and several other DNA repair proteins including XPF/ERCC1 and Mre11/Rad50/Nbs1 (40,43), indicating that CSB interaction with TRF2 may be dependent upon a specific functional requirement.

Analysis of domain mapping suggests that the TRFH domain of TRF2 is sufficient and required for its interaction with CSB. The TRFH domain of TRF2 has been shown to interact with proteins containing the Y/FxLxP motif (17,18). CSB contains one YxLxP motif corresponding to amino acids 402-406 but also seven degenerate Y/FxLxx motifs spread throughout the entire protein. Double mutations at positions L404 and P406 did not abrogate CSB interaction with TRF2 (T.R.H. Mitchell and X.D. Zhu, unpublished data). These results, in conjunction with our finding that multiple domains of CSB are engaged in its interaction with TRF2 raise the possibility that TRF2 might interact with degenerate Y/FxLxx motifs of CSB. Alternatively TRF2 may interact with CSB through a mechanism independent of Y/FxLxP motifs. Future studies are required to investigate the mechanism underlying CSB interaction with TRF2.

The physical interaction between TRF2 and CSB raises the possibility that TRF2 may play a role in recruiting and/or modulating CSB function at telomeres. We have observed localization of CSB at a small subset of human telomeres. Several shelterin accessory proteins have been reported to localize at one or a few human telomeres including HP1, BLM, PNUITS and MCPH1 (52-54). Perhaps, like these shelterin accessory factors, CSB might be needed by only a few telomeres at a given time although we cannot rule out the possibility that the colocalization of CSB with a few telomeres may be coincidental.

We have shown that overexpression of wild type CSB has little effect on the telomere association of TRF2 but results in a reduction in the amount of telomere-bound TRF1, a negative mediator of telomerase-dependent telomere elongation. Perhaps, the reduction in the level of telomere-bound TRF1 may in part contribute to the telomerase-

dependent telomere elongation observed in CSB-expressing hTERT-GM10905 cells. We have not been able to detect any interaction between CSB and endogenous TRF1 (T.R.H Mitchell and X.D. Zhu, unpublished data), suggesting that the effect of CSB on TRF1 binding to telomeric DNA may be indirect.

While we have observed a greater accumulation of telomere loss in CS primary fibroblast GM739 (p19) and GM1428 cells (p15) than in the control cells GM38 (p19) and GM9503 (p18), no significant difference in the formation of telomere loss has been detected between the heterozygote mother GM10901 and her CS offspring GM10905. It is possible that the lack of difference in telomere loss between the heterozygote mother and her CS offspring may be due to CSB haploinsufficiency. Alternatively, the level of accumulation of telomere loss observed in CS cells may vary depending upon their genetic background.

We have found that while knockdown of CSB leads to a reduction in the level of TERRA, overexpression of wild type CSB can have an opposite effect on the level of TERRA in CS cells. Introduction of wild type CSB into CS cells hTERT-GM10905 results in a decrease in the level of TERRA whereas introduction of wild type CSB into CS cells GM16095 leads to an increase in the level of TERRA. Both CS cell lines carry a nonsense mutation (Supplementary Table S1), which converts R735 to a stop codon in GM10905 (22,55) and K337 to a stop codon in GM16095 (27). The level of overexpressed CSB in hTERT-GM10905 cells is comparable to that in GM16095 (N. Batenburg, T.R.H. Mitchell and X.D. Zhu, unpublished data), suggesting that it is unlikely that exogenously-expressed CSB may account for its opposite effect on the level of TERRA in these two cell lines.

Although both cell lines do not express full length CSB, GM10905 cells express a CSB-PiggyBac fusion protein (Figure. 5D) (56), which is not present in GM16095 (27). CSB-PiggyBac is a product of alternative splicing involving the first 5 exons of CSB and a conserved PiggyBac transposable element (PGBD3) located within the intron 5 of the CSB gene (56). How overexpression of CSB differentially affects the level of TERRA remains unknown. Our finding suggests that the nature of CSB mutations may play a role in influencing TERRA expression. Taken together, our data suggest that CSB is required for maintaining the homeostatic level of TERRA, excess expression or depletion of which has been shown to impair the maintenance of telomere length and integrity (5,6,57,58).

We have shown that CSB mutations or CSB depletion promotes the formation of telomere doublets, also known as fragile telomeres (9,51). It has been shown that fragile telomeres can arise from a defect in telomere replication (9,51). Consistent with this notion, we have observed that treatment with aphidicolin further induces the formation of telomere doublets in CS cells, suggesting that telomere replication is compromised in CS cells. It is likely that the compromised telomere replication in CS cells may be in part caused by misregulation of TERRA, an integral component of telomere heterochromatin. Perhaps misregulation of TERRA associated with CS cells could lead to an altered telomere heterochromatin, which could impede the progression of replication fork.

Acknowledgements

We are grateful to Titia de Lange (Rockefeller University) for providing various reagents, including TRF2 cDNA, retroviral vectors and antibodies to TRF1, TRF2 and hRap1. We

thank John R. Walker for providing critical comments. N.L.B., T.R.H.M. and X.D.Z. designed experiments, interpreted the data and wrote the manuscript. N.L.B. and T.R.H.M. performed all experiments described. T.R.H.M. and D.M.L. conceptualized and performed initial experiments identifying the interaction between CSB and TRF2. D.M.L. and A.J.R. provided intellectual input.

Funding

Cancer Research Society (grant number 16208) to X.-D.Z. and funding from Canadian Cancer Society to A.J.R. (grant number 16066). T.R.H.M is a holder of Ontario Graduate Scholarship.

Conflict of interest statement

None declared.

2.2.6 Figures and figure legends

Figure 1 Batenburg et al.

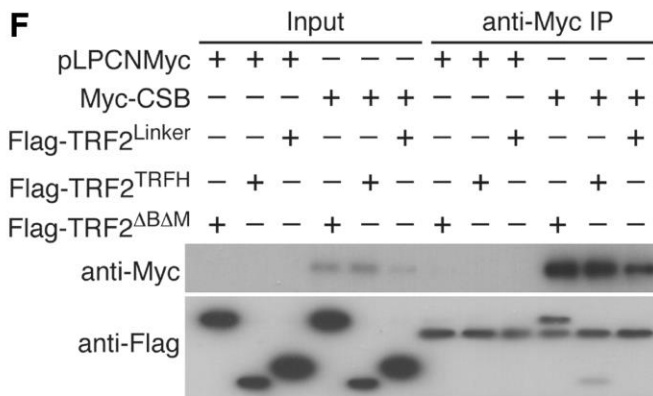
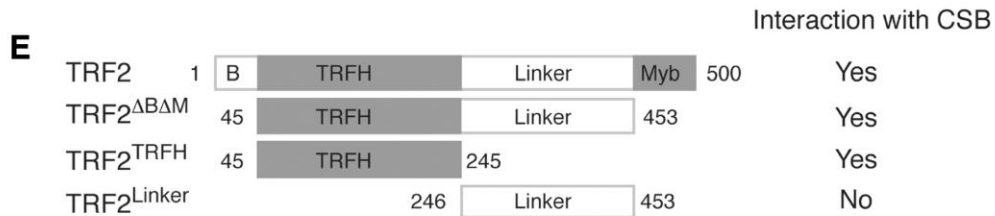
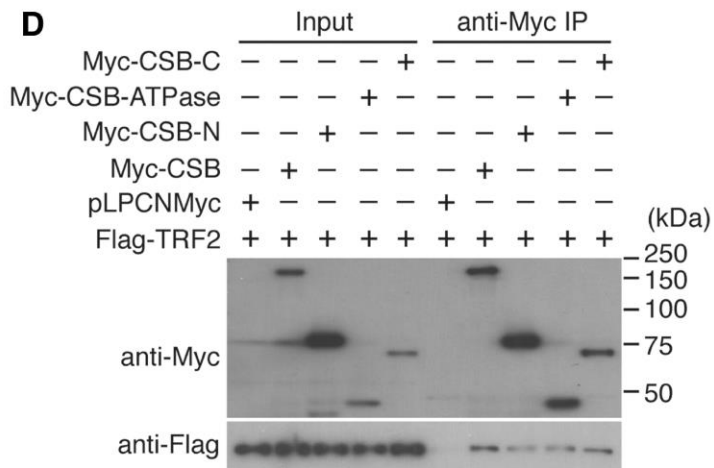
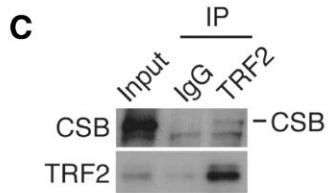
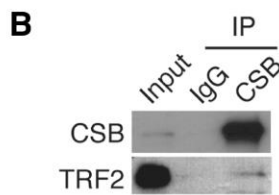
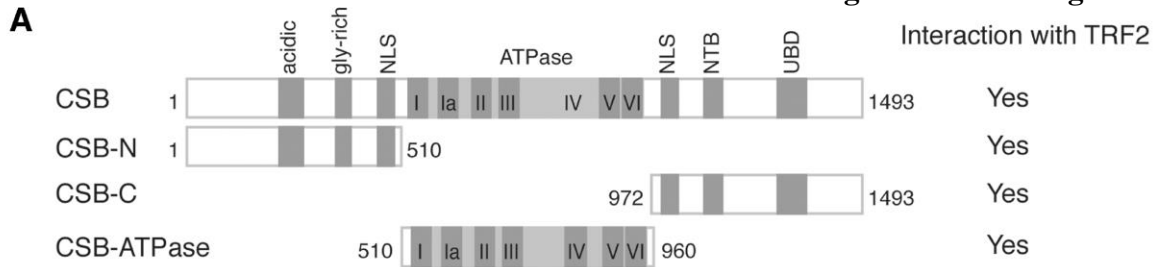


Figure 1. CSB interacts physically with TRF2. **(A)** Schematic diagram of CSB. NLS, NTB and UBD stand for nuclear localization sequence, nucleotide binding domain and ubiquitin binding domain respectively. **(B)** Coimmunoprecipitation with HeLa cell extracts and anti-CSB antibody. Anti-IgG IP was used as a negative control. Immunoblotting was carried out with anti-CSB or anti-TRF2 antibody. **(C)** Coimmunoprecipitation with HeLa nuclear extracts and anti-TRF2 antibody. Anti-IgG IP was used as a negative control. Immunoblotting was carried out with anti-CSB or anti-TRF2 antibody. **(D)** Immunoprecipitation with anti-Myc antibody was carried out with protein extracts from 293T cells coexpressing Flag-TRF2 in conjunction with either the vector alone, Myc-CSB, Myc-CSB-N, Myc-CSB-ATPase or Myc-CSB-C. Immunoblotting was performed with anti-Myc or anti-Flag antibody. **(E)** Schematic diagram of TRF2. B stands for basic domain. **(F)** Immunoprecipitation with anti-Myc antibody was carried out with protein extracts from 293T cells coexpressing the vector or Myc-CSB in conjunction with Flag-TRF2^{linker}, Flag-TRF2^{TRFH} or Flag-TRF2^{ΔBΔM}. Immunoblotting was performed with anti-Myc or anti-Flag antibody.

Figure 2 Batenburg et al.

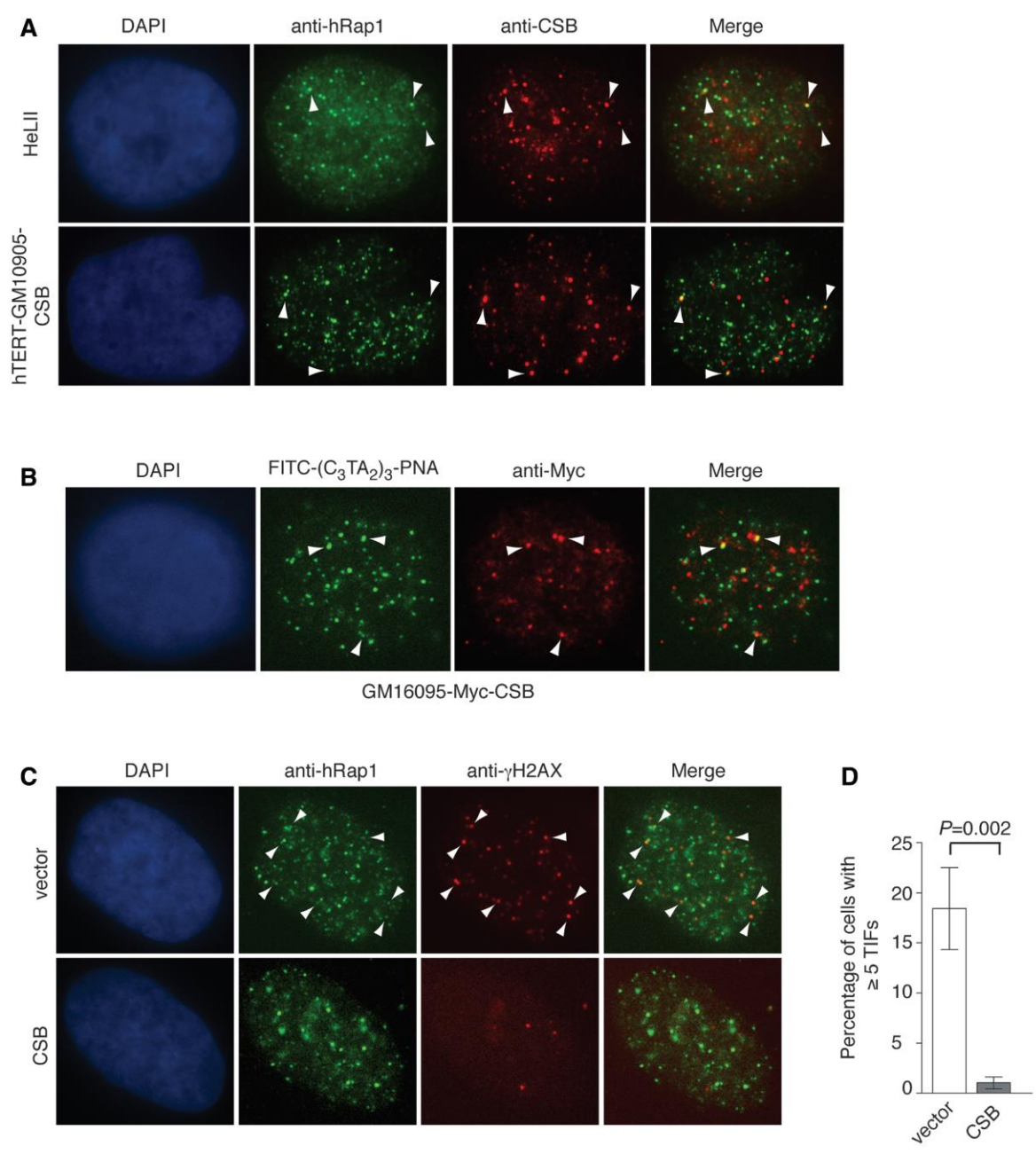


Figure 2. CSB localizes at a small subset of human telomeres and prevents the formation of TIFs in CS cells. **(A)** Analysis of indirect immunofluorescence (IF) on HeLaII and CSB-complemented hTERT-GM10905 cells. IF was performed with mouse anti-CSB (red) in conjunction with rabbit anti-hRap1 (green). Cells were extracted with detergent prior to fixation by formaldehyde to remove soluble proteins. Cell nuclei were stained with DAPI shown in blue. Arrowheads indicate the overlap between anti-CSB and anti-hRap1 staining. **(B)** Analysis of IF-FISH on GM16095 cells expressing Myc-CSB. IF-FISH analysis was performed with anti-Myc antibody (red) in conjunction with a FITC-conjugated (CCCTAA)₃-containing PNA probe (green). Cell nuclei were stained with DAPI shown in blue. Arrowheads indicate the colocalization of CSB with telomeric DNA. **(C)** Indirect immunofluorescence using anti-hRap1 in conjunction with anti- γ -H2AX was performed with fixed hTERT-GM10905 cells expressing either the vector alone or wild type CSB. Arrowheads indicate sites of colocalization of γ H2AX and hRap1. **(D)** Quantification of percentage of cells with five or more TIFs. For each cell line, a total of 300 cells from three independent experiments were scored. Standard deviations from three independent experiments are indicated.

Figure 3 Batenburg et al.

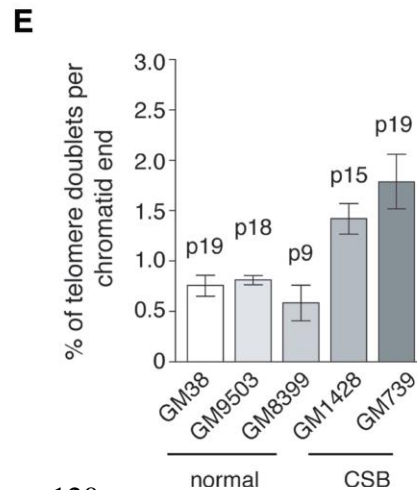
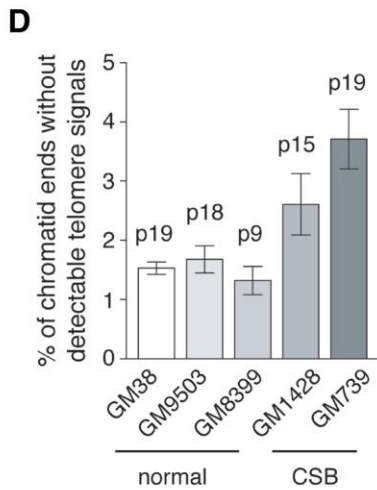
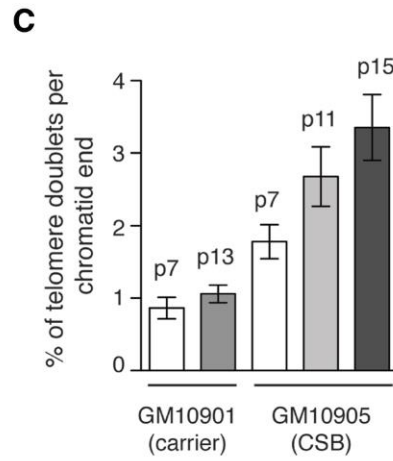
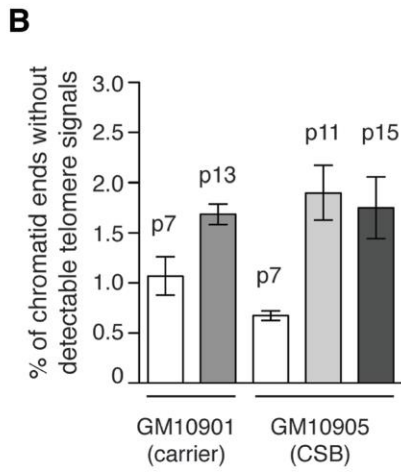
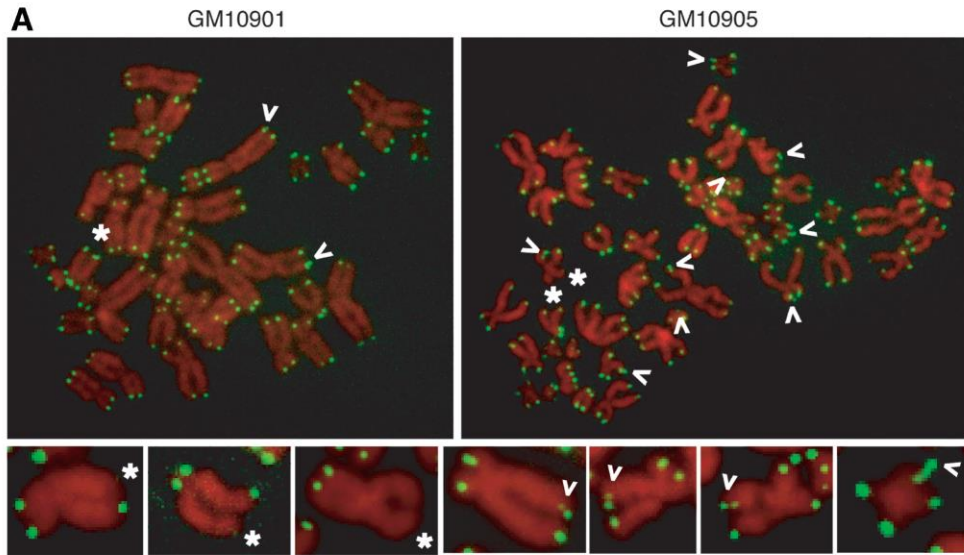


Figure 3. CS primary fibroblasts carrying CSB mutations accumulate telomere doublets. (A) Analysis of metaphase chromosomes from GM10901 and GM10905. Chromosomes were stained with DAPI and false colored in red. Telomeric DNA was detected by FISH using a FITC-conjugated (CCCTAA)₃-containing PNA probe (green). Open arrows represent telomere doublets whereas asterisks indicate telomere loss. Enlarged images of chromosomes with telomere doublets or telomere loss are shown at the bottom. (B-E) Quantification of telomere loss or telomere doublets from indicated cell lines. For each cell line, a total of 2410 to 2699 chromosomes from 60 metaphase cells were scored in a blind manner for the presence of telomere loss (B & D) as well as telomere doublets in (C & E). Standard deviations derived from three independent experiments are indicated. Passage numbers of cell lines used are indicated above the bars.

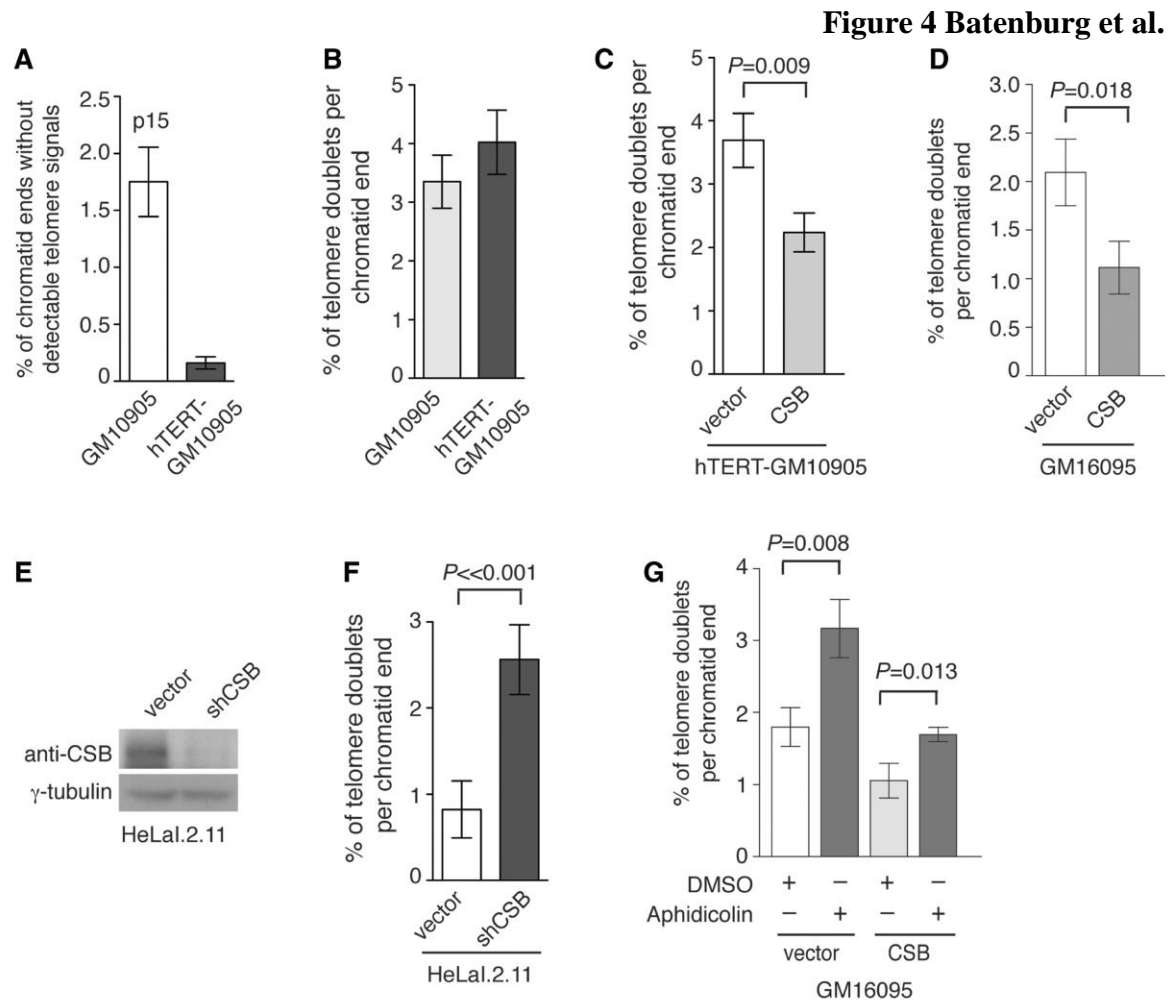


Figure 4. CSB is required to prevent the formation of telomere doublets. (A) Quantification of telomere loss from indicated cell lines. For each cell line, a total of at least 2649 to 2668 chromosomes from 60 metaphase cells were scored in a blind manner. Standard deviations derived from three independent experiments are indicated. (B) Quantification of telomere doublets from indicated cell lines. For each cell line, a total of 2649 to 2668 chromosomes from 60 metaphase cells were scored in a blind manner. Standard deviations derived from three independent experiments are indicated. (C) Quantification of telomere doublets from

hTERT-GM10905 cells expressing indicated constructs. For each cell line, a total of 2707 to 2754 chromosomes from 60 metaphase cells were scored in a blind manner. Standard deviations derived from three independent experiments are indicated. **(D)** Quantification of telomere doublets from GM16095 cells expressing indicated constructs. For each cell line, a total of 4774 to 4923 chromosomes from 60 metaphase cells were scored in a blind manner. Standard deviations derived from three independent experiments are indicated. **(E)** Western analysis of CSB expression. CSB was stably knocked down in HeLaI.2.11 cells. Immunoblotting was performed with anti-CSB or anti- γ -tubulin antibody. The latter was used as a loading control. **(F)** Quantification of telomere doublets from HeLaI.2.11 cells expressing the vector alone or pRS-shCSB. For each cell line, a total of 2678 to 2961 chromosomes from at least 43 metaphase cells were scored in a blind manner. Standard deviations derived from three independent experiments are indicated. **(G)** Quantification of telomere doublets from GM16095 cells expressing indicated constructs. Cells were treated with DMSO or aphidicolin (0.2 μ M) for 16 hr. For each cell line, a total of 3879 to 4321 chromosomes from 51-53 metaphase cells were scored in a blind manner. Standard deviations derived from three independent experiments are indicated.

Figure 5 Batenburg et al.

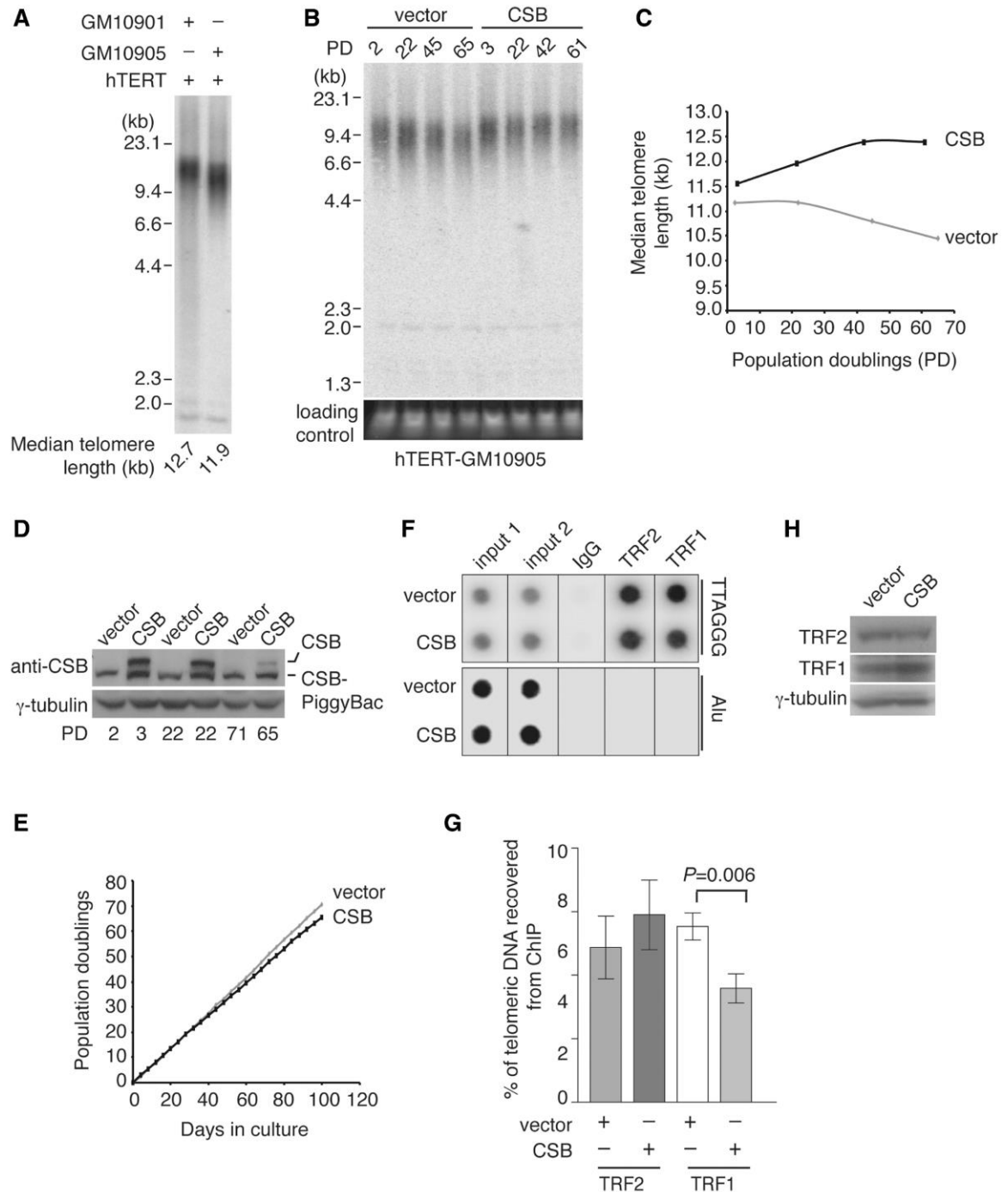


Figure 5. CSB is required for telomere length maintenance. (A) Genomic blot of telomeric restriction fragments from hTERT-immortalized GM10901 and GM10905 cells. About 3

μg of *RsaI/HinfI*-digested genomic DNA from each sample was used for gel electrophoresis. DNA molecular weight markers are shown on the left of the blot. Median telomere length of indicated cell lines are shown on the bottom of the blot. **(B)** Genomic blots of telomeric restriction fragments from hTERT-GM10905 cells expressing either the vector alone or wild type CSB as indicated above the lanes. About 3 μg of *RsaI/HinfI*-digested genomic DNA from each sample was used for gel electrophoresis. Population doublings (PD) are indicated above the lanes whereas DNA molecular weight markers are shown on the left of the blots. The bottom panel, taken from an ethidium bromide-stained agarose gel, is used as a loading control. **(C)** Median telomere length of indicated cell lines was plotted against population doublings. **(D)** Western analysis of CSB expression in hTERT-GM10905 cells. Immunoblotting was performed with anti-CSB or anti- γ -tubulin antibody. The indicated CSB-PiggyBac fusion protein is a product of alternative splicing involving the first 5 exons of CSB and a conserved PiggyBac transposable element (PGBD3) located within the intron 5 of the CSB gene (56). **(E)** Growth curve of hTERT-GM10905 cells expressing various constructs as indicated. The number of PDs was plotted against days in culture. **(F)** Dot blots of ChIPs with anti-TRF1 or anti-TRF2 antibody. ChIPs were performed with lysates from hTERT-GM10905 cells expressing either the vector alone or wild type CSB. Anti-IgG ChIP was used as a control. **(G)** Quantification of ChIPs from (E). The signals from dot blots were quantified by ImageQuant (IQ) analysis. Standard deviations from three independent experiments are shown. **(H)** Western analysis of protein expression. Immunoblotting was carried out with anti-TRF1, anti-TRF2 or anti- γ -tubulin antibody.

Figure 6 Batenburg et al.

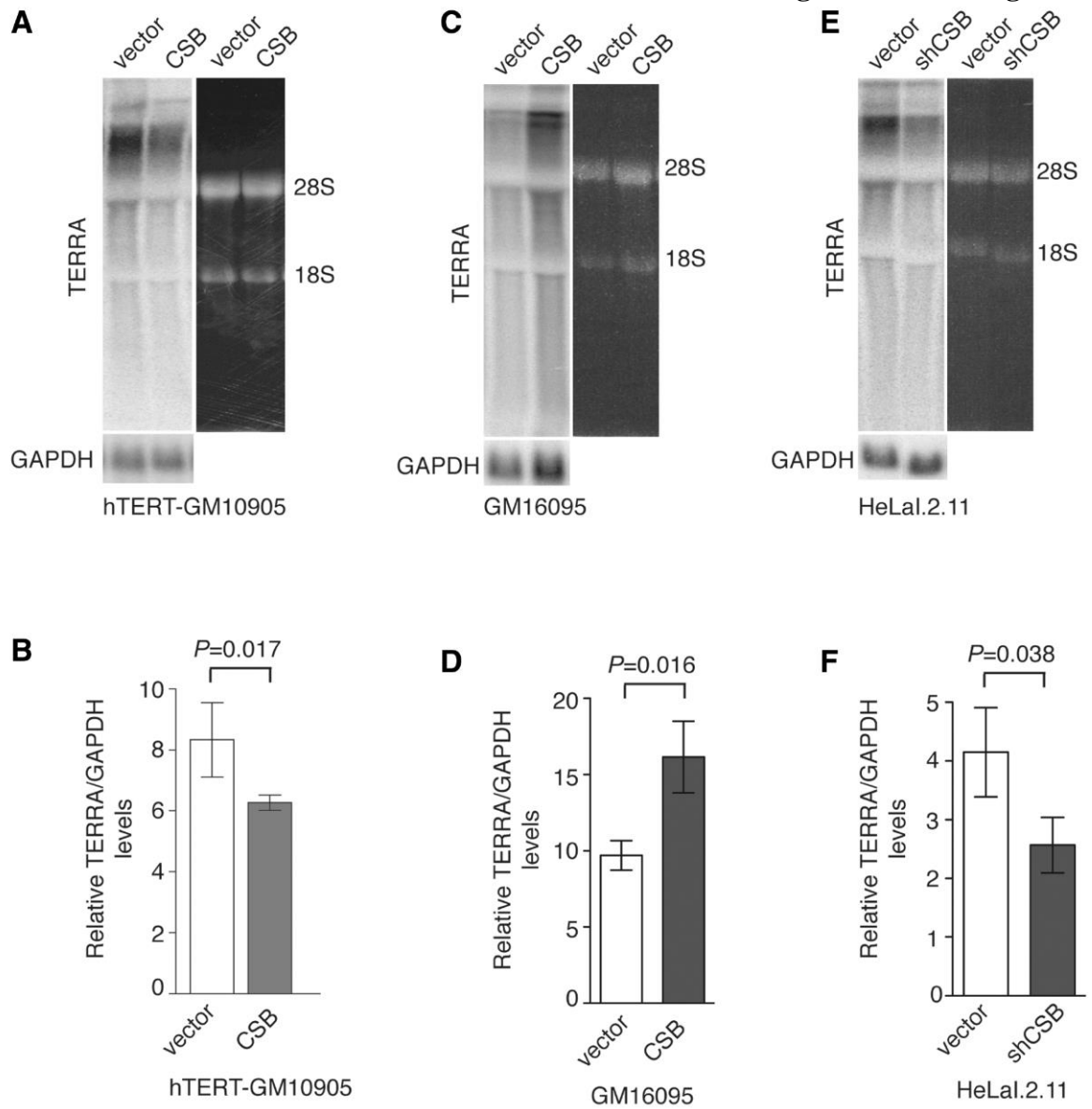


Figure 6. CSB is required for maintaining the homeostatic level of TERRA. **(A)** Analysis of TERRA expression from hTERT-GM10905 cells expressing the vector alone or CSB. Northern blotting was performed with a ³²P-labeled telomeric DNA-containing probe shown on the left top panel. The northern blot of GAPDH shown on the left bottom panel was used as a loading control. The right panel was taken from the ethidium bromide-stained agarose gel. The position of 28S or 18S ribosomal RNA is indicated. **(B)** Quantification of relative TERRA levels from (A). The signals from northern blots were quantified by ImageQuant analysis. The TERRA signal from each lane was normalized to the GAPDH signal in the corresponding lane, giving rise to the relative level of TERRA to GAPDH. **(C)** Northern analysis of TERRA expression from GM16095 cells expressing the vector alone or wild type CSB. The northern blot of GAPDH shown on the left bottom panel was used as a loading control. The right panel was taken from the ethidium bromide-stained agarose gel. The position of 28S or 18S ribosomal RNA is indicated. **(D)** Quantification of relative TERRA levels from (C). Quantification was performed as described in (B). **(E)** Northern analysis of TERRA expression from HeLaI.2.11 cells stably expressing the vector alone or pRS-shCSB. The northern blot of GAPDH shown on the left bottom panel was used as a loading control. The right panel was taken from the ethidium bromide-stained agarose gel. The position of 28S or 18S ribosomal RNA is indicated. **(F)** Quantification of relative TERRA levels from (E). Quantification was performed as described in (B).

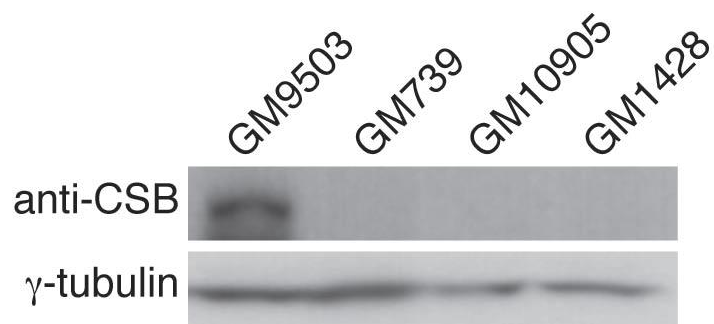
Supplementary Figure S1 Batenburg et al.

Figure S1. Western analysis of CSB expression in normal and CS primary fibroblasts.

Immunoblotting was carried out with anti-CSB or anti- γ -tubulin antibody. The latter was used as a loading control.

Supplementary Figure S2 Batenburg et al.

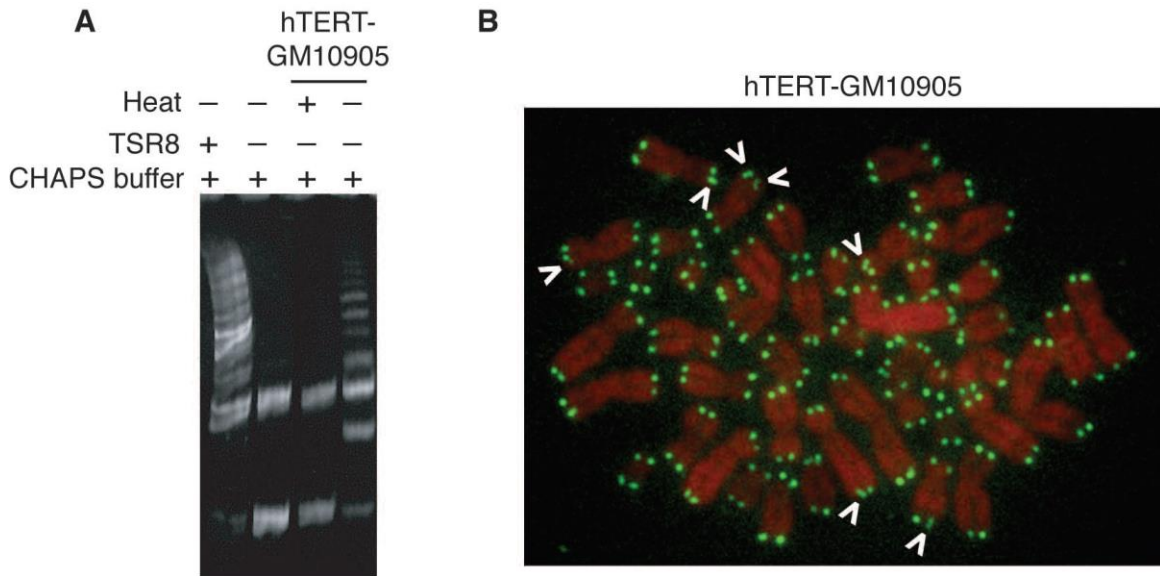


Figure S2. (A) Analysis of hTERT expression in GM10905 cells. One thousand cells of hTERT immortalized GM10905 cells were used to measure telomerase activity. TSR8 was used as a positive control whereas 3-[(3-cholamidopropyl)-dimethylammonio]-1-propanesulfonate buffer (CHAPS) was used as a negative control. (B) Analysis of metaphase chromosomes from hTERT-GM10905. Chromosomes were stained with DAPI and false colored in red. Telomeric DNA was detected by FISH using a FITC-conjugated (CCCTAA)₃-containing PNA probe (green).

Supplementary Figure S3 Batenburg et al.

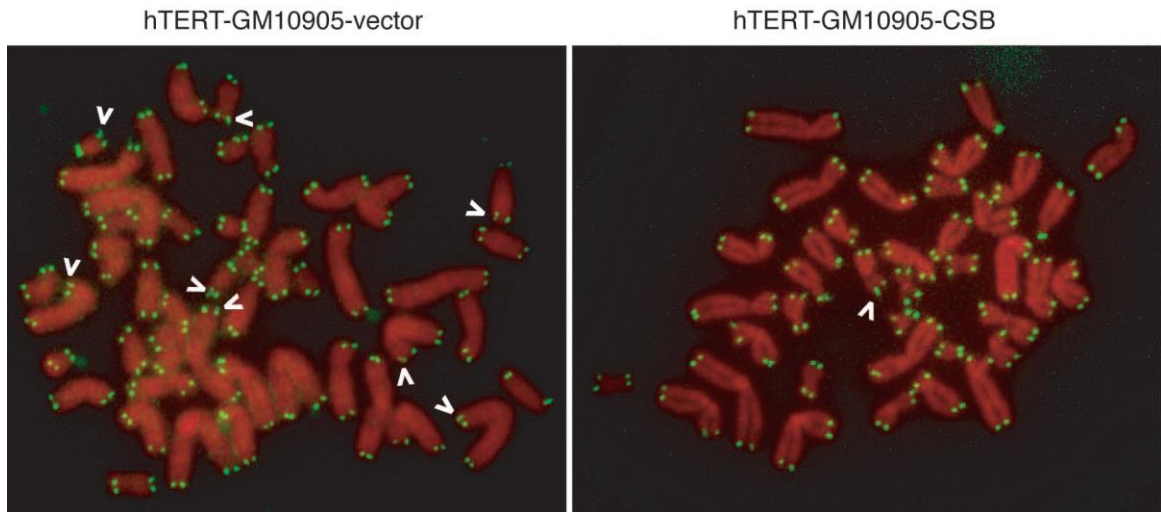


Figure S3. Analysis of metaphase chromosomes from hTERT-GM10905 stably expressing either the vector alone or wild type CSB. Chromosomes were stained with DAPI and false colored in red. Telomeric DNA was detected by FISH using a FITC-conjugated (CCCTAA)₃-containing PNA probe (green). Open arrows represent telomere doublets.

Supplementary Figure S4 Batenburg et al.

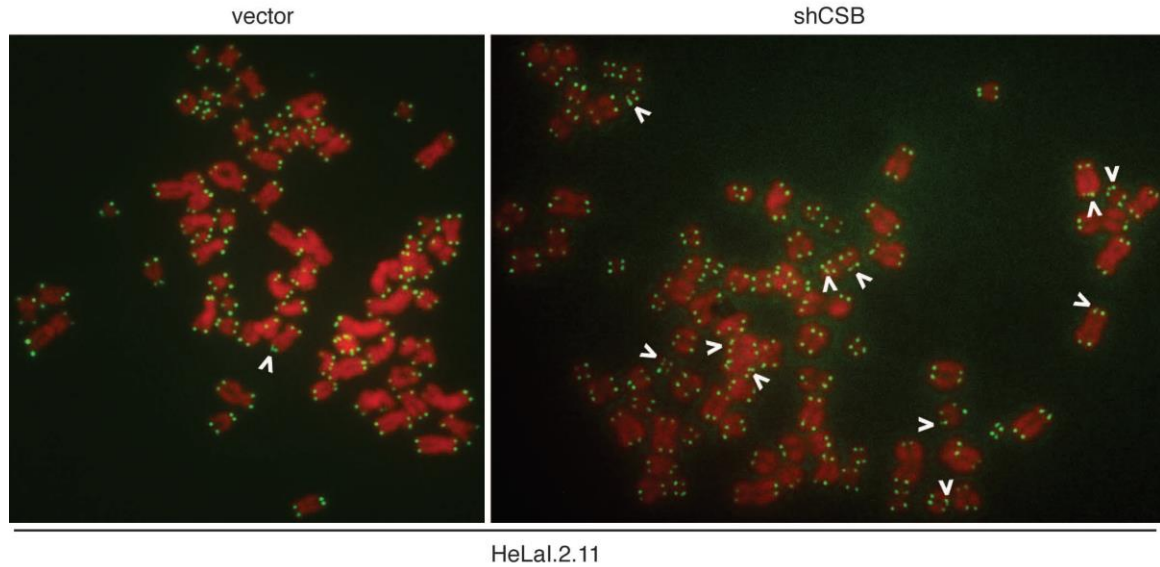


Figure S4. Analysis of metaphase chromosomes from HeLaI.2.11 stably expressing either the vector alone or pRS-shCSB. Chromosomes were stained with DAPI and false colored in red. Telomeric DNA was detected by FISH using a FITC-conjugated (CCCTAA)₃-containing PNA probe (green). Open arrows represent telomere doublets.

Supplementary Table S1. Summary of normal and CS primary fibroblast cell lines used.

Cell Line	Age at Biopsy	CSB Allele 1	CSB Allele 2	Source
GM38	9 YR	Normal	Normal	NIGMS
GM9503	10 YR	Normal	Normal	NIGMS
GM8399	19 YR	Normal	Normal	NIGMS
GM10901	42 YR	R735X	Normal	NIGMS
GM10905	10 YR	R735X	R735X	NIGMS
GM739	3 YR	R377X	R857X	NIGMS
GM1428	8 YR	N/A	N/A	NIGMS

2.2.7 References

1. de Lange, T. (2005) Shelterin: the protein complex that shapes and safeguards human telomeres. *Genes Dev*, **19**, 2100-2110.
2. Palm, W. and de Lange, T. (2008) How shelterin protects Mammalian telomeres. *Annu Rev Genet*, **42**, 301-334.
3. Liu, D., O'Connor, M.S., Qin, J. and Songyang, Z. (2004) Telosome, a mammalian telomere-associated complex formed by multiple telomeric proteins. *J Biol Chem*, **279**, 51338-51342.
4. Walker, J.R. and Zhu, X.D. (2012) Post-translational modification of TRF1 and TRF2 and their roles in telomere maintenance. *Mechanisms of ageing and development*, **133**, 421-434.
5. Azzalin, C.M., Reichenbach, P., Khoriantuli, L., Giulotto, E. and Lingner, J. (2007) Telomeric repeat containing RNA and RNA surveillance factors at mammalian chromosome ends. *Science*, **318**, 798-801.
6. Deng, Z., Norseen, J., Wiedmer, A., Riethman, H. and Lieberman, P.M. (2009) TERRA RNA binding to TRF2 facilitates heterochromatin formation and ORC recruitment at telomeres. *Mol Cell*, **35**, 403-413.
7. Takai, H., Smogorzewska, A. and de Lange, T. (2003) DNA damage foci at dysfunctional telomeres. *Curr Biol*, **13**, 1549-1556.
8. Wang, R.C., Smogorzewska, A. and de Lange, T. (2004) Homologous recombination generates T-loop-sized deletions at human telomeres. *Cell*, **119**, 355-368.
9. Sfeir, A., Kosiyatrakul, S.T., Hockemeyer, D., MacRae, S.L., Karlseder, J., Schildkraut, C.L. and de Lange, T. (2009) Mammalian telomeres resemble fragile sites and require TRF1 for efficient replication. *Cell*, **138**, 90-103.
10. Mitchell, T.R., Glenfield, K., Jeyanthan, K. and Zhu, X.D. (2009) Arginine methylation regulates telomere length and stability. *Molecular and cellular biology*, **29**, 4918-4934.
11. Broccoli, D., Smogorzewska, A., Chong, L. and de Lange, T. (1997) Human telomeres contain two distinct Myb-related proteins, TRF1 and TRF2. *Nature genetics*, **17**, 231-235.
12. Bilaud, T., Brun, C., Ancelin, K., Koering, C.E., Laroche, T. and Gilson, E. (1997) Telomeric localization of TRF2, a novel human telobox protein. *Nat Genet*, **17**, 236-239.
13. Chong, L., van Steensel, B., Broccoli, D., Erdjument-Bromage, H., Hanish, J., Tempst, P. and de Lange, T. (1995) A human telomeric protein. *Science*, **270**, 1663-1667.
14. van Steensel, B. and de Lange, T. (1997) Control of telomere length by the human telomeric protein TRF1 [see comments]. *Nature*, **385**, 740-743.
15. Smogorzewska, A., van Steensel, B., Bianchi, A., Oelmann, S., Schaefer, M.R., Schnapp, G. and de Lange, T. (2000) Control of human telomere length by TRF1 and TRF2. *Mol Cell Biol*, **20**, 1659-1668.

16. Ancelin, K., Brunori, M., Bauwens, S., Koering, C.E., Brun, C., Ricoul, M., Pommier, J.P., Sabatier, L. and Gilson, E. (2002) Targeting assay to study the cis functions of human telomeric proteins: evidence for inhibition of telomerase by TRF1 and for activation of telomere degradation by TRF2. *Molecular and cellular biology*, **22**, 3474-3487.
17. Chen, Y., Yang, Y., van Overbeek, M., Donigian, J.R., Baciú, P., de Lange, T. and Lei, M. (2008) A shared docking motif in TRF1 and TRF2 used for differential recruitment of telomeric proteins. *Science*, **319**, 1092-1096.
18. Kim, H., Lee, O.H., Xin, H., Chen, L.Y., Qin, J., Chae, H.K., Lin, S.Y., Safari, A., Liu, D. and Songyang, Z. (2009) TRF2 functions as a protein hub and regulates telomere maintenance by recognizing specific peptide motifs. *Nat Struct Mol Biol*, **16**, 372-379.
19. van Steensel, B., Smogorzewska, A. and de Lange, T. (1998) TRF2 protects human telomeres from end-to-end fusions. *Cell*, **92**, 401-413.
20. Celli, G.B. and de Lange, T. (2005) DNA processing is not required for ATM-mediated telomere damage response after TRF2 deletion. *Nat Cell Biol*, **7**, 712-718.
21. Stevensner, T., Muftuoglu, M., Aamann, M.D. and Bohr, V.A. (2008) The role of Cockayne Syndrome group B (CSB) protein in base excision repair and aging. *Mech Ageing Dev*, **129**, 441-448.
22. Laugel, V., Dalloz, C., Durand, M., Sauvanaud, F., Kristensen, U., Vincent, M.C., Pasquier, L., Odent, S., Cormier-Daire, V., Gener, B. *et al.* (2009) Mutation update for the CSB/ERCC6 and CSA/ERCC8 genes involved in Cockayne syndrome. *Hum Mutat*, **31**, 113-126.
23. van der Horst, G.T., van Steeg, H., Berg, R.J., van Gool, A.J., de Wit, J., Weeda, G., Morreau, H., Beems, R.B., van Kreijl, C.F., de Gruijl, F.R. *et al.* (1997) Defective transcription-coupled repair in Cockayne syndrome B mice is associated with skin cancer predisposition. *Cell*, **89**, 425-435.
24. Leech, R.W., Brumback, R.A., Miller, R.H., Otsuka, F., Tarone, R.E. and Robbins, J.H. (1985) Cockayne syndrome: clinicopathologic and tissue culture studies of affected siblings. *J Neuropathol Exp Neurol*, **44**, 507-519.
25. Mallery, D.L., Tanganelli, B., Colella, S., Steingrimsdottir, H., van Gool, A.J., Troelstra, C., Stefanini, M. and Lehmann, A.R. (1998) Molecular analysis of mutations in the CSB (ERCC6) gene in patients with Cockayne syndrome. *Am J Hum Genet*, **62**, 77-85.
26. Eisen, J.A., Sweder, K.S. and Hanawalt, P.C. (1995) Evolution of the SNF2 family of proteins: subfamilies with distinct sequences and functions. *Nucleic Acids Res*, **23**, 2715-2723.
27. Troelstra, C., van Gool, A., de Wit, J., Vermeulen, W., Bootsma, D. and Hoeijmakers, J.H. (1992) ERCC6, a member of a subfamily of putative helicases, is involved in Cockayne's syndrome and preferential repair of active genes. *Cell*, **71**, 939-953.
28. Anindya, R., Mari, P.O., Kristensen, U., Kool, H., Giglia-Mari, G., Mullenders, L.H., Foustieri, M., Vermeulen, W., Egly, J.M. and Svejstrup, J.Q. (2010) A

- ubiquitin-binding domain in Cockayne syndrome B required for transcription-coupled nucleotide excision repair. *Mol Cell*, **38**, 637-648.
29. Hoeijmakers, J.H. (2001) Genome maintenance mechanisms for preventing cancer. *Nature*, **411**, 366-374.
 30. Tuo, J., Jaruga, P., Rodriguez, H., Dizdaroglu, M. and Bohr, V.A. (2002) The cockayne syndrome group B gene product is involved in cellular repair of 8-hydroxyadenine in DNA. *J Biol Chem*, **277**, 30832-30837.
 31. Tuo, J., Jaruga, P., Rodriguez, H., Bohr, V.A. and Dizdaroglu, M. (2003) Primary fibroblasts of Cockayne syndrome patients are defective in cellular repair of 8-hydroxyguanine and 8-hydroxyadenine resulting from oxidative stress. *Faseb J*, **17**, 668-674.
 32. Bradsher, J., Auriol, J., Proietti de Santis, L., Iben, S., Vonesch, J.L., Grummt, I. and Egly, J.M. (2002) CSB is a component of RNA pol I transcription. *Molecular Cell*, **10**, 819-829.
 33. Selby, C.P. and Sancar, A. (1997) Cockayne syndrome group B protein enhances elongation by RNA polymerase II. *Proceedings of the National Academy of Sciences of the United States of America*, **94**, 11205-11209.
 34. Kyng, K.J., May, A., Brosh, R.M., Jr., Cheng, W.H., Chen, C., Becker, K.G. and Bohr, V.A. (2003) The transcriptional response after oxidative stress is defective in Cockayne syndrome group B cells. *Oncogene*, **22**, 1135-1149.
 35. Balajee, A.S., May, A., Dianov, G.L., Friedberg, E.C. and Bohr, V.A. (1997) Reduced RNA polymerase II transcription in intact and permeabilized Cockayne syndrome group B cells. *Proceedings of the National Academy of Sciences of the United States of America*, **94**, 4306-4311.
 36. Newman, J.C., Bailey, A.D. and Weiner, A.M. (2006) Cockayne syndrome group B protein (CSB) plays a general role in chromatin maintenance and remodeling. *Proc Natl Acad Sci U S A*, **103**, 9613-9618.
 37. Wu, Y., Zagal, N.J., Rainbow, A.J. and Zhu, X.D. (2007) XPF with mutations in its conserved nuclease domain is defective in DNA repair but functions in TRF2-mediated telomere shortening. *DNA Repair (Amst)*, **6**, 157-166.
 38. Ye, J.Z., Hockemeyer, D., Krutchinsky, A.N., Loayza, D., Hooper, S.M., Chait, B.T. and de Lange, T. (2004) POT1-interacting protein PIP1: a telomere length regulator that recruits POT1 to the TIN2/TRF1 complex. *Genes Dev*, **18**, 1649-1654.
 39. Liu, F., Yu, Z.J., Sui, J.L., Bai, B. and Zhou, P.K. (2006) siRNA-mediated silencing of Cockayne Syndrome group B gene potentiates radiation-induced apoptosis and antiproliferative effect in HeLa cells. *Chin Med J (Engl)*, **119**, 731-739.
 40. Zhu, X.D., Kuster, B., Mann, M., Petrini, J.H. and Lange, T. (2000) Cell-cycle-regulated association of RAD50/MRE11/NBS1 with TRF2 and human telomeres. *Nat Genet*, **25**, 347-352.
 41. Li, B., Oestreich, S. and de Lange, T. (2000) Identification of human Rap1: implications for telomere evolution. *Cell*, **101**, 471-483.

42. Karlseder, J., Smogorzewska, A. and de Lange, T. (2002) Senescence induced by altered telomere state, not telomere loss. *Science*, **295**, 2446-2449.
43. Zhu, X.D., Niedernhofer, L., Kuster, B., Mann, M., Hoeijmakers, J.H. and de Lange, T. (2003) ERCC1/XPF removes the 3' overhang from uncapped telomeres and represses formation of telomeric DNA-containing double minute chromosomes. *Mol Cell*, **12**, 1489-1498.
44. Loayza, D. and De Lange, T. (2003) POT1 as a terminal transducer of TRF1 telomere length control. *Nature*, **424**, 1013-1018.
45. Wu, Y., Xiao, S. and Zhu, X.D. (2007) MRE11-RAD50-NBS1 and ATM function as co-mediators of TRF1 in telomere length control. *Nat Struct Mol Biol*, **14**, 832-840.
46. McKerlie, M. and Zhu, X.D. (2011) Cyclin B-dependent kinase 1 regulates human TRF1 to modulate the resolution of sister telomeres. *Nat Commun*, **2:371 doi: 10.1038/ncomms1372**.
47. Lansdorp, P.M., Verwoerd, N.P., van de Rijke, F.M., Dragowska, V., Little, M.T., Dirks, R.W., Raap, A.K. and Tanke, H.J. (1996) Heterogeneity in telomere length of human chromosomes. *Hum Mol Genet*, **5**, 685-691.
48. McKerlie, M., Lin, S. and Zhu, X.D. (2012) ATM regulates proteasome-dependent subnuclear localization of TRF1, which is important for telomere maintenance. *Nucleic acids research*, **40**, 3975-3989.
49. Wu, Y., Mitchell, T.R. and Zhu, X.D. (2008) Human XPF controls TRF2 and telomere length maintenance through distinctive mechanisms. *Mech Ageing Dev*, **129**, 602-610.
50. Li, B. and de Lange, T. (2003) Rap1 affects the length and heterogeneity of human telomeres. *Mol Biol Cell*, **14**, 5060-5068.
51. Martinez, P., Thanasoula, M., Munoz, P., Liao, C., Tejera, A., McNees, C., Flores, J.M., Fernandez-Capetillo, O., Tarsounas, M. and Blasco, M.A. (2009) Increased telomere fragility and fusions resulting from TRF1 deficiency lead to degenerative pathologies and increased cancer in mice. *Genes Dev*, **23**, 2060-2075.
52. Canudas, S., Houghtaling, B.R., Bhanot, M., Sasa, G., Savage, S.A., Bertuch, A.A. and Smith, S. (2011) A role for heterochromatin protein 1gamma at human telomeres. *Genes & development*, **25**, 1807-1819.
53. Barefield, C. and Karlseder, J. (2012) The BLM helicase contributes to telomere maintenance through processing of late-replicating intermediate structures. *Nucleic acids research*.
54. Kim, H., Lee, O.H., Xin, H., Chen, L.Y., Qin, J., Chae, H.K., Lin, S.Y., Safari, A., Liu, D. and Songyang, Z. (2009) TRF2 functions as a protein hub and regulates telomere maintenance by recognizing specific peptide motifs. *Nature structural & molecular biology*, **16**, 372-379.
55. Colella, S., Nardo, T., Botta, E., Lehmann, A.R. and Stefanini, M. (2000) Identical mutations in the CSB gene associated with either Cockayne syndrome or the DeSanctis-cacchione variant of xeroderma pigmentosum. *Human molecular genetics*, **9**, 1171-1175.

56. Newman, J.C., Bailey, A.D., Fan, H.Y., Pavelitz, T. and Weiner, A.M. (2008) An abundant evolutionarily conserved CSB-PiggyBac fusion protein expressed in Cockayne syndrome. *PLoS genetics*, **4**, e1000031.
57. Maicher, A., Kastner, L., Dees, M. and Luke, B. (2012) Deregulated telomere transcription causes replication-dependent telomere shortening and promotes cellular senescence. *Nucleic acids research*.
58. Pfeiffer, V. and Lingner, J. (2012) TERRA Promotes Telomere Shortening through Exonuclease 1-Mediated Resection of Chromosome Ends. *PLoS genetics*, **8**, e1002747.
59. Saltman, D., Morgan, R., Cleary, M.L. and de Lange, T. (1993) Telomeric structure in cells with chromosome end associations. *Chromosoma*, **102**, 121–128.

Chapter 3

Cockayne syndrome group B protein regulates DNA double-strand break repair and checkpoint activation

3.1 Preface

Cells derived from CS patients are sensitive to DSB-inducing agents such as ionizing radiation (IR) (Leadon & Cooper, 1993; Tuo *et al*, 2002b, 2003), camptothecin (CPT) (Squires *et al*, 2012) and etoposide (Elli *et al*, 1996), suggesting that CSB plays a role in DNA DSB repair. The work presented in this chapter clearly describe a novel role for CSB in DNA DSB repair, specifically in regulating the choice between the two main pathways non-homologous end-joining (NHEJ) and homologous recombination (HR). These findings advance our understanding of the defects associated with loss of CSB and provide further evidence for the link between DSB repair and aging.

The work in this chapter was published in the *EMBO Journal* on May 12, 2015, on pages 1399-1416, volume 34, issue 10, DOI: 10.15252/embj.201490041. I performed all of the experiments in this chapter with the exception of the GFP reporter assay in Figure 2D and cell cycle analysis by FACS in Supplementary Figure S2, which was completed by Elizabeth Thompson in Dr. Eric Hendrickson's lab. Dr. Eric Hendrickson also provided rAAV constructs and helped us establish the rAAV-based gene targeting protocol. The experimental design was a collaborative effort between myself and Dr. Xu-Dong Zhu. Th writing of the manuscript was a collaborative effort between myself and Dr. Xu-Dong Zhu with input from other authors.

3.2 Publication – Cockayne syndrome group B protein regulates DNA double-strand break repair and checkpoint activation

Article



Cockayne syndrome group B protein regulates DNA double-strand break repair and checkpoint activation

Nicole L Batenburg¹, Elizabeth L Thompson², Eric A Hendrickson² & Xu-Dong Zhu^{1,*}

*Corresponding author:

Xu-Dong Zhu
Department of Biology, LSB438
McMaster University
1280 Main St. West
Hamilton, Ontario
Canada L8S4K1
Phone: (905) 525-9140 ext. 27737
Fax: (905)522-6066
Email: zhuxu@mcmaster.ca

3.2.1 Abstract

Mutations of CSB account for the majority of Cockayne syndrome (CS), a devastating hereditary disorder characterized by physical impairment, neurological degeneration and segmental premature aging. Here we report the generation of a human CSB-knockout cell line. We find that CSB facilitates HR and represses NHEJ. Loss of CSB or a CS-associated CSB mutation abrogating its ATPase activity impairs the recruitment of BRCA1, RPA and Rad51 proteins to damaged chromatin but promotes the formation of 53BP1-Rif1 damage foci in S and G2 cells. Depletion of 53BP1 rescues the formation of BRCA1 damage foci in CSB-knockout cells. In addition, knockout of CSB impairs the ATM- and Chk2-mediated DNA damage responses, promoting a premature entry into mitosis. Furthermore, we show that CSB accumulates at sites of DNA double-strand breaks (DSBs) in a transcription-dependent manner. The kinetics of DSB-induced chromatin association of CSB is distinct from that of its UV-induced chromatin association. These results reveal novel, important functions of CSB in regulating the DNA DSB repair pathway choice as well as G2/M checkpoint activation.

3.2.2 Introduction

DNA double-strand breaks (DSBs) are one of the most lethal forms of DNA damage and can promote tumorigenesis if not repaired properly. Eukaryotic cells have evolved a complex network to sense and repair DSBs. Ataxia telangiectasia mutated (ATM), a kinase, is responsible for transducing the DNA damage signal through phosphorylation of many proteins essential for the activation of the DNA damage checkpoint, cell cycle arrest, DNA

repair or apoptosis (Shiloh, 2003; Lukas et al, 2011). Specifically, upon DSB induction, ATM phosphorylates the histone variant H2AX at serine 139, giving rise to γ H2AX (Rogakou et al, 1998, 1999). γ H2AX plays a key role in marking damaged chromatin and in directing the recruitment of DNA damage signaling and DNA repair proteins into repair centers, also known as ‘foci’ (Lukas et al, 2011; Chapman et al, 2012).

There exist two major pathways responsible for repairing DSBs: nonhomologous end joining (NHEJ) and homologous recombination (HR) (Chapman et al, 2012; McKerlie et al, 2013). NHEJ can ligate two broken ends in the absence of sequence homology, whereas HR, largely error-free, requires sequence homology and is often restricted to the S and G2 phases of the cell cycle during which sister chromatids are present. The choice of which DNA DSB repair path-way is utilized is highly regulated, and two tumor suppressor proteins BRCA1 and 53BP1 play pivotal roles in influencing the fate of the repair of DSBs by either HR or NHEJ (Chapman et al, 2012). BRCA1 promotes HR (Xie et al, 2007; Cao et al, 2009; Bouwman et al, 2010; Bunting et al, 2010), perhaps by facilitating DNA end resection (Bunting et al, 2010), an early step of HR marked by the generation of RPA-coated single-stranded DNA (RPA-ssDNA), whereas 53BP1 and its effector Rif1 are found to antagonize BRCA1 at DSBs to promote NHEJ (Xie et al, 2007; Cao et al, 2009; Bouwman et al, 2010; Bunting et al, 2010; Chapman et al, 2013; Di Virgilio et al, 2013; Escribano-Diaz et al, 2013). A perturbation in the recruitment of BRCA1 or 53BP1 to damaged chromatin can lead to an error in the choice of the DNA DSB repair pathway, which can promote genomic instability, an underlying hallmark of cancer and aging.

Cockayne syndrome (CS) is a devastating hereditary disorder characterized by physical impairment, neurological degeneration and segmental premature aging. The majority of CS cases are caused by mutations in the ERCC6 gene, which encodes Cockayne syndrome group B protein (CSB). CSB is required for transcription-coupled nucleotide excision repair (Troelstra et al, 1992; van der Horst et al, 1997) and has also been implicated in chromatin remodeling (Newman et al, 2006), oxidative damage repair (Stevnsner et al, 2008), interstrand crosslink repair (Iyama et al, 2015), mitochondrial function (Aamann et al, 2010; Scheibye-Knudsen et al, 2012), telomere maintenance (Batenburg et al, 2012) and transcription-associated DNA recombination (Gottipati & Helleday, 2009; Savolainen et al, 2010). CSB is also known to play key roles in transcription and modulation of the stress response (Velez-Cruz & Egly, 2013). CSB contains a central SWI/SNF-like ATPase domain and possesses an DNA-dependent ATPase activity that is important for its chromatin remodeling and UV repair functions (Citterio et al, 1998; Selzer et al, 2002; Cho et al, 2013).

CSB-deficient cells derived from CS patients are best known for their hypersensitivity to UV light because of their defect in transcription-coupled nucleotide excision repair (Troelstra et al, 1992; van der Horst et al, 1997). However, they are also sensitive to several other types of DNA damaging agents including ionizing radiation (IR) (Leadon & Cooper, 1993; Tuo et al, 2002, 2003), camptothecin (CPT) (Squires et al, 1993) and etoposide (Etop) (Elli et al, 1996), all of which are known to induce DNA DSBs. It has been suggested that a defect in base excision repair in CSB-deficient CS cells may contribute to their sensitivity to IR (Tuo et al, 2002, 2003). However, CSB has recently

been implicated in the processing of CPT-induced R-loops into DNA DSBs (Sollier et al, 2014), suggesting that it may play a role in DNA DSB repair.

Most CSB-deficient cell lines derived from CS patients carry compound heterozygous CSB mutations, making them less than ideal for mutational analysis of CSB function and speak for a need for human CSB-knockout cells. Here we report the generation of a human CSB-knockout cell line, which we used to demonstrate that CSB has novel, important roles in regulating the choice of DNA DSB repair pathways. We show that CSB accumulates at sites of DNA DSBs in a transcription-dependent manner. Moreover, the loss of CSB promoted NHEJ-mediated repair of DNA DSBs but impaired HR-mediated repair of DNA DSBs. The absence of CSB promoted the recruitment of 53BP1 and Rif1 in S/G2 cells at the expense of blocking BRCA1 association with damaged chromatin. Introduction of wild-type CSB fully suppressed the increase in 53BP1 and Rif1 damage foci formation in CSB-knockout cells, whereas the introduction of CSB carrying a CS associated W851R mutation in its conserved ATPase domain failed to do so. We propose that CSB represses NHEJ in S/G2 cells to facilitate the HR repair of DNA DSBs and that CSB's ATPase activity is important for its role in regulating this choice of DNA DSB repair. In addition, we find that CSB is needed for the activation of the ATM- and Chk2-dependent DNA damage responses. Furthermore, we find that the ATPase activity of CSB, which is essential for its UV-induced chromatin association, is dispensable for its DSB-induced chromatin association, suggesting that CSB association with DSBs is distinct from its association with UV-induced damaged chromatin. Our work suggests that dysregulation of DNA DSB repair resulting from defects in CSB could play a role in CS pathology.

3.2.3 *Materials and methods*

Plasmids and antibodies

The retroviral expression constructs for wild-type CSB and the shRNA against CSB or 53BP1 have been described (Batenburg et al, 2012; McKerlie et al, 2013). The QuickChange site-directed mutagenesis kit (Agilent Technologies) was used to generate CSB mutant W851R.

Antibodies used include Rad50, Mre11 and Nbs1 (Zhu et al, 2000) (kindly provided by John Petrini, Memorial Sloan-Kettering Cancer Center); Rif1 (Escribano-Diaz et al, 2013) (generously provided by Daniel Durocher, Samuel Lunenfeld Research Institute); 53BP1 (BD Biosciences); BRCA1 (MS110, Abcam); BRCA1 (Millipore); ATM (clone 2C1, Novus Biologicals); ATM (Ab-3, Calbiochem); ATM-pS1981 (10H11.E12, Cell Signaling); cyclin A (6E6, Abcam); CSB/ERCC6 (A301-354A, Bethyl Laboratories); ERCC6 (553C5a, Fitzgerald); Chk1 (FL-476, Santa Cruz); Chk1-pS317 (A300-163A, Bethyl Laboratories); Chk2 (H300, Santa Cruz); Chk2-pT68 (Cell Signaling); γ -H2AX (Millipore); H3-pS10 (Cell Signaling); KAP1-pS824 (ab70369, Abcam); KAP1 (NB500-158, Novus Biologicals); Rad51 (ab213, Abcam); Rad51 (Santa Cruz); RPA70 (a kind gift from James Ingles, University of Toronto); RPA32 (9H8, Abcam); RPA32-pS4/pS8 (Bethyl Laboratories); SMC1-pS966 (NB100-206, Novus Biologicals); SMC1 (NB100-204, Novus Biologicals); PGBD3 (Fitzgerald); and c-tubulin (GTU88, Sigma).

Cell culture, retroviral infection and treatments

Cells were grown in DMEM with 10% fetal bovine serum supplemented with non-essential amino acids, L-glutamine, 100 U/ml penicillin and 0.1 mg/ml streptomycin. Phoenix, hTERT-RPE and HeLa-DR-GFP cells were respective gifts from Titia de Lange (Rockefeller University), Prasad Jallepalli (Memorial Sloan-Kettering Cancer Center) and Daniel Durocher (Samuel Lunenfeld Research Institute). GM16095 and the parental line GM10905 for hTERT-GM1095 were obtained from the NIGMS Human Genetic Cell Repository (Coriell Institute for Medical Research). rAAV-293 cells were from Stratagene. Retroviral gene delivery was carried out as described (Wu et al, 2007a, 2008).

To induce DNA DSBs, cells were treated with either 10 μ M Etop (Sigma) or 1 μ M CPT (Sigma) for 1 h at 37°C. IR was delivered from a Cs-137 source at McMaster University (Gammacell 1000). For UV treatment, cells were exposed to UVC (254 nm) generated by a germicidal lamp (Model G8T5, GE) as described (Wu et al, 2007b). To inhibit transcription, cells were treated with either 50 μ M DRB (Cayman Chemical) or 1 μ g/ml actinomycin D (Sigma) for 2 h at 37°C except where specified. KU55933 (10 μ M, Sigma) and NU7026 (1 μ M, Sigma) were used to inhibit ATM and DNA-PKcs, respectively.

Generation of CSB knockout in hTERT-RPE cells

All primers used in the generation of the CSB-knockout cell line are shown in Supplementary Table S1. Construction of targeting vectors was performed as described (Kohli et al, 2004). The primer sets 313/314 and 315/316 were used to amplify the right

and left arms flanking exon 5 of the ERCC6 locus, respectively, using genomic DNA harvested from hTERT-RPE cells. The amplified right and left arms of exon 5 were mixed with a 4-kb PvuI fragment derived from the NeDaKO-Neo plasmid, followed by PCR using primers 313 and 316. The resulting fusion PCR product (4.4 kb) was purified, digested with NotI and ligated with the NotI-linearized pAAV-MCS plasmid, giving rise to pAAV-Neo-CSB.

Viral packaging and infection of target cells were done essentially as described (Kohli et al, 2004). Briefly, AAV-293 cells at about 60% confluency were cotransfected with the targeting vector (pAAV-Neo-CSB), pAAV-RC and pHelper plasmids using Lipofectamine 2000 (Invitrogen). Forty-eight hours post-transfection, cells were harvested and subjected to three cycles of freezing and thawing (liquid N₂ for 10 min, vortexed for 30 s and then thawed at 37°C for 10 min). The viral supernatant was collected by centrifugation at 14,000 g for 2 min and stored at 80°C.

For infection, the virus was added dropwise to hTERT-RPE cells grown at about 70–80% confluency. Forty-eight hours post-infection, cells were trypsinized and plated in 96-well plates at a density of 2,000 cells per well in media containing 1 mg/ml G418 (Invitrogen). Two weeks later, single colonies were identified and transferred to 24-well plates for expansion.

To screen for CSB targeting events, genomic DNA from cells grown in 24-well plates was harvested using the Qiagen Puregene Cell Kit according to manufacturer's instructions, followed by PCR reactions with two different sets of primers (364/365 and

366/367). Retargeting was examined by PCR screening for the presence of exon 5 using the primer set 378/367.

Immunofluorescence

Immunofluorescence (IF) was performed as described (Mitchell et al, 2009; McKerlie & Zhu, 2011) except for visualizing Rad51 and CSB. For Rad51 IF, cells grown on coverslips were fixed in PBS-buffered 2% paraformaldehyde at room temperature for 10 min. For CSB IF, cells grown on coverslips were fixed in PBS-buffered 4% paraformaldehyde at room temperature for 10 min. Following three washes in PBS, cells were then permeabilized in 0.5% Triton X-100 for 5 min before proceeding to blocking as described (Zhu et al, 2003; Mitchell & Zhu, 2014) except that the blocking buffer was made with 0.1× PBS. All cell images were recorded on a Zeiss Axio-plan 2 microscope with a Hamamatsu C4742-95 camera and processed in Open Lab.

Differential salt extraction of chromatin and immunoblotting

Protein extracts, differential salt extraction of chromatin and immunoblotting were performed as described (Wu et al, 2007a; McKerlie et al, 2012; Ye & de Lange, 2004).

Northern analysis of CSB transcripts

Northern analysis was performed as described (Batenburg et al, 2012) except that a PCR product corresponding to CSB nucleotide 1–1,398 was used to generate the radioactively labeled probe.

Random integration assays

For random integration assays, cells were infected with 15 μ l of the indicated rAAV adenoviral lysates as described and then plated in media containing 1 mg/ml G418 at 300,000 cells/per 10-cm plate. Following incubation for 12 days, colonies were fixed and stained at room temperature for 10 min with a solution containing 50% methanol, 7% acetic acid and 0.1% Coomassie blue. Colonies consisting of more than 32 cells were scored. To assess plating efficiency, infected cells were plated in media without G418. The number of colonies counted on plates without G418 was normalized to the number of cells seeded to give rise to plating efficiency.

GFP reporter assays and FACS analysis

To assess NHEJ activity, the reporter plasmid pEGFP-Pem1-Ad2 was used as described (Fattah et al, 2010). In brief, Lipofectamine LTX plus reagent (Invitrogen) was used to transfect parental and CSB-KO cells with an I-SceI-expressing plasmid, pCherry and pEGFP-Pem1-Ad2 in a ratio of 1:0.5:1 according to the manufacturer's instructions. Forty-eight hours post-transfection, cells were harvested and subjected to FACS analysis.

To assess HR activity, HeLa-DR-GFP cells were first transfected with either pRS or shCSB using Lipofectamine 2000 reagents (Invitrogen) according to the manufacturer's instructions. Twenty-four hours after the first transfection, cells were transfected with an I-SceI-expressing plasmid and pCherry in a ratio of 4:1. Forty-eight hours after the second transfection, cells were harvested and subjected to FACS analysis. For FACS analysis, cells were harvested, washed in 1 \times PBS and fixed in PBS-buffered 4% paraformaldehyde. FACS

analysis was performed using a Becton-Dickinson LSRII located at the McMaster University flow cytometry facility, Hamilton, Canada. The number of cells positive for both GFP and pCherry was normalized to the total number of pCherry-positive cells, giving rise to the percentage of GFP-positive cells.

For cell cycle analysis of parental and CSB-KO cells, two million cells were fixed in 80% ethanol. Fixed cells were then washed twice with PBS, followed by incubation in PBS containing 100 $\mu\text{g/ml}$ RNase A and 50 $\mu\text{g/ml}$ propidium iodide at 37°C for 30 min. FACS analysis was performed on a FACS Calibur instrument and analyzed using FlowJo (vX.0.7).

Clonogenic survival and G2/M checkpoint assays

For clonogenic survival assays, 4 to 6 h prior to Etop or CPT treatment, cells were seeded in triplicate at 200/300 cells (0 to 250 μM CPT and 0 to 5 μM Etop) or 800/2,400 cells (10 μM Etop) for parental and CSB-KO, respectively, per 6-cm plate. After 1 h of CPT or Etop treatment, the drug was washed off with PBS and fresh growth medium was added. For IR treatment, cells were counted, irradiated and seeded in triplicate at 200 or 300 cells for parental and CSB-KO, respectively, per 6-cm plate, followed by replacement with fresh media after a 24-h incubation. For PARP1 inhibitor treatment, cells were seeded in triplicate at 200 and 300 cells for parental and CSB-KO, respectively, except for that 600 knockout cells were seeded for 2 μM olaparib treatment. Twenty-four hours post-seeding, cells were treated with olaparib and allowed to grow in the presence of olaparib for the entirety of the experiments. Ten days later, colonies were fixed and stained at room

temperature for 10 min with a solution containing 50% methanol, 7% acetic acid and 0.1% Coomassie blue. Colonies consisting of more than 32 cells were scored.

The G2/M checkpoint assay was performed as described (McKerlie et al, 2013). Briefly, cells seeded on coverslips were treated with 2 Gy IR and allowed to recover in the incubator. Following 1 h, 4 h and 8 h incubations, cells were gently washed with PBS, fixed with paraformaldehyde and then processed for immunofluorescence with anti-H3-pS10 antibody.

Neutral comet assays

Neutral comet assays were carried out as described (Dhawan et al, 2002) with minor modifications. Cells were mixed with 1% agarose, and the mixture was dropped onto slides pre-coated with 1% agarose. Cells on the slides were lysed in comet lysis buffer (100 mM EDTA, 2.5 M NaCl, 10 mM Tris, 1% Triton X-100 pH 10) overnight at 4°C in the dark. The slides were then incubated in 1× TBE buffer (9 mM Tris, 9 mM boric acid, 2 mM EDTA pH 8.0) for 30 min at 4°C in the dark. Following gel electrophoresis run at 0.8 V/cm for 30 min in cold 1× TBE buffer, the slides were dehydrated in 70% ethanol for 30 min, air-dried and stained with SYBR Green I (Invitrogen). ImageJ (v1.49) was used with the Open Comet (v1.3) plugin to analyze at least 200 cells for each sample. The tail moment (TM) represents the product of the tail length (TL) and the fraction of DNA in the comet tail ($TM = \%DNA \text{ in tail} \times TL/100$). The data were plotted using Prism (v5.03) to create a box and whisker graph where the whiskers correspond to the 10–90 percentiles. A non-

parametric Mann–Whitney rank-sum t-test was used to derive P-values specifically for comet assays.

Statistical analysis

A Student's two-tailed unpaired t-test was used to derive all P-values except where specified.

3.2.4 Results

Generation of a human CSB-knockout cell line

Most CSB-deficient cell lines derived from CS patients carry compound heterozygous CSB mutations, making them less than ideal for mutational analysis of CSB function. To address this problem, we decided to create a human CSB-knockout cell line by targeting exon 5, the largest exon of CSB, through recombinant adeno-associated virus (rAAV)-mediated gene targeting technology (Fig 1A). For these studies, we selected the telomerized human retinal pigment epithelial (hTERT-RPE) cell line since these cells are diploid, wild-type for all known DNA repair genes and have successfully been utilized for gene targeting experiments (Kohli et al, 2004; Burkard et al, 2007; Di Nicolantonio et al, 2008). After the first round, we screened 280 clones and obtained two clones (L3A2 and M1D3) that were correctly targeted (Fig 1B). The clone L3A2 was used in the second round of gene targeting. After screening 1,158 clones, 46 correctly targeted clones were obtained; however, only one of them (28-C4) corresponded to the desired genotype in which both copies of exon 5 had been disrupted (Fig 1B). The other 45 clones comprised cells in which retargeting to

the already (first round) targeted allele had occurred. The absence of CSB expression in the clone 28-C4 was subsequently confirmed by Northern (Fig 1C) and Western analyses with two independent anti-CSB antibodies (Fig 1D and E).

Alternative splicing of exon 5 of CSB with the gene PGBD3, which is located within intron 5 of CSB, instead of exon 6 of CSB, gives rise to a CSB:PGBD3 fusion protein (Newman et al, 2008). Therefore, we also examined the expression of CSB:PGBD3 in 28-C4 cells. Western analysis with an antibody raised against either the N-terminus of CSB, which is present in CSB:PGBD3, or PGBD3 revealed no expression of the CSB:PGBD3 fusion protein in 28-C4 cells (Fig 1E and F). On the other hand, expression of PGBD3 was not disrupted (Fig 1F). These results demonstrated that CSB:PGBD3 is also knocked out in clone 28-C4, and hereafter, we refer to clone 28-C4 as CSB-knockout (CSB-KO) cells.

Loss of CSB promotes NHEJ but impairs HR, rendering cells sensitive to DNA DSB-inducing agents

We observed that the respective frequency of the random integration of two independent targeting vectors (CSB-rAAV and CCR5-rAAV) in the CSB-KO cells was a 2.65-fold and a 1.74-fold higher than in the parental hTERT-RPE cells (Fig 2A), indicating that the loss of CSB may promote random integration. It has been suggested that the random integration of gene targeting vectors is mediated by NHEJ (Kotin et al, 1992; Kan et al, 2014), and therefore, we examined whether inhibition of DNA-PKcs, a kinase directly engaged in NHEJ, might affect the frequency of the random integration in CSB-KO cells. Treatment

with NU7026, a specific inhibitor of DNA-PKcs (Veuger et al, 2003), severely impaired the frequency of random integration of either CSB-rAAV or CCR5-rAAV targeting vector in both parental and CSB-KO cells (Supplementary Fig S1A and B), although it did not abolish the increased frequency of random integration in CSB-KO cells (Supplementary Fig S1A and B). These results suggest that random integration is mediated at least in part by NHEJ. Although we cannot rule out the possibility that the increased frequency of random integration in CSB-KO cells is not epistatic to NHEJ deficiency, it is possible that the residual NHEJ activity in cells treated with the DNA-PKcs inhibitor might be sufficient to support the increased frequency of random integration in the CSB-KO cells.

To further investigate the role of CSB in regulating NHEJ-mediated DNA DSB repair, we employed a well-established NHEJ reporter plasmid pEGFP-Pem1-Ad2 (Seluanov et al, 2004), which contains the GFP gene disrupted by the insertion of an I-SceI restriction enzyme site. Repair of I-SceI-induced DNA DSBs by NHEJ restores GFP expression in pEGFP-Pem1-Ad2. NHEJ-mediated repair of I-SceI-induced DSBs was significantly upregulated in CSB-KO cells when compared with parental cells (Fig 2B), further supporting the notion that CSB negatively regulates NHEJ-mediated DSB repair.

An upregulation in NHEJ-mediated DSB repair can have a consequence on the repair of DSBs by HR, and therefore, we also asked whether loss of CSB might affect HR-mediated DSB repair. To address this question, we employed a HeLa cell line stably expressing a well-established HR reporter DR-GFP (Escribano-Diaz et al, 2013), which also contains the GFP gene disrupted by the insertion of an I-SceI restriction enzyme site. In this instance, however, repair of I-SceI-induced DNA DSBs by HR restores GFP

expression in HeLa cells. The knockdown of CSB led to a significant reduction in HR-mediated repair of I-SceI-induced DSBs (Fig 2C and D), suggesting that CSB facilitates HR-mediated DSB repair.

In support of the notion that CSB regulates DNA DSB repair pathway choice, CSB-KO cells were sensitive to a range of DSB-inducing agents including IR, Etop and CPT (Fig 2E–G), in agreement with previous findings (Squires et al, 1993; Elli et al, 1996; Tuo et al, 2002, 2003). CPT is known to induce DSBs specifically in S phase (Ryan et al, 1991); however, we did not observe any significant difference in the cell cycle profile between parental and CSB-KO cells (Supplementary Fig S2), suggesting that the increased sensitivity of CSB-KO cells to CPT is not likely due to a change in their S phase profile.

It has been suggested that CPT can also induce DNA DSBs in a transcription-dependent manner (Sakasai et al, 2010), and therefore, we asked whether the hypersensitivity of CSB-KO cells to CPT might be dependent upon transcription. To address this question, we treated both parental and CSB-KO cells with the transcription inhibitor DRB for 1 h, followed by the incubation with CPT in the presence of DRB for another 1 h. Treatment with DRB resulted in a slight increase in the sensitivity of both parental and CSB-KO cells to CPT (Fig 2H), which was not significantly different, suggesting that the increased sensitivity of CSB-KO cells to CPT is unlikely to be mediated solely by transcription-dependent damage.

Loss of CSB impairs the recruitment of BRCA1 and HR repair factors to sites of DNA damage

Analysis of indirect immunofluorescence with anti- γ H2AX revealed that CSB-KO cells were able to form IR-induced γ H2AX foci indistinguishable from the parental cells 1 h post-IR (2 Gy) exposure (Supplementary Fig S3A and B), suggesting that the absence of CSB does not prevent the recruitment of γ H2AX to sites of DNA DSBs. However, we observed that the CSB-KO cells exhibited a small—but significant—accumulation of IR-induced γ H2AX foci 4 and 8 h post-IR (Supplementary Fig S3B). Further analysis revealed that this increase in the formation of IR-induced γ H2AX foci was restricted to cyclin A (a marker for cells in the S/G2 phases of the cell cycle)-positive CSB-KO cells (Fig 3A; Supplementary Fig S3C), suggesting that CSB-KO cells may be compromised in HR-mediated repair of DSBs in S/G2, in agreement with our earlier finding that depletion of CSB impairs HR-mediated repair of I-SceI-induced DSBs (Fig 2D).

BRCA1, a tumor suppressor protein, plays a key role in directing DNA DSBs to HR repair (Xie et al, 2007; Cao et al, 2009; Bouwman et al, 2010; Bunting et al, 2010), and therefore, we examined the recruitment of BRCA1 to sites of DNA damage in CSB-KO cells. We observed a significant reduction in the formation of IR-induced BRCA1 foci in CSB-KO cells (Fig 3B; Supplementary Fig S3D). Further analysis of dual indirect immunofluorescence with an anti-BRCA1 antibody in conjunction with an anti-cyclin A antibody revealed that the reduction in the formation of IR-induced BRCA1 foci in the knockout cells was largely confined to cyclin A-positive cells (Fig 3C; Supplementary Fig

S3E). On the other hand, the loss of CSB did not lead to any detectable change in the level of BRCA1 expression (Supplementary Fig S3F). Taken together, these results suggest that CSB is important for the recruitment of BRCA1 to sites of DNA damage in S/G2 cells.

The effect of the loss of CSB on the recruitment of proteins directly involved in DNA DSB repair was also examined. CSB-KO cells were compromised in forming not only IR-induced foci of RPA (Fig 3D), a readout commonly used for DNA end resection (Huertas & Jackson, 2009; McKerlie et al, 2013), but also IR-induced foci of Rad51 (Fig 3E), a HR recombinase. In addition, CSB-KO cells were sensitive to olaparib (Fig 3F), a PARP1 inhibitor known to be toxic to cells deficient in HR (Chapman et al, 2013; Escribano-Diaz et al, 2013). Collectively, these results demonstrate that CSB plays an important role in facilitating HR repair in S/G2 cells.

As CSB is known to be involved in transcription, we also investigated whether the observed impairment of IR-induced Rad51 foci in CSB-KO cells might be transcription dependent. To address this question, we treated parental and CSB-KO cells with a transcription inhibitor (actinomycin D or DRB) prior to IR treatment. Pretreatment with actinomycin D or DRB severely impaired the formation of IR-induced Rad51 foci formation in both parental and CSB-KO cells that stained positive for cyclin A (Fig 3G), in agreement with previous finding that Rad51 recruitment to sites of DNA DSBs is transcription dependent (Aymard et al, 2014). On the other hand, pretreatment with actinomycin D or DRB did not abolish the decrease in IR-induced Rad51 foci formation observed in CSB-KO cells (Fig 3G), suggesting that transcription-dependent damage is not likely to be the main cause for the impaired Rad51 foci formation in the CSB-KO cells.

Loss of CSB leads to an accumulation of 53BP1 and Rif1 at sites of DNA damage in S/G2 cells

To investigate whether the observed defect in recruiting HR factors in CSB-KO cells might be associated with a concomitant increase in recruiting NHEJ-promoting factors to the sites of DSBs, the formation of IR-induced foci of 53BP1 and Rif1, both of which are known to inhibit BRCA1 and to promote NHEJ (Chapman et al, 2013; Di Virgilio et al, 2013; Escribano-Diaz et al, 2013; Feng et al, 2013; Zimmermann et al, 2013), was examined. Analysis of indirect immunofluorescence with anti-53BP1 revealed that CSB-KO cells were not only competent in forming IR-induced 53BP1 foci (Fig 4A; Supplementary Fig S4A) but also displayed a significant supernumerary accumulation of IR-induced 53BP1 foci 4 and 8 h post-IR (Fig 4A). Similarly, an excess accumulation of IR-induced Rif1 foci in CSB-KO cells (Fig 4B; Supplementary Fig S4B) was observed. Again, the accumulation of IR-induced Rif1 foci was predominantly confined to CSB-KO cells staining positive for cyclin A (Fig 4C; Supplementary Fig S4B), suggesting that the loss of CSB promotes NHEJ activity in S/G2 cells, which is in agreement with our earlier findings that the loss of CSB promoted NHEJ-mediated repair of I-SceI-induced DSBs (Fig 2B).

CSB-KO cells are sensitive to olaparib (Fig 3F). To investigate whether the observed increase in NHEJ activity in S/G2 cells might contribute to the sensitivity of the CSB-KO cells to olaparib, 53BP1 was knocked down with two independent shRNA constructs (Supplementary Fig S4C). The knockdown of 53BP1 fully suppressed the sensitivity of the knockout cells to olaparib (Fig 4D), and this suppression was specific to

olaparib since the 53BP1 knockdown did not suppress the UV sensitivity of the CSB-KO cells (Fig 4E). In addition, the knockdown of 53BP1 rescued the formation of IR-induced BRCA1 foci in the CSB-KO cells (Fig 4F). Taken together, these results demonstrate that CSB is important for suppressing NHEJ in S/G2, which, in turn, supports the HR-mediated repair of DSBs.

Loss of CSB impairs the ATM-mediated DNA damage response and promotes a premature exit from the G2/M checkpoint

Upon the induction of DNA DSBs, ATM, a master regulator of the DNA damage response, is activated through its autophosphorylation at S1981 (Bakkenist & Kastan, 2003). To investigate whether loss of CSB might affect ATM activation, both parental and CSB-KO cells were exposed to 5 Gy of IR. The parental cells displayed a robust ATM phosphorylation at S1981 as early as 15 min post-IR (Fig 5A), consistent with previous findings (Bakkenist & Kastan, 2003; McKerlie et al, 2013). In contrast, the level of ATM phosphorylation at S1981 was severely impaired in the CSB-KO cells after IR (Fig 5A) although the level of ATM expression in the knockout cells was indistinguishable from that in the parental cells (Fig 5A). A loss in the level of ATM phosphorylation at S1981 was also observed in the knockout cells following treatment with Etop (Supplementary Fig S5A). Furthermore, the IR-induced phosphorylation of KAP1, SMC1, H2AX and Chk2, downstream targets of ATM, was also impaired in the CSB-KO cells (Fig 5A). Little change in Chk1 phosphorylation was detected in the CSB-KO cells (Supplementary Fig S5B). Loss of CSB also had little effect on the expression level of KAP1, SMC1, H2AX,

Chk1 and Chk2 (Fig 5B). Taken together, these results suggest that loss of CSB impairs ATM-mediated DNA damage response.

CSB has been suggested to play a role in transcription, and therefore, formally it was possible that the loss of CSB might affect the expression of DNA damage response factors important for the regulation of ATM activation. Following the induction of DNA DSBs, ATM activation requires the Mre11/Rad50/Nbs1 complex (Lee & Paull, 2004, 2005). Western analysis revealed that the levels of Mre11, Rad50 and Nbs1 expression in CSB-KO cells were indistinguishable from that in parental cells (Fig 5B), suggesting that the compromised ATM activation observed in the CSB-KO cells is unlikely due to a loss in the level of the Mre11/Rad50/Nbs1 complex. Furthermore, we found that pretreatment with the transcription inhibitor DRB or actinomycin D did not abrogate the reduction in the level of ATM phosphorylation at S1981 in the CSB-KO cells (Fig 5C), suggesting that the compromised ATM activation in the CSB-KO cells is not likely to be mediated by active transcription.

Although CSB-KO cells were able to enter an G2/M arrest immediately following the treatment with IR (Fig 5D), they exhibited premature exit from the G2/M checkpoint (Fig 5D). Earlier we have shown that CSB-KO cells promote NHEJ (Fig 2B). To investigate whether an increase in NHEJ-mediated fast repair of DNA DSBs might contribute to the observed premature entry of CSB-KO cells into mitosis, we performed neutral comet assays with both parental (WT) and CSB-KO cells that were either mock or IR treated. The comet tail moment in the CSB-KO cells was indistinguishable from that in the parental (WT) cells 15 min, 30 min or 1 h after 10 Gy IR (Fig 5E), suggesting that the

premature exit of CSB-KO cells from the G2/M checkpoint is not likely to be due to a difference in the efficiency of fast DSB repair.

Inhibition of ATM abrogates IR-induced Rif1 foci formation in CSB-KO cells

The formation of IR-induced Rif1 foci is dependent upon ATM activation (Chapman et al, 2013; Escribano-Diaz et al, 2013). Moreover, CSB-KO cells exhibit an impairment in ATM activation (Fig 5A) but are competent in forming IR-induced Rif1 foci (Fig 4C; Supplementary Fig S4B). To investigate whether the ATM activity might mediate the accumulation of IR-induced Rif1 foci in the CSB-KO cells, we treated both parental and CSB-KO cells with KU55933, a specific inhibitor for ATM, prior to 2 Gy IR treatment. The preincubation with KU55933 abrogated the IR-induced Rif1 foci formation in both parental and CSB-KO cells (Supplementary Fig S4D), in agreement with previous findings (Chapman et al, 2013; Escribano-Diaz et al, 2013). Taken together, these results suggest that Rif1 recruitment to sites of DNA DSBs may not require a full level of ATM activation.

CSB, but not the CSB:PGBD3 fusion protein, is the main factor responsible for facilitating HR repair of DNA DSBs

The deletion of exon 5 of CSB leads to loss of expression of both CSB and the CSB:PGBD3 fusion protein from the CSB locus (Fig 1E). To investigate whether CSB or CSB-PGBD3 was responsible for the observed defect in recruiting HR factors to sites of DSBs in the CSB-KO cells, we generated derivative CSB-KO cell lines stably expressing CSB, CSB:PGBD3 or an empty vector (Supplementary Fig S6A). The introduction of CSB, but not the CSB-PGBD3 fusion protein, was able to suppress the sensitivity of the knockout

cells to olaparib (Supplementary Fig S6B). In addition, the introduction of CSB, but not the CSB:PGBD3 fusion, was able to rescue Etop-induced foci of RPA and Rad51 (Supplementary Fig S6C and D). From these results, we conclude that CSB is the main factor from the CSB locus responsible for promoting HR-mediated repair of DSBs.

Recruitment of DSB repair factors to sites of DNA damage is misregulated in cells derived from CS patients

To investigate whether the defect in HR-mediated repair of DSBs in the CSB-KO cells might be cell type specific, we examined the recruitment of DSB repair factors to sites of DSBs in two cell lines derived from CS patients lacking functional CSB (hTERT-GM10905 and GM16095). hTERT-GM10905 is a telomerase-immortalized CS cell line carrying a homozygous nonsense mutation at position 735 (R735X) of CSB, whereas GM16095 is a SV40-transformed CS cell line with heterozygous compound mutations of K377X and R857X (Batenburg et al, 2012). Through retroviral infection, two pairs of isogenic cell lines stably expressing either wild-type CSB or the vector alone were generated. The introduction of wild-type CSB into these two CS cell lines led to a significant decrease in the percentage of cells with IR-induced 53BP1 foci (Supplementary Fig S7A) and simultaneously resulted in a significant increase in the number of cyclin A-positive cells with IR-induced foci of BRCA1, RPA and Rad51 (Supplementary Fig S7B–D), suggesting that CS cells lacking functional CSB are also defective in HR-mediated DSB repair. In support of this notion, the introduction of CSB into GM16095 cells also enhanced cell survival in response to the treatment with olaparib (Supplementary Fig S7E), consistent

with a previous report that CS cells are hypersensitive to PARP inhibition (Thorslund et al, 2005). Furthermore, the introduction of CSB into GM16905 cells suppressed their sensitivity to CPT and Etop (Supplementary Fig S7F and G). Taken together, these results demonstrate that DNA DSB repair is misregulated in CS cells lacking functional CSB.

CSB is found to accumulate at sites of DSBs in a transcription-dependent manner

To investigate whether CSB may be associated with sites of DSBs, dual indirect immunofluorescence with an anti-CSB antibody in conjunction with an anti-53BP1 antibody in cells treated with no IR or 10 Gy IR was performed. About 40 to 50% of cells exhibited IR-induced damage foci of CSB 8 h post-IR, and these CSB damage foci all contained 53BP1 (Fig 6A), a marker for DSBs (Daley & Sung, 2014; Panier & Boulton, 2014), suggesting that CSB accumulates at sites of DSBs.

CSB is engaged in transcription, and we therefore asked whether transcription might regulate CSB accumulation at sites of DSBs. To address this question, cells were treated with the transcription inhibitor actinomycin D or DRB prior to 10 Gy IR treatment. Treatment with actinomycin D or DRB severely impaired the formation of IR-induced CSB damage foci (Fig 6B), indicating that CSB accumulation at sites of DSBs is dependent upon active transcription.

The ATPase activity of CSB is dispensable for its DSB-induced chromatin association

To gain further insights into the CSB association with DSB-induced damaged chromatin, differential salt extraction of chromatin from hTERT-RPE cells that were mock-treated or treated with either CPT or Etop was performed. Treatment with CPT or Etop led to a

significant increase in the association of CSB with chromatin (lane 2 versus lanes 5, 8, 11 and 14 in Fig 6C and lane 2 versus lanes 5, 8 and 11 in Fig 6D). At 8 h after release from treatment with either Etop or CPT, approximately 50% of the CSB was found associated with chromatin (Fig 6C, lane 2 versus lane 14 and Fig 6D, lane 2 versus lane 11), supporting the notion that CSB is recruited to damaged chromatin following the induction of DNA DSBs. On the other hand, proportionally, UV-induced CSB association with chromatin peaked 2 h post-UV treatment and was largely lost 4 h post-UV (Supplementary Fig S8A, lane 8 versus lane 11), in agreement with previous findings (Lake et al, 2010). Taken together, these results suggest that the kinetics of CPT- and Etop-induced CSB association with chromatin is distinct from that of UV-induced CSB association with chromatin.

CSB contains a conserved SWI/SNF-like ATPase domain and exhibits a DNA-dependent ATPase activity (Citterio et al, 1998) that is required for its UV-induced chromatin association (Lake et al, 2010). Amino acid substitutions in the conserved ATPase domain are found in CS patients, and the W851R mutation abrogates the ATPase activity of CSB and its UV-induced chromatin association (Lake et al, 2010). To investigate whether the ATPase activity of CSB might be important for its DSB-induced chromatin association, we generated derivative CSB-KO cells stably expressing either wild-type CSB, CSB carrying the W851R mutation or the vector alone (Supplementary Fig S8B). In undamaged (untreated) cells, we reproducibly observed chromatin association of mutant CSB-W851R at a level higher than that of wild-type CSB (Fig 6E and F; Supplementary Fig S8C and D). Upon Etop treatment, mutant CSB-W851R was able to exhibit DSB-induced chromatin association (Fig 6F). On the other hand, we failed to detect any increase

in the proportion of CSB associated with chromatin following UV treatment (Supplementary Fig S8D) although wild-type CSB exhibited UV-induced chromatin association (Supplementary Fig S8C), in agreement with previous findings (Lake et al, 2010). Analysis of multiple protein markers, either cytoplasmic or chromatin bound (c-tubulin, TRF2 or H2AX), revealed that the chromatin salt fractionation procedure was done consistently between the CSB-KO cells expressing CSB-W851R and the CSB-KO cells expressing wild-type CSB (Fig 6E and F; Supplementary Fig S8C and D). Taken together, these results suggest that DSB-induced chromatin association of CSB is distinct from its UV-induced chromatin association and that the ATPase activity of CSB is dispensable for its DSB-induced chromatin association.

The ATPase activity of CSB is essential for suppressing NHEJ to facilitate HR-mediated repair of DSBs in S/G2 cells

To investigate whether the ATPase activity of CSB might be important for regulating the choice of DNA DSB repair pathways, we examined the recruitment of 53BP1/Rif1 and BRCA1 to sites of DSBs in CSB-KO cells stably expressing vector alone, wild-type CSB or CSB harboring the W851R mutation. Introduction of wild-type CSB into CSB-knockout cells suppressed the number of cells with IR-induced foci of 53BP1 and Rif1 (Fig 7A and B). This suppression was not detectable in CSB-KO cells expressing the mutant CSB-W851R (Fig 7A and B). The reduction in IR-induced Rif1 foci, resulting from introduction of wild-type CSB, was only observed in the knockout cells staining positive for cyclin A

(Fig 7C), suggesting that the ATPase activity of CSB is important for suppressing NHEJ-mediated repair of DNA DSBs in S/G2 cells.

Additionally, analysis of indirect immunofluorescence with anti-BRCA1 antibody revealed that introduction of wild-type CSB rescued the formation of IR-induced BRCA1 foci in CSB-KO cells, whereas CSB carrying the W851R mutation failed to do so (Fig 7D). Further-more, while introduction of wild-type CSB into CSB-KO cells promoted cell survival after treatment with olaparib (Fig 7E), CSB carrying the W851R mutation was unable to suppress the sensitivity of the knockout cells to olaparib (Fig 7E). Taken together, these results suggest that while the ATPase activity of CSB is not important for chromatin recruitment, it is important for its ability to facilitate the HR-mediated repair of DSBs.

The ATPase activity of CSB is important for the maintenance of the G2/M checkpoint

When introduced into the CSB-KO cells, wild-type CSB was able to rescue the level of IR-induced ATM phosphorylation at S1981, most noticeable at 15 min post-IR treatment (Fig 8A). On the other hand, no rescue was detected in the CSB-KO cells complemented with CSB carrying the W851R mutation (Fig 8A). In addition, we reproducibly observed a rescue in the level of Chk2 phosphorylation 1 h post-IR treatment in CSB-KO cells complemented with wild-type CSB and such a rescue was not seen in CSB-KO cells complemented with CSB carrying the W851R mutation (Fig 8A). Furthermore, the introduction of wild-type CSB into CSB-KO cells was able to suppress their premature exit from the G2/M checkpoint, whereas introduction of CSB carrying a W851R mutation failed to do so (Fig 8B). Introduction of CSB carrying a W851R mutation also failed to suppress

the sensitivity of CSB-KO cells to IR exposure (Fig 8C). Collectively, these results suggest that the ATPase activity of CSB is important for facilitating the maintenance of the G2/M checkpoint and cell survival in response to the induction of DNA DSBs.

3.2.5 Discussion

In this report, we uncover a novel but important function of CSB in regulating the choice of DNA DSB repair pathways. Our work suggests that CSB facilitates BRCA1-mediated HR repair by repressing the accumulation of NHEJ-promoting factors 53BP1 and Rif1 at sites of DNA DSBs in S and G2 cells (Fig 8D). Furthermore, we have demonstrated that CSB is needed for maintaining the ATM- and Chk2-mediated DNA damage checkpoint (Fig 8D), preventing premature entry of cells into mitosis following the induction of DNA DSBs.

We observed a large asymmetry in the ratio of targeting versus retargeting in the recovery of null clones. Although a large asymmetry in gene targeting typically is found to be associated with genes whose function is critical to cell viability (Dang et al, 2006; Hucl et al, 2008; Ruis et al, 2008; Oh et al, 2013), homozygous CSB mutations leading to the complete absence of CSB protein have been reported in patients (Horibata et al, 2004; Hashimoto et al, 2008; Laugel et al, 2008). Several lines of evidence strongly argue against the possibility that the observed phenotype of the CSB null clone may be due to a secondary mutation. Firstly, introduction of wild-type CSB rescued the defect of the CSB-knockout cells in the choice of DNA DSB repair pathways as well as the maintenance of G2/M checkpoint. Secondly, dysregulation in the choice of DNA DSB repair pathways was also

detected in two independent CSB-deficient cell lines derived from CSB patients. Thirdly, endogenous CSB was found to accumulate at sites of DSBs.

Most patient-derived CSB null cell lines that are available are skin fibroblasts whereas the CSB-KO cells described here are retinal pigment epithelial cells in origin. CS patients are known to exhibit segmental premature aging in certain cell types that are not skin fibroblasts. Therefore, we anticipate that our CSB null clone will provide an added value for understanding the pathology of CS.

CSB has recently been implicated in processing R-loops into DNA DSBs (Sollier et al, 2014). R-loop-dependent DNA DSBs led to a robust DNA damage response including phosphorylation of KAP1, which is sensitive to CSB knockdown (Sollier et al, 2014). We have observed an impaired KAP1 phosphorylation as well as ATM- and Chk2-mediated DNA damage response in CSB-KO cells following ionizing radiation. Conceivably, the fewer R-loop-dependent DNA DSBs resulting from the absence of CSB in the CSB-KO cells may in part account for the reduction in their ATM-dependent damage response (Fig 8D). Treatment with the transcription inhibitor DRB or actinomycin D did not abolish the impaired ATM phosphorylation in CSB-KO cells, suggesting that active transcription may not be needed for CSB to regulate ATM activation.

We have reproducibly found that the introduction of wild-type CSB into CSB-KO cells rescued the level of Chk2 phosphorylation at 1h post-IR but not at 15 min post-IR whereas Chk2 phosphorylation was robust in parental (WT) cells 15 min post-IR. It is possible that the kinetics of Chk2 phosphorylation in CSB-KO cells complemented with

wild-type CSB may be different from that in parental (WT) cells. Future studies will be needed to investigate the nature of this difference.

CSB requires its ATPase activity to maintain ATM activation and to regulate DNA DSB repair pathway choice. CSB has been reported to exhibit ATP-dependent chromatin remodeling activity *in vitro* (Citterio et al, 2000; Cho et al, 2013). Chromatin remodeling is known to influence DNA DSB repair (Goodarzi et al, 2010; Chapman et al, 2012). It is possible that CSB may facilitate DNA DSB repair pathway choice through its ATP-dependent chromatin remodeling activity. Alternatively, CSB might regulate the repair pathway choice through its interactions with chromatin modifying factors. Recently, it has been reported that the chromatin context can influence the choice of DNA DSB repair pathways, especially in S and G2 phases of the cell cycle during which both pathways are available to the cell (Aymard et al, 2014; Carvalho et al, 2014; Jha & Strahl, 2014; Pai et al, 2014; Pfister et al, 2014). For example, in human cells, tri-methylation of H3K36 has been suggested to promote DNA end resection and repair of DSBs via HR (Aymard et al, 2014; Pfister et al, 2014) and modification of H3K9 has been implicated in the DSB response in heterochromatin that is preferentially repaired by HR (Chiolo et al, 2011). CSB has been found, in different contexts, to associate with numerous chromatin modifying and remodeling factors such as NuRD (Xie et al, 2012), SMARCA5 (Aydin et al, 2014) as well as histone methyltransferase G9A (Yuan et al, 2007) and acetyltransferase PCAF (Shen et al, 2013), while the yeast homolog of CSB, Rad26, has been reported to genetically interact with the H3K36 methyltransferase SET2 (Jha & Strahl, 2014).

Although transcription inhibition did not abolish the impairment of CSB-KO cells in IR-induced Rad51 foci formation and ATM activation, it abrogated the accumulation of CSB at sites of DNA DSBs. These results suggest that CSB association with DSB-induced damaged chromatin may be regulated distinctively from its role in HR and ATM activation. This notion is further supported by our finding that CSB requires its ATPase activity to facilitate IR-induced Rad51 foci and ATM activation but its ATPase activity is dispensable for its association with DSB-induced damaged chromatin. CSB has previously been reported to possess both ATP-dependent and ATP-independent functions (Wong et al, 2007; Lake et al, 2010).

Mutant CSB-W851R lacking its ATPase activity is competent in DSB-induced chromatin association but defective in UV-induced chromatin association, the latter of which is in line with previous findings (Lake et al, 2010). These results suggest that CSB may use distinct mechanisms to interact with UV-induced DNA damage and DSBs, which is not unprecedented. The chromatin remodeling protein SMARCA5 (also known as SNF2H) does not require its ATPase activity to localize to DSBs, but it does so for its localization to UV-induced DNA damage (Lan et al, 2010; Aydin et al, 2014).

CSB-KO cells exhibit an accumulation of IR-induced 53BP1 foci. Previously, it has been reported that depletion of CSB leads to a decrease in the formation of a specific subset of CPT-induced 53BP1 foci, referred to as type I foci, which are dose dependent and only seen in RPA-negative cells (Sakai et al, 2012). CPT also induces the formation of type II foci of 53BP1, which is not dose dependent and persists after CPT treatment (Sakai et al, 2012). However, whether depletion of CSB might affect CPT-induced type II foci of 53BP1

was not investigated, and therefore, our findings cannot be strictly compared to the previous report. Future studies will be needed to investigate the effect of knockout of CSB on CPT-induced type I and type II foci formation.

CS cells deficient in CSB are known to be sensitive to IR-induced DNA damage as well as to the topoisomerase poisons CPT and Etop (Squires et al, 1993; Elli et al, 1996; Tuo et al, 2002, 2003). However, the multiplicity of the forms of DNA damage generated by these cellular treatments may have contributed to obscure our understanding of CSB as a DNA DSB repair protein. IR, for instance, produces not only DSBs but also oxidative damage and single-strand breaks. Indeed, a defect in repairing oxidative damage may contribute to the sensitivity of CS cells to IR (Stevnsner et al, 2008). Similarly, camptothecin and etoposide generate not only DSBs but also topoisomerase–DNA adducts, which are thought to be removed by base excision repair (Caldecott, 2008). Our finding that CSB accumulates at sites of DSBs and regulates the choice of the DNA DSB repair pathways suggests for the first time that dysregulation in DNA DSB repair may at least in part contribute to the hypersensitivity of CS cells to DSB-inducing agents. In support of this notion, depletion of 53BP1 rescued the formation of BRCA1 damage foci in CSB-knockout cells and fully suppressed their sensitivity to olaparib, a PARP1 inhibitor known to be toxic to cells deficient in HR. Our finding raises a new possibility that targeting 53BP1 might be clinically beneficial to CS patients.

Acknowledgements

We would like to thank Daniel Durocher, James Ingles, Titia de Lange, Prasad Jallepalli and John Petrini for providing cell lines and antibodies. We are indebted to Daniel Durocher and John R. Walker for their insightful suggestions. John R. Walker is also thanked for his critical reading of the manuscript. This work is supported by funding from Canadian Institutes of Health Research to X.-D.Z. Work in the Hendrickson laboratory was supported by the NIH (GM088351) and the NCI (CA15446). N.L.B. is a holder of Ontario Graduate Scholarship.

Author contributions

NLB and ELT performed the experiments. NLB, EAH and X-DZ designed the experiments. NLB and XDZ wrote the paper.

Conflict of interest

The authors declare that they have no conflict of interest.

3.2.6 *Figures and figure legends*

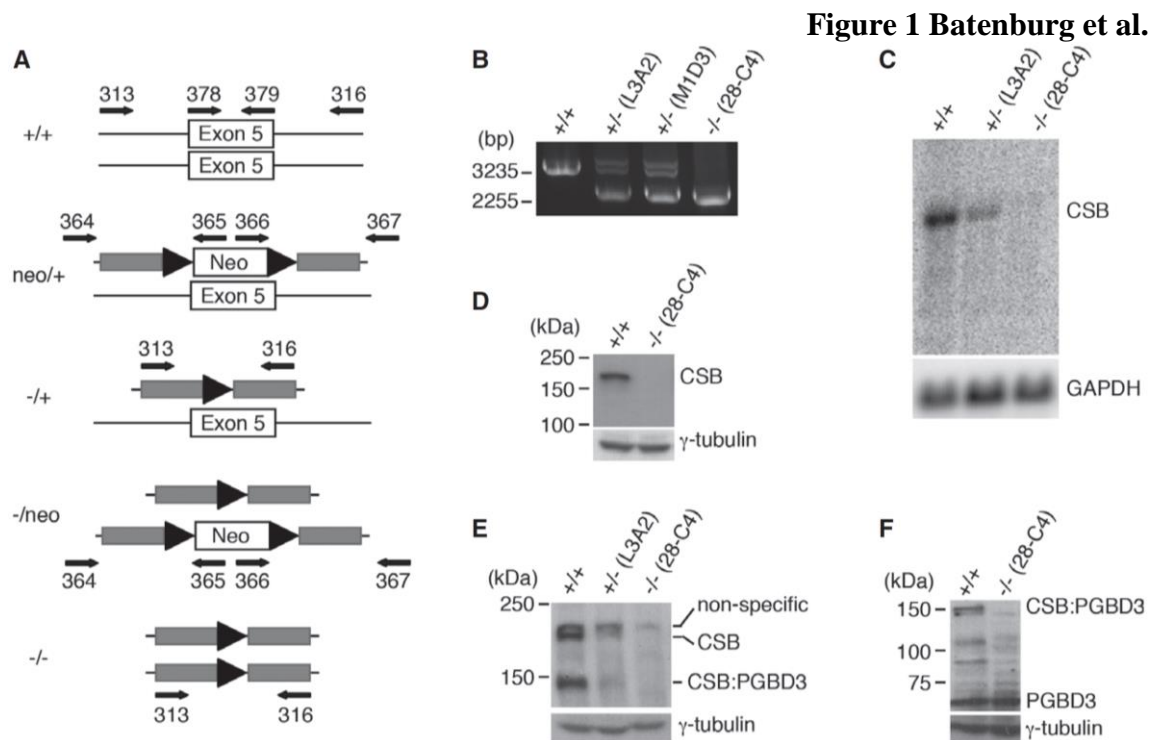


Figure 1. Generation of CSB-KO cells. **(A)** Schematic diagram of rAAV-mediated gene targeting of exon 5 of CSB. Grey horizontal bars represent homology arms flanking exon 5 of CSB. Black arrowheads represent loxP sites. **(B)** Analysis of PCR products amplified with the primer set 313 and 316 and genomic DNA isolated from parental hTERT-RPE cells, the heterozygote cell clones (L3A2 and M1D3) and the CSB homozygous cell clone (28-C4). Molecular weight markers corresponding to 3225 bp and 2255 bp are indicated on the left. **(C)** Northern blot analysis of RNA isolated from parental hTERT-RPE cells, the heterozygous cell clone L3A2 and the homozygous cell clone 28-C4. GAPDH was used as a loading control. **(D)** Western analysis with an antibody against the C-terminus of CSB (Abcam). γ -tubulin was used as a loading control in this and subsequent figures. **(E)** Western analysis with an antibody against the N-terminus of CSB (Bethyl). **(F)** Western analysis with an antibody against PGBD3.

Figure 2 Batenburg et al.

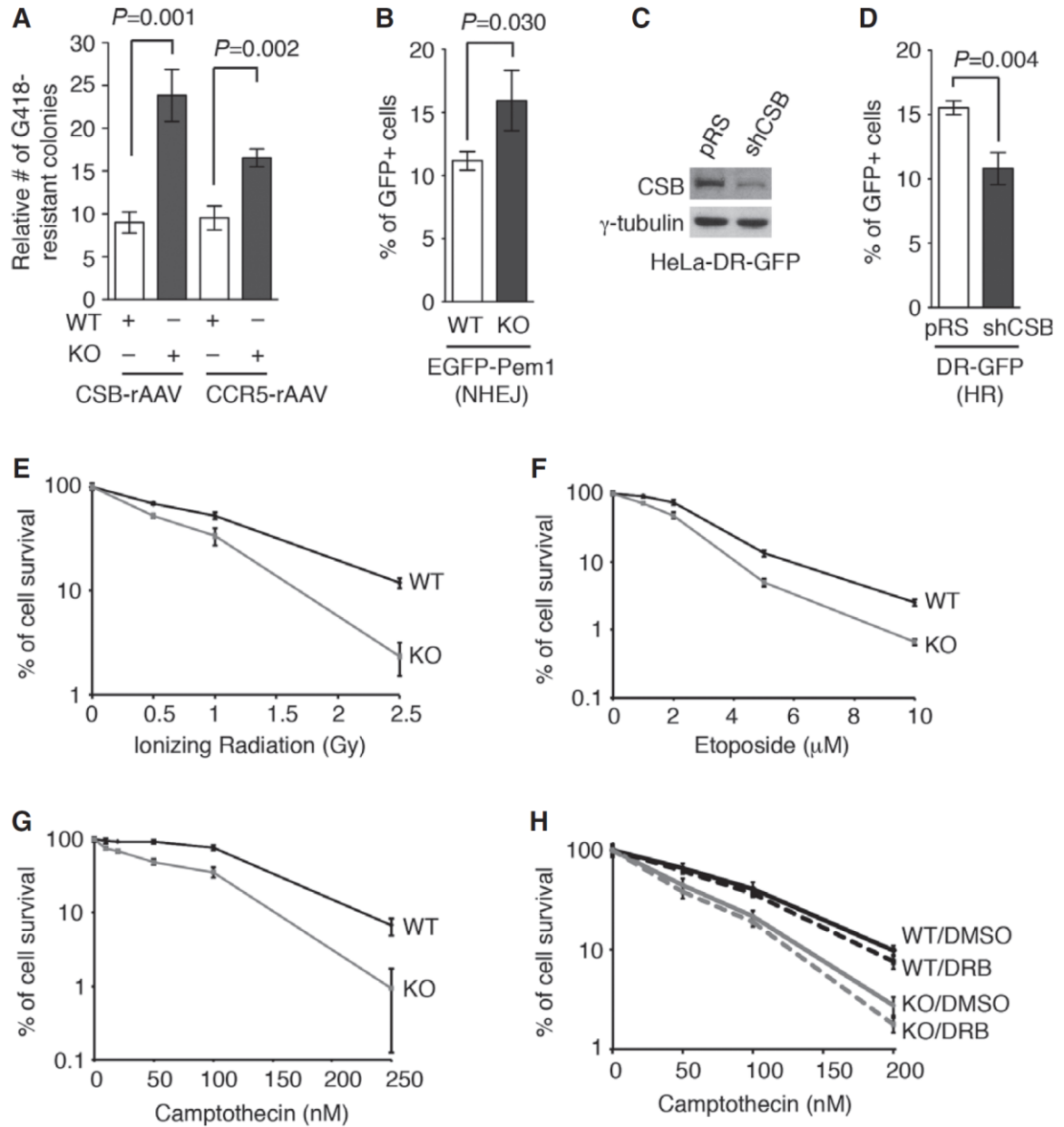


Figure 2. Loss of CSB promotes NHEJ, impairs HR and renders cells sensitive to DSB-inducing agents. **(A)** Quantification of the frequency of random integration of two independent rAAV targeting vectors (CSB-rAAV and CCR-rAAV). **(B)** NHEJ-mediated repair of *I-SceI*-induced DNA DSBs. The parental (WT) and the CSB-KO (KO) cells were cotransfected with pEGFP-Pem1-Ad2, pCherry and *I-SceI* expression constructs. The number of cells positive for both GFP and pCherry was normalized to the total number of pCherry-positive cells, giving rise to the percentage of normalized GFP-positive cells. Standard deviations from three independent experiments are indicated. **(C)** Western analysis of CSB in HeLa-DR-GFP transiently transfected with the vector alone or shCSB. **(D)** HR-mediated repair of *I-SceI*-induced DNA DSBs. HeLa-DR-GFP transiently expressing the vector alone or shCSB were cotransfected with pCherry and *I-SceI* expression constructs. The percentage of normalized GFP-positive cells was calculated as described in (B). Standard deviations from three independent experiments are indicated. **(E-G)** Clonogenic survival assays of the parental (WT) and the CSB-KO (KO) cells following various doses of ionizing radiation (IR) (E), etoposide (Etop) (F) or camptothecin (CPT) (G). Standard deviations from at least three experiments are indicated. **(H)** Clonogenic survival assays. Both WT and CSB-KO cells were treated with 50 μ M DRB, prior to the addition of various doses of CPT. Standard deviations from at least three experiments are indicated.

Figure 3 Batenburg et al.

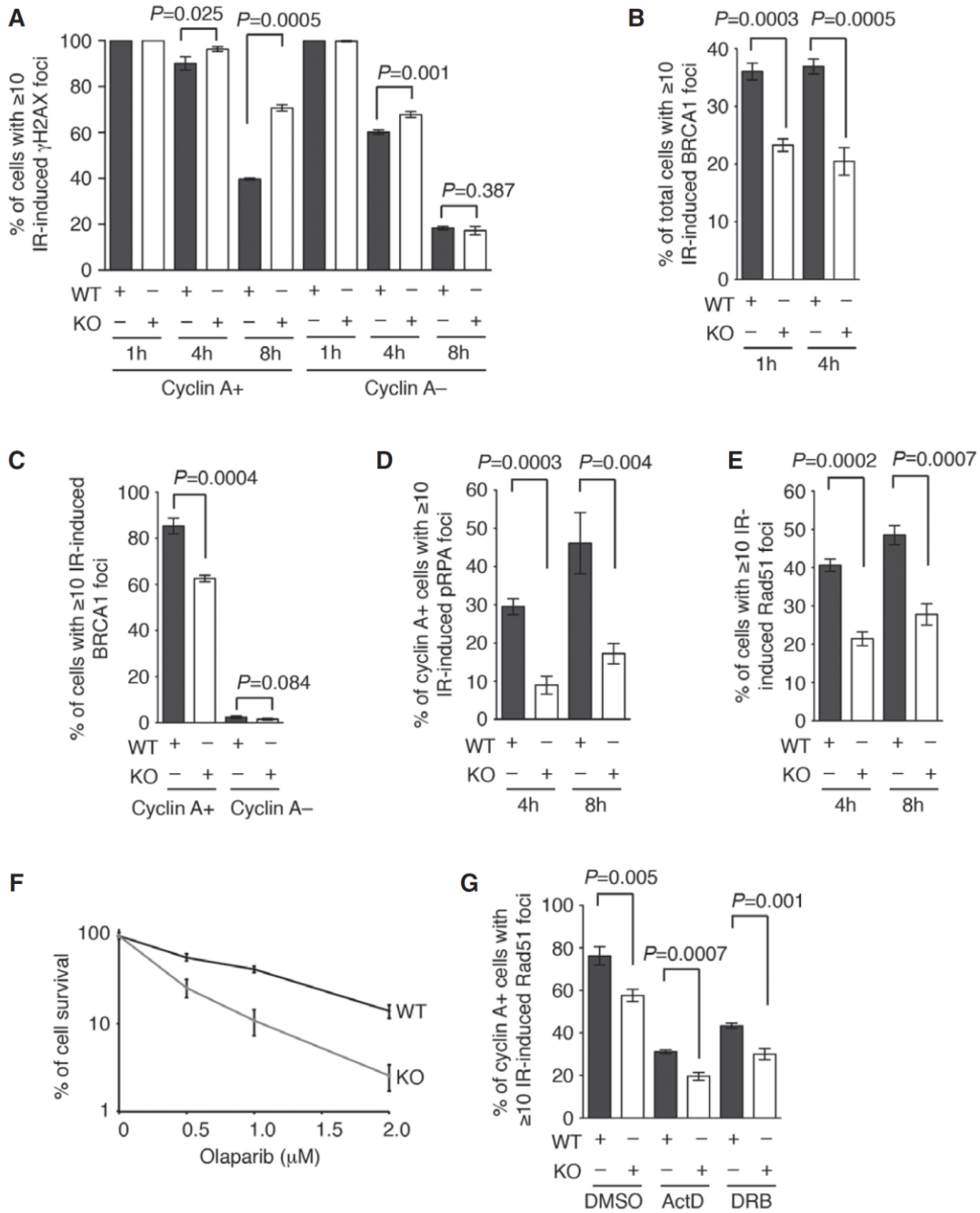


Figure 3. Knockout of CSB impairs HR-mediated DNA DSB repair in S and G2 cells.

(A) Quantification of percentage of cyclin A-positive and cyclin A-negative cells exhibiting 10 or more IR-induced γ H2AX foci. Both parental (WT) and CSB-KO (KO)

cells were treated with 2 Gy IR and fixed 1 h, 4 h and 8 hr post IR. A total of at least 1500 cells from three independent experiments were scored in blind. Standard deviations from three independent experiments are indicated. **(B)** Quantification of the percentage of cells with 10 or more IR-induced BRCA1 foci. Cells (WT and KO) were treated with 2 Gy IR and fixed 1 hr and 4 hr post IR. A total of at least 1500 cells from three independent experiments were scored in blind. Standard deviations from three independent experiments are indicated. **(C)** Quantification of percentage of cyclin A-positive and cyclin A-negative cells displaying 10 or more IR-induced BRCA1 foci. Cells were treated with 2 Gy IR and scored as described in (B). Standard deviations from three independent experiments are indicated. **(D)** Quantification of the percentage of cyclin A-positive cells with 10 or more IR-induced RPA32-pS4/pS8 foci. Cells (WT and KO) were treated with 10 Gy IR and fixed 4 hr and 8 hr post IR. A total of 750 cells were scored in blind. Standard deviations from three independent experiments are indicated. **(E)** Quantification of percentage of cells with 10 or more IR-induced Rad51 foci. Cells (WT and KO) were treated with 10 Gy IR and fixed 4 hr and 8 hr post IR. A total of 750 cells were scored in blind. Standard deviations from three independent experiments are indicated. **(F)** Clonogenic survival assays of olaparib-treated parental (WT) and CSB-KO (KO) cells as indicated. Standard deviations from three independent experiments are indicated. **(G)** Quantification of percentage of cells with 10 or more IR-induced Rad51 foci. Cells (WT and KO) were treated with actinomycin D (1 μ g/ml) or DRB (50 μ M) prior to 10 Gy IR and then fixed 8 hr post IR. A total of at least 1500 cells were scored in blind. Standard deviations from three independent experiments are indicated.

Figure 4 Batenburg et al.

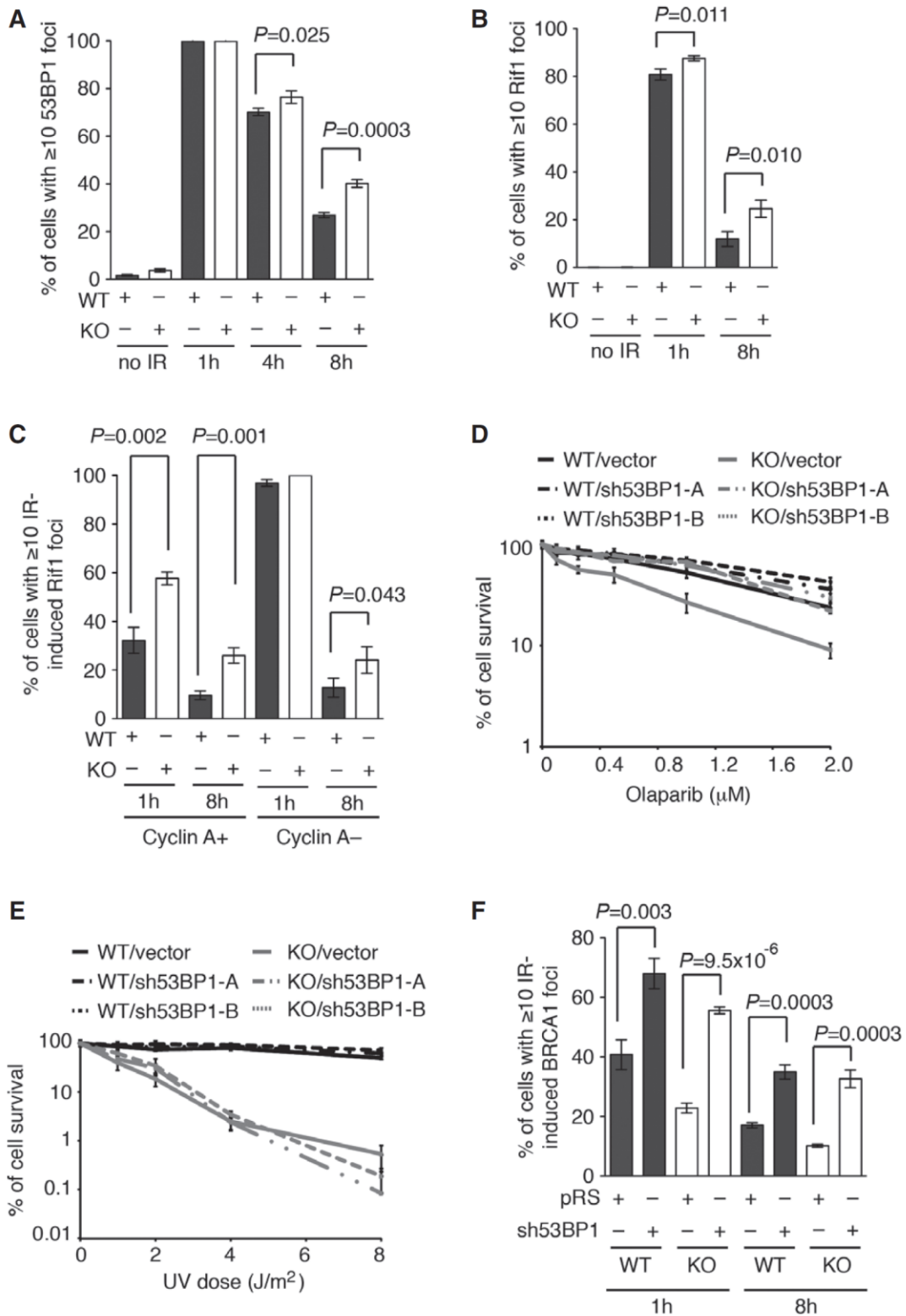


Figure 4. Loss of CSB leads to an accumulation of NHEJ-promoting factors at sites of DNA DSBs in S and G2 cells. **(A)** Quantification of percentage of cells with 10 or more IR-induced 53BP1 foci. Cells (WT and KO) were treated with 2 Gy IR and fixed 1 hr, 4 hr and 8 hr post IR. A total of 1500 cells were scored in blind. Standard deviations from three independent experiments are indicated. **(B)** Quantification of percentage of cells with 10 or more IR-induced Rif1 foci. Cells (WT and KO) were treated with 2 Gy IR and fixed 1 hr and 8 hr post IR. A total of 750 cells were scored in blind. Standard deviations from three independent experiments are indicated. **(C)** Quantification of the percentage of cyclin A-positive and cyclin A-negative cells with 10 or more IR-induced Rif1 foci. Cells were treated and scored as described in (B). Standard deviations from three independent experiments are indicated. **(D)** Clonogenic survival assays of olaparib-treated parental (WT) and CSB-KO (KO) cells stably expressing the vector alone, sh53BP1-A or sh53BP1-B as indicated. Standard deviations from three independent experiments are indicated. **(E)** Clonogenic survival assays of UV-treated parental (WT) and CSB-KO (KO) cells stably expressing the vector alone, sh53BP1-A or sh53BP1-B as indicated. Standard deviations from three independent experiments are indicated. **(F)** Quantification of percentage of cells with 10 or more IR-induced BRCA1 foci. Parental (WT) and knockout (KO) stably expressing the vector (pRS) alone or sh53BP1-A were treated with 2 Gy IR and fixed 1 hr and 8 hr post IR. A total of at least 1500 cells were scored in blind. Standard deviations from three independent experiments are indicated.

Figure 5 Batenburg et al.

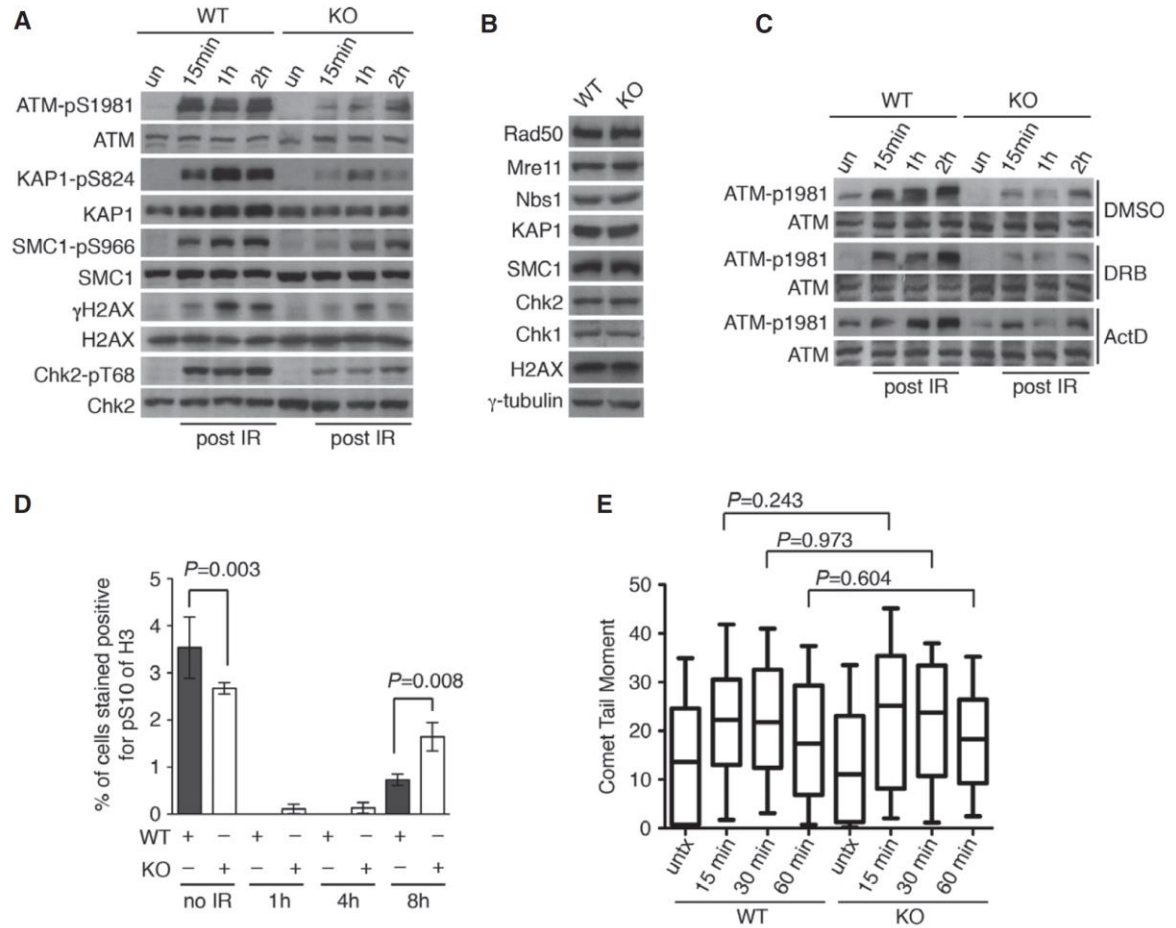


Figure 5. Loss of CSB impairs ATM- and Chk2-dependent DNA damage checkpoint. **(A)** Western analysis of the parental (WT) and the CSB-KO (KO) cells either mock-treated or treated with 5 Gy IR. Immunoblotting was performed with anti-ATM-pS1981, anti-ATM, anti-KAP1-pS824, anti-KAP1, anti-SMC1-pS966, anti-SMC1, anti- γ H2AX, anti-H2AX, anti-Chk2-pT68 and anti-Chk2 antibodies. **(B)** Western analysis of WT and CSB-KO cells. Immunoblotting was performed with anti-Rad50, anti-Mre11, anti-Nbs1, anti-KAP1, anti-SMC1, anti-Chk2, anti-Chk1, anti-H2AX and anti- γ -tubulin antibodies. The anti- γ -tubulin blot was used as a loading control. **(C)** Western analysis. WT and CSB-KO cells were treated with DMSO, DRB or actinomycin D (ActD) prior to 5 Gy IR. Immunoblotting was performed with anti-ATM-pS1981 and anti-ATM antibodies. **(D)** Quantification of the percentage of cells staining positive for H3-pS10. For each cell line, at least 3000 cells were scored in blind. Standard deviations from three independent experiments are indicated. **(E)** Quantification of comet tail moment. Both WT and CSB-KO cells were treated with 10 Gy IR and harvested for comet assays 15 min, 30 min and 1 hr post IR. At least 200 cells were scored for each sample.

Figure 6 Batenburg et al.

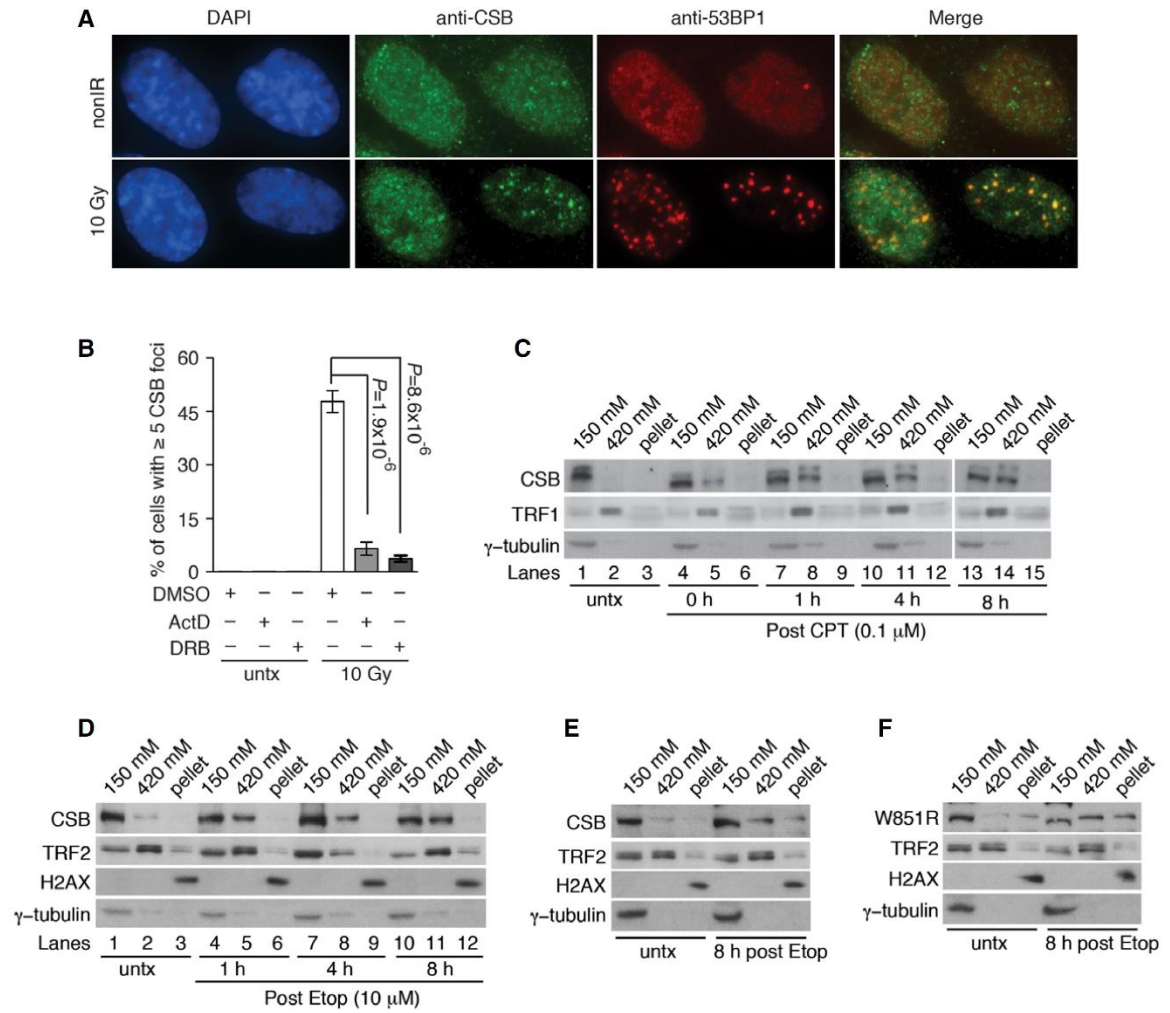


Figure 6. CSB is associated with chromatin following induction of DNA DSBs. **(A)** Analysis of indirect immunofluorescence with an anti-CSB antibody in conjunction with an anti-53BP1 antibody. hTERT-RPE cells were treated with 10 Gy IR and fixed 8 hr post IR. Cell nuclei were stained with DAPI in blue. **(B)** CSB accumulation at sites of DNA DSBs is severely impaired by actinomycin D or DRB treatment. Quantification of hTERT-RPE cells with five or more IR-induced CSB damage foci in cells. Cells were treated with actinomycin D (1 $\mu\text{g}/\text{ml}$, ActD) for 1 hr or DRB (50 μM) for 2 hr prior to 10 Gy IR and maintained in the drugs for 8 hr post IR. A total of at least 1500 cells were scored in blind. Standard deviations from three independent experiments are indicated. **(C-D)** Analysis of differential salt extraction of chromatin. hTERT-RPE cells were treated with 0.1 μM CPT (C) or 10 μM Etop (D) for 1 hr and then released from drugs for various time points as indicated. Immunoblotting was performed with anti-CSB antibody. The anti-TRF1, anti-TRF2, anti-H2AX and anti- γ -tubulin blots were used as controls for differential salt extraction. **(E-F)** Analysis of differential salt extraction of chromatin. The CSB-KO cells stably expressing either wild type CSB (E) or mutant CSB-W851R (F) were treated with 10 μM etoposide (Etop) for 1 hr and then released from Etop for 8 hr. Immunoblotting was performed with anti-CSB, anti-TRF2, anti-H2AX and anti- γ -tubulin antibodies.

Figure 7 Batenburg et al.

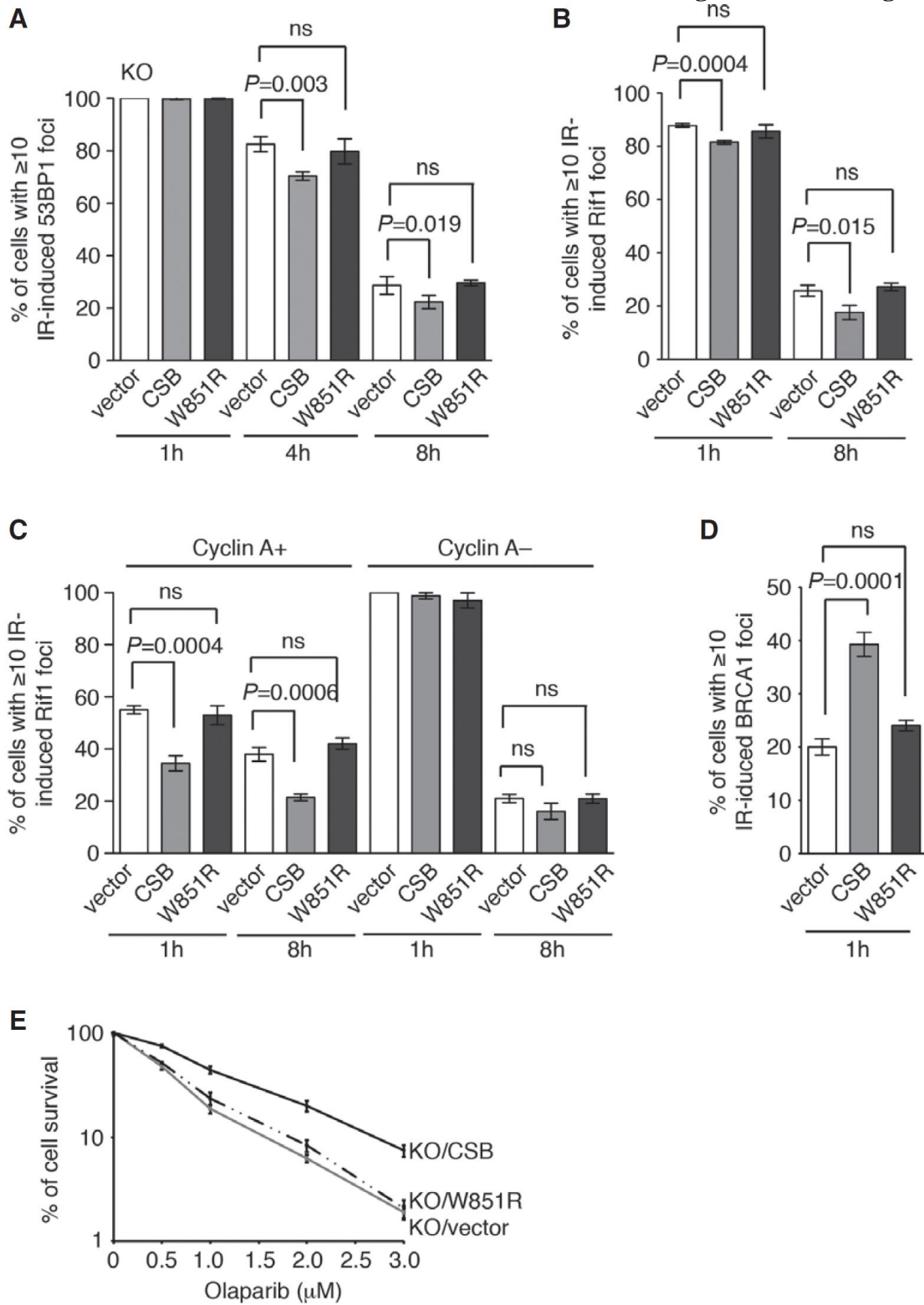


Figure 7. CSB carrying a W851R mutation is unable to suppress the recruitment of NHEJ-promoting factors to sites of DNA DSBs in S and G2 cells. **(A)** Quantification of percentage of cells with 10 or more IR-induced 53BP1 foci. CSB-KO cells stably expressing wild-type CSB, CSB-W851R or the vector alone were treated with 2 Gy IR and fixed 1 hr 4 hr and 8 hr post IR. A total of 1500 cells were scored in blind for each cell line. Standard deviations from three independent experiments are indicated. **(B)** Quantification of percentage of cells with 10 or more IR-induced Rif1 foci. CSB-KO cells stably expressing wild-type CSB, CSB-W851R or the vector alone were treated with 2 Gy IR and fixed 1 hr and 8 hr post IR. A total of 1500 cells were scored in blind for each cell line. Standard deviations from three independent experiments are indicated. **(C)** Quantification of percentage of cyclin A-positive and cyclin A-negative cells with 10 or more IR-induced Rif1 foci. Cells were treated and fixed as described in **(B)**. A total of 750 cells were scored in blind for each cell line. Standard deviations from three independent experiments are indicated. **(D)** Quantification of percentage of cells with 10 or more IR-induced BRCA1 foci. Cells were treated with 2 Gy IR and fixed 1 hr post IR. A total of 1500 cells were scored in blind for each cell line. Standard deviations from three independent experiments are indicated. **(E)** Clonogenic survival assays of olaparib-treated CSB-KO cells stably expressing wild-type CSB, CSB-W851R or the vector alone as indicated. Standard deviations from three independent experiments are indicated.

Figure 8 Batenburg et al.

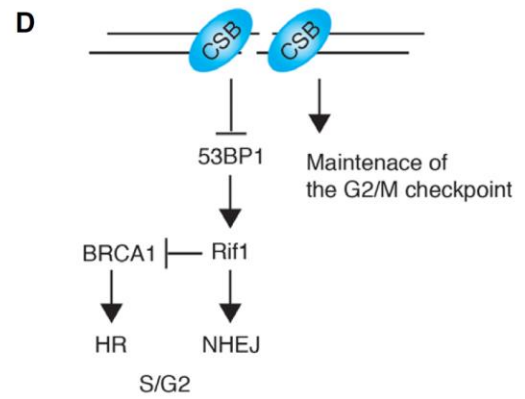
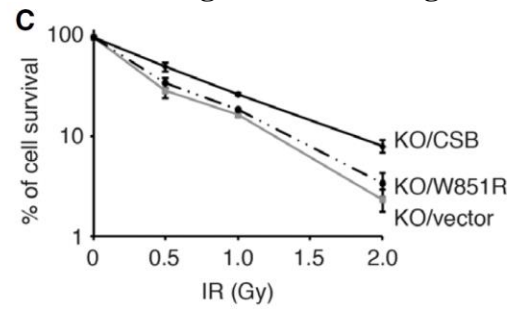
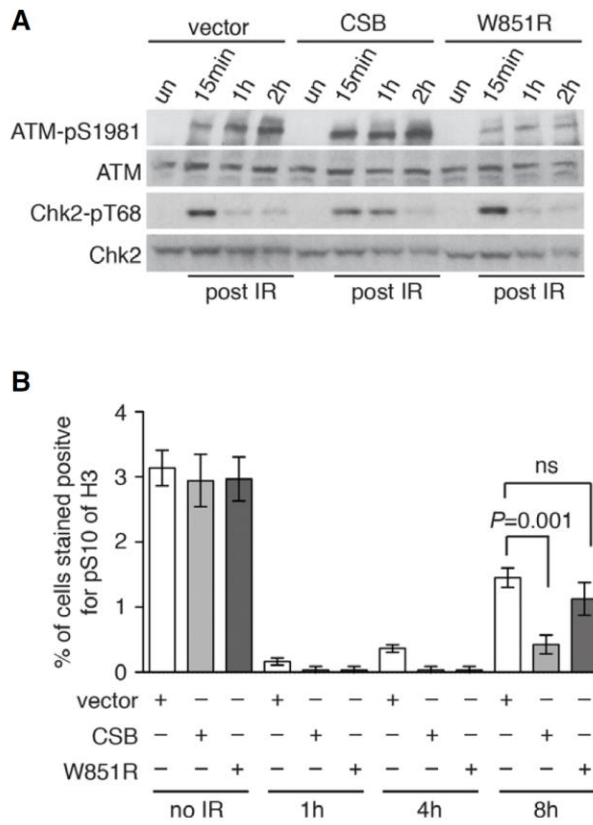


Figure 8. The ATPase activity of CSB is needed for maintaining the ATM- and Chk2-mediated DNA damage checkpoint. **(A)** Western analysis of CSB-KO cells stably expressing wild-type CSB, CSB-W851R or the vector alone as indicated. Cells were either mock-treated or treated with 5 Gy IR. Immunoblotting was performed with anti-ATM, anti-ATM-pS1981, anti-Chk2 and anti-Chk2-pT68 antibodies. **(B)** Quantification of the percentage of cells stained positive for H3-pS10. Cells were either mock-treated or treated with 2 Gy IR. For each cell line, at least 3000 cells were scored in blind. Standard deviations from three independent experiments are indicated. **(C)** Clonogenic survival assays of IR-treated CSB-KO (KO) cell stably expressing wild-type CSB, CSB-W851R or the vector alone as indicated. Standard deviations from three independent experiments are indicated. **(D)** Model for the role of CSB in repressing NHEJ and maintaining the G2/M checkpoint. See the text for more information.

Supplementary Figure 1 Batenburg et al.

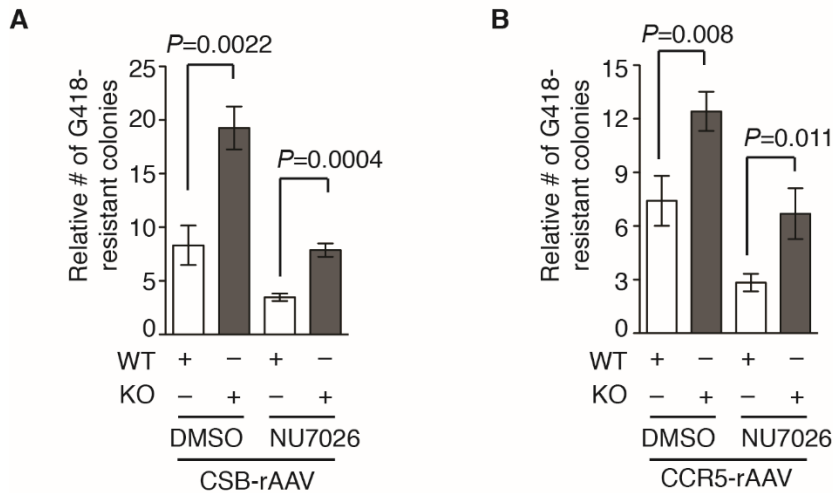


Figure S1. Treatment of DNA-PKcs inhibitor impairs the frequency of random integration in both parental (WT) and CSB-KO (KO) cells. **(A)** Quantification of the frequency of random integration of the CSB-rAAV targeting vector. Both WT and KO cells were infected with adeno-associated virus expressing the targeting vector in the presence of either DMSO or 1 μ M NU7026, a specific inhibitor of DNA-PKcs, for 48 hr. **(B)** Quantification of the frequency of random integration of the CCR5-rAAV targeting vector. Cells were treated as described in (A).

Supplementary Figure 2 Batenburg et al.

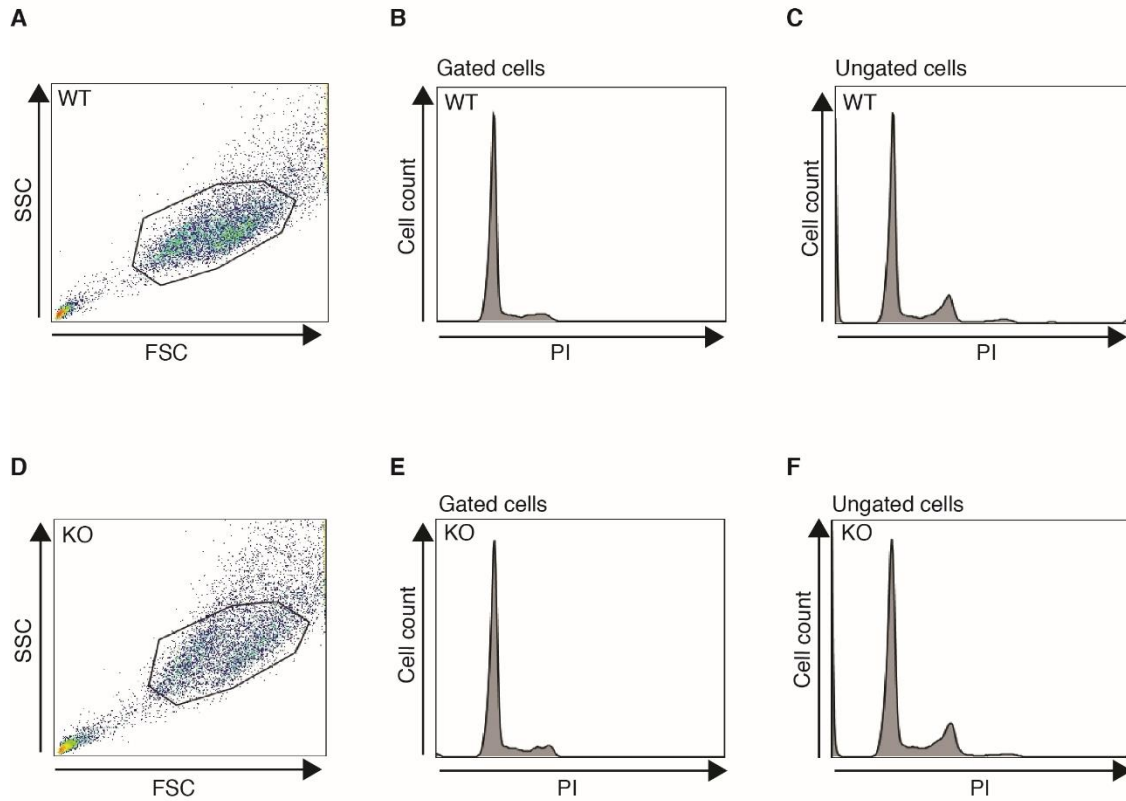


Figure S2. Normal cell cycle analysis of asynchronous parental (WT) and CSB-KO (KO) cells. FACS analysis cells labeled with 50 $\mu\text{g/ml}$ PI for wild type (WT) cells (A-C) and CSB-KO cells (D-F). (A and D) Cells gated on forward light scatter (FSC) versus side scatter (SSC). (B and E) Gated cells; (C and F) Ungated cells analyzed by PI staining.

Supplementary Figure 3 Batenburg et al.

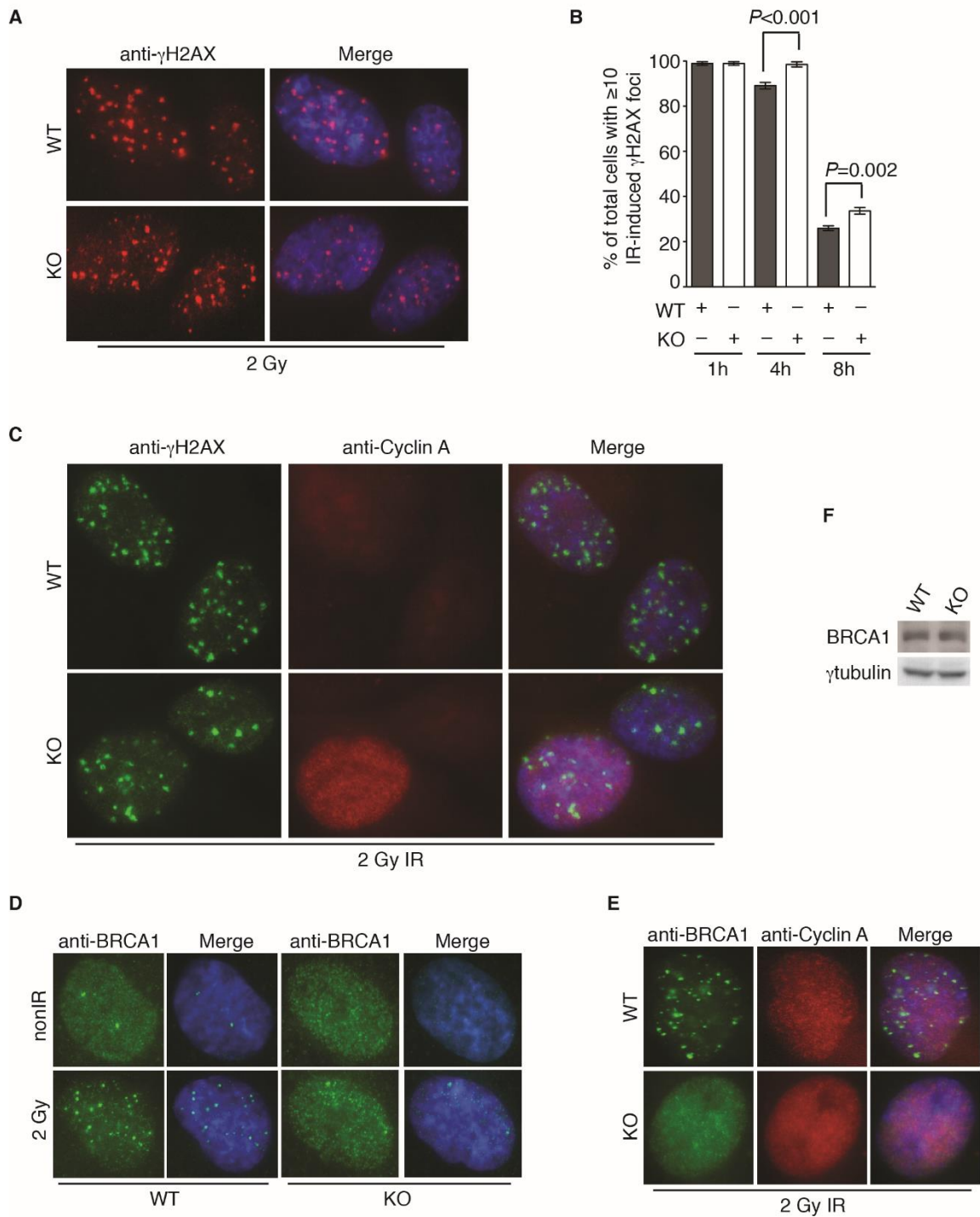


Figure S3. Knockout of CSB impairs the repair of DNA DSBs. **(A)** Analysis of indirect immunofluorescence with anti- γ H2AX antibody. Both parental (WT) and CSB-KO (KO) cells were treated with 2 Gy and fixed 1 hr post IR. Cell nuclei were stained with DAPI in blue. **(B)** Quantification of the percentage of cells with 10 or more IR-induced γ H2AX foci. Cells were treated with 2 Gy and fixed 1 hr, 4 hr and 8 hr post IR. A total of over 1500 cells from three independent experiments were scored in blind for each cell line fixed at each indicated time point. Standard deviations from three independent experiments are indicated. **(C)** Analysis of indirect immunofluorescence with anti- γ H2AX antibody in conjunction with anti-cyclin A antibody. Both parental (WT) and CSB-KO (KO) cells were treated with 2 Gy and fixed 1 hr post IR. Cell nuclei were stained with DAPI in blue. **(D)** Analysis of indirect immunofluorescence with anti-BRCA1 antibody. Cells were treated as in (C). Cell nuclei were stained with DAPI in blue. **(E)** Analysis of indirect immunofluorescence with anti-BRCA1 antibody in conjunction with anti-cyclin A antibody. Cells were treated as in (C). **(F)** Western analysis with anti-BRCA1 antibody. Immunoblotting was performed with anti-BRCA1 antibody. The γ -tubulin blot was used as a loading control.

Supplementary Figure 4 Batenburg et al.

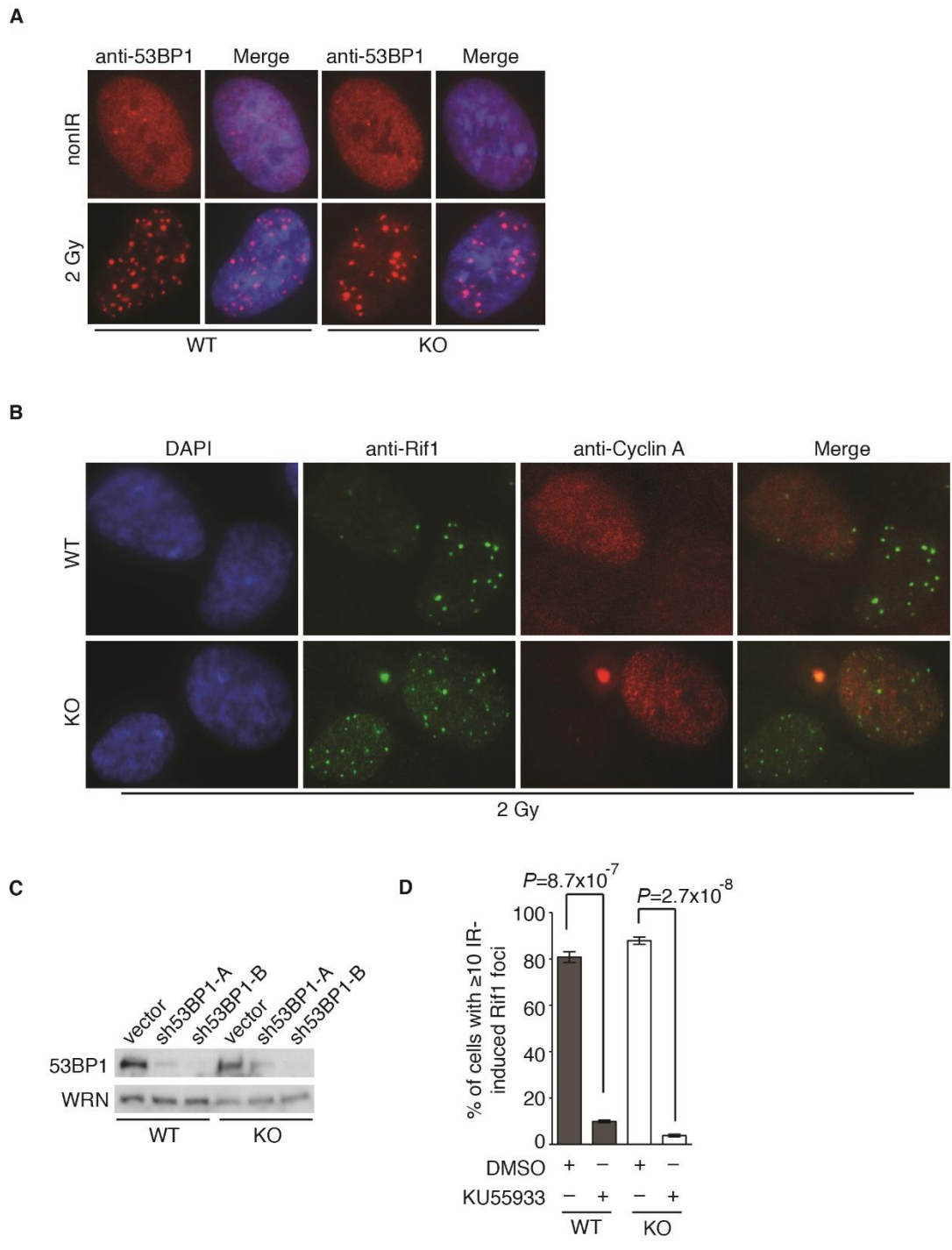


Figure S4. Knockout of CSB leads to an accumulation of NHEJ-promoting factors at sites of DNA DSBs in S and G2 cells. **(A)** Analysis of indirect immunofluorescence with anti-53BP1 antibody. Both parental (WT) and CSB-KO (KO) cells were treated with 2 Gy and fixed 1 hr post IR. Cell nuclei were stained with DAPI in blue. **(B)** Analysis of indirect immunofluorescence with anti-Rif1 antibody in conjunction with anti-cyclin A antibody. Cells were treated as in (A). **(C)** Western analysis of parental (WT) and CSB-KO (KO) cells stably expressing the vector alone or two independent shRNA against 53BP1 (sh53BP1-A and sh53BP1-B) as indicated. Immunoblotting was carried out with anti-53BP1 antibody. WRN was used as a loading control. **(D)** Quantification of the percentage of cells with 10 or more IR-induced Rif1 foci. WT and CSB-KO cells were treated with DMSO or 10 μ M KU55933, a specific inhibitor of ATM, prior to 2 Gy IR, and then fixed 1 hr post IR. At least of 1500 cells were scored in blind. Standard deviations from three independent experiments are indicated.

Supplementary Figure 5 Batenburg et al.

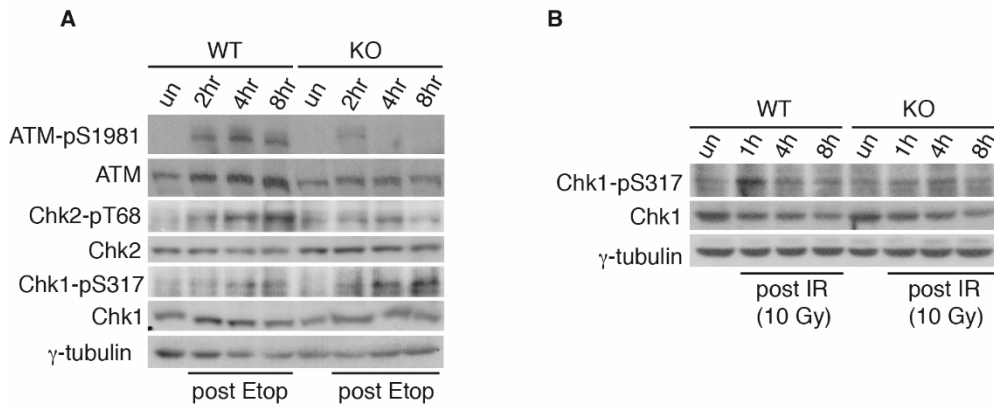


Figure S5. Knockout of CSB impairs the maintenance of the ATM- and Chk2-mediated DNA damage checkpoint. **(A)** Western analysis of parental (WT) and CSB-KO (KO) cells. Cells were either mock-treated or treated with 10 μ M etoposide (Etop) and then harvested at various time points post release from Etop as indicated. Immunoblotting was performed with anti-ATM, anti-ATM-pS1981, anti-Chk2, anti-Chk2-pT68, anti-Chk1, anti-Chk1-pS317 and anti- γ -tubulin antibodies. **(B)** Western analysis of parental (WT) and CSB-KO (KO) cells. Cells were either mock treated or treated with 10 Gy IR and then harvested at various time points post IR as indicated. Immunoblotting was performed with anti-Chk1, anti-Chk1-pS317 and anti- γ -tubulin antibodies.

Supplementary Figure 6 Batenburg et al.

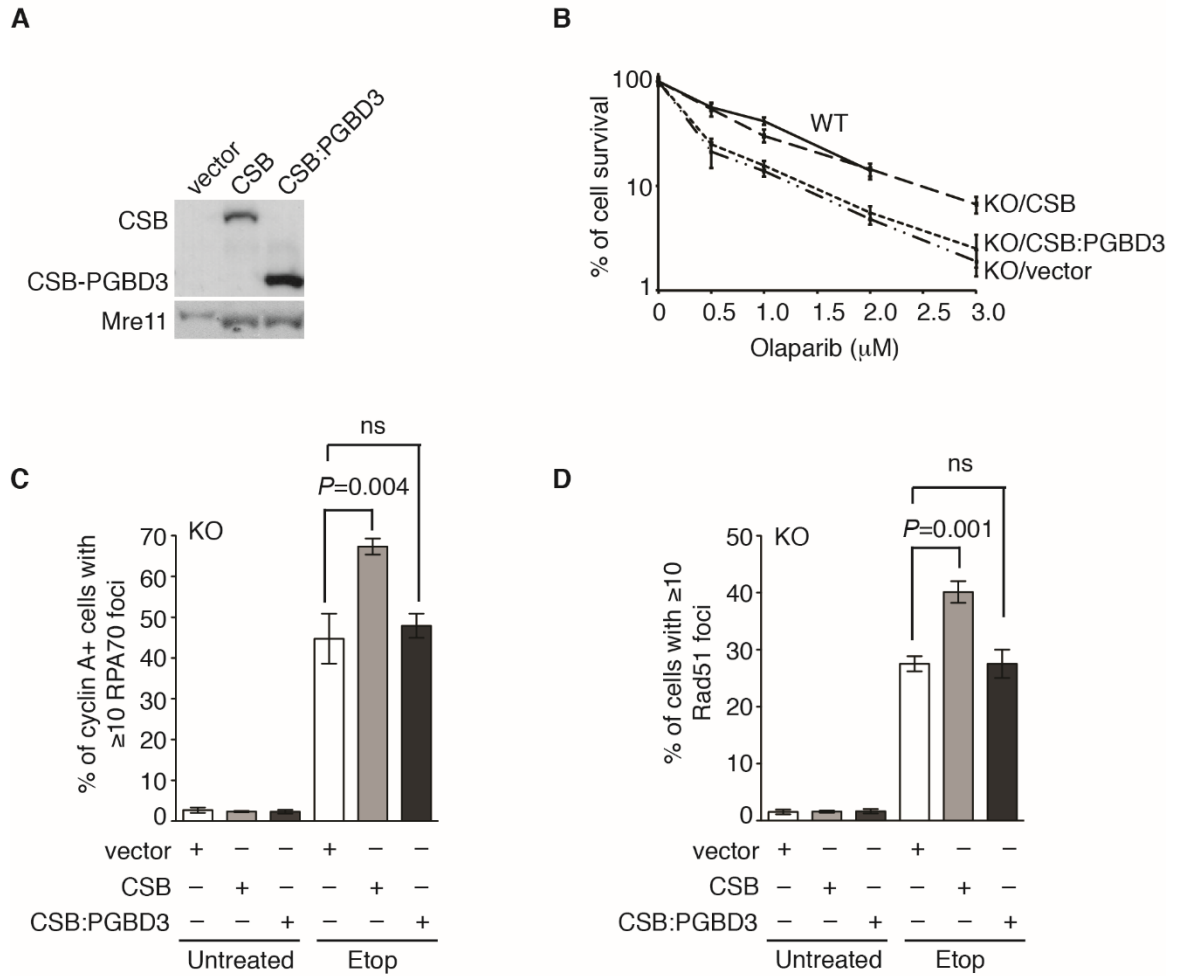


Figure S6. Introduction of CSB but not CSB:PGBD3 alone suppresses the defect in the recruitment of HR factors to sites of DNA DSBs. **(A)** Western analysis of the CSB-KO cells stably expressing CSB or CSB:PGBD3. Immunoblotting was performed with an antibody against the N-terminus of CSB. Mre11 was used as a loading control. **(B)** Clonogenic survival assays of olaparib-treated CSB-KO (KO) cells stably expressing CSB, CSB:PGBD3 or the vector alone as indicated. Standard deviations from three independent experiments are indicated. **(C)** Quantification of the percentage of cyclin A-positive cells with 10 or more etoposide-induced RPA foci. CSB-KO cells stably expressing CSB, CSB:PGBD3 or the vector alone were treated with 10 μ M etoposide (Etop) for 1 hr and fixed 8 hr post release from Etop. A total of 1500 cells from three independent experiments were scored in blind for each cell line at each indicated time point. Standard deviations from three independent experiments are indicated. **(D)** Quantification of the percentage of cells with 10 or more etoposide-induced Rad51 foci. Cells were treated and scored as in (C). Standard deviations from three independent experiments are indicated.

Supplementary Figure 7 Batenburg et al.

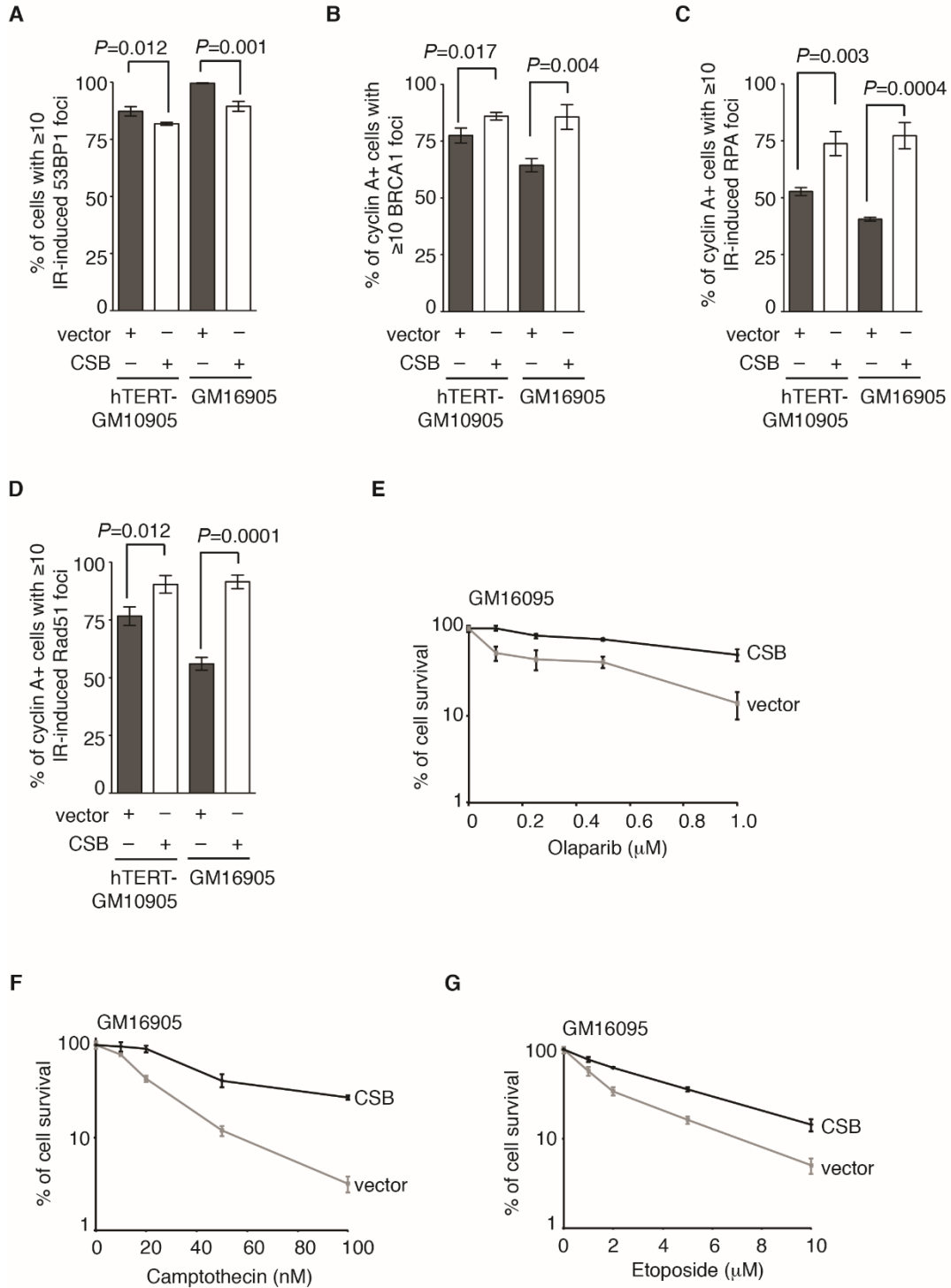


Figure S7. Recruitment of DSB repair factors to sites of DNA damage is misregulated in cells derived from CS patients. **(A)** Quantification of percentage of cells with 10 or more IR-induced 53BP1 foci. GM16095 and hTERT-GM10905 cells stably expressing either the vector alone or wild type CSB were treated with 2 Gy IR and fixed 1 hr post IR. A total of 1500 cells were scored in blind for each cell line. Standard deviations from three independent experiments are indicated. **(B)** Quantification of percentage of cyclin A-positive cells with 10 or more IR-induced BRCA1 foci. Two pair of isogenic CS cell lines (hTERT-GM10905 and GM16095) stably expressing either the vector alone or wild-type CSB were treated with 2 Gy IR and fixed 1 hr post IR. A total of 750 cells were scored in blind for each cell line. Standard deviations from three independent experiments are indicated. **(C)** Quantification of percentage of cyclin A-positive cells with 10 or more IR-induced RPA foci. GM16095 and hTERT-GM10905 cells stably expressing either the vector alone or wild-type CSB were treated with 10 Gy IR and fixed 8 hr post IR. A total of 750 cells were scored in blind for each cell line. Standard deviations from three independent experiments are indicated. **(D)** Quantification of percentage of cyclin A-positive cells with 10 or more IR-induced Rad51 foci. Cells were treated and scored as in (C). Standard deviations from three independent experiments are indicated. **(E)** Clonogenic survival assays of olaparib-treated GM16095 cells stably expressing wild type CSB or the vector alone as indicated. Standard deviations from three independent experiments are indicated. **(F)** Clonogenic survival assays of CPT-treated GM16095 cells stably expressing wild-type CSB or the vector alone as indicated. Standard deviations from three independent experiments are indicated. **(G)** Clonogenic survival assays of Etop-treated GM16095 cells

stably expressing wild type CSB or the vector alone as indicated. Standard deviations from three independent experiments are indicated.

Supplementary Figure 8 Batenburg et al.

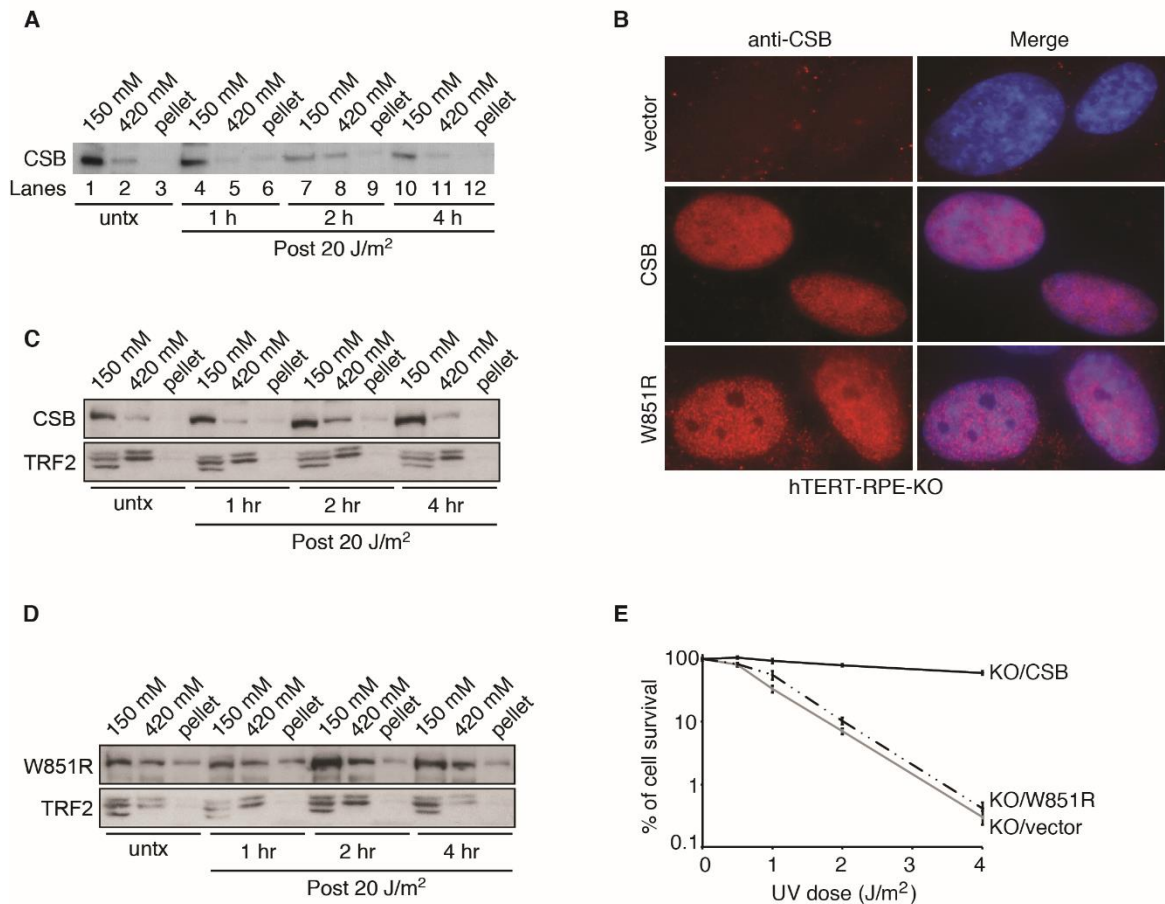


Figure S8. The W851R mutation abrogates UV-induced chromatin association of CSB and its function in UV repair. **(A)** Analysis of differential salt extraction of chromatin of parental cells following treatment with 20 J/m². Immunoblotting was performed with anti-CSB antibody. **(B)** Analysis of indirect immunofluorescence with anti-CSB antibody. The CSB-KO cells were complemented with wild-type CSB, CSB-W851R or the vector alone.

Cell nuclei were stained with DAPI in blue. **(C-D)** Analysis of differential salt extraction of chromatin. The CSB-KO cells stably expressing wild-type CSB (C) or mutant CSB-W851R (D) were either mock-treated or treated with UV (20 J/m²). Cells were harvested post UV treatment at various time points as indicated. Immunoblotting was performed with anti-CSB antibody. The anti-TRF2 blot was used as a control. **(E)** Clonogenic survival assays of UV-treated knockout (KO) cell stably expressing CSB, CSB-W851R or the vector alone as indicated. Standard deviations from three independent experiments are indicated.

3.2.7 References

- Aamann MD, Sorensen MM, Hvitby C, Berquist BR, Muftuoglu M, Tian J, de Souza-Pinto NC, Scheibye-Knudsen M, Wilson DM, 3rd, Stevnsner T, Bohr VA (2010) Cockayne syndrome group B protein promotes mitochondrial DNA stability by supporting the DNA repair association with the mitochondrial membrane. *FASEB J* **24**: 2334-2346
- Aydin OZ, Marteiijn JA, Ribeiro-Silva C, Rodriguez Lopez A, Wijgers N, Smeenk G, van Attikum H, Poot RA, Vermeulen W, Lans H (2014) Human ISWI complexes are targeted by SMARCA5 ATPase and SLIDE domains to help resolve lesion-stalled transcription. *Nucleic Acids Res* **42**: 8473-8485
- Aymard F, Bugler B, Schmidt CK, Guillou E, Caron P, Briois S, Iacovoni JS, Daburon V, Miller KM, Jackson SP, Legube G (2014) Transcriptionally active chromatin recruits homologous recombination at DNA double-strand breaks. *Nat Struct Mol Biol* **21**: 366-374
- Bakkenist CJ, Kastan MB (2003) DNA damage activates ATM through intermolecular autophosphorylation and dimer dissociation. *Nature* **421**: 499-506
- Batenburg NL, Mitchell TR, Leach DM, Rainbow AJ, Zhu XD (2012) Cockayne Syndrome group B protein interacts with TRF2 and regulates telomere length and stability. *Nucleic Acids Res* **40**: 9661-9674
- Bouwman P, Aly A, Escandell JM, Pieterse M, Bartkova J, van der Gulden H, Hiddingh S, Thanasoula M, Kulkarni A, Yang Q, Haffty BG, Tommiska J, Blomqvist C, Drapkin R, Adams DJ, Nevanlinna H, Bartek J, Tarsounas M, Ganesan S, Jonkers J (2010) 53BP1 loss rescues BRCA1 deficiency and is associated with triple-negative and BRCA-mutated breast cancers. *Nat Struct Mol Biol* **17**: 688-695
- Bunting SF, Callen E, Wong N, Chen HT, Polato F, Gunn A, Bothmer A, Feldhahn N, Fernandez-Capetillo O, Cao L, Xu X, Deng CX, Finkel T, Nussenzweig M, Stark

- JM, Nussenzweig A (2010) 53BP1 inhibits homologous recombination in Brca1-deficient cells by blocking resection of DNA breaks. *Cell* **141**: 243-254
- Burkard ME, Randall CL, Laroche S, Zhang C, Shokat KM, Fisher RP, Jallepalli PV (2007) Chemical genetics reveals the requirement for Polo-like kinase 1 activity in positioning RhoA and triggering cytokinesis in human cells. *Proc Natl Acad Sci U S A* **104**: 4383-4388
- Caldecott KW (2008) Single-strand break repair and genetic disease. *Nat Rev Genet* **9**: 619-631
- Cao L, Xu X, Bunting SF, Liu J, Wang RH, Cao LL, Wu JJ, Peng TN, Chen J, Nussenzweig A, Deng CX, Finkel T (2009) A selective requirement for 53BP1 in the biological response to genomic instability induced by Brca1 deficiency. *Mol Cell* **35**: 534-541
- Carvalho S, Vitor AC, Sridhara SC, Martins FB, Raposo AC, Desterro JM, Ferreira J, de Almeida SF (2014) SETD2 is required for DNA double-strand break repair and activation of the p53-mediated checkpoint. *Elife* **3**: e02482
- Chapman JR, Barral P, Vannier JB, Borel V, Steger M, Tomas-Loba A, Sartori AA, Adams IR, Batista FD, Boulton SJ (2013) RIF1 Is essential for 53BP1-dependent nonhomologous end joining and suppression of DNA double-strand break resection. *Mol Cell* **49**: 858-871
- Chapman JR, Taylor MR, Boulton SJ (2012) Playing the end game: DNA double-strand break repair pathway choice. *Mol Cell* **47**: 497-510
- Chiolo I, Minoda A, Colmenares SU, Polyzos A, Costes SV, Karpen GH (2011) Double-strand breaks in heterochromatin move outside of a dynamic HP1a domain to complete recombinational repair. *Cell* **144**: 732-744
- Cho I, Tsai PF, Lake RJ, Basheer A, Fan HY (2013) ATP-dependent chromatin remodeling by Cockayne syndrome protein B and NAP1-like histone chaperones is required for efficient transcription-coupled DNA repair. *PLoS Genet* **9**: e1003407
- Citterio E, Rademakers S, van der Horst GT, van Gool AJ, Hoeijmakers JH, Vermeulen W (1998) Biochemical and biological characterization of wild-type and ATPase-deficient Cockayne syndrome B repair protein. *J Biol Chem* **273**: 11844-11851
- Citterio E, Van Den Boom V, Schnitzler G, Kanaar R, Bonte E, Kingston RE, Hoeijmakers JH, Vermeulen W (2000) ATP-dependent chromatin remodeling by the Cockayne syndrome B DNA repair-transcription-coupling factor. *Mol Cell Biol* **20**: 7643-7653
- Daley JM, Sung P (2014) 53BP1, BRCA1, and the choice between recombination and end joining at DNA double-strand breaks. *Mol Cell Biol* **34**: 1380-1388
- Dang LH, Chen F, Ying C, Chun SY, Knock SA, Appelman HD, Dang DT (2006) CDX2 has tumorigenic potential in the human colon cancer cell lines LOVO and SW48. *Oncogene* **25**: 2264-2272
- Dhawan A, Anderson D, de Pascual-Teresa S, Santos-Buelga C, Clifford MN, Ioannides C (2002) Evaluation of the antigenotoxic potential of monomeric and dimeric flavanols, and black tea polyphenols against heterocyclic amine-induced DNA damage in human lymphocytes using the Comet assay. *Mut Res* **515**: 39-56

- Di Nicolantonio F, Arena S, Gallicchio M, Zecchin D, Martini M, Flonta SE, Stella GM, Lamba S, Cancelliere C, Russo M, Geuna M, Appendino G, Fantozzi R, Medico E, Bardelli A (2008) Replacement of normal with mutant alleles in the genome of normal human cells unveils mutation-specific drug responses. *Proc Natl Acad Sci U S A* **105**: 20864-20869
- Di Virgilio M, Callen E, Yamane A, Zhang W, Jankovic M, Gitlin AD, Feldhahn N, Resch W, Oliveira TY, Chait BT, Nussenzweig A, Casellas R, Robbiani DF, Nussenzweig MC (2013) Rif1 prevents resection of DNA breaks and promotes immunoglobulin class switching. *Science* **339**: 711-715
- Elli R, Chessa L, Antonelli A, Petrinelli P, Ambra R, Marcucci L (1996) Effects of topoisomerase II inhibition in lymphoblasts from patients with progeroid and "chromosome instability" syndromes. *Cancer Genet Cytogenet* **87**: 112-116
- Escribano-Diaz C, Orthwein A, Fradet-Turcotte A, Xing M, Young JT, Tkac J, Cook MA, Rosebrock AP, Munro M, Canny MD, Xu D, Durocher D (2013) A cell cycle-dependent regulatory circuit composed of 53BP1-Rif1 and BRCA1-CtIP controls DNA repair pathway choice. *Mol Cell* **49**: 872-883
- Fattah F, Lee EH, Weisensel N, Wang Y, Lichter N, Hendrickson EA (2010) Ku regulates the non-homologous end joining pathway choice of DNA double-strand break repair in human somatic cells. *PLoS Genet* **6**: e1000855
- Feng L, Fong KW, Wang J, Wang W, Chen J (2013) RIF1 counteracts BRCA1-mediated end resection during DNA repair. *J Biol Chem* **288**: 11135-11143
- Goodarzi AA, Jeggo P, Lobrich M (2010) The influence of heterochromatin on DNA double strand break repair: Getting the strong, silent type to relax. *DNA repair* **9**: 1273-1282
- Gottipati P, Helleday T (2009) Transcription-associated recombination in eukaryotes: link between transcription, replication and recombination. *Mutagenesis* **24**: 203-210
- Hashimoto S, Suga T, Kudo E, Ihn H, Uchino M, Tateishi S (2008) Adult-onset neurological degeneration in a patient with Cockayne syndrome and a null mutation in the CSB gene. *J Invest Dermatol* **128**: 1597-1599
- Horibata K, Iwamoto Y, Kuraoka I, Jaspers NG, Kurimasa A, Oshimura M, Ichihashi M, Tanaka K (2004) Complete absence of Cockayne syndrome group B gene product gives rise to UV-sensitive syndrome but not Cockayne syndrome. *Proc Natl Acad Sci U S A* **101**: 15410-15415
- Hucl T, Rago C, Gallmeier E, Brody JR, Gorospe M, Kern SE (2008) A syngeneic variance library for functional annotation of human variation: application to BRCA2. *Cancer Res* **68**: 5023-5030
- Huertas P, Jackson SP (2009) Human CtIP mediates cell cycle control of DNA end resection and double strand break repair. *J Biol Chem* **284**: 9558-9565
- Iyama T, Lee SY, Berquist BR, Gileadi O, Bohr VA, Seidman MM, McHugh PJ, Wilson DM, 3rd (2015) CSB interacts with SNM1A and promotes DNA interstrand crosslink processing. *Nucleic Acids Res* **43**: 247-258
- Jha DK, Strahl BD (2014) An RNA polymerase II-coupled function for histone H3K36 methylation in checkpoint activation and DSB repair. *Nat Commun* **5**: 3965

- Kan Y, Ruis B, Lin S, Hendrickson EA (2014) The mechanism of gene targeting in human somatic cells. *PLoS Genet* **10**: e1004251
- Kohli M, Rago C, Lengauer C, Kinzler KW, Vogelstein B (2004) Facile methods for generating human somatic cell gene knockouts using recombinant adeno-associated viruses. *Nucleic Acids Res* **32**: e3
- Kotin RM, Linden RM, Berns KI (1992) Characterization of a preferred site on human chromosome 19q for integration of adeno-associated virus DNA by non-homologous recombination. *EMBO J* **11**: 5071-5078
- Lake RJ, Geyko A, Hemashettar G, Zhao Y, Fan HY (2010) UV-induced association of the CSB remodeling protein with chromatin requires ATP-dependent relief of N-terminal autorepression. *Mol Cell* **37**: 235-246
- Lan L, Ui A, Nakajima S, Hatakeyama K, Hoshi M, Watanabe R, Janicki SM, Ogiwara H, Kohno T, Kanno S, Yasui A (2010) The ACF1 complex is required for DNA double-strand break repair in human cells. *Mol Cell* **40**: 976-987
- Laugel V, Dalloz C, Stary A, Cormier-Daire V, Desguerre I, Renouil M, Fourmaintraux A, Velez-Cruz R, Egly JM, Sarasin A, Dollfus H (2008) Deletion of 5' sequences of the CSB gene provides insight into the pathophysiology of Cockayne syndrome. *Eur J Hum Genet* **16**: 320-327
- Leadon SA, Cooper PK (1993) Preferential repair of ionizing radiation-induced damage in the transcribed strand of an active human gene is defective in Cockayne syndrome. *Proc Natl Acad Sci U S A* **90**: 10499-10503
- Lee JH, Paull TT (2004) Direct activation of the ATM protein kinase by the Mre11/Rad50/Nbs1 complex. *Science* **304**: 93-96
- Lee JH, Paull TT (2005) ATM activation by DNA double-strand breaks through the Mre11-Rad50-Nbs1 complex. *Science* **308**: 551-554
- Lukas J, Lukas C, Bartek J (2011) More than just a focus: The chromatin response to DNA damage and its role in genome integrity maintenance. *Nat Cell Biol* **13**: 1161-1169
- McKerlie M, Lin S, Zhu XD (2012) ATM regulates proteasome-dependent subnuclear localization of TRF1, which is important for telomere maintenance. *Nucleic Acids Res* **40**: 3975-3989
- McKerlie M, Walker JR, Mitchell TR, Wilson FR, Zhu XD (2013) Phosphorylated (pT371)TRF1 is recruited to sites of DNA damage to facilitate homologous recombination and checkpoint activation. *Nucleic Acids Res* **41**: 10268-10282
- McKerlie M, Zhu XD (2011) Cyclin B-dependent kinase 1 regulates human TRF1 to modulate the resolution of sister telomeres. *Nat Commun* **2**:371 doi: **10.1038/ncomms1372**
- Mitchell TR, Glenfield K, Jeyanthan K, Zhu XD (2009) Arginine methylation regulates telomere length and stability. *Mol Cell Biol* **29**: 4918-4934
- Mitchell TR, Zhu XD (2014) Methylated TRF2 associates with the nuclear matrix and serves as a potential biomarker for cellular senescence. *Aging (Albany NY)* **6**: 248-263

- Newman JC, Bailey AD, Fan HY, Pavelitz T, Weiner AM (2008) An abundant evolutionarily conserved CSB-PiggyBac fusion protein expressed in Cockayne syndrome. *PLoS Genet* **4**: e1000031
- Newman JC, Bailey AD, Weiner AM (2006) Cockayne syndrome group B protein (CSB) plays a general role in chromatin maintenance and remodeling. *Proc Natl Acad Sci U S A* **103**: 9613-9618
- Oh S, Wang Y, Zimbric J, Hendrickson EA (2013) Human LIGIV is synthetically lethal with the loss of Rad54B-dependent recombination and is required for certain chromosome fusion events induced by telomere dysfunction. *Nucleic Acids Res* **41**: 1734-1749
- Pai CC, Deegan RS, Subramanian L, Gal C, Sarkar S, Blaikley EJ, Walker C, Hulme L, Bernhard E, Codlin S, Bahler J, Allshire R, Whitehall S, Humphrey TC (2014) A histone H3K36 chromatin switch coordinates DNA double-strand break repair pathway choice. *Nat Commun* **5**: 4091
- Panier S, Boulton SJ (2014) Double-strand break repair: 53BP1 comes into focus. *Nat Rev Mol Cell Biol* **15**: 7-18
- Pfister SX, Ahrabi S, Zalmas LP, Sarkar S, Aymard F, Bachrati CZ, Helleday T, Legube G, La Thangue NB, Porter AC, Humphrey TC (2014) SETD2-dependent histone H3K36 trimethylation is required for homologous recombination repair and genome stability. *Cell Rep* **7**: 2006-2018
- Rogakou EP, Boon C, Redon C, Bonner WM (1999) Megabase chromatin domains involved in DNA double-strand breaks in vivo. *J Cell Biol* **146**: 905-916
- Rogakou EP, Pilch DR, Orr AH, Ivanova VS, Bonner WM (1998) DNA double-stranded breaks induce histone H2AX phosphorylation on serine 139. *J Biol Chem* **273**: 5858-5868
- Ruis BL, Fattah KR, Hendrickson EA (2008) The catalytic subunit of DNA-dependent protein kinase regulates proliferation, telomere length, and genomic stability in human somatic cells. *Mol Cell Biol* **28**: 6182-6195
- Ryan AJ, Squires S, Strutt HL, Johnson RT (1991) Camptothecin cytotoxicity in mammalian cells is associated with the induction of persistent double strand breaks in replicating DNA. *Nucleic Acids Res* **19**: 3295-3300
- Sakai A, Sakasai R, Kakeji Y, Kitao H, Maehara Y (2012) PARP and CSB modulate the processing of transcription-mediated DNA strand breaks. *Genes Genet Syst* **87**: 265-272
- Sakasai R, Teraoka H, Takagi M, Tibbetts RS (2010) Transcription-dependent activation of ataxia telangiectasia mutated prevents DNA-dependent protein kinase-mediated cell death in response to topoisomerase I poison. *J Biol Chem* **285**: 15201-15208
- Savolainen L, Cassel T, Helleday T (2010) The XPD subunit of TFIIH is required for transcription-associated but not DNA double-strand break-induced recombination in mammalian cells. *Mutagenesis* **25**: 623-629
- Scheibye-Knudsen M, Ramamoorthy M, Sykora P, Maynard S, Lin PC, Minor RK, Wilson DM, 3rd, Cooper M, Spencer R, de Cabo R, Croteau DL, Bohr VA (2012)

- Cockayne syndrome group B protein prevents the accumulation of damaged mitochondria by promoting mitochondrial autophagy. *J Exp Med* **209**: 855-869
- Seluanov A, Mittelman D, Pereira-Smith OM, Wilson JH, Gorbunova V (2004) DNA end joining becomes less efficient and more error-prone during cellular senescence. *Proc Natl Acad Sci U S A* **101**: 7624-7629
- Selzer RR, Nyaga S, Tuo J, May A, Muftuoglu M, Christiansen M, Citterio E, Brosh RM, Jr., Bohr VA (2002) Differential requirement for the ATPase domain of the Cockayne syndrome group B gene in the processing of UV-induced DNA damage and 8-oxoguanine lesions in human cells. *Nucleic Acids Res* **30**: 782-793
- Shen M, Zhou T, Xie W, Ling T, Zhu Q, Zong L, Lyu G, Gao Q, Zhang F, Tao W (2013) The chromatin remodeling factor CSB recruits histone acetyltransferase PCAF to rRNA gene promoters in active state for transcription initiation. *PLoS One* **8**: e62668
- Shiloh Y (2003) ATM and related protein kinases: safeguarding genome integrity. *Nat Rev Cancer* **3**: 155-168
- Sollier J, Stork CT, Garcia-Rubio ML, Paulsen RD, Aguilera A, Cimprich KA (2014) Transcription-coupled nucleotide excision repair factors promote R-loop-induced genome instability. *Mol Cell* **56**: 777-785
- Squires S, Ryan AJ, Strutt HL, Johnson RT (1993) Hypersensitivity of Cockayne's syndrome cells to camptothecin is associated with the generation of abnormally high levels of double strand breaks in nascent DNA. *Cancer Res* **53**: 2012-2019
- Stevnsner T, Muftuoglu M, Aamann MD, Bohr VA (2008) The role of Cockayne Syndrome group B (CSB) protein in base excision repair and aging. *Mech Ageing Dev* **129**: 441-448
- Thorslund T, von Kobbe C, Harrigan JA, Indig FE, Christiansen M, Stevnsner T, Bohr VA (2005) Cooperation of the Cockayne syndrome group B protein and poly(ADP-ribose) polymerase 1 in the response to oxidative stress. *Mol Cell Biol* **25**: 7625-7636
- Troelstra C, van Gool A, de Wit J, Vermeulen W, Bootsma D, Hoeijmakers JH (1992) ERCC6, a member of a subfamily of putative helicases, is involved in Cockayne's syndrome and preferential repair of active genes. *Cell* **71**: 939-953
- Tuo J, Jaruga P, Rodriguez H, Bohr VA, Dizdaroglu M (2003) Primary fibroblasts of Cockayne syndrome patients are defective in cellular repair of 8-hydroxyguanine and 8-hydroxyadenine resulting from oxidative stress. *FASEB J* **17**: 668-674
- Tuo J, Jaruga P, Rodriguez H, Dizdaroglu M, Bohr VA (2002) The cockayne syndrome group B gene product is involved in cellular repair of 8-hydroxyadenine in DNA. *J Biol Chem* **277**: 30832-30837
- van der Horst GT, van Steeg H, Berg RJ, van Gool AJ, de Wit J, Weeda G, Morreau H, Beems RB, van Kreijl CF, de Gruijl FR, Bootsma D, Hoeijmakers JH (1997) Defective transcription-coupled repair in Cockayne syndrome B mice is associated with skin cancer predisposition. *Cell* **89**: 425-435
- Velez-Cruz R, Egly JM (2013) Cockayne syndrome group B (CSB) protein: at the crossroads of transcriptional networks. *Mech Ageing Dev* **134**: 234-242

- Veuger SJ, Curtin NJ, Richardson CJ, Smith GC, Durkacz BW (2003) Radiosensitization and DNA repair inhibition by the combined use of novel inhibitors of DNA-dependent protein kinase and poly(ADP-ribose) polymerase-1. *Cancer Res* **63**: 6008-6015
- Wong HK, Muftuoglu M, Beck G, Imam SZ, Bohr VA, Wilson DM, 3rd (2007) Cockayne syndrome B protein stimulates apurinic endonuclease 1 activity and protects against agents that introduce base excision repair intermediates. *Nucleic Acids Res* **35**: 4103-4113
- Wu Y, Mitchell TR, Zhu XD (2008) Human XPF controls TRF2 and telomere length maintenance through distinctive mechanisms. *Mech Ageing Dev* **129**: 602-610
- Wu Y, Xiao S, Zhu XD (2007a) MRE11-RAD50-NBS1 and ATM function as co-mediators of TRF1 in telomere length control. *Nat Struct Mol Biol* **14**: 832-840
- Wu Y, Zagal NJ, Rainbow AJ, Zhu XD (2007b) XPF with mutations in its conserved nuclease domain is defective in DNA repair but functions in TRF2-mediated telomere shortening. *DNA Repair (Amst)* **6**: 157-166
- Xie A, Hartlerode A, Stucki M, Odate S, Puget N, Kwok A, Nagaraju G, Yan C, Alt FW, Chen J, Jackson SP, Scully R (2007) Distinct roles of chromatin-associated proteins MDC1 and 53BP1 in mammalian double-strand break repair. *Mol Cell* **28**: 1045-1057
- Xie W, Ling T, Zhou Y, Feng W, Zhu Q, Stunnenberg HG, Grummt I, Tao W (2012) The chromatin remodeling complex NuRD establishes the poised state of rRNA genes characterized by bivalent histone modifications and altered nucleosome positions. *Proc Natl Acad Sci U S A* **109**: 8161-8166
- Ye JZ, de Lange T (2004) TIN2 is a tankyrase 1 PARP modulator in the TRF1 telomere length control complex. *Nat. Genet.* **36**: 618-623.
- Yuan X, Feng W, Imhof A, Grummt I, Zhou Y (2007) Activation of RNA polymerase I transcription by cockayne syndrome group B protein and histone methyltransferase G9a. *Mol Cell* **27**: 585-595
- Zhu XD, Kuster B, Mann M, Petrini JH, Lange T (2000) Cell-cycle-regulated association of RAD50/MRE11/NBS1 with TRF2 and human telomeres. *Nat Genet* **25**: 347-352
- Zhu XD, Niedernhofer L, Kuster B, Mann M, Hoeijmakers JH, de Lange T (2003) ERCC1/XPF removes the 3' overhang from uncapped telomeres and represses formation of telomeric DNA-containing double minute chromosomes. *Mol Cell* **12**: 1489-1498
- Zimmermann M, Lottersberger F, Buonomo SB, Sfeir A, de Lange T (2013) 53BP1 regulates DSB repair using Rif1 to control 5' end resection. *Science* **339**: 700-704

Chapter 4

ATM and CDK2 control chromatin remodeler CSB inhibit RIF1 in DSB repair pathway choice

4.1 Preface

The work included in this chapter serves to expand upon the function of CSB in DNA DSB repair. Specifically, how CSB is recruited to DSBs and what function it has at DSBs to regulate DNA DSB repair pathway choice. This work describes the mechanism in which CSB is recruited to DSBs, the chromatin remodeling activity that CSB has at DSBs, and how this activity is regulated by post-translational modification. These findings demonstrate that CSB functions *in vivo* as a chromatin remodeler and that phosphorylation plays an important role in regulating CSB function.

The work presented in this chapter has been submitted for publication in Nature Communications. Majority of the experiments were performed by myself. John R. Walker cloned all CSB constructs used, performed sequence analysis and computer modeling of WHD in Supplementary Figure S2, immunoprecipitated Flag-CSB used for mass spectrometry analysis in Supplementary Figure S7a, and produced recombinant CSB used in Figure 7d. Sylvie Noordermeer performed mass spectrometry analysis of Flag-CSB in Supplementary Figure S7a. Nathalie Moatti performed the FACS analysis of DR-GFP assays in Figure 5i and Supplementary Figure S7f. The experimental design was a collaborative effort between myself, John R. Walker and Xu-Dong Zhu. The writing of the manuscript was a collaborative effort from myself, John R. Walker and Xu-Dong Zhu with input from other authors.

4.2 Submitted Manuscript - ATM and CDK2 control chromatin remodeler CSB inhibit RIF1 in DSB repair pathway choice

Nicole L. Batenburg¹, John R. Walker¹, Sylvie M. Noordermeer^{2,3}, Nathalie Moatti², Daniel Durocher² and Xu-Dong Zhu^{1,*}

¹Department of Biology, McMaster University, Hamilton, Ontario, Canada L8S 4K1

²Lunenfeld-Tanenbaum Research Institute, Mount Sinai Hospital, 600 University Avenue, Toronto, Ontario, Canada M5G 1X5

³Current address: Department of Human Genetics, Leiden University Medical Centre, Leiden, The Netherlands.

Running title: Control of CSB by ATM and CDK2 in RIF1 inhibition

*Corresponding author:

Xu-Dong Zhu
Department of Biology, LSB438
McMaster University
1280 Main St. West
Hamilton, Ontario
Canada L8S4K1
Phone: (905) 525-9140 ext. 27737
Fax: (905)522-6066
Email: zhuxu@mcmaster.ca

4.2.1 Abstract

CSB, a member of the SWI2/SNF2 superfamily, is implicated in DNA double-strand break (DSB) repair. However how it regulates this repair process is poorly understood. Here we uncover that CSB interacts via its newly-identified winged helix domain with RIF1, an effector of 53BP1, and that this interaction mediates CSB recruitment to DSBs in S phase. At DSBs, CSB remodels chromatin by evicting histones, which limits RIF1 and its effector MAD2L2 but promotes BRCA1 accumulation. The chromatin remodeling activity of CSB requires not only damage-induced phosphorylation on S10 by ATM but also cell cycle-dependent phosphorylation on S158 by cyclin A-CDK2. Both modifications modulate the interaction of the CSB N-terminal region with its ATPase domain, the activity of which has been previously reported to be autorepressed by the N-terminal region. These results suggest that ATM and CDK2 control the chromatin remodeling activity of CSB in the regulation of DSB repair pathway choice.

Key words: CSB/RIF1/ATM/CDK2/Chromatin Remodeling/DNA double strand break repair

4.2.2 Introduction

DNA double strand breaks (DSBs), one of the most lethal forms of DNA damage, can threaten genomic integrity and promote tumorigenesis or premature aging if not repaired properly. Eukaryotic cells have evolved two mechanistically distinct pathways to repair DSBs: nonhomologous end joining (NHEJ) and homologous recombination (HR)^{1,2}. NHEJ

can ligate two broken ends in the absence of sequence homology whereas HR uses homologous sequences as a template to repair broken DNA. While NHEJ is active throughout interphase, HR is primarily confined to S and G2 phases when sister chromatids are present. The choice of DSB repair pathways is highly regulated during the cell cycle, with two proteins 53BP1 and BRCA1 playing pivotal but antagonizing roles in this process³⁻⁷. 53BP1 blocks BRCA1 and promotes NHEJ in G1 through its downstream effector RIF1⁸⁻¹². Phosphorylation of 53BP1 by ATM on its N-terminal region promotes RIF1 recruitment to DSBs, which prevents DNA end resection and channels DSBs towards NHEJ. In S/G2 phases, BRCA1 antagonizes 53BP1, perhaps through repositioning 53BP1 on the damaged chromatin^{3,13}. BRCA1 also blocks RIF1 from DSBs in S phase^{8-10,14}, paving the way for the initiation of DNA end resection. Aberrant selection of NHEJ or HR can lead to genomic instability^{1,2}.

Upon induction of DSBs, the chromatin structure needs to be modified to facilitate efficient access to DSBs¹⁵. Modification of chromatin structure includes histone post-translational modification, histone exchange, histone mobilization and histone removal. The latter three contribute to chromatin disassembly. In mammalian cells, limited or local nucleosome disassembly occurs in G1 phase when DSBs are repaired by NHEJ whereas extensive nucleosome disassembly is associated with HR in S/G2 cells¹⁶⁻¹⁹. How nucleosome disassembly is controlled in a cell-cycle dependent manner remains unclear. Many ATP-dependent chromatin remodeling complexes participate in chromatin disassembly to allow for efficient DSB repair¹⁵, however the exact mechanism by which

these complexes are regulated locally to remodel chromatin and to facilitate DSB repair remains poorly understood.

Cockayne syndrome (CS), a devastating hereditary disorder, is characterized by physical impairment, neurological degeneration and segmental premature aging. The majority of CS patients carry mutations in the *ERCC6* gene encoding Cockayne syndrome group B protein (CSB). CSB is a multifunctional protein that participates in a number of cellular processes including transcription²⁰, transcription-coupled repair^{21,22}, oxidative damage²³, mitochondria function^{24,25}, telomere maintenance²⁶ and DSB repair²⁷⁻²⁹. CSB forms IR-induced damage foci and regulates DSB repair pathway choice²⁷. Loss of CSB induces RIF1 accumulation at DSBs specifically in S/G2 cells²⁷, thereby hindering BRCA1 recruitment to DSBs. However how CSB is recruited to DSBs and what it does at DSBs to facilitate efficient HR remains unclear. CSB contains a central SWI2/SNF2-like ATPase domain and its *in vitro* ATPase activity is autoinhibited by its N-terminal region^{30,31}, but the physiological mechanism that permits release of its ATPase activity is unknown. Furthermore, CSB possesses ATP-dependent chromatin remodeling activity *in vitro*^{30,32,33}, however, whether CSB may function as a chromatin remodeler *in vivo* has not yet been demonstrated.

Here we uncover that CSB interacts with RIF1 and is recruited by RIF1 to DSBs in S/G2. This interaction is modulated by the C-terminal domain (CTD) of RIF1 and a newly-identified winged helix domain (WHD) at the C-terminus of CSB. We demonstrate that CSB is a chromatin remodeler *in vivo*, evicting histones from chromatin surrounding DSBs. The N-terminus of CSB is necessary for its chromatin remodeling activity, disruption of

which induces RIF1 accumulation at DSBs in S/G2 but impairs BRCA1, RAD51 and HR. The chromatin remodeling activity of CSB at DSBs is controlled by two phosphorylation events, one being damage-induced S10 phosphorylation by ATM and the other being cell-cycle-regulated S158 phosphorylation by cyclin A-CDK2. Both S10 and S158 phosphorylations modulate the interaction of CSB N-terminus with its ATPase domain. Taken together, these results led us to propose that CSB phosphorylations by ATM and CDK2 function as molecular signals to unlock its chromatin remodeling activity, perhaps by releasing the autoinhibition of its N-terminus. Subsequent nucleosome disassembly by CSB at DSBs inhibits RIF1 and paves the way for BRCA1-mediated HR.

4.2.3 Materials and methods

Plasmids, siRNA and antibodies

Retroviral expression constructs for wild type CSB and ATPase-dead mutant CSB-W851R have been described^{26,27}. Wild type CSB was used as a template to generate various CSB deletion alleles, which were cloned into the retroviral expression vector pLPC-NMyc²⁶, mammalian expression vector mCherry-LacR-NLS⁹ or the bacterial expression pHis-parallel-2⁵¹. The QuickChange site-directed mutagenesis kit (Agilent Technologies) was used to generate CSB mutants S10A, S10D, S158A and S158D. The primers used to clone CSB deletions and point mutations are available upon request. To generate pBabe-neo-ddI-PpoI expression construct, pBabe-ddI-PpoI¹⁸ (#49052, Addgene) was digested with *Bam*HI and *Sal*I and two inserts (a 267-bp *Bam*HI-*Sal*I fragment and a 1.5-kb *Bam*HI fragment) were

sequentially ligated into BamHI-SalI-linearized pBabe-Neo (a kind gift from Titia de Lange, Rockefeller University). Inserts of all plasmids was confirmed by DNA sequencing.

The sequence of siRNA against RIF1 (Dhamacon) as well as the expression constructs (pDEST-mCherry-LacR and pDEST-EGFP) carrying either siRIF1-resistant wild type RIF1 or various RIF1 deletion alleles have been described⁹. The GFP-PTIP expression construct⁴⁰ was a generous gift from André Nussenzweig and Jeremy Daniel.

Rabbit polyclonal anti-pS10 and anti-pS158 antibodies were developed by Cocalico Biologicals against respective CSB peptides containing phosphorylated serine 10 (NEGIPHS-pS-QTQEQDC) (Bio-Synthesis Inc) and phosphorylated serine 158 (NKIIEQL-pS-PQAATSR) (Bio-Synthesis Inc). Other antibodies used include RIF1 (sc55979, Santa Cruz); MAD2L2 (sc135977, Santa Cruz); 53BP1 (612522, BD Biosciences); BRCA1 (MS110, Abcam); BRCA1 (07-434, Millipore); Cyclin A (6E6, Abcam); CSB/ERCC6 (A301-354A, Bethyl Laboratories); ERCC6 (553C5a, Fitzgerald); γ -H2AX (Millipore); RAD51 (generously provided by Jan Hoeijmakers, Erasmus University); SMARCAD1 (A301-593A, Bethyl Laboratory); anti-Myc (9E10, Calbiochem); FK2 (04-263, Millipore); H2A (ab18255, Abcam); H2B (ab1790, Abcam); mCherry (NBP2-25157, Novus Biologicals); γ -tubulin (GTU88, Sigma).

Cell culture and drug treatment

All cells were grown in DMEM medium with 10% fetal bovine serum supplemented with non-essential amino acids, L-glutamine, 100 U/ml penicillin and 0.1 mg/ml streptomycin. Cell lines used: hTERT-RPE parental and CSB knockout²⁷, Phoenix²⁶ (a kind gift from

Titia de Lange, Rockefeller University), U2OS⁵² (ATCC), U2OS-265³⁴ (a kind gift from Roger Greenberg, University of Pennsylvania), U2OS-DR-GFP⁹, HCT116⁵³ (Life Technology), GM16666A^{54,55} (Coriell) and GM166667^{54,55} (Coriell). Parental cells were tested for mycoplasma contamination and were authenticated by STR DNA profiling. Retroviral gene delivery was carried out as described^{56,57} to generate stable cell lines. DNA and siRNA transfections were carried out with respective JetPRIME[®] transfection reagent (Polyplus) and Lipofectamine RNAiMax (Invitrogen) according to their respective manufacturer's instructions.

To induce expression of FokI, U2OS-265 cells were treated with both 1 μ M Shield-1 (CheminPharma) and 4-hydroxytosterone (4-OHT, Abcam) for 6 h or for the indicated time. IR was delivered from a Cs-137 source at McMaster University (Gammacell 1000). Roscovitine (20 μ M, Sigma), KU55933 (10 μ M, Sigma), VE-821 (10 μ M, Selleckchem), NU7026 (10 μ M, Sigma) were used to inhibit CDK, ATM, ATR and DNA-PKcs respectively.

Mass spectrometric analysis of phosphorylated CSB

Approximately 12 million U2OS cells stably expressing Flag-tagged CSB were treated with 20 Gy IR and the whole cell extracts were prepared as described^{58,59}. Flag-tagged CSB was immunoprecipitated from whole-cell extracts of approximately 12 million cells as described⁵⁸. Affinity purification of Flag-CSB was carried out with FLAG[®] purification kit (Sigma) according to the manufacturer's instruction. Following the final wash in 50 mM ammonium bicarbonate (ABC), pH 8.0, the resin containing Flag-CSB was digested with

1 µg trypsin in 200 µl ABC buffer overnight at 37°C. The next day, a fresh 0.5 µg trypsin was added and the mixture was incubated for another 3 h. Following centrifugation, the supernatant was transferred to a keratin-free tube and fully dried. The dried peptides were reconstituted in 2% formic acid and diluted 1:5 with lactic acid solution [25% lactic acid, 60% acetonitrile (ACN), 2.5% trifluoroacetic acid (TFA)]. Phosphorylated peptides were enriched on titanium-oxide (Ti-O₂) tips (GL Sciences, Tokyo, Japan) that were equilibrated consecutively with 100% H₂O, 100% methanol and lactic acid solution. Following loading of the sample, tips were washed consecutively with lactic acid solution, 80% ACN plus 0.1% TFA, 0.1% TFA and 2x H₂O. Phosphorylated peptides were eluted with 400 mM NH₄OH. Peptides were dried and reconstituted in 5% formic acid and loaded onto a fused silica 12 cm analytical column packed in-house with 3.5 µm Zorbax C18 material (Agilent Technology). Peptides were analyzed using an Orbitrap ELITE (Thermo Scientific) coupled to an Eksigent nanoLC ultra (AB SCIEX). Peptides were eluted from the column using a 90 min period cycle with a linear gradient from 2% to 35% ACN in 0.1% formic acid. Tandem MS spectra were acquired in a data-dependent mode for the top 10 most abundant ions using collision induced dissociation. Acquired spectra were searched against the human Refseq_V53 database using Mascot.

CRISPR/Cas9 genome editing of CSB

U2OS, U2OS-265, U2OS-DR-GFP and HCT116 cells were transiently transfected with sgRNA (AGAATTGCCACTCTGAACGG)⁵³ targeting CSB and expressed from the pX459 vector⁶⁰ (#48139, Addgene) containing Cas9 followed by the 2A-Puromycin

cassette. The next day, cells were selected with puromycin for 2 days and subcloned to allow for the formation of single colonies. Individual clones were screened by immunofluorescence with anti-CSB antibody (Fitzgerald) for the loss of CSB. CSB null clones were further confirmed by immunoblotting using anti-CSB antibody (Bethyl). Subsequently, any off-target effects from sgRNA were ruled out by clonogenic UV survival assays of CSB null clones complemented with either vector alone or Myc-tagged CSB. Only CSB null clones whose UV sensitivity were fully suppressed by wild type CSB were used in this study.

Cell synchronization and FACS analysis

Cell synchronization was done essentially as described^{52,59} with some modifications. Cells were treated with 2 mM thymidine for 16 h, followed by washing in PBS three times and then released into fresh media for 9 h. Subsequently, cells were arrested again with 2 mM thymidine for 16 h and washed in PBS for three times before their release into fresh media for various time points as indicated. For cell cycle analysis, two million cells from each of indicated time points were fixed and processed as described⁵². FACS analysis was performed on a FACSCalibur instrument and analyzed using FlowJo (v10.2). For induction of FokI expression in synchronized U2OS-265 cells, Shield-1 and 4-OHT were added 2 h prior to a given time point as indicated.

U2OS-DR-GFP WT and CSB knockout cells were transfected with indicated constructs along with an *I-SceI*-expressing plasmid using JetPRIME[®] transfection reagents (Polyplus). U2OS WT and CSB-KO cells were cotransfected with pEGFP-Pem1-Ad2 and

I-SceI expression constructs. 48 hr post transfection, cells were harvested, fixed and subjected to FACS analysis as described²⁷. A total of 10,000 cells per cell line were scored for each independent experiment. FACS analysis was performed on a FACSCalibur instrument.

Immunoprecipitation and immunoblotting

Immunoprecipitation (IP) with endogenous proteins was carried out as described¹⁴ with minor modifications. Untreated HCT116 cells or HCT116 cells collected 1 h post 20 Gy IR were lysed in NETN buffer [20 mM Tris-HCl, pH 8.0, 100 mM NaCl, 1 mM EDTA, 0.5% NonidetTM P-40 Substitute (Sigma), 1 mM PMSF, 1 µg/ml aprotinin, 1 µg/ml leupeptin, 1 µg/ml pepstatin, 1 mM NaF, 1 mM NaVO₄, 50 mM Na-β-glycerolphosphate] on ice for 30 min. For each IP, 5 mg of cell lysate was precleared with 30 µl protein G sepharose beads (GE Healthcare) for 1 h at 4°C, followed by incubation with primary antibody (1-2 µg) overnight at 4°C. Precipitates were then washed 4 times in NETN buffer containing 300 mM NaCl, and immunoblotted with indicated antibodies. IP with an anti-Myc antibody in 293T cells co-overexpressed Myc-CSB-C and various mCherry-LacR-RIF1-CTD alleles was done as described²⁶. Immunoblotting was performed as described²⁷.

Chromatin immunoprecipitation (ChIP)

ChIP and I-PpoI-induced DSB assays were carried out as described^{18,61} with minor modifications. Cells stably expressing pBabe-neo-ddI-PpoI were first treated with Shield-1 (1 µM) for 3 h and then with 4-OHT (1 µM) for 15 min. Following fixation in 1% PBS-

buffered formaldehyde for 10 min, cells were resuspended in 20X cell pellet volume of cell lysis buffer I [10 mM HEPES pH 6.5, 10 mM EDTA, 0.5 mM EGTA, 0.25% Triton X-100, 1 mM PMSF, 1 µg/ml aprotinin, 1 µg/ml leupeptin, 1 µg/ml pepstatin, 1 mM NaF, 1 mM NaVO₄, 50 mM Na-β-glycerolphosphate] and incubated on ice for 10 min. Following centrifugation, cell pellets were washed in cell lysis buffer II [10 mM HEPES pH 6.5, 1 mM EDTA, 0.5 mM EGTA, 200 mM NaCl] and then resuspended in nuclei lysis buffer [50 mM Tris-HCl pH8.1, 10 mM EDTA, 0.5% SDS]. Both cell lysis buffer II and nuclei lysis buffer contained phosphatase and protease inhibitors as described in cell lysis buffer I. Following incubation on ice for 10 min, the cell lysate was sonicated and clarified through centrifugation.

For each ChIP, 200 µl of the cell lysate was diluted 1:5 in IP dilution buffer [1% Triton X-100, 2 mM EDTA, 20 mM Tris-HCl pH8.1, 150 mM NaCl]. Out of 1 ml diluted lysate, 20 µl was set aside as input control and the remaining was precleared with protein G sepharose beads (GE Healthcare) preblocked with BSA and tRNA and then incubated with primary antibody (1 µg) overnight at 4°C. Precipitates were washed once in low salt buffer [150 mM NaCl, 0.1% SDS, 1% Triton X-100, 2 mM EDTA, 20 mM Tris-HCl pH8.0, 1 mM PMSF, 1 µg/ml aprotinin, 1 µg/ml leupeptin, 1 µg/ml pepstatin], once in high salt buffer [500 mM NaCl, 0.1% SDS, 1% Triton X-100, 2 mM EDTA, 20 mM Tris-HCl pH8.0], twice in LiCl buffer [0.25 M LiCl, 1% NonidetTM P-40 Substitute, 1% deoxycholic acid, 1 mM EDTA, 10 mM Tris-HCl pH 8.0] and then once in TE buffer [10 mM Tris-HCl pH 8.0, 1 mM EDTA]. The IP DNA was eluted twice in elution buffer [0.1 M NaHCO₃,

1% SDS] at 65°C for 15 min. Subsequently, the IP DNA, along with the input DNA (equivalent to 2% of lysate used for IP), were treated with RNase A at 37°C for 1 h and then with proteinase K at 55°C for 1 h. Following incubation overnight at 65°C to reverse the crosslink, the DNA was purified with phenol/chloroform, precipitated with ethanol in the presence of 20 µg glycogen (Roche), resuspended in 10 mM Tris-HCl, pH 8.5 and then used for PCR or qPCR. Primers for PCR and real-time PCR are listed in Supplementary Tables 1 and 2. For PCR reactions, the products were run on a 2% agarose gel, stained with ethidium bromide and analyzed with ImageJ (NIH). Each PCR product of GAPDH from IP DNA was normalized to that from input DNA as internal control, giving rise to the ChIP efficiency. For real-time PCR, the threshold cycle (Ct) value of qPCR reactions for GAPDH of each IP DNA was normalized to that of input DNA as internal control, giving rise to ChIP efficiency. Each PCR or qPCR product of the I-PpoI locus on chromosome 1 was first normalized to that from input DNA as internal control and then normalized to the corresponding ChIP efficiency. The y-axis in figures displaying ChIP results represents the relative occupancy normalized to the untreated control.

Assays of DSB induction in ddI-PpoI cells

Cells stably expressing pBabe-neo-ddI-PpoI were first treated with Shield-1 (1 µM) for 3 h and then with 4-OHT (1 µM) for 15 min. After washing twice in PBS, cells were collected and genomic DNA was isolated using the Gentra Puregene Cell kit (Qiagen) according to the manufacturer's protocol. qPCR was performed using primers (Supplementary Table 2) flanking the I-PpoI site on chromosome 1. The Ct values of qPCR from I-PpoI site was

then normalized to the Ct values of qPCR from the GAPDH gene using the $\Delta\Delta\text{Ct}$ method, giving rise to the percentage of the I-PpoI-induced DSB on chromosome 1 as described¹⁸.

Immunofluorescence

Immunofluorescence (IF) was performed as described^{26,27}. All cell images were recorded on a Zeiss Axioplan 2 microscope with a Hamamatsu C4742-95 camera and processed in Open Lab.

To quantify recruitment of BRCA1, RIF1 and SMARCAD1 to FokI-induced DSBs, fixed cells were co-immunostained with anti-BRCA1, anti-RIF1 or anti-SMARCAD1 antibody in conjunction with γH2AX . The γH2AX signal was used to mark the area of FokI-induced damage and the intensity of BRCA1, RIF1 or SMARCAD1 within the marked area was measured. To quantify the intensity of Myc-CSB at FokI-induced DSBs in RIF1-depleted cells, the mCherry signal was used to mark the area of damage and the intensity of Myc-CSB within that area was measured. The intensity of BRCA1, RIF1, SMARCAD1 or Myc-CSB at FokI-induced DSBs marked by γH2AX or mCherry was normalized respectively to their intensity of the same size area but away from the FokI-induced damage site in the same nucleus, giving rise to normalized signal intensity. All images for a given experiment were captured on the same day with the same exposure time. All analyses were carried out on unmodified images with ImageJ software (NIH). Data were represented as scatter plot graphs with the mean indicated. *P* values were derived using a two-tailed Mann-Whitney test.

Recombinant CSB proteins and *in vitro* kinase assays

Production of 6xHis-tagged wild type and mutant CSB carrying amino acids from 2 to 322 was carried out essentially as described^{58,62} with minor modifications. Induction of CSB proteins was carried out overnight with 1 mM isopropylthiogalactoside at room temperature. The cell pellet was resuspended in Binding buffer [20 mM Tris-HCl pH8.0, 500 mM NaCl, 10 mM imidazole, 1 mM PMSF] and lysed by sonication. Triton X-100 was then added to 0.1% and the lysate was shaken at 4°C for 30 min. Following centrifugation, the supernatant was incubated with nickel resin (Qiagen) at 4°C for 2 h. The beads were washed once in Binding buffer, three times in Wash buffer [20 mM Tris-HCl, pH 8.0, 500 mM NaCl, 50 mM imidazole, 10 mM β -mercaptoethanol and 1 mM PMSF] and then eluted three times with an elution buffer [20 mM Tris-HCl, pH 8.0, 500 mM NaCl, 880 mM imidazole and 10 mM β -mercaptoethanol]. The elutions were combined and dialysed against a dialysis buffer [20 mM HEPES pH7.9, 500 mM NaCl, 20% glycerol, 3 mM MgCl₂ and 1mM DTT]. For cyclin A/CDK2 kinase assays, 2.5 μ g of His-tagged wild type and mutant CSB fragments was incubated with or without 50 ng of active recombinant cyclin A/CDK2 (14-488, Millipore) in the presence of ATP according to the manufacturer's protocol.

Clonogenic survival assays

Clonogenic survival assays were done as described²⁷.

Statistical analysis

A Student's two-tailed unpaired t test was used to derive all *P* values except for where specified.

Data availability

All data used in this study are available within the article, Supplementary files, or available from the authors upon request.

4.2.4 Results

RIF1 interacts with CSB and recruits it to DSBs

To investigate the mechanism by which CSB is recruited to DSBs, we employed a well-established reporter osteosarcoma cell line U2OS-265³⁴, which has the 256 copy lac operator array integrated into a single site on chromosome 1p3.6. Overexpression of the FokI nuclease domain fused to mCherry-LacR (mCherry-LacR-FokI) in the reporter cells resulted in a robust production of DSBs within the lac operator array. Both endogenous CSB and Myc-CSB were found to accumulate at FokI-induced DSBs (Fig. 1a and 1b), in agreement with previous reports that CSB is recruited to DSBs²⁷⁻²⁹.

Myc-CSB accumulation at FokI-induced DSBs was sensitive to ATM inhibition (Fig. 1c), loss of 53BP1 (Fig. 1d) and RIF1 (Fig. 1e and 1f), prompting us to investigate if CSB might interact with RIF1 since RIF1 recruitment to DSBs is entirely dependent upon ATM and 53BP1^{8,9,11}. Coimmunoprecipitation with anti-CSB antibody in HCT116 cells brought down RIF1 but not 53BP1 (Fig. 1g). The CSB interaction with RIF1 was also confirmed in a reverse immunoprecipitation with anti-RIF1 antibody (Fig. 1h). The

discrepancy between the amount of CSB brought down by anti-RIF1 antibody and the amount of RIF1 brought down by anti-CSB antibody may imply that CSB might not interact with RIF1 in a 1:1 stoichiometry, however we cannot rule out the possibility that this discrepancy might be due to a difference in IP efficiency. As a control, coimmunoprecipitation with anti-RIF1 antibody brought down 53BP1 but not CSB in CSB knockout HCT116 cells (Fig. 1h), suggesting that CSB interaction with RIF1 is specific. Furthermore, treatment with ionizing radiation did not significantly affect CSB interaction with RIF1 (Fig. 1g and 1h). These results reveal that CSB interacts with RIF1 independently of not only 53BP1 but also damage induction.

To gain further insights into CSB interaction with RIF1, we returned to the reporter U2OS-265 cell line. In the absence of 4-hydroxytamoxifen and shield-1, this reporter cell line does not express mCherry-LacR-FokI and can be used for analysis of protein-protein interactions with a bait protein fused to mCherry-LacR. Full length RIF1 and RIF1 deletion alleles containing only the heat repeats (RIF1-N) or lacking the heat repeats (RIF1-C) were fused to mCherry-LacR (Fig. 2a). Their ability to recruit Myc-CSB or Myc-CSB deletion alleles containing the N-terminal region (CSB-N), the central ATPase domain (CSB-ATPase) or the C-terminal region (CSB-C) (Fig. 2b, top panel) to the lac operator array was examined in U2OS-265 cells. We observed a robust interaction between mCherry-LacR-RIF1-C and Myc-CSB-C (Fig. 2c and 2d, Supplementary Fig. 1a and 1b). The level of expression of mCherry-LacR-RIF1-FL was much lower than that of mCherry-LacR-RIF1-N and mCherry-LacR-RIF1-C in U2OS-265 cells (Supplementary Fig. 1c), which

likely contributed to the poor interaction observed between mCherry-LacR-RIF1-FL and Myc-CSB.

Deletion analysis revealed that the CTD of RIF1 was necessary and sufficient for its interaction with Myc-CSB-C (Fig. 2e and 2f, Supplementary Fig. 2a). While deletion of CTDI subdomain did not affect mCherry-LacR-RIF1-CTD interaction with Myc-CSB-C at the lac operator array (Fig. 2e, Supplementary Fig. 2a), it moderately affected the ability of mCherry-LacR-RIF1-CTD to coimmunoprecipitate with Myc-CSB-C (Fig. 2f). On the other hand, deletion of the CTDIII subdomain abrogated the ability of mCherry-LacR-RIF1-CTD not only to interact with Myc-CSB-C at the lac operator array but also to coimmunoprecipitate with Myc-CSB-C (Fig. 2e and 2f, Supplementary Fig. 2a), suggesting that the CTDIII subdomain is necessary for RIF1 interaction with CSB. mCherry-LacR-CTDIII was observed to interact with Myc-CSB-C at the lac operator array (Fig. 2e, Supplementary Fig. 2a) but failed to coimmunoprecipitate Myc-CSB-C (Fig. 2f), the latter suggesting that CTDIII alone may not be sufficient to mediate RIF1 interaction with CSB. The discrepancy in the observed CTDIII interaction with CSB-C may be in part due to the difference in experimental conditions.

To investigate the role of the CTDIII subdomain of RIF1 in recruiting CSB to DSBs, we knocked down RIF1 in U2OS-265 cells and complemented RIF1-depleted cells with either the vector alone, siRIF1-resistant RIF1-FL or siRIF1-resistant RIF1- Δ CTDIII. RIF1 knockdown significantly affected CSB accumulation at FokI-induced DSBs (Fig. 2g), in agreement with our earlier finding (Fig. 1d). While introduction of EGFP-RIF1-FL rescued CSB accumulation at FokI-induced DSBs (Fig. 2g, Supplementary Fig. 2b), overexpression

of EGFP-RIF1- Δ CTDIII failed to do so (Fig. 2g, Supplementary Fig. 2b). These results suggest that the CTDIII subdomain of RIF1 is necessary for recruiting CSB to DSBs.

CSB interacts with RIF1 via a newly-identified WHD

Deletion of the last 65 amino acids of CSB drastically affected Myc-CSB-C interaction with mCherry-LacR-RIF1-C in U2OS-265 cells (Fig. 3a, Supplementary Fig. 3a). Further deletion of previously-described UBD domain³⁵ did not lead to any further reduction in Myc-CSB-C interaction with mCherry-LacR-RIF1-C (Fig. 3a, Supplementary Fig. 3a), suggesting that the last 65 amino acids of CSB is necessary for its interaction with RIF1. Profile-profile alignment and fold-recognition using the program FFAS³⁶ revealed that the last 76 amino acids of CSB resembled a winged helix domain (WHD) (Supplementary Fig. 4a). Additional protein threading trials using PHYRE (<http://www.sbg.bio.ic.ac.uk/>) strengthened our original prediction and further revealed that sequences belonging to more distantly related CSB homologs such as the yeast Rad26 were also likely to fold into the WHD, suggesting that this domain is evolutionarily conserved. Computer modeling of this domain on reported crystal structure of the WHD of the general transcription factor TFIIF³⁷ suggested that L1470, W1486 and L1488 of CSB, all of which are evolutionarily conserved (Supplementary Fig. 4b), contributed to the hydrophobic core formation of the CSB WHD (Supplementary Fig. 4c). To gain further insight into the role of this newly-identified WHD, we generated CSB mutant alleles carrying simultaneous mutations of W1486 and L1488 to glycines (GG) or simultaneous mutations of L1470, W1486 and L1488 to glycines (GGG). Both Myc-CSB-C-GG and Myc-CSB-C-GGG were severely defective in their interaction

with mCherry-LacR-RIF1-C (Fig. 3a, Supplementary Fig. 3a), indistinguishable from Myc-CSB-C lacking the WHD (Myc-CSB-C- Δ WHD) (Fig. 3a, Supplementary Fig. 3a), suggesting that the WHD of CSB mediates its interaction with RIF1.

While Myc-CSB was readily recruited to FokI-induced DSBs, neither Myc-CSB-GG nor Myc-CSB-GGG were able to accumulate at FokI-induced DSBs (Fig. 3b, Supplementary Fig. 3b), underscoring the importance of the WHD in mediating CSB accumulation at DSBs.

It has been reported that CSB regulates DSB pathway choice²⁷. In agreement with the previous finding²⁷, knockout of CSB in U2OS-265 cells (Supplementary Fig. 3c) resulted in an increase in accumulation of RIF1 and its effector MAD2L2^{38,39} at FokI-induced DSBs (Fig. 3c and 3d, Supplementary Fig. 3d). On the other hand, loss of CSB did not affect GFP-PTIP recruitment to FokI-induced DSBs (Fig. 3e), suggesting that CSB specifically restricts the RIF1-MAD2L2 pathway but not the parallel PTIP pathway⁴⁰. RIF1-MAD2L2 accumulation in CSB knockout cells was accompanied by an impairment in BRCA1 accumulation at FokI-induced DSBs (Fig. 3f, Supplementary 3e). In support of the observed impairment in BRCA1 accumulation, CSB null cells exhibited reduced DSB repair by HR but increased DSB repair by NHEJ (Fig. 3g and 3h). Introduction of Myc-CSB into U2OS-265 CSB knockout cells not only suppressed RIF1 but also restored BRCA1 accumulation at FokI-induced DSBs (Fig. 3i and 3j). On the other hand, neither Myc-CSB-GG nor Myc-CSB-GGG were able to dampen RIF1 and restore BRCA1 accumulation in U2OS-265 CSB knockout cells (Fig. 3i and 3j). These results suggest that

the WHD of CSB is necessary for its function in regulating DSB pathway choice. These results further imply that CSB acts as an inhibitor of RIF1.

RIF1 recruits CSB to DSBs in S phase

Analysis of the dynamics of Myc-CSB accumulation at FokI-induced DSBs in synchronized U2OS-265 cells revealed that CSB recruitment to DSBs was cell cycle regulated, peaking in S phase (Fig. 4a). Cell synchronization did not significantly affect the induction of DSBs by FokI (Fig. 4b). At 0 h post release from a double thymidine block, about 6% of cells exhibited Myc-CSB accumulation at FokI-induced DSBs (Fig. 4a). This number increased sharply to about 30% at 2 h post release and peaked to about 38% at 6 h post release when the majority of cells (62.6%) were in S phase (Fig. 4a, Supplementary Fig. 5a). A dramatic decline in the number of cells exhibiting Myc-CSB accumulation was detected 16 h post release when the majority of cells (58.2%) were in G1 (Fig. 4a, Supplementary Fig. 5a),

RIF1 accumulation at FokI-induced DSBs was at the highest level in cells 0 hr post release when the majority of cells were arrested in G1 (Fig. 4a, Supplementary Fig. 5a), in agreement with a previous finding that RIF1 is largely recruited to sites of DSBs in G1 cells⁹. RIF1 accumulation started to decline as cells entered S phase and continued to decline as cells progressed through S and G2, dipping to the lowest level at 10 h post release when cells were enriched in G2/M (Fig. 4a and Supplementary Fig. 5a). Despite this decline, a substantial number of cells retained RIF1 at FokI-induced DSBs in S/G2 phase, particularly from 2 h to 6 h post release (45%, 44% and 38% at respective 2h, 4h, and 6h

post release) (Fig. 4a). These results prompted us to ask if this pool of RIF1 might be responsible for the sharp increase in CSB recruitment to FokI-induced DSBs observed earlier from 2 h to 6 h post release. To address this question, we turned to 53BP1 knockout cells to avoid any potential replication defect associated with RIF1 deficiency⁴¹. Knockout of 53BP1 did not alter the cell cycle profile of U2OS-265 cells (Supplementary Fig. 5b) nor did it affect expression of RIF1 or CSB (Fig. 4c). While knockout of 53BP1 did not affect the induction of DSBs by FokI (Fig. 4d), it completely abrogated RIF1 accumulation at FokI-induced DSBs (Fig. 4e), the latter in agreement with the previous finding that RIF1 recruitment to IR-induced DSBs is dependent upon 53BP1⁹. Recruitment of Myc-CSB to FokI-induced DSBs was also severely impaired in 53BP1 knockout U2OS-265 cells at 2 h, 4 h and 6 h post release (Fig. 4f). These results suggest that RIF1 is responsible for recruiting CSB to DSBs in S phase.

CSB inhibits RIF1 but promotes BRCA1 in S/G2

Our earlier finding that CSB acts as an inhibitor of RIF1 prompted us to ask if this inhibition might occur in S/G2 phase. Loss of CSB did not affect the induction of DSBs by FokI (Fig. 4g) but prevented the decline in RIF1 accumulation at the FokI-induced DSBs in cells from 2 h to 8 h post release from a double thymidine block (Fig. 4h). RIF1 accumulation at FokI-induced DSBs in CSB null cells was similar to that in wild type cells at 12 h post release when cells started to exit G2/M and were enriched in G1 (Fig. 4h, Supplementary Fig. 5a), further supporting the notion that CSB inhibits RIF1 specifically in S/G2. The elevated accumulation of RIF1 in S/G2 was associated with a decrease in BRCA1 accumulation at

FokI-induced DSBs (Fig. 4i), which was unlikely due to a loss of BRCA1 expression in CSB knockout cells (Fig. 4j). These results reveal that CSB inhibits RIF1 but promotes BRCA1 in S/G2.

CSB evicts histones from chromatin flanking DNA DSBs *in vivo*

CSB is reported to be a chromatin remodeler *in vitro*^{32,33}, however whether it does so *in vivo* has not yet been demonstrated. To investigate if CSB might function as a chromatin remodeler at DSBs, we employed a well-established inducible ddI-PpoI expression construct¹⁸, which was stably integrated into both hTERT-RPE wild type and CSB knockout cells (Supplementary Fig. 6a). I-PpoI has a number of cleavage sites in the human genome¹⁸, including a unique site on chromosome 1. Neither the ability of I-PpoI to induce DSBs nor the percentage of I-PpoI-induced cleavage on chromosome 1 was affected by loss of CSB in hTERT-RPE cells (Supplementary Fig. 6b-6d).

ChIP analysis revealed that loss of both histone H2A and H2B from chromatin surrounding the unique I-PpoI cleavage site on human chromosome 1 in hTERT-RPE wild type cells was visible one hour following I-PpoI induction and peaked two hours post I-PpoI induction (Fig. 5a and 5b), in agreement with previous observations that histones are removed from chromatin surrounding DSBs to accommodate HR-mediated repair^{18,42,43}. On average 45-50% of loss of H2A and H2B was observed 2 h post I-PpoI induction (Fig. 5a and 5b) and this effect was similar to that previously-reported^{16,18}. At 2 h post induction, the average frequency of I-PpoI-induced cleavage was 21% (Supplementary Fig. 6d).

Previously I-PpoI was reported to cleave this locus at a frequency of ~30% in MCF7 cells¹⁸. Perhaps the cleavage frequency by I-PpoI may vary depending upon the cell type.

On the other hand, induction of I-PpoI did not lead to any significant removal of H2A and H2B from the I-PpoI cleavage site on chromosome 1 in hTERT-RPE CSB knockout cells (Fig. 5c and 5d). To further substantiate the role of CSB in removing H2A and H2B from damaged chromatin, we generated hTERT-RPE-ddIPpoI-CSB KO cells stably expressing the vector alone, Myc-CSB or Myc-CSB carrying a ATPase-dead mutation of W851R mutation^{27,30}. We then examined histone H2A and H2B occupancy in these cell lines 2 h post induction of I-PpoI expression when loss of H2A and H2B was observed earlier to peak in hTERT-RPE parental cells. This time point was also used in experiments below for analysis of other CSB mutant alleles. While wild type CSB rescued I-PpoI-induced loss of H2A and H2B from the I-PpoI cleavage site on chromosome 1 in CSB knockout cells, the ATPase-dead mutant CSB-W851R failed to do so (Fig. 5e and 5f). Together, these results demonstrate that CSB functions as a chromatin remodeler *in vivo* and that its ATP-dependent chromatin remodeling activity is essential for displacing histones from chromatin flanking DSBs.

Earlier we have shown that loss of CSB impairs BRCA1 accumulation at FokI-induced DSBs (Fig. 3f). BRCA1 is reported to mediate ubiquitylation of H2A that is recognized by the ubiquitin-binding CUE domain of chromatin remodeler SMARCAD1¹³. Formally it was possible that loss of histone displacement in CSB null cells might have resulted from impaired recruitment of SMARCAD1 at DSBs. However we did not detect any significant change in SMARCAD1 recruitment to FokI-induced DSBs in CSB null

cells (Supplementary Fig. 7a-7b). Combined with previous reports that CSB is a chromatin remodeler *in vitro*^{30,32,33}, our finding further supports the notion that CSB functions as a chromatin remodeler *in vivo*. Furthermore, our finding implies that CSB may act independently of SMARCAD1 in promoting HR-mediated DSB repair.

Chromatin remodeling by CSB N-terminus inhibits RIF1 at DSBs

The N-terminus of CSB has been implicated in autoregulation of its ATPase activity *in vitro*³⁰⁻³² and thus we asked if CSB N terminus might regulate its chromatin remodeling activity *in vivo*. Deletion analysis revealed that deleting the first 30 amino acids from CSB N-terminus (CSB- Δ N30) was sufficient to abrogate its ability to displace H2A and H2B from the I-PpoI cleavage site on chromosome 1 in hTERT-RPE-ddIPpoI-CSB KO cells (Fig. 6a and 6b). The inability of Myc-CSB- Δ N30 to displace H2A and H2B from damaged chromatin was unlikely due to its lack of expression or a defect in its recruitment to DSBs (Fig. 6c and 6d). These results suggest that CSB N-terminus is necessary for its *in vivo* chromatin remodeling activity at DSBs.

Previously it has been reported that CSB limits IR-induced RIF1 foci formation specifically in S/G2 cells²⁷. When stably introduced into hTERT-RPE CSB null cells, Myc-CSB- Δ N30 failed to fully suppress IR-induced RIF1 foci formation in cells staining positive for cyclin A, a marker for S/G2 cells (Fig. 6e). The inability of Myc-CSB- Δ N30 to suppress RIF1 foci formation was accompanied by a lack of rescue in IR-induced BRCA1 and RAD51 foci formation (Fig. 6f and 6g). Overexpression of Myc-CSB- Δ N30 failed to suppress the sensitivity of hTERT-RPE CSB null cells, which were proficient for

both BRCA1²⁷ and BRCA2 (unpublished data, N.L. Batenburg and X.D. Zhu), to olaparib treatment (Fig. 6h). Myc-CSB- Δ N30 also failed to promote HR in the reporter U2OS-DR-GFP CSB KO cells (Fig. 6i and 6j). These results suggest that the chromatin remodeling activity of CSB is necessary to suppress RIF1 but promote BRCA1-mediated HR in S/G2.

ATM controls the chromatin remodeling activity of CSB

Analysis of the first 30 amino acids of CSB revealed three closely-spaced SQ/TQ motifs (S¹⁰Q, T¹²Q and S²⁰Q), which are commonly found in DNA damage response proteins that are substrates of ATM/ATR⁴⁴. Clonogenic survival assays revealed that although Myc-CSB carrying a nonphosphorylatable mutation of either T12A or S20A behaved like wild type CSB in suppressing the sensitivity of CSB null cells to olaparib (Supplementary Fig. 8a and 8b), Myc-CSB carrying a nonphosphorylatable mutation of S10A failed to suppress the sensitivity of CSB null cells to olaparib (Supplementary Fig. 8c). On the other hand, Myc-CSB carrying a phosphomimic mutation of S10D was fully competent in suppressing the sensitivity of CSB null cells to olaparib (Supplementary Fig. 8c). All CSB mutants were expressed at a level comparable to wild type CSB (Supplementary Fig. 8d). These results suggest that CSB phosphorylation on S10 is important for its function in DSB repair.

Western analysis with an antibody raised against a peptide carrying phosphorylated S10 revealed that both endogenous CSB and Myc-CSB were phosphorylated on S10 following induction of IR-induced DNA damage and that little CSB-pS10 was detected in undamaged cells (Fig. 7a and 7b). CSB phosphorylation on S10 was sensitive to the ATM inhibitor KU55933, but not the ATR inhibitor VE-821 or the DNA-PKcs inhibitor NU7026

(Fig. 7c). Introduction of wild type ATM into ATM-deficient GM16666A cells rescued IR-induced CSB phosphorylation on S10 (Fig. 7d). Together, these results reveal that ATM is the main kinase responsible for damage-induced CSB phosphorylation on S10. ATM-deficient GM16666A cells carry a homozygous frameshift mutation at codon 762 of the *ATM* gene and no ATM protein is detected in these cells⁴⁵ (Fig. 7d). The residual signal of CSB-pS10 observed in GM16666A cells might result from an activity of another kinase in the absence of ATM.

ChIP analysis revealed that following induction of I-PpoI, Myc-CSB-S10A failed to displace H2A and H2B from the I-PpoI cleavage site on chromosome 1 whereas Myc-CSB-S10D was able to do so (Fig. 7e and 7f). The inability of Myc-CSB-S10A to evict H2A and H2B was unlikely due to a lack of protein expression (Supplementary Fig. 8e). Furthermore, both Myc-CSB-S10A and Myc-CSB-S10D were recruited to FokI-induced DSBs, indistinguishable from Myc-CSB (Supplementary Fig. 8f). Collectively, these results suggest that ATM controls the chromatin remodeling activity of CSB at DSBs through damage-induced S10 phosphorylation.

When stably introduced into hTERT-RPE CSB KO cells, overexpression of Myc-CSB-S10A failed to suppress IR-induced RIF1 foci formation in cyclin A-positive cells whereas overexpression of Myc-CSB-S10D was able to do so (Fig. 7g). In addition, IR-induced BRCA1 and RAD51 foci formation was compromised in CSB null cells complemented with Myc-CSB-S10A but not in CSB null cells complemented with Myc-CSB-S10D (Fig. 7h and 7i). These results suggest that ATM-dependent chromatin

remodeling activity of CSB is part of the mechanism that suppresses RIF1 but promotes BRCA1 and RAD51 at DSBs in S/G2 cells.

CDK2 controls the chromatin remodeling activity of CSB

Mass spectrometric analysis of Flag-CSB immunoprecipitated from IR-treated cells revealed a robust phosphorylation of S158 (S¹⁵⁸P) (Supplementary Fig. 9a), which fits the consensus sequence (S/TP) for cyclin-dependent kinases. Western analysis with an antibody raised against phosphorylated S158 confirmed that S158 was phosphorylated *in vivo* (Fig. 8a and 8b). Analysis of synchronized cell lysates revealed that CSB phosphorylation on S158, which was absent in CSB null cells (Supplementary Fig. 9d), was reproducibly detected above the background level at 6 h post release from a double thymidine block, continued to increase as cells progressed through S/G2/M but declined sharply when cells returned to G1, 16 h post release (Fig. 8b and Supplementary Fig. 9b and 9c). Treatment with the CDK inhibitor roscovitine severely affected S158 phosphorylation (Fig. 8c). Furthermore, S158 was an *in vitro* substrate of cyclin A-CDK2 (Fig. 8d). Together, these results suggest that cyclin A-CDK2 is a kinase responsible for CSB phosphorylation on S158 in S/G2 phase.

ChIP analysis revealed that Myc-CSB carrying a nonphosphorylatable mutation of S158A failed to rescue the displacement of H2A and H2B from the I-PpoI cleavage site on chromosome 1 in CSB null cells whereas Myc-CSB carrying a phosphomimic mutation of S158D was fully competent to do so (Fig. 8e and 8f). The level of CSB-S158A expression was comparable to that of wild type CSB and CSB-S158D (Supplementary Fig. 9e). Both

Myc-CSB-S158A and Myc-CSB-S158D were recruited to FokI-induced DSBs, indistinguishable from Myc-CSB (Supplementary Fig. 9f). These results suggest that CSB phosphorylation on S158 by cyclin A-CDK2 controls its chromatin remodeling at DSBs in S/G2 cells.

When stably introduced into hTERT-RPE CSB KO cells (Supplementary Fig. 9g), Myc-CSB-S158A failed to suppress IR-induced RIF1 foci formation in cyclin A-positive cells (Fig. 8g), failed to rescue IR-induced BRCA1 and RAD51 foci formation and failed to support cell survival in response to olaparib treatment (Fig. 8h and 8i, Supplementary Fig. 9h). Myc-CSB-S158A also failed to promote HR in U2OS-DR-GFP CSB KO cells (Supplementary Fig. 9i). On the other hand, Myc-CSB-S158D was fully competent in suppressing IR-induced RIF1 foci formation in cyclin A-positive CSB null cells and facilitating efficient HR as evidenced by a complete rescue in IR-induced BRCA1 and RAD51 foci formation, HR-mediated repair as well as cell survival of CSB null cells in response to olaparib treatment (Fig. 8h-8i, Supplementary Fig. 9h and 9i). Collectively, these results suggest that cyclin A-CDK2 controls the chromatin remodeling activity of CSB at DSBs to promote efficient HR.

Phosphorylation controls CSB intramolecular interaction

The CSB N-terminal region (CSB-N) is reported to be engaged in an intramolecular interaction with the ATPase domain to autoregulate its ATPase activity *in vitro*^{30,31}. In agreement with previous findings, we observed a robust interaction of Myc-CSB-N with mCherry-LacR-CSB-ATPase at the lac operator array (Fig. 9a and 9b). No interaction of

Myc-CSB-N with mCherry-LacR-CSB-C was detected (Fig. 9a and 9b). We found that a single mutation of either S10A or S158A impaired the interaction of Myc-CSB-N with mCherry-LacR-CSB-ATPase whereas a single mutation of either S10D or S158D did not affect the interaction of Myc-CSB-N with mCherry-LacR-CSB-ATPase (Fig. 9c). Further analysis of double mutations of either S10AS158A or S10DS158D revealed that CSB phosphorylations on S10 and S158 acted in the same epistatic pathway to promote the interaction of its N-terminal region with its ATPase domain. These results imply that these two phosphorylation events serve as molecular gates to modulate intramolecular interactions of CSB N-terminal region with its ATPase domain.

4.2.5 Discussion

The work presented here has uncovered that RIF1 interacts with CSB and recruits it to DSBs in S phase. We have demonstrated that CSB inhibits RIF1 through its damage- and cell cycle-dependent chromatin remodeling activity at DSBs. Our data suggest a model in which CSB phosphorylations on S10 by ATM and on S158 by cyclin A-Cdk2 serve as molecular signals governing its chromatin remodeling activity at DSBs, which inhibits RIF1 but promotes BRCA1-mediated HR (Fig. 9d). Furthermore, our data provide the first direct evidence that CSB functions as a chromatin remodeler *in vivo*.

It has been reported that RIF1 interacts with 53BP1 and that its recruitment to DSBs is entirely dependent upon 53BP1⁸⁻¹². Our finding that RIF1 can form a subcomplex with CSB independently of 53BP1 and damage induction suggests that CSB may be recruited to DSBs in the form of this subcomplex via RIF1 interaction with 53BP1 (Fig. 8d). However

we cannot rule out the possibility that CSB may be recruited to DSBs via the RIF1-53BP1 complex. Previously it has been reported that CSB recruitment to DSBs is dependent upon transcription²⁷. RNA is reported to mediate 53BP1 and RIF1 recruitment to DSBs^{46,47}. Perhaps CSB recruitment by RIF1 to DSBs might also be regulated by transcription, which would require future investigation.

We have shown that RIF1 interacts with CSB through its conserved CTD. The CTD of RIF1 has been implicated in binding BLM to promote recovery of stalled replication forks⁴⁸. Knockdown of BLM did not affect CSB recruitment to FokI-induced DSBs (N.L. Batenburg and X.D. Zhu, unpublished data), suggesting that it is unlikely that RIF1 mediates CSB recruitment to DSBs through BLM.

Through sequence analysis, secondary structural predictions and protein threading, we have uncovered that the very C-terminus of CSB harbours a cryptic winged helix domain (WHD), which shares closest resemblance to the WHD of general transcription factors TFIIF subunits A and B, TFIID subunit of TAF1, ELL and ELL2 as well as the chromatin assembly factor CAF1. The WHD of CSB, which spans from amino acids 1417 to 1493, overlaps with the previously-reported ubiquitin binding domain (UBD) of CSB³⁵, which spans amino acids 1399 to 1428. In particular, computer modeling suggests that the two leucines 1427 and 1428, which have previously been implicated in the function of the UBD in UV repair³⁵, are contained within helix 1 of the WHD. Further structural and functional analysis is needed to clarify the role of this region in regulating CSB activity.

The CSB WHD is predicted to be evolutionarily conserved from yeast to human. The WHD, frequently found in transcription factors, transcription regulators and helicases,

is a versatile domain that is implicated in protein-DNA and protein-protein interactions⁴⁹. Recent studies suggest that the last 30 amino acids of CSB is necessary for its interaction with RNAPII in transcription-coupled UV repair⁵⁰. Our finding that CSB interacts with RIF1 through its WHD in DSB repair supports the notion that the CSB WHD acts as a protein-protein interaction module to mediate its interaction with different partners depending upon the type of DNA repair process.

The CSB N-terminal region is implicated in an intramolecular interaction with its ATPase domain and autosuppresses its ATPase activity *in vitro*^{30,31}, perhaps through binding to the ATPase domain. On the other hand, the CSB N-terminal region is reported to couple ATP hydrolysis to chromatin remodeling³². However how the CSB N-terminal region binds its ATPase domain to regulate its ATP-dependent chromatin remodeling activity remains elusive. We have shown that the CSB N-terminal region interacts with its ATPase domain and that this interaction is modulated by two CSB phosphorylation events on its N-terminal S10 and S158, both of which are necessary for its *in vivo* chromatin remodeling activity at DSBs. We envision a model in which in the absence of DSBs, the CSB N-terminal region is docked on its ATPase domain in such a manner that its ATPase activity is restricted. Upon induction of DSBs, ATM- and CDK2-dependent CSB phosphorylations on S10 and S158 promote CSB conformational change so that its N-terminal region is now docked at a different location on its ATPase domain (Fig. 9d). This new docking frees its ATPase activity needed for its chromatin remodeling activity. In the absence of these two phosphorylation events, CSB- Δ N30, CSB-S10A and CSB-S158A mutants would not be able to undergo protein conformational change needed for the new

docking of its N-terminal region. Our finding that CSB phosphorylations on S10 and S158 stimulate CSB-N interaction with CSB-ATPase suggests that these two phosphorylation events might create an interface favorable for these two domains to interact. We propose that these two phosphorylation events act together as molecular signals to trigger the release of the autoinhibition of its N-terminal region on its ATPase domain in S/G2 cells (Fig. 9d). Subsequently the chromatin remodeling activity of CSB at DSBs evicts histones and disassembles nucleosomes, limiting RIF1 accumulation but paving the way for BRCA1-mediated HR activity in S/G2 (Fig. 9d). Our finding that the activation of CSB chromatin remodeling activity at DSBs requires not only a DNA damage signal but also a signal indicating the correct phase of the cell cycle suggests that these two signals are needed to restrict displacement of histones by CSB to damaged S/G2 cells, perhaps helping guard against unwarranted extensive chromatin disassembly by CSB in undamaged cells or damaged G1 cells.

Acknowledgments

We would like to thank Titia de Lange for phoenix cells, Jan Hoeijmakers for the RAD51 antibody, Roger Greenberg for U2OS-265 cells, André Nussenzweig and Jeremy Daniel for the GFP-PTIP expression construct. Sebastien Landry is thanked for generating U2OS-265 53BP1 KO cells. This work is supported by funding from Canadian Institutes of Health Research to D.D. (FDN143343) and to X.-D.Z. (MOP-285822). N.L.B. is a holder of Ontario Graduate Scholarship.

Author Contributions

N.L.B. initiated the project and performed the majority of the experiments. J.R.W. carried out the sequence alignment and computer modeling of WHD, cloned all CSB mutants, immunoprecipitated Flag-CSB, produced recombinant CSB and assisted with IR experiments. S.M.N. conducted the mass spectrometric analysis of Flag-CSB. N.M. conducted the FACS analysis of DR-GFP assays. All authors contributed to data analysis and interpretation. X.D.Z. designed the project and wrote the paper with N.L.B., J.R.W., and with input from other authors.

Conflict of interest

The authors declare no competing financial interests.

4.2.6 *Figure and figure legends*

Figure 1 Batenburg et al.

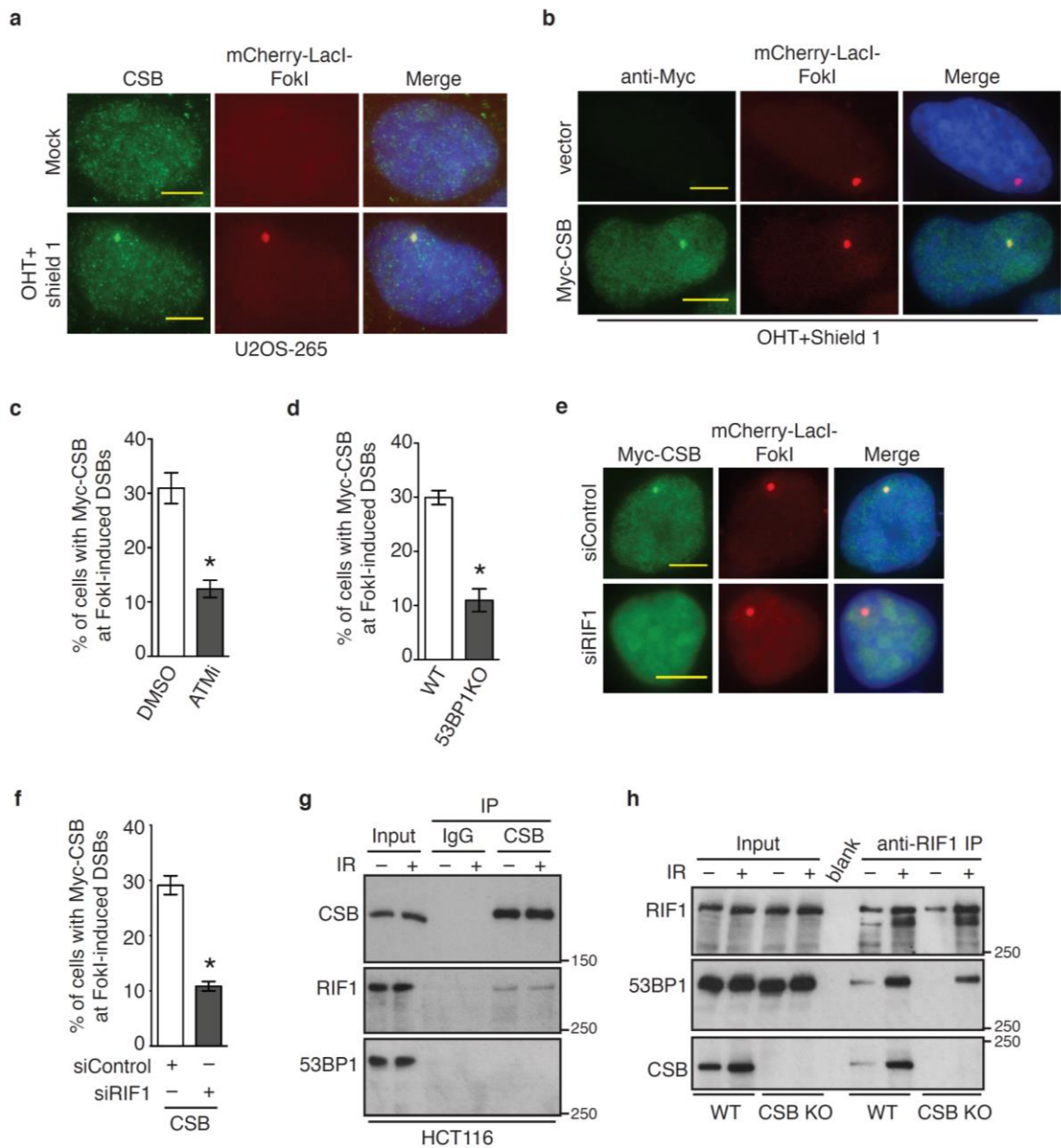


Figure 1. CSB interacts with RIF1 and is recruited by RIF1 to FokI-induced DSBs. (a) Immunofluorescence of U2OS-265 cells with or without induction of FokI expression. Fixed cells were stained with an anti-CSB antibody. Nuclei were stained with DAPI in blue

in this and following figures. Scale bars, 5 μm . **(b)** Immunofluorescence of U2OS-265 cells expressing Myc-tagged CSB with or without induction of FokI expression. Fixed cells were stained with anti-Myc antibody. Scale bars, 5 μm . **(c)** Quantification of the percentage of U2OS-265 cells with Myc-CSB accumulated at FokI-induced DSBs. U2OS-265 cells were treated with DMSO or ATM inhibitor KU55933 for 1 h prior to induction of FokI expression. A total of 250 Myc-expressing cells were scored for each independent experiment in a blind manner. Standard deviations, referred to as SDs in this and the subsequent figures, from three independent experiments are indicated. $*P < 0.05$. **(d)** Quantification of the percentage of parental and 53BP1 KO U2OS-265 cells with Myc-CSB accumulated at FokI-induced DSBs. Scoring was done as described in 1c. SDs from three independent experiments are indicated. $*P < 0.05$. **(e)** Immunofluorescence with an anti-Myc antibody. 48 h prior to FokI induction, U2OS-265 cells were transfected with siRNA against scramble DNA (siControl) or RIF1 (siRIF1). Scale bars, 5 μm . **(f)** Quantification of the percentage of siControl- and siRIF1-expressing U2OS-265 cells with Myc-CSB accumulated at FokI-induced DSBs. Scoring was done as described in 1c. SDs from three independent experiments are indicated. $*P < 0.05$. **(g)** Coimmunoprecipitation with IgG and anti-CSB antibody in HCT116 cells treated with or without 20 Gy IR. Immunoblotting was performed with anti-CSB, anti-RIF1 and anti-53BP1 antibodies. Protein molecular weight markers in kDa are indicated in this and the subsequent figures. **(h)** Coimmunoprecipitation with anti-RIF1 antibody in parental (WT) and CSB knockout (KO) HCT116 cells treated with or without 20 Gy IR. Immunoblotting was performed with anti-RIF1, anti-53BP1 and anti-CSB antibodies.

Figure 2 Batenburg et al.

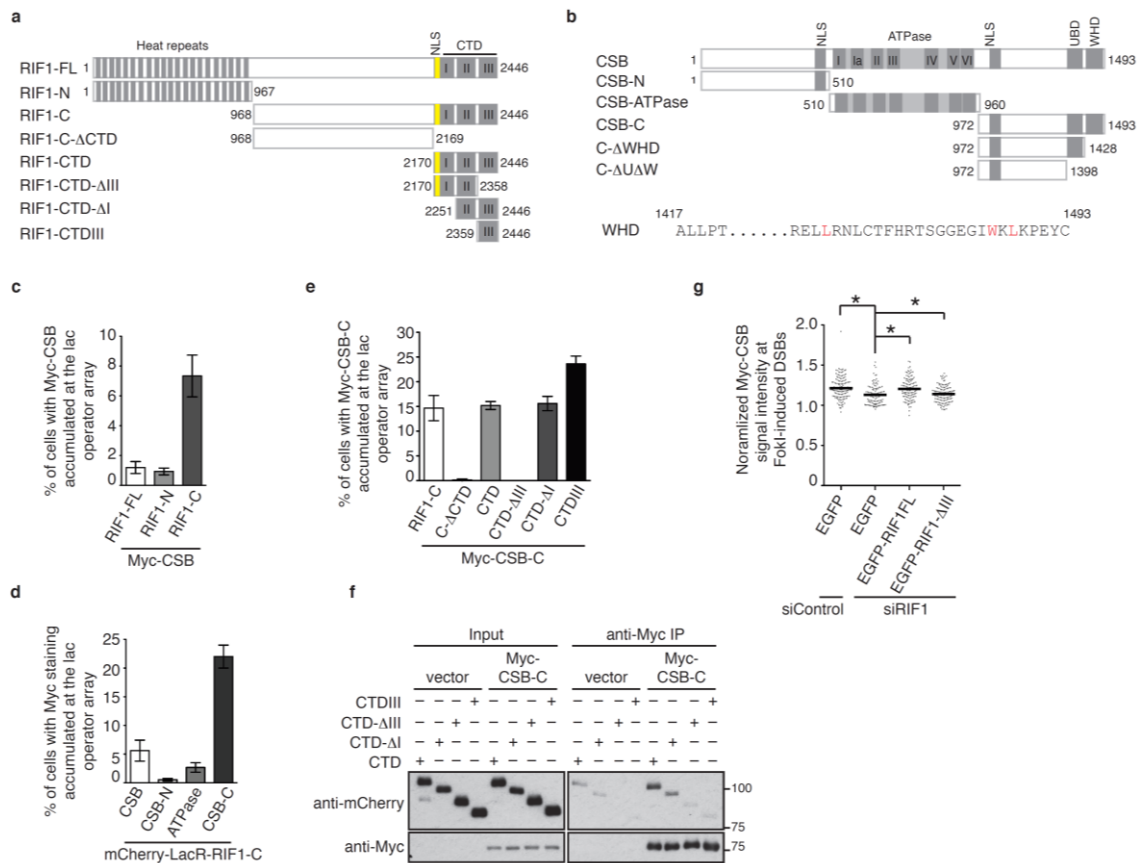


Figure 2. RIF1 interacts with CSB and recruits CSB to DSBs via its CTD domain. **(a)** Schematic diagram of RIF1. NLS: nuclear localization signal; CTD: C-terminal domain. **(b)** Schematic diagram of CSB. NLS: nuclear localization signal; UBD: ubiquitin binding domain; WHD: winged helix domain. **(c)** Quantification of the percentage of cells exhibiting Myc-CSB accumulated at the lac operator array. U2OS-265 cells were co-transfected with Myc-CSB and various mCherry-LacR-RIF1 alleles as indicated. A total of 250 cells positive for Myc-CSB expression were scored for each independent experiment in a blind manner. SDs from three independent experiments are indicated. **(d)**

Quantification of the percentage of cells exhibiting Myc staining accumulated at the lac operator array. U2OS-265 cells were co-transfected with mCherry-LacR-RIF1-C and various Myc-tagged CSB alleles as indicated. A total of 250 cells positive for expression of various Myc-tagged CSB alleles as indicated were scored for each independent experiment in a blind manner. SDs from three independent experiments are indicated. (e) Quantification of the percentage of cells exhibiting Myc-CSB-C accumulated at the lac operator array. U2OS-265 cells were co-transfected with Myc-CSB-C and various mCherry-LacR-RIF1-C alleles as indicated. A total of 250 cells positive for Myc-CSB-C expression were scored for each independent experiment in a blind manner. SDs from three independent experiments are indicated. (f) Coimmunoprecipitation with anti-Myc antibody in 293T cells expressing the vector alone or Myc-CSB-C in conjunction with various mCherry-LacR-CTD alleles as indicated. Immunoblotting was done with anti-Myc and anti-mCherry antibodies. (g) Quantification of the intensity of Myc-CSB signal at the site of FokI-induced DSBs. 24 hr post transfection with siControl or siRIF1, U2OS-265 cells were transfected with the EGFP vector alone or various siRIF1-resistant EGFP-RIF1 alleles as indicated and induced for FokI expression 48 hr post transfection. Analysis of Myc-CSB signal intensity was only done for cells positive for expression of Myc-CSB, EGFP and mCherry-LacR-FokI. The respective numbers of cells analyzed for siControl/EGFP, siRIF1/EGFP, siRIF1/EGFP-RIF1 and siRIF1/EGFP-Rif-DCTDIII were 131, 107, 120 and 124. * $P < 0.05$.

Figure 3 Batenburg et al.

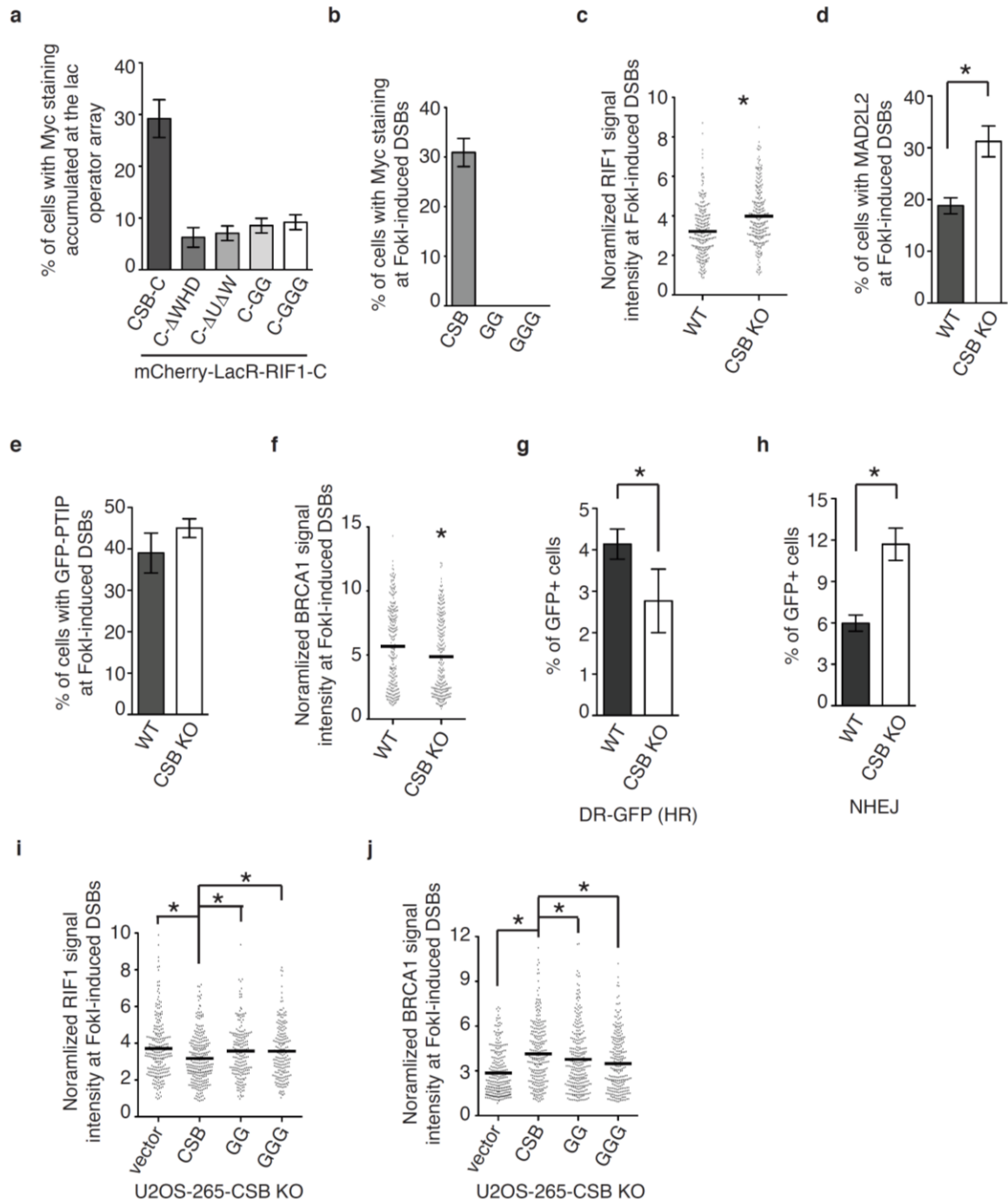


Figure 3. CSB interacts with RIF1 via its a newly-identified winged helix domain (WHD) and inhibits RIF1 at DSBs. **(a)** Quantification of the percentage of cells exhibiting Myc staining accumulated at the lac operator array in U2OS-265 cells co-transfected with indicated alleles. A total of 250 cells positive for Myc staining were scored for each independent experiment in a blind manner. SDs from three independent experiments are indicated. **(b)** Quantification of the percentage of cells exhibiting Myc staining at the site of FokI-induced DSBs. A total of 250 U2OS-265 cells expressing various Myc-tagged CSB alleles as indicated were scored for each independent experiment in a blind manner. SDs from three independent experiments are indicated. **(c)** Quantification of the intensity of RIF1 signal at the site of FokI-induced DSBs. The respective numbers of cells analyzed for parental and CSB KO were 275 and 277. * $P < 0.05$. **(d)** Quantification of the percentage of cells exhibiting MAD2L2 at the site of FokI-induced DSBs. A total of 500-550 cells were scored for each independent experiment in a blind manner. SDs from three independent experiments are indicated. **(e)** Quantification of the percentage of cells exhibiting GFP-PTIP at the site of FokI-induced DSBs. A total of 500 cells were scored for each independent experiment in a blind manner. SDs from three independent experiments are indicated. **(f)** Quantification of the intensity of BRCA1 signal at the site of FokI-induced DSBs. The respective numbers of cells analyzed for parental and CSB KO were 282 and 294. * $P < 0.05$. **(g)** HR-mediated repair of *I-SceI*-induced DSBs in U2OS-DR-GFP WT and CSB-KO cells. SDs from three independent experiments are indicated. **(h)** NHEJ-mediated repair of *I-SceI*-induced DSBs. SDs from three independent experiments are indicated. **(i)** Quantification of the intensity of RIF1 signal at the site of FokI-induced DSBs. The

respective numbers of cells analyzed for the vector alone, Myc-CSB, Myc-CSB-GG and Myc-CSB-GGG were 298, 304, 204 and 209. * $P < 0.05$. (j) Quantification of the intensity of BRCA1 signal at the site of FokI-induced DSBs. The respective numbers of cells analyzed for the vector alone, Myc-CSB, Myc-CSB-GG and Myc-CSB-GGG were 279, 270, 291, 258. * $P < 0.05$.

Figure 4 Batenburg et al.

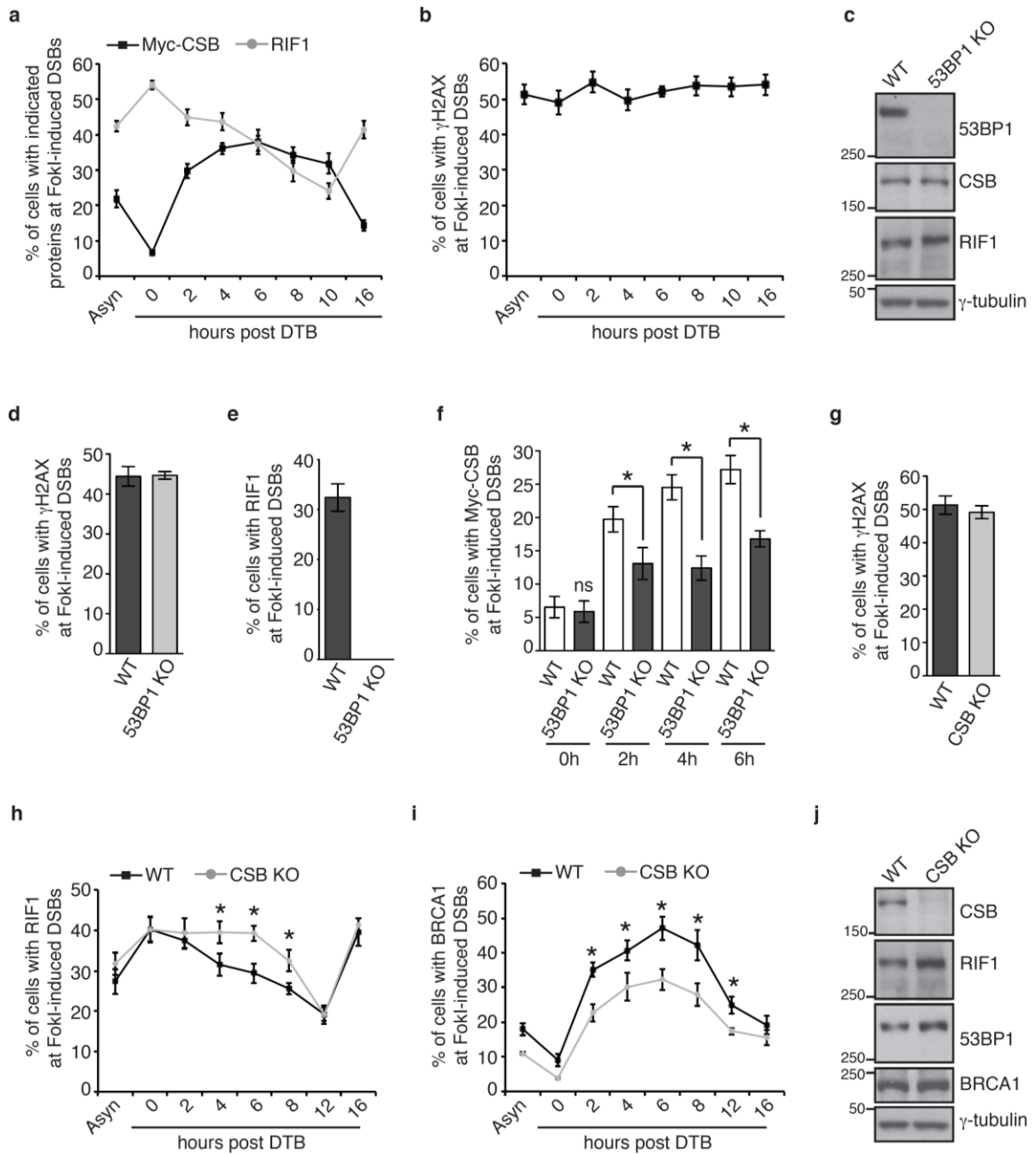


Figure 4. RIF1 recruits CSB to FokI-induced DSBs in S phase, which in turn inhibits RIF1.

(a) Quantification of the percentage of synchronized Myc-CSB-expressing U2OS-265 cells exhibiting indicated proteins at FokI-induced DSBs. For Myc-CSB, a total of 250 Myc-CSB-expressing cells were scored for each independent experiment in blind. For RIF1, a total of 500-550 cells were scored in blind for each independent experiment. SDs from three independent experiments are indicated. (b) Quantification of the percentage of synchronized Myc-CSB-expressing U2OS-265 cells exhibiting γ H2AX at FokI-induced DSBs. A total of 500-550 cells were scored in blind for each independent experiment. SDs from three independent experiments are indicated. (c) Western analysis of U2OS-265 parental (WT) and 53BP1 KO cells. The γ -tubulin blot was used as a loading control here and the following figures. (d) Quantification of the percentage of U2OS-265 WT and 53BP1 KO cells with γ H2AX at FokI-induced DSBs. Scoring was done as in 3b. SDs from three independent experiments are indicated. (e) Quantification of the percentage of U2OS-265 WT and 53BP1 KO cells with RIF1 at FokI-induced DSBs. Scoring was done as in 3b. SDs from three independent experiments are indicated. (f) Quantification of the percentage of synchronized Myc-CSB-expressing WT and 53BP1 KO U2OS-265 cells with Myc-CSB at FokI-induced DSBs. A total of 250 Myc-CSB-expressing cells were scored for each independent experiment in blind. SDs from three independent experiments are indicated. * $P < 0.05$. (g) Quantification of the percentage of U2OS-265 WT and CSB-KO cells with γ H2AX at FokI-induced DSBs. Scoring was done as in 3b. SDs from three independent experiments are indicated. (h) Quantification of the percentage of synchronized U2OS-265

WT and CSB KO cells with RIF1 at FokI-induced DSBs. Scoring was done as in 3b. SDs from three independent experiments are indicated. * $P < 0.05$. (i) Quantification of the percentage of synchronized U2OS-265 WT and CSB KO cells with BRCA1 at FokI-induced DSBs. Scoring was done as in 3b. SDs from three independent experiments are indicated. * $P < 0.05$. (j) Western analysis of U2OS-265 WT and CSB KO cells.

Figure 5 Batenburg et al.

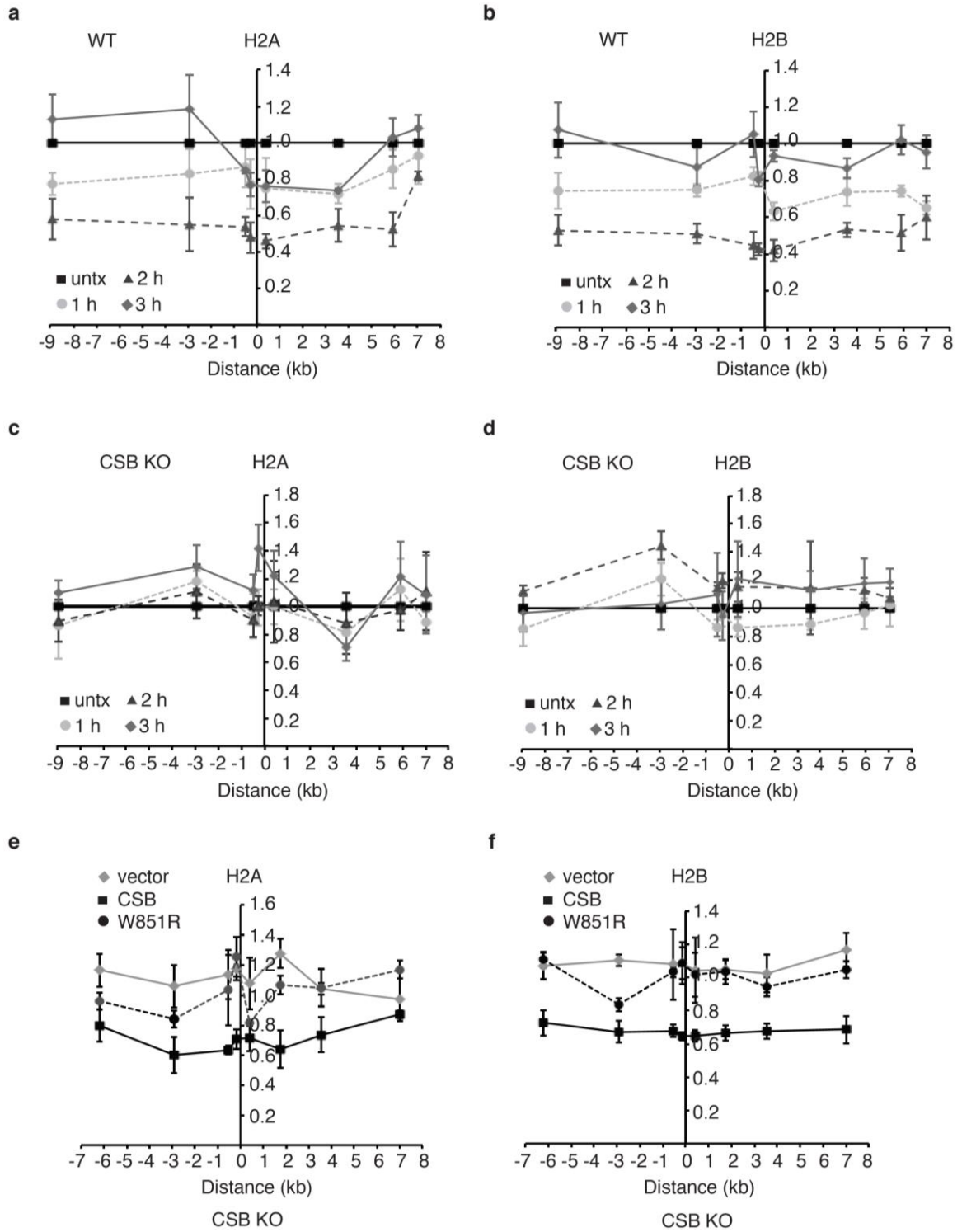


Figure 5. CSB is a chromatin remodeler and evicts histones from the chromatin surrounding I-PpoI-induced DSBs *in vivo*. **(a)** Relative occupancy of histone H2A in ddI-PpoI-expressing hTERT-RPE parental cells. Cells were either untreated (untx) or treated with Shield-1 and 4-OHT and then harvested at indicated times. The x-axis represents the distance in kb upstream and downstream from the I-PpoI-induced DSB on chromosome 1, which was set as 0. The y-axis represents the relative occupancy of H2A of treated cells relative to untreated cells. Standard error of the mean (SEM) from three independent experiments are indicated. **(b)** Relative occupancy of histone H2B in ddI-PpoI-expressing hTERT-RPE parental cells. Both x- and y-axes are as described in 5a. SEM from three independent experiments are indicated. **(c)** Relative occupancy of histone H2A in ddI-PpoI-expressing hTERT-RPE CSB KO cells. Both x- and y-axes are as described in 4a. SEM from three independent experiments are indicated. **(d)** Relative occupancy of histone H2B in ddI-PpoI-expressing hTERT-RPE CSB KO cells. Both x- and y-axes are as described in 5a. SEM from three independent experiments are indicated. **(e)** Relative occupancy of histone H2A in ddI-PpoI-expressing hTERT-RPE CSB KO cells complemented with the vector alone, Myc-tagged wild type CSB or Myc-tagged mutant CSB-W851R. Both x- and y-axes are as described in 5a. SEM from three independent experiments are indicated. **(f)** Relative occupancy of histone H2B in ddI-PpoI-expressing hTERT-RPE CSB KO cells complemented with the vector alone, Myc-tagged wild type CSB or Myc-tagged mutant CSB-W851R. Both x- and y-axes are as described in 5a. SEM from three independent experiments are indicated.

Figure 6 Batenburg et al.

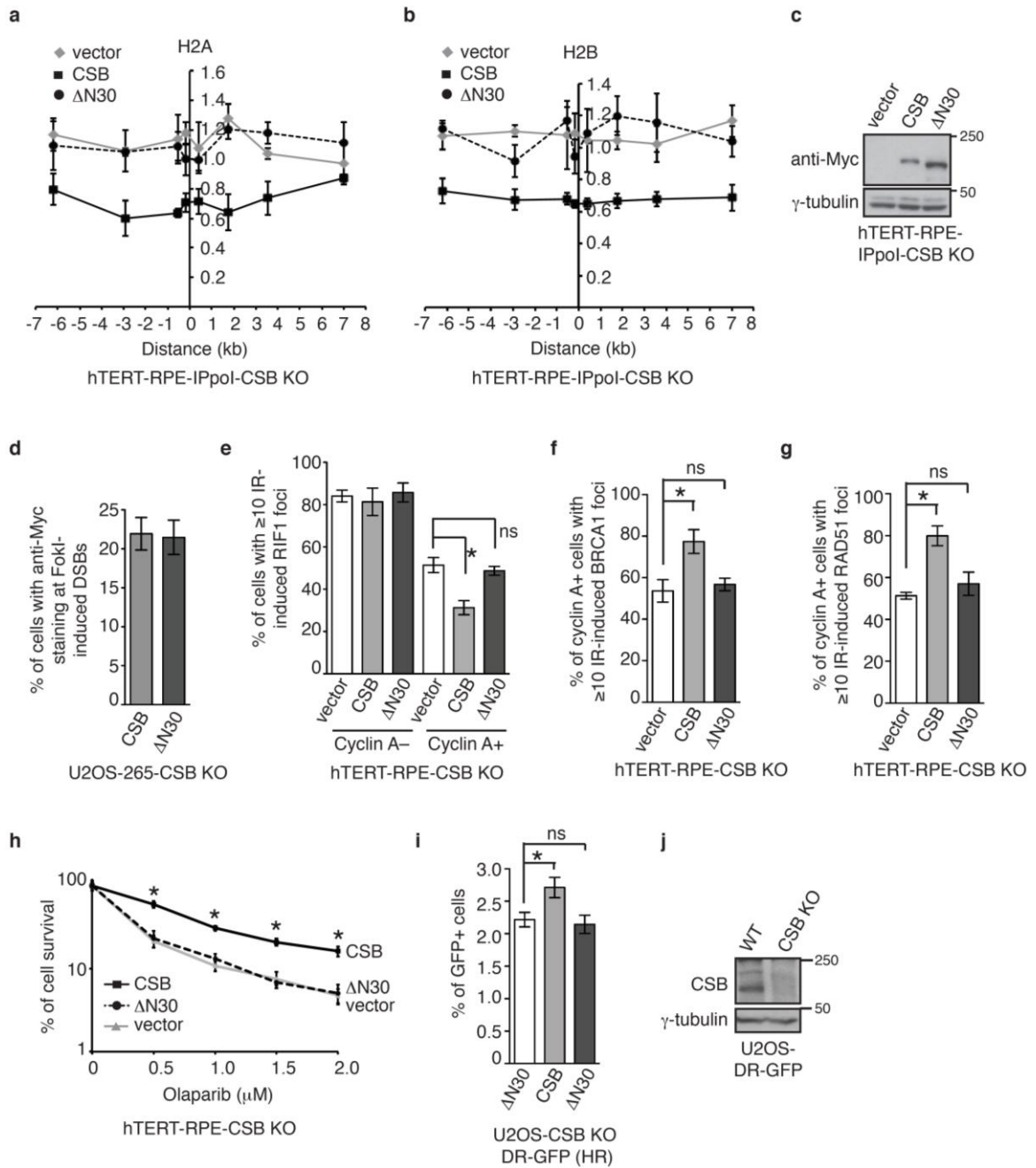


Figure 6. The N-terminus of CSB mediates its chromatin remodeling activity to repress RIF1 accumulation at sites of DSBs. **(a)** Relative occupancy of histone H2A in ddI-PpoI-expressing CSB KO hTERT-RPE cells complemented with various alleles as indicated. Both x- and y-axes are as described in 5a. SEM from three independent experiments are indicated. **(b)** Relative occupancy of histone H2B in ddI-PpoI-expressing CSB KO hTERT-RPE cells complemented with various alleles as indicated. Both x- and y-axes are as described in 5a. SEM from three independent experiments are indicated. **(c)** Western analysis of hTERT-RPE-IPpoI-CSB KO cells expressing various alleles as indicated. **(d)** Quantification of the percentage of Myc-CSB and Myc-CSB- Δ N30-expressing U2OS-265 cells exhibiting anti-Myc staining at FokI-induced DSBs. A total of 250 cells positive for anti-Myc staining were scored for each independent experiment in a blind manner. SDs from three independent experiments are indicated. **(e)** Quantification of the percentage of cyclin A- and cyclin A+ cells with 10 or more IR-induced RIF1 foci. hTERT-RPE CSB KO cells stably expressing various alleles as indicated were treated with 2 Gy IR and fixed 1 hr post IR. A total of 500-550 cells were scored for each independent experiment in a blind manner. SDs from three independent experiments are indicated. * $P < 0.05$. ns: $P > 0.05$. **(f)** Quantification of the percentage of cyclin A+ cells with ≥ 10 IR-induced BRCA1 foci. Scoring was done as in 6e. SDs from three independent experiments are indicated. * $P < 0.05$. ns: $P > 0.05$. **(g)** Quantification of the percentage of cyclin A+ cells with 10 or more IR-induced RAD51 foci. hTERT-RPE CSB KO cells stably expressing various alleles as indicated were treated with 2 Gy IR and fixed 4 hr post IR. Scoring was done as in 6e. SDs from three independent experiments are indicated. * $P < 0.05$. ns: $P > 0.05$. **(h)** Clonogenic

survival assays of olaparib-treated hTERT-RPE CSB-KO cells complemented with various alleles as indicated. SDs from three independent experiments are indicated. * $P < 0.05$ for comparison between CSB and $\Delta N30$. (i) HR-mediated repair of I-SceI-induced DNA DSBs. SDs from three independent experiments are indicated. * $P < 0.05$. ns: $P > 0.05$. (j) Western analysis of U2OS-DR-GFP parental and CSB KO cells.

Figure 7 Batenburg et al.

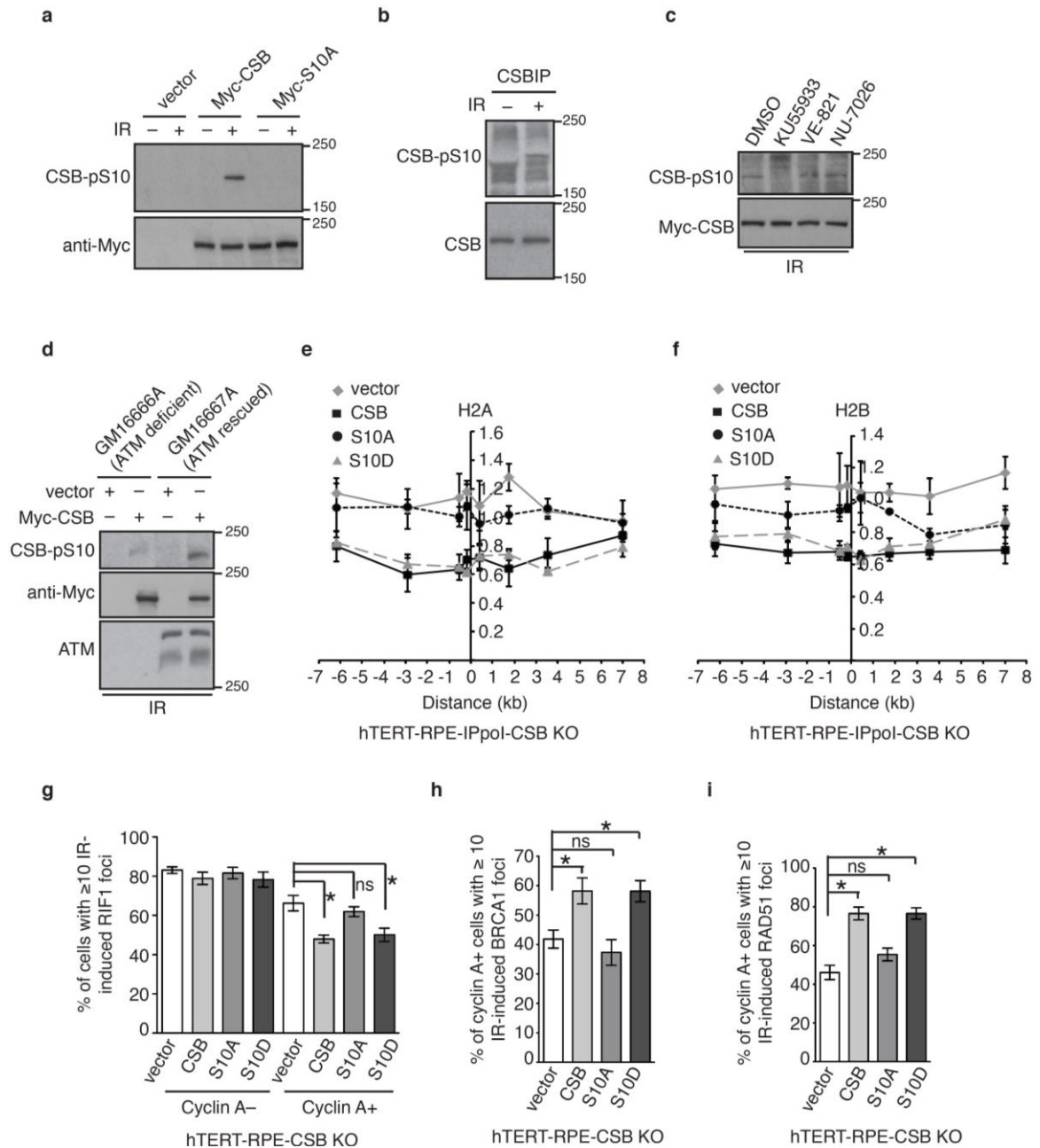


Figure 7. ATM controls the chromatin remodeling activity of CSB through S10 phosphorylation. (a) Western analysis of U2OS CSB KO cells stably expressing various

alleles as indicated. Cells were either treated with or without 10 Gy IR. **(b)** Western analysis of anti-CSB immunoprecipitates from HCT116 cells treated with or without 10 Gy IR. **(c)** Western analysis. Myc-CSB-expressing U2OS CSB KO cells were treated with DMSO, ATM inhibitor KU55933, ATR inhibitor VE-821 or DNA-PKcs inhibitor NU-7026 for 1 h prior to 10 Gy IR. **(d)** Western analysis of ATM-deficient GM16666A and ATM-complemented GM16667A cells. Cells were transfected with the vector alone or Myc-CSB, followed by treatment with 10 Gy IR 48 hr post transfection. **(e)** Relative occupancy of histone H2A in ddi-PpoI-expressing hTERT-RPE CSB KO cells complemented with various alleles as indicated. Both x- and y-axes are as described in 5a. SEM from three independent experiments are indicated. **(f)** Relative occupancy of histone H2B in ddi-PpoI-expressing hTERT-RPE CSB KO cells complemented with various alleles as indicated. Both x- and y-axes are as described in 5a. SEM from three independent experiments are indicated. **(g)** Quantification of the percentage of cyclin A- and cyclin A+ cells with 10 or more IR-induced RIF1 foci. hTERT-RPE CSB KO cells stably expressing various alleles as indicated were treated with 2 Gy IR and fixed 1 hr post IR. A total of 500-550 cells were scored for each independent experiment in a blind manner. SDs from three independent experiments are indicated. * $P < 0.05$. ns: $P > 0.05$. **(h)** Quantification of the percentage of cyclin A+ cells with ≥ 10 IR-induced BRCA1 foci. Scoring was done as in 7g. SDs from three independent experiments are indicated. * $P < 0.05$. ns: $P > 0.05$. **(i)** Quantification of the percentage of cyclin A+ cells with 10 or more IR-induced RAD51 foci. Cells were treated with 2 Gy IR and fixed 4 hr post IR. Scoring was done as in 7g. SDs from three independent experiments are indicated. * $P < 0.05$. ns: $P > 0.05$.

Figure 8 Batenburg et al.

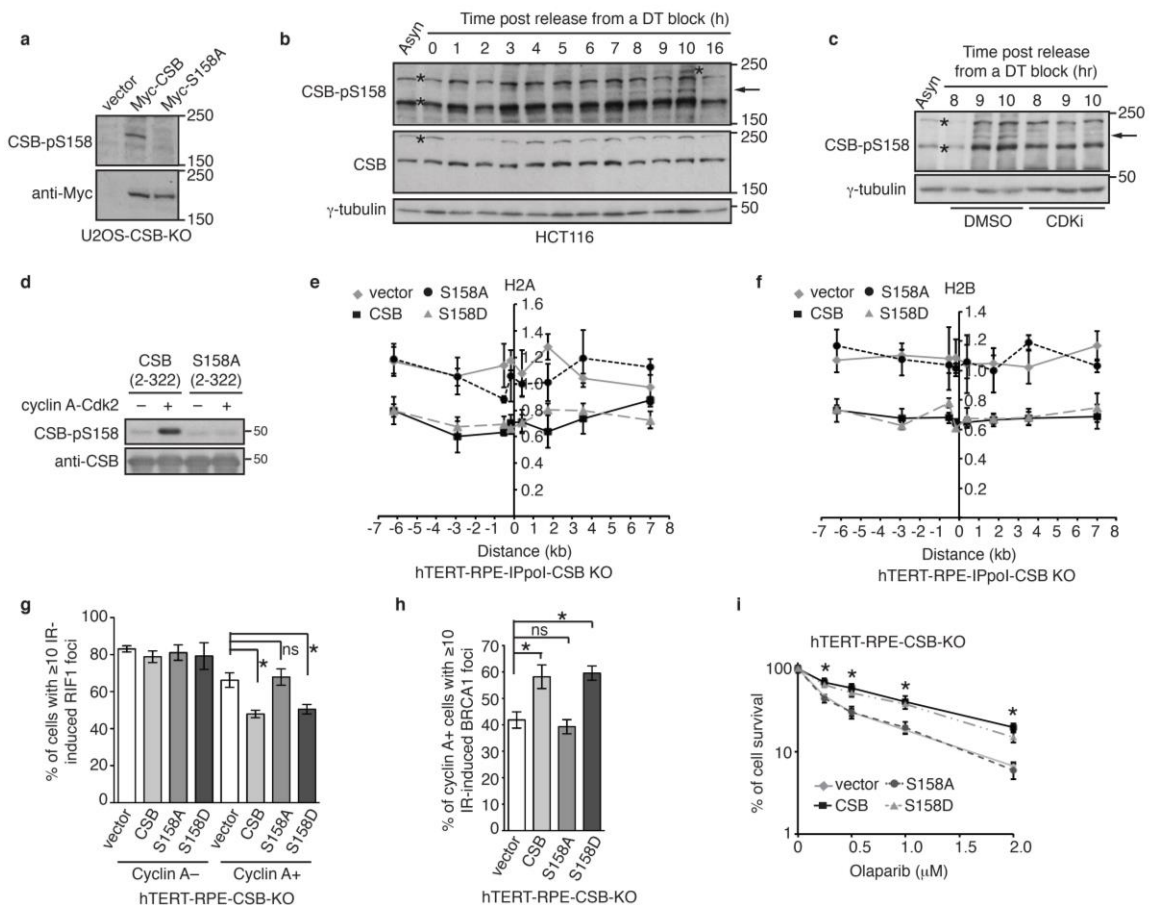


Figure 8. Cyclin A-CDK2 controls the chromatin remodeling activity of CSB through S158 phosphorylation. **(a)** Western analysis of U2OS-CSB-KO cells stably expressing the vector alone, Myc-CSB or Myc-CSB carrying a S158A mutation. Immunoblotting was performed with anti-CSB-pS158 and anti-Myc antibodies. **(b)** Western analysis of synchronized HCT116 cells. The arrow indicates the position of CSB-pS158. Asterisks indicate non-specific bands. **(c)** Western analysis. Asynchronous and synchronized HCT116 cells post release from a double thymidine block as indicated were treated with DMSO or the CDK inhibitor roscovitine. The arrow indicates the position of CSB-pS158. Asterisks indicate non-specific bands. **(d)** *In vitro* kinase assays with recombinant cyclin A-CDK2 and

bacteria-expressed recombinant CSB fragments as indicated. **(e)** Relative occupancy of histone H2A in ddI-PpoI-expressing hTERT-RPE CSB KO cells complemented with various alleles as indicated. Both x- and y-axes are as described in 5a. SEM from three independent experiments are indicated. **(f)** Relative occupancy of histone H2B in ddI-PpoI-expressing hTERT-RPE CSB KO cells complemented with various alleles as indicated. Both x- and y-axes are as described in 5a. SEM from three independent experiments are indicated. **(g)** Quantification of the percentage of cyclin A- and cyclin A+ cells with 10 or more IR-induced RIF1 foci. hTERT-RPE CSB KO cells stably expressing various alleles as indicated were treated with 2 Gy IR and fixed 1 hr post IR. A total of 500-550 cells were scored for each independent experiment in a blind manner. SDs from three independent experiments are indicated. * $P < 0.05$. ns: $P > 0.05$. **(h)** Quantification of the percentage of cyclin A+ cells with ≥ 10 IR-induced BRCA1 foci. Scoring was done as in 8g. SDs from three independent experiments are indicated. * $P < 0.05$. ns: $P > 0.05$. **(i)** Clonogenic survival assays of olaparib-treated hTERT-RPE CSB-KO cells complemented with various alleles as indicated. SDs from three independent experiments are indicated. * $P < 0.05$ for comparison between CSB and S158A.

Figure 9 Batenburg et al.

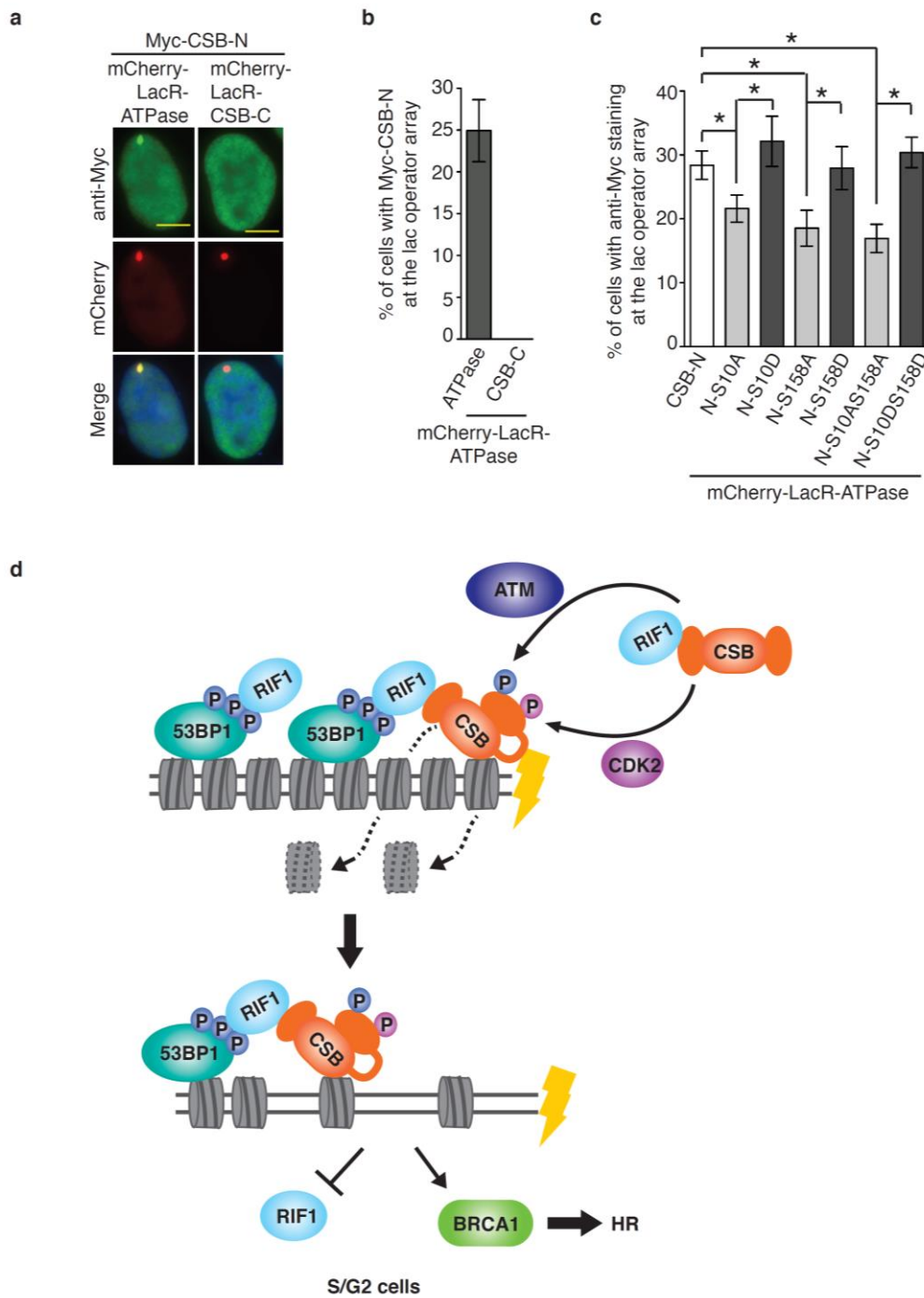
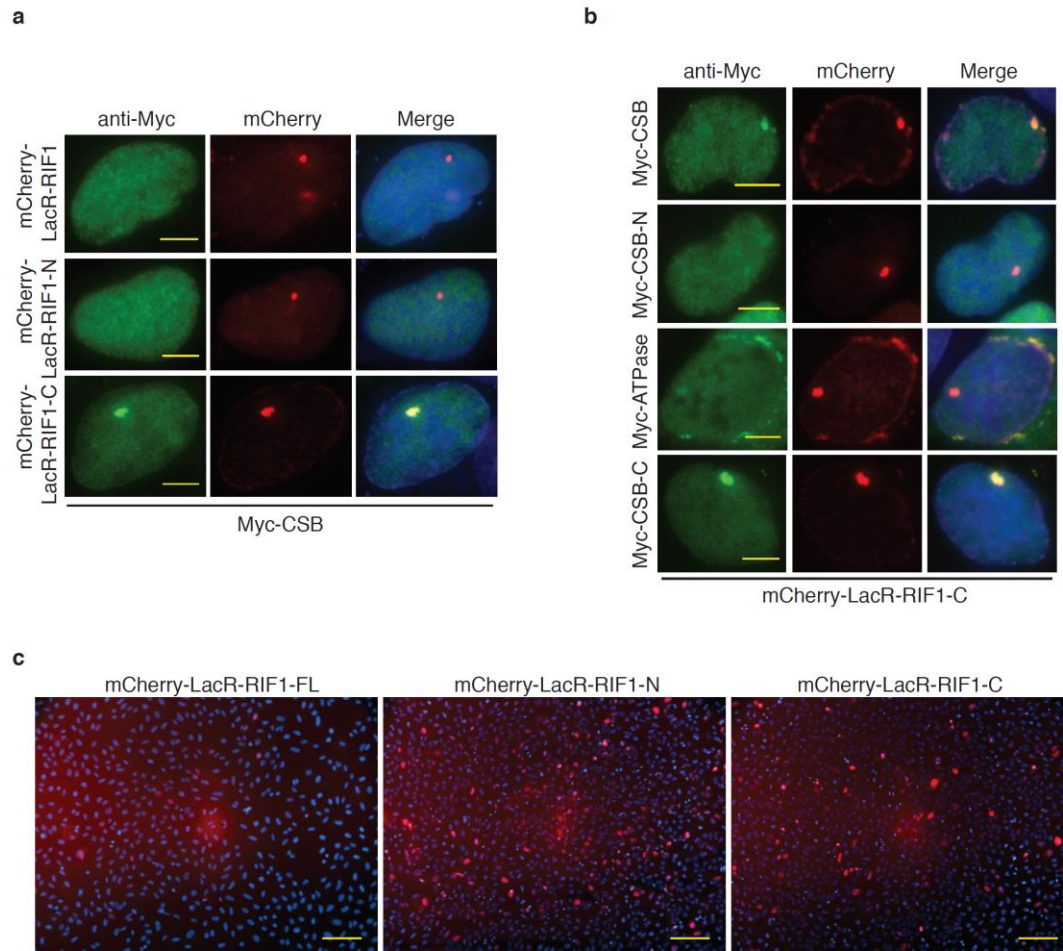


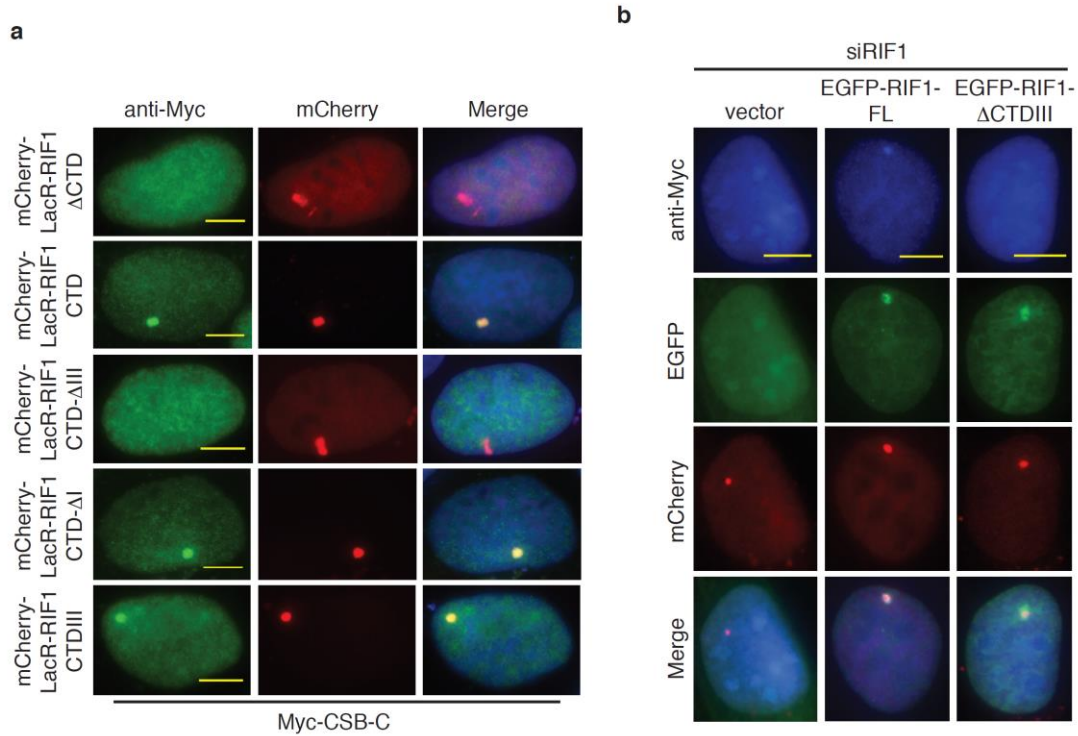
Figure 9. CSB phosphorylations on S10 and S158 modulate its intramolecular interaction between the N-terminus and the ATPase domain. **(a)** Immunofluorescence of U2OS-265 cells transfected with Myc-CSB-N in conjunction with either mCherry-LacR-CSB-ATPase or mCherry-LacR-CSB-C. Scale bars, 5 μ m. **(b)** Quantification of the percentage of U2OS-265 cells from (a) with anti-Myc staining at FokI-induced DSBs. A total of 250 Myc-expressing cells were scored for each independent experiment in a blind manner. SDs from three independent experiments are indicated. **(c)** Quantification of the percentage of U2OS-265 cells with anti-Myc staining at FokI-induced DSBs. U2OS-265 were co-transfected with various alleles as indicated. A total of 250 Myc-expressing cells were scored for each independent experiment in a blind manner. SDs from three independent experiments are indicated. * $P < 0.05$. **(d)** Model for control of CSB chromatin remodeling activity by ATM and CDK2 in DNA DSB repair pathway choice in S/G2. See the text for details.

Supplimentary Figure 1 Batenburg et al.



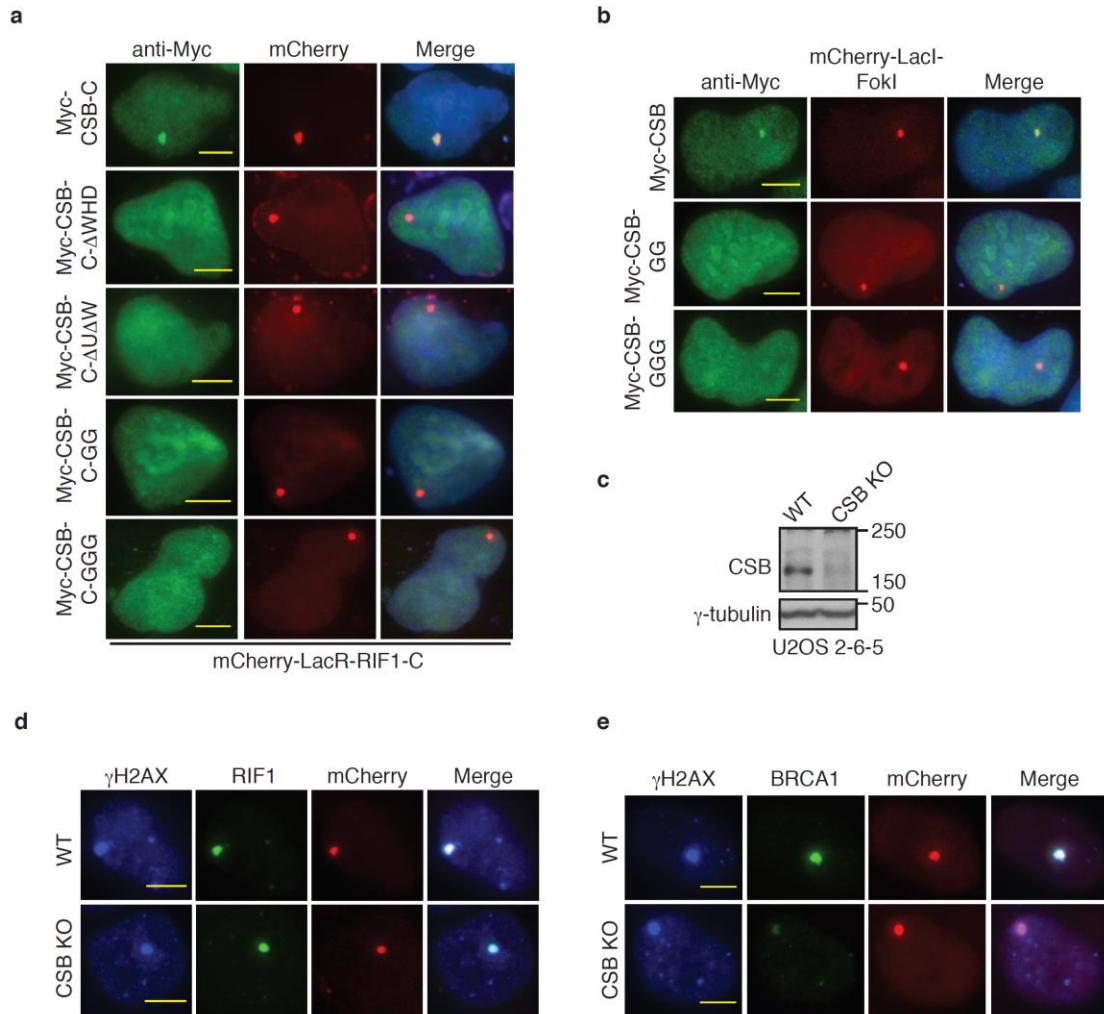
Supplementary Figure 1. RIF1-C interacts with CSB-C. **(a)** Immunofluorescence of U2OS-265 cells that were co-transfected with Myc-CSB and various mCherry-LacR-RIF1 alleles as indicated. Cell nuclei were stained with DAPI in blue in this and subsequent figures. Scale bars, 5 μ m. **(b)** Immunofluorescence of U2OS-265 cells that were co-transfected with mCherry-LacR-RIF1-C and various Myc-tagged CSB alleles as indicated. Scale bars, 5 μ m. **(c)** Immunofluorescence of expression of mCherry-LacR-RIF1 alleles in U2OS-265 cells from (a). Scale bars, 50 μ m.

Supplimentary Figure 2 Batenburg et al.



Supplementary Figure 2. RIF1 interacts with CSB and recruits CSB to sites of DSBs through its CTD. **(a)** Immunofluorescence of U2OS-265 cells that were co-transfected with Myc-CSB-C and various mCherry-LacR-RIF1 alleles as indicated. Scale bars, 5 μ m. **(b)** Immunofluorescence. 24 hr post transfection with siControl and siRIF1, U2OS-265 cells were transfected with the vector alone (EGFP), EGFP-RIF1-FL or EGFP-RIF1- Δ CTDIII and then induced for FokI expression 48 hr post transfection. Fixed cells were immunostained with anti-Myc antibody (in blue). Scale bars, 5 μ m.

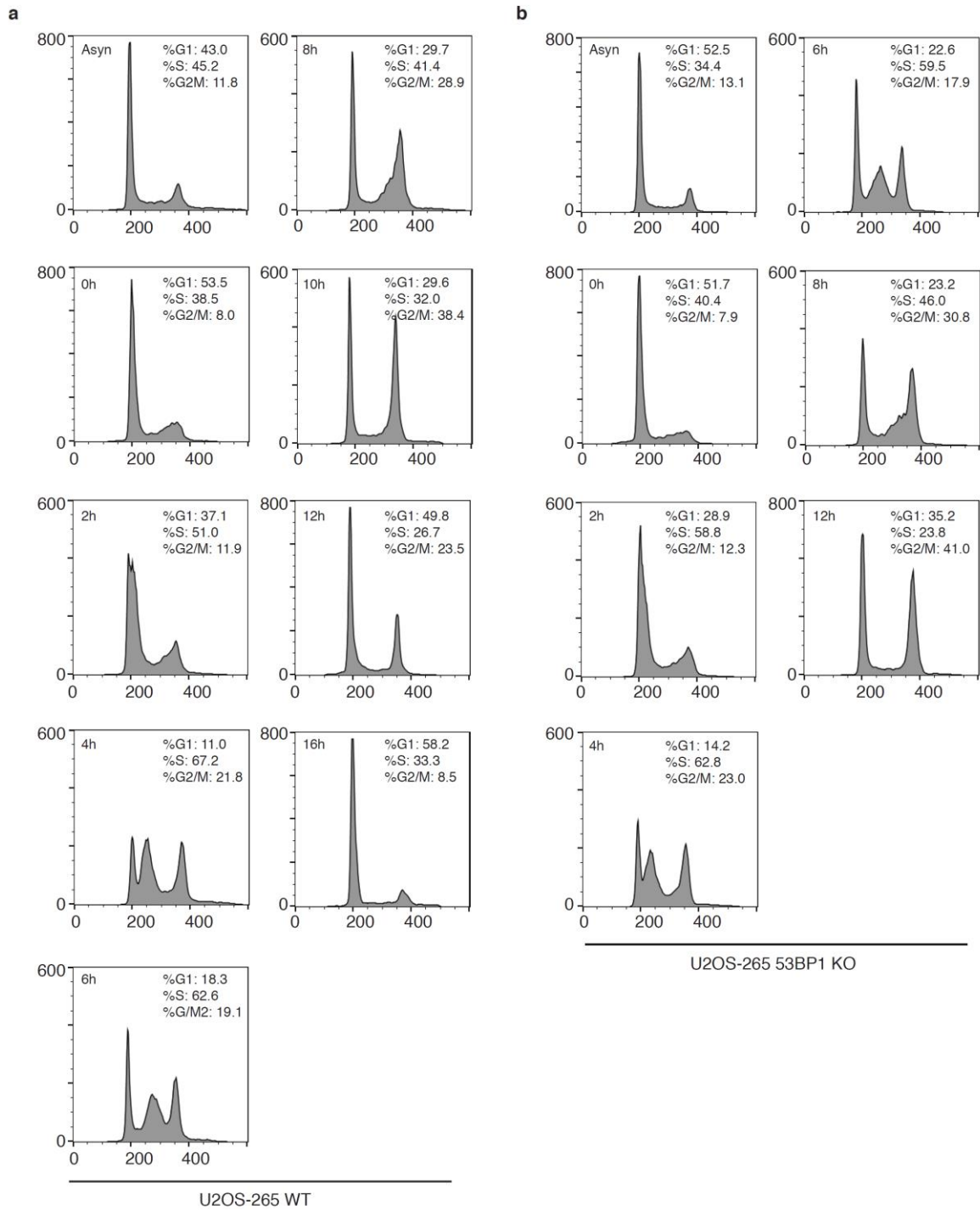
Supplementary Figure 3 Batenburg et al.



Supplementary Figure 3. The WHD of CSB is necessary for its interaction with RIF1 and its recruitment to the site of FokI-induced DSBs. **(a)** Immunofluorescence of U2OS-265 cells that were co-transfected with mCherry-LacR-RIF1-C and various Myc-tagged CSB alleles as indicated. Scale bars, 5 μ m. **(b)** Immunofluorescence of U2OS-265 cells expressing various Myc-tagged CSB alleles as indicated. 48 hr post transfection, cells were induced for FokI expression and fixed 6 h post FokI induction. Scale bars, 5 μ m. **(c)** Western analysis of wild type (WT) and CSB knockout U2OS-265 cells. The γ -tubulin blot was used as a loading control in this and subsequent figures. **(d)** Immunofluorescence of U2OS-265 parental and CSB KO cells. Cells were fixed 4 h post FokI induction and co-stained with anti-RIF1 and anti- γ H2AX antibodies. γ H2AX staining was used to mark the FokI-induced damage site. Scale bars, 5 μ m. **(e)** Immunofluorescence of U2OS-265 parental and CSB KO cells. Cells were fixed 4 h post FokI induction and co-stained with anti-BRCA1 and anti- γ H2AX antibodies. γ H2AX staining was used to mark the FokI-induced damage site. Scale bars, 5 μ m.

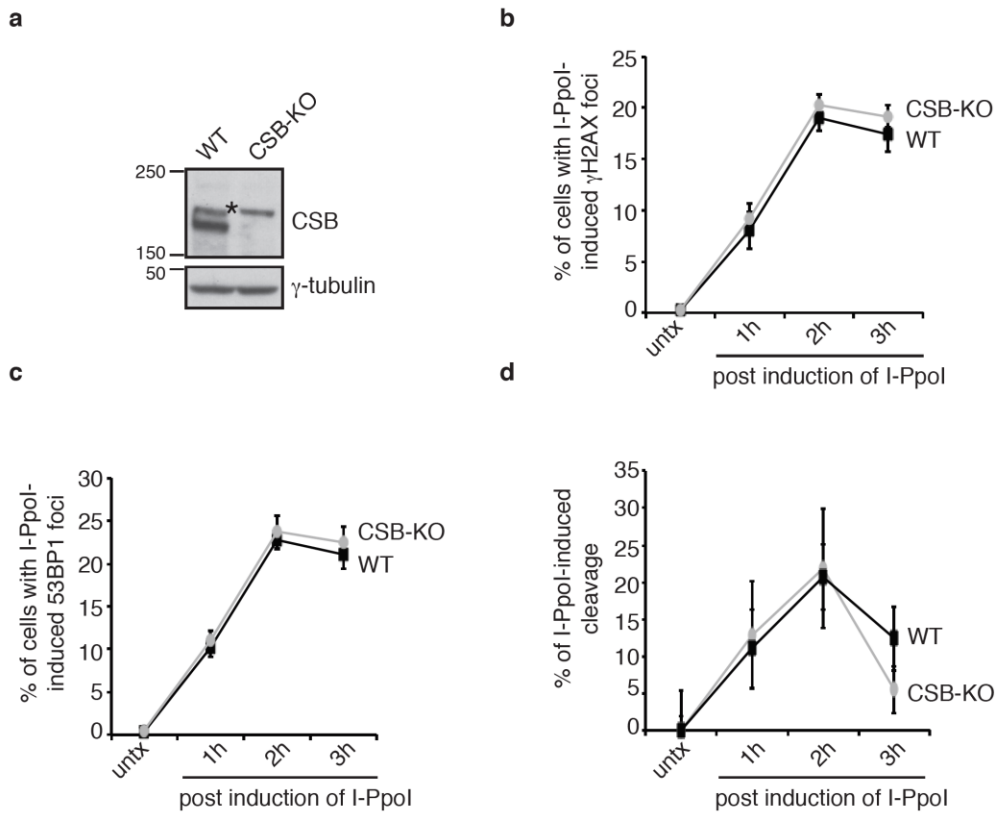
by the server JPRED4 (www.compbio.dundee.ac.uk/jpred4) is indicated underneath the sequence of CSB. Identical amino acids to those found in CSB are colored in grey; similar amino acids (charged RHKDE, polar uncharged STNQY, hydrophobic AVILMFWCPG) are colored in cyan. For CSB, the sequence is colored according to whether a match is made to an amino acid of a structural homolog in the order of preference: identical>similar>no match. Asterisks indicate the amino acids in CSB that were mutated in this study. **(b)** Sequence alignment of the WHD of CSB homologs from human to yeast. Identical amino acids in homologs to those found in CSB are colored in grey; similar amino acids as in (a) are colored in cyan. For CSB, sequence coloring is as in (a). Accession numbers are: NP_000115.1 (*Homo sapiens*); XP_009438634 (*Pan troglodytes*); XP_534944 (*Canis lupus familiaris*); NP_001100766 (*Rattus norvegicus*); XP_421656 (*Gallus gallus*); XP_007442212 (*Python bivittatus*); OCA28283 (*Xenopus tropicalis*); XP_005815483 (*Xiphophorus maculatus*); KFM67945 (*Stegodyphus mimosarum*); XP_014774958 (*Octopus bimaculoides*); NP_179466 (*Arabidopsis thaliana*); XP_002502040 (*Micromonas commoda*); AJR54981 (*Saccharomyces cerevisiae* YJM689). **(c)** Cartoon representation of three-dimensional structure of the WHD of human CSB based on the C-terminal domain of the RAP74 subunit of the human transcription factor IIF (PDB 1I27) as generated from FFAS³⁶ alignment. Helices are shown in purple; β strands are in yellow; random coils are in green. Three amino acids that were mutated in this study are shown in stick representation. The figure was generated using PyMOL (www.pymol.org).

Supplementary Figure 5 Batenburg et al.



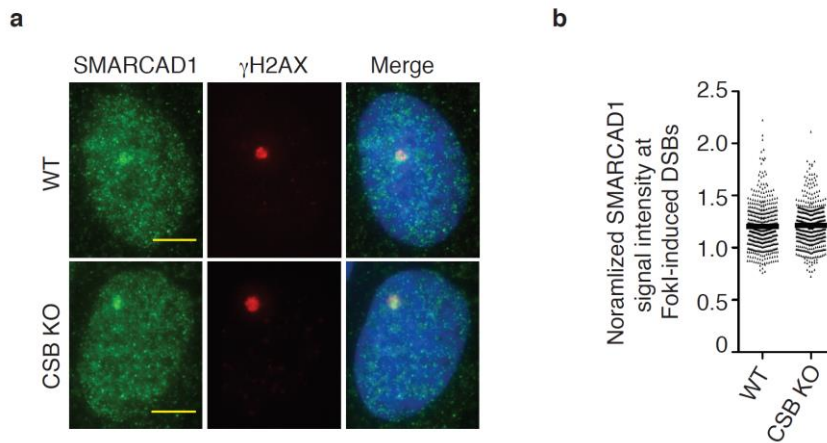
Supplementary Figure 5. Loss of 53BP1 has little effect on cell cycle progression. **(a)** FACS analysis of synchronized parental U2OS-265 cells. y axis, cell number; x axis, relative DNA content on the basis of staining with propidium iodide; 0-16 h, cells were released for 0-16 h from a double thymidine block; Asyn, asynchronous population. **(b)** FACS analysis of synchronized U2OS-265 53BP1 KO cells. y axis, cell number; x axis, relative DNA content on the basis of staining with propidium iodide; 0-12 h, cells were released for 0-12 h from a double thymidine block; Asyn, asynchronous population.

Supplementary Figure 6 Batenburg et al.



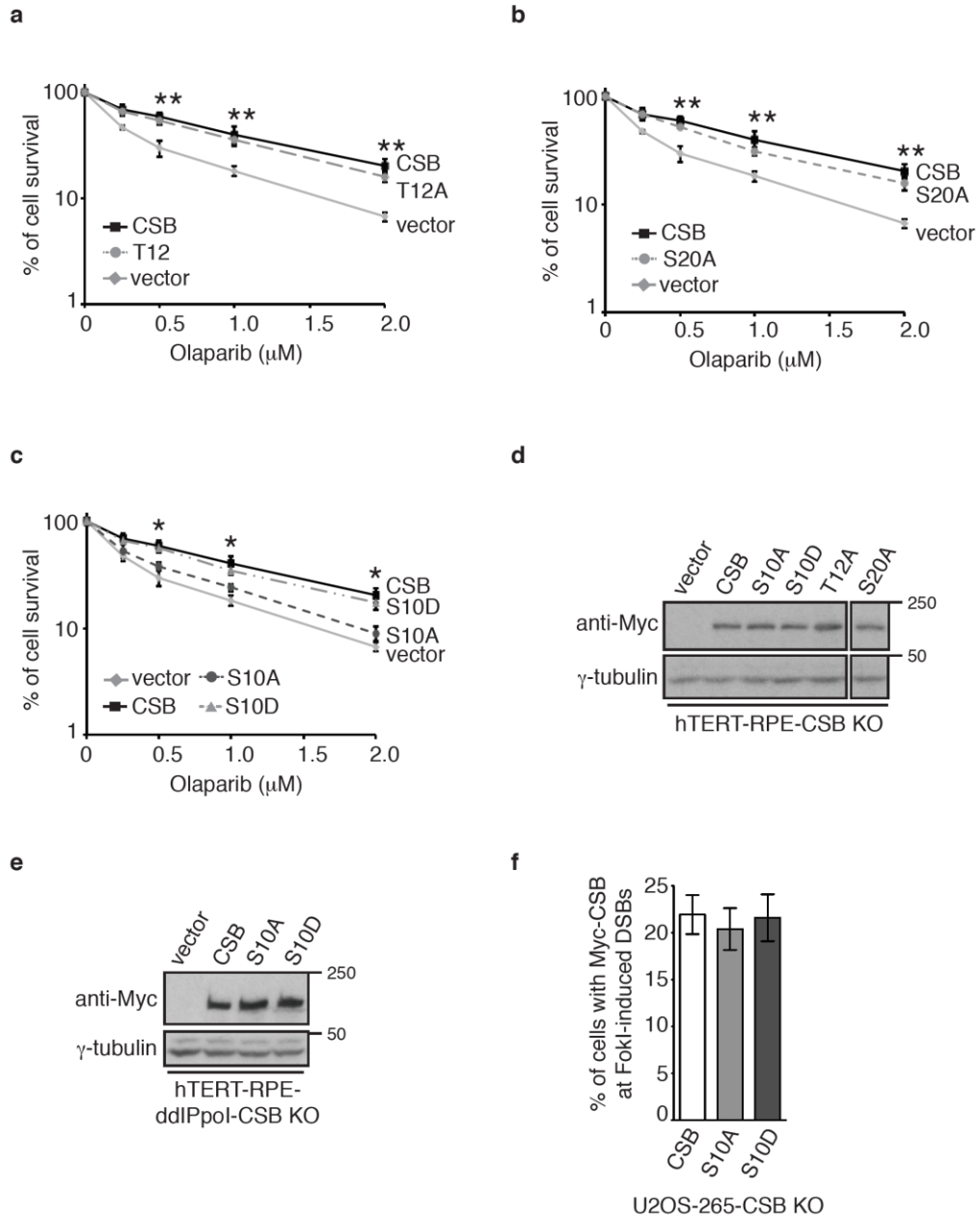
Supplementary Figure 6. Knockout of CSB does not affect the production of I-PpoI-induced DNA cleavage. **(a)** Western analysis of hTERT-RPE WT and CSB KO cells. The asterisk indicates the non-specific band. **(b)** Quantification of the percentage of hTERT-RPE parental (WT) and CSB KO cells exhibiting I-PpoI-induced γ H2AX foci. A minimum of 500 cells were scored for each independent experiment in a blind manner. SDs from three independent experiments are indicated. **(c)** Quantification of the percentage of hTERT-RPE parental (WT) and CSB KO cells exhibiting I-PpoI-induced 53BP1 foci. Scoring was done as in 6b. SDs from three independent experiments are indicated. **(d)** Quantification of the percentage of I-PpoI-induced DNA cleavage from hTERT-RPE WT and CSB KO cells on chromosome 1. SDs from three independent experiments are indicated.

Supplementary Figure 7 Batenburg et al.



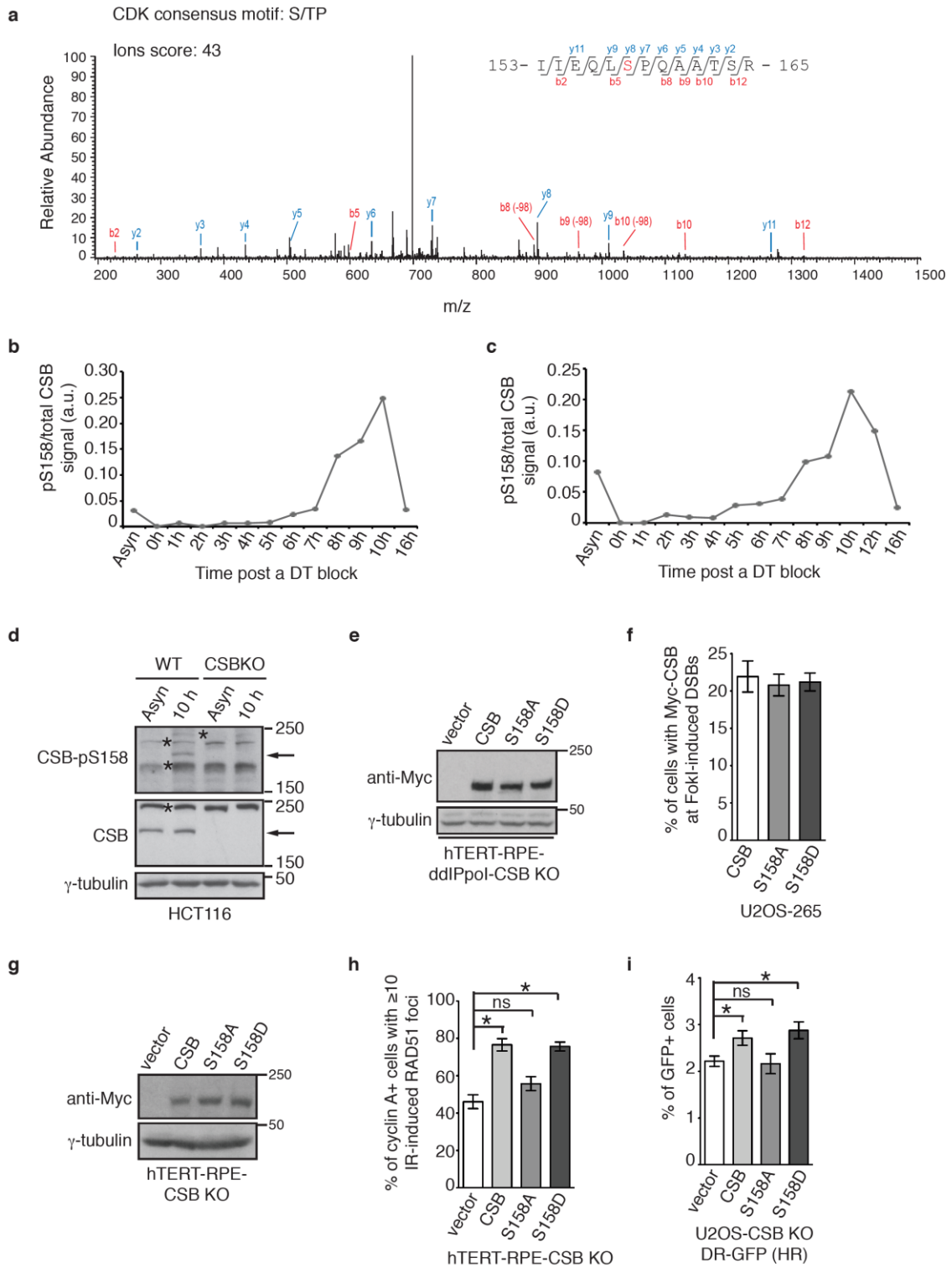
Supplementary Figure 7. Loss of CSB does not affect SMARCAD1 recruitment to sites of FokI-induced DSBs. **(a)** Immunofluorescence of U2OS-265 WT and CSB KO cells. Cells were fixed 6 h post FokI induction and co-stained with anti-SMARCAD1 and anti- γ H2AX antibodies. γ H2AX staining was used to mark the FokI-induced damage site. Scale bars, 5 μ m. **(b)** Quantification of the intensity of SMARCAD1 signal at the site of FokI-induced DSBs from (a). Cells positive for γ H2AX were used for analysis of SMARCAD1 signal intensity. The respective numbers of cells analyzed for WT and CSB KO were 469 and 470.

Supplementary Figure 8 Batenburg et al.



Supplementary Figure 8. CSB phosphorylation on S10 is necessary to support cell survival in response to the PARP inhibitor olaparib. **(a-c)** Clonogenic survival assays of olaparib-treated hTERT-RPE CSB-KO cells complemented with the vector alone or various Myc-tagged CSB alleles as indicated. Standard deviations from three independent experiments are indicated. $**P>0.05$ for comparison between CSB and T12A (a), between CSB and S20A (b). $*P<0.05$ for comparison between CSB and S10A (c). **(d)** Western analysis of hTERT-RPE CSB-KO cells stably expressing the vector alone or various Myc-tagged CSB alleles as indicated. **(e)** Western analysis of ddi-PpoI-expressing hTERT-RPE CSB-KO cells stably expressing the vector alone or various Myc-tagged CSB alleles as indicated. **(f)** Quantification of the percentage of Myc-CSB, Myc-CSB-S10A and Myc-CSB-S10D-expressing U2OS-265 cells exhibiting anti-Myc staining at FokI-induced DSBs. A total of 250 cells positive for anti-Myc staining were scored for each independent experiment in a blind manner. SDs from three independent experiments are indicated.

Supplementary Figure 9 Batenburg et al.



Supplementary Figure 9. CSB phosphorylation on S158 is necessary for HR-mediated repair of DSBs. **(a)** Fragmentation spectrum of a tryptic peptide surrounding pS158 (indicated in red) of CSB identified by MS/MS analysis of immunoprecipitated and phospho-enriched Flag-CSB. The peptide shown was identified with a Mascot ions score of 43 and an expect score of 0.0044. **(b)** Quantification of the CSB-pS158 signal from the western shown in Fig. 8b. Quantification was done with ImageJ. **(c)** Quantification of the CSB-pS158 signal from a second western using an independently prepared synchronized cell lysate. Quantification was done with ImageJ. **(d)** Western analysis of HCT116 WT and CSB KO cells that were either asynchronous (Asyn) or 10 h post release from a double thymidine block. The arrow indicates the position of CSB-pS158. Asterisks indicate non-specific bands. **(e)** Western analysis of ddI-PpoI-expressing hTERT-RPE CSB-KO cells complemented with the vector alone, various Myc-tagged CSB alleles. **(f)** Quantification of the percentage of Myc-CSB, Myc-CSB-S158A and Myc-CSB-S158D-expressing U2OS-265 cells exhibiting anti-Myc staining at FokI-induced DSBs. A total of 250 cells positive for anti-Myc staining were scored for each independent experiment in a blind manner. SDs from three independent experiments are indicated. **(g)** Western analysis of hTERT-RPE CSB-KO cells stably expressing the vector alone or various Myc-tagged CSB alleles as indicated. **(h)** Quantification of the percentage of cyclin A+ cells with 10 or more IR-induced RAD51 foci. hTERT-RPE CSB KO cells stably expressing the vector alone or various Myc-tagged CSB alleles as indicated were treated with 2 Gy IR and fixed 4 hr post IR. A minimum of 500 cells were scored for each independent experiment in a blind manner. SDs from three independent experiments are indicated. * $P < 0.05$. ns: $P > 0.05$. **(i)**

HR-mediated repair of I-SceI-induced DNA DSBs. SDs from three independent experiments are indicated. * $P < 0.05$. ns: $P > 0.05$.

Supplementary Table 1

Description	Primer Sequence	Size (bp)
Oligos for PCR ChIP assay, (I-PpoI cut site at 0 bp)		
-8921	5'-GCAAGGGCTCATGAATGATAGTC-3'	263bp
	5'-CTTCCCATTTCAGAATTGTGATGAG-3'	
-6245	5'-GCCTAAATGCCTCTTTCTACTGG-3'	236bp
	5'-GACACGGTTTTAGTGGAATGAGG-3'	
-2930	5'-CTCTTAAACACTGGGTGCCTTTC-3'	252bp
	5'-CACAGCCAGTAAATGACAGAAATGG-3'	
-496	5'-CTCCAGGGCATCCTTAGTGTT-3'	214bp
	5'-CAACGAGTATACTTGGGATGCG-3'	
-281	5'-CTTTGCTGCTTTTTCTTCTTCTCC-3'	241bp
	5'-GACTTCTTTCCACCAAGTCTTC-3'	
408	5'-GTTCCATTATCTGAAGAGCGTC-3'	238bp
	5'-CAAGGTCCTCAGCTTGTAAGG-3'	
1756	5'-GGTTGTTACACCCTTTCTGAG-3'	251bp
	5'-CCTGACTCACAGTAGACCCTC-3'	
3559	5'-GCTTTGGCTTGTAACCCACAAC-3'	231bp
	5'-GAGTGTCTATCTACAGTGAGCCC-3'	
5900	5'-CAGAGATGGAGGACAATTATGATGTG-3'	257bp
	5'-GCATGATCCTAAATTGTATGTACAGC-3'	
7014	5'-GCATTCTGGAGTTCCTTGCTG-3'	233bp
	5'-GCACTTCCTTATCTCCACTCTTCC-3'	
GAPDH site	5'-AAGCTTGTCATCAATGGAAATCCCATC-3'	548 bp
	5'-CTCAGACGGCAGGTCAGGTCCACCAC-3'	

Supplementary Table 2

Description	Primer Sequence	Size (bp)
Oligos for real-time PCR ChIP assay (I-PpoI cut site at 0 bp)		
-6195	5'-TGACCTAAGGAACGAGCTAAACC-3'	126bp
	5'-GAGTAGGGGGAGTCCACAAGTC-3'	
-2907	5'-CAGTGGGTGGATTAACCTCTCTGA-3'	122bp
	5'-CCAACATCCATTTGTTAGTTCCCTT-3'	
-527	5'-CATGTATGTGGTCAGGACCTCC-3'	136bp
	5'-GAGAGAGAACTGACAATTGGGTTG-3'	
-168	5'-CCCAACTCCTTCACCAGCAAAT-3'	123bp
	5'-GGAGATGACTTCTTTCCCACCAAG-3'	
408	5'-GTTCCCATTATCTGAAGAGCGTC-3'	144bp
	5'-GTTGGATGGCTCTGATAGTTACAA -3'	
1756	5'-CACACCCTTTCTGAGTACACTGAGA -3'	122bp
	5'- GTCTTGTGACCTAATAGCGGAGAA-3'	
3559	5'-GCTTTGGCTTGTAACCCACAAC-3'	131bp
	5'-GATGCTGCTCATACCCAATGTA-3'	
7014	5'- GCATTCTGGAGTTCCTTGCTG -3'	95bp
	5'- CTAATGCACCCACTCATGCTTT -3'	
Oligos for real-time PCR DSB-induction assay		
I-PpoI site at chromosome 1 (flanking the I-PpoI site)	5'-CTTGGTGGGAAAGAAGTCATCTCC -3'	142bp
	5'-CTCTTCCACTGTGGTATGAAACCT-3'	
GAPDH site	5'-GGCTTGCCCTGTCCAGTTAAT-3'	103bp
	5'-CTAGCTCAGCTGCACCCTTTA -3'	

4.2.7 References

- 1 Chapman, J. R., Taylor, M. R. & Boulton, S. J. Playing the end game: DNA double-strand break repair pathway choice. *Mol Cell* **47**, 497-510, doi:10.1016/j.molcel.2012.07.029 (2012).
- 2 Hustedt, N. & Durocher, D. The control of DNA repair by the cell cycle. *Nat Cell Biol* **19**, 1-9, doi:10.1038/ncb3452 (2016).
- 3 Chapman, J. R., Sossick, A. J., Boulton, S. J. & Jackson, S. P. BRCA1-associated exclusion of 53BP1 from DNA damage sites underlies temporal control of DNA repair. *J Cell Sci* **125**, 3529-3534, doi:10.1242/jcs.105353 (2012).
- 4 Bouwman, P. *et al.* 53BP1 loss rescues BRCA1 deficiency and is associated with triple-negative and BRCA-mutated breast cancers. *Nat Struct Mol Biol* **17**, 688-695, doi:10.1038/nsmb.1831 (2010).
- 5 Bunting, S. F. *et al.* 53BP1 inhibits homologous recombination in Brca1-deficient cells by blocking resection of DNA breaks. *Cell* **141**, 243-254, doi:10.1016/j.cell.2010.03.012 (2010).
- 6 Cao, L. *et al.* A selective requirement for 53BP1 in the biological response to genomic instability induced by Brca1 deficiency. *Mol Cell* **35**, 534-541, doi:10.1016/j.molcel.2009.06.037 (2009).
- 7 Kass, E. M., Moynahan, M. E. & Jasin, M. Loss of 53BP1 is a gain for BRCA1 mutant cells. *Cancer Cell* **17**, 423-425, doi:10.1016/j.ccr.2010.04.021 (2010).
- 8 Chapman, J. R. *et al.* RIF1 Is essential for 53BP1-dependent nonhomologous end joining and suppression of DNA double-strand break resection. *Mol Cell* **49**, 858-871, doi:10.1016/j.molcel.2013.01.002 (2013).
- 9 Escribano-Diaz, C. *et al.* A cell cycle-dependent regulatory circuit composed of 53BP1-Rif1 and BRCA1-CtIP controls DNA repair pathway choice. *Mol Cell* **49**, 872-883, doi:10.1016/j.molcel.2013.01.001 (2013).
- 10 Feng, L., Fong, K. W., Wang, J., Wang, W. & Chen, J. RIF1 counteracts BRCA1-mediated end resection during DNA repair. *J Biol Chem* **288**, 11135-11143, doi:10.1074/jbc.M113.457440 (2013).
- 11 Di Virgilio, M. *et al.* Rif1 prevents resection of DNA breaks and promotes immunoglobulin class switching. *Science* **339**, 711-715, doi:10.1126/science.1230624 (2013).
- 12 Zimmermann, M., Lottersberger, F., Buonomo, S. B., Sfeir, A. & de Lange, T. 53BP1 regulates DSB repair using Rif1 to control 5' end resection. *Science* **339**, 700-704, doi:10.1126/science.1231573 (2013).
- 13 Densham, R. M. *et al.* Human BRCA1-BARD1 ubiquitin ligase activity counteracts chromatin barriers to DNA resection. *Nat Struct Mol Biol* **23**, 647-655, doi:10.1038/nsmb.3236 (2016).
- 14 Zhang, H. *et al.* A cell cycle-dependent BRCA1-UHRF1 cascade regulates DNA double-strand break repair pathway choice. *Nat Commun* **7**, 10201, doi:10.1038/ncomms10201 (2016).

- 15 Lans, H., Marteijn, J. A. & Vermeulen, W. ATP-dependent chromatin remodeling in the DNA-damage response. *Epigenetics Chromatin* **5**, 4, doi:10.1186/1756-8935-5-4 (2012).
- 16 Li, X. & Tyler, J. K. Nucleosome disassembly during human non-homologous end joining followed by concerted HIRA- and CAF-1-dependent reassembly. *Elife* **5**: e15129, doi:10.7554/eLife.15129 (2016).
- 17 Berkovich, E., Monnat, R. J., Jr. & Kastan, M. B. Roles of ATM and NBS1 in chromatin structure modulation and DNA double-strand break repair. *Nat Cell Biol* **9**, 683-690, doi:10.1038/ncb1599 (2007).
- 18 Goldstein, M., Derheimer, F. A., Tait-Mulder, J. & Kastan, M. B. Nucleolin mediates nucleosome disruption critical for DNA double-strand break repair. *Proc Natl Acad Sci U S A* **110**, 16874-16879, doi:10.1073/pnas.1306160110 (2013).
- 19 Sunavala-Dossabhoy, G. & De Benedetti, A. Tousled homolog, TLK1, binds and phosphorylates Rad9; TLK1 acts as a molecular chaperone in DNA repair. *DNA Repair* **8**, 87-102, doi:10.1016/j.dnarep.2008.09.005 (2009).
- 20 Velez-Cruz, R. & Egly, J. M. Cockayne syndrome group B (CSB) protein: at the crossroads of transcriptional networks. *Mech Ageing Dev* **134**, 234-242, doi:10.1016/j.mad.2013.03.004 (2013).
- 21 Troelstra, C. *et al.* ERCC6, a member of a subfamily of putative helicases, is involved in Cockayne's syndrome and preferential repair of active genes. *Cell* **71**, 939-953 (1992).
- 22 van der Horst, G. T. *et al.* Defective transcription-coupled repair in Cockayne syndrome B mice is associated with skin cancer predisposition. *Cell* **89**, 425-435 (1997).
- 23 Stevnsner, T., Muftuoglu, M., Aamann, M. D. & Bohr, V. A. The role of Cockayne Syndrome group B (CSB) protein in base excision repair and aging. *Mech Ageing Dev* **129**, 441-448 (2008).
- 24 Aamann, M. D. *et al.* Cockayne syndrome group B protein promotes mitochondrial DNA stability by supporting the DNA repair association with the mitochondrial membrane. *FASEB J.* **24**, 2334-2346, doi:10.1096/fj.09-147991 (2010).
- 25 Scheibye-Knudsen, M. *et al.* Cockayne syndrome group B protein prevents the accumulation of damaged mitochondria by promoting mitochondrial autophagy. *J Exp Med* **209**, 855-869, doi:10.1084/jem.20111721 (2012).
- 26 Batenburg, N. L., Mitchell, T. R., Leach, D. M., Rainbow, A. J. & Zhu, X. D. Cockayne Syndrome group B protein interacts with TRF2 and regulates telomere length and stability. *Nucleic Acids Res.* **40**, 9661-9674, doi:10.1093/nar/gks745 (2012).
- 27 Batenburg, N. L., Thompson, E. L., Hendrickson, E. A. & Zhu, X. D. Cockayne syndrome group B protein regulates DNA double-strand break repair and checkpoint activation. *EMBO J.* **34**, 1399-1416, doi:10.15252/embj.201490041 (2015).

- 28 Iyama, T. & Wilson, D. M., 3rd. Elements That Regulate the DNA Damage Response of Proteins Defective in Cockayne Syndrome. *J Mol Biol* **428**, 62-78, doi:10.1016/j.jmb.2015.11.020 (2016).
- 29 Wei, L. *et al.* DNA damage during the G0/G1 phase triggers RNA-templated, Cockayne syndrome B-dependent homologous recombination. *Proc Natl Acad Sci USA* **112**, E3495-3504, doi:10.1073/pnas.1507105112 (2015).
- 30 Lake, R. J., Geyko, A., Hemashettar, G., Zhao, Y. & Fan, H. Y. UV-induced association of the CSB remodeling protein with chromatin requires ATP-dependent relief of N-terminal autorepression. *Mol Cell* **37**, 235-246, doi:10.1016/j.molcel.2009.10.027 (2010).
- 31 Wang, L. *et al.* Regulation of the Rhp26ERCC6/CSB chromatin remodeler by a novel conserved leucine latch motif. *Proc. Natl. Acad. Sci. U S A* **111**, 18566-18571, doi:10.1073/pnas.1420227112 (2014).
- 32 Cho, I., Tsai, P. F., Lake, R. J., Basheer, A. & Fan, H. Y. ATP-dependent chromatin remodeling by Cockayne syndrome protein B and NAP1-like histone chaperones is required for efficient transcription-coupled DNA repair. *PLoS Genet* **9**, e1003407, doi:10.1371/journal.pgen.1003407 (2013).
- 33 Citterio, E. *et al.* ATP-dependent chromatin remodeling by the Cockayne syndrome B DNA repair-transcription-coupling factor. *Mol Cell Biol* **20**, 7643-7653 (2000).
- 34 Shanbhag, N. M., Rafalska-Metcalf, I. U., Balane-Bolivar, C., Janicki, S. M. & Greenberg, R. A. ATM-dependent chromatin changes silence transcription in cis to DNA double-strand breaks. *Cell* **141**, 970-981, doi:10.1016/j.cell.2010.04.038 (2010).
- 35 Anindya, R. *et al.* A ubiquitin-binding domain in Cockayne syndrome B required for transcription-coupled nucleotide excision repair. *Mol Cell* **38**, 637-648 (2010).
- 36 Xu, D., Jaroszewski, L., Li, Z. & Godzik, A. FFAS-3D: improving fold recognition by including optimized structural features and template re-ranking. *Bioinformatics* **30**, 660-667, doi:10.1093/bioinformatics/btt578 (2014).
- 37 Kamada, K., De Angelis, J., Roeder, R. G. & Burley, S. K. Crystal structure of the C-terminal domain of the RAP74 subunit of human transcription factor IIF. *Proc Natl Acad Sci USA* **98**, 3115-3120, doi:10.1073/pnas.051631098 (2001).
- 38 Boersma, V. *et al.* MAD2L2 controls DNA repair at telomeres and DNA breaks by inhibiting 5' end resection. *Nature* **521**, 537-540, doi:10.1038/nature14216 (2015).
- 39 Xu, G. *et al.* REV7 counteracts DNA double-strand break resection and affects PARP inhibition. *Nature* **521**, 541-544, doi:10.1038/nature14328 (2015).
- 40 Callen, E. *et al.* 53BP1 mediates productive and mutagenic DNA repair through distinct phosphoprotein interactions. *Cell* **153**, 1266-1280, doi:10.1016/j.cell.2013.05.023 (2013).
- 41 Foti, R. *et al.* Nuclear Architecture Organized by Rif1 Underpins the Replication-Timing Program. *Mol Cell* **61**, 260-273, doi:10.1016/j.molcel.2015.12.001 (2016).
- 42 Wu, S. *et al.* A YY1-INO80 complex regulates genomic stability through homologous recombination-based repair. *Nat. Struct. Mol. Biol.* **14**, 1165-1172, doi:10.1038/nsmb1332 (2007).

- 43 Tsukuda, T., Fleming, A. B., Nickoloff, J. A. & Osley, M. A. Chromatin remodelling at a DNA double-strand break site in *Saccharomyces cerevisiae*. *Nature* **438**, 379-383, doi:10.1038/nature04148 (2005).
- 44 Traven, A. & Heierhorst, J. SQ/TQ cluster domains: concentrated ATM/ATR kinase phosphorylation site regions in DNA-damage-response proteins. *BioEssays* **27**, 397-407, doi:10.1002/bies.20204 (2005).
- 45 Ziv, Y. *et al.* Recombinant ATM protein complements the cellular A-T phenotype. *Oncogene* **15**, 159-167, doi:10.1038/sj.onc.1201319 (1997).
- 46 Li, L. *et al.* Role for RIF1-interacting partner DDX1 in BLM recruitment to DNA double-strand breaks. *DNA Repair* **55**, 47-63, doi:10.1016/j.dnarep.2017.05.001 (2017).
- 47 Pryde, F. *et al.* 53BP1 exchanges slowly at the sites of DNA damage and appears to require RNA for its association with chromatin. *J Cell Sci* **118**, 2043-2055, doi:10.1242/jcs.02336 (2005).
- 48 Xu, D. *et al.* Rif1 provides a new DNA-binding interface for the Bloom syndrome complex to maintain normal replication. *EMBO J* **29**, 3140-3155, doi:10.1038/emboj.2010.186 (2010).
- 49 Harami, G. M., Gyimesi, M. & Kovacs, M. From keys to bulldozers: expanding roles for winged helix domains in nucleic-acid-binding proteins. *Trends Biochem Sci* **38**, 364-371, doi:10.1016/j.tibs.2013.04.006 (2013).
- 50 Sin, Y., Tanaka, K. & Saijo, M. The C-terminal Region and SUMOylation of Cockayne Syndrome Group B Protein Play Critical Roles in Transcription-coupled Nucleotide Excision Repair. *J Biol Chem* **291**, 1387-1397, doi:10.1074/jbc.M115.683235 (2016).
- 51 Sheffield, P., Garrard, S. & Derewenda, Z. Overcoming expression and purification problems of RhoGDI using a family of "parallel" expression vectors. *Protein Expr Purif* **15**, 34-39 (1999).
- 52 Wilson, F. R., Ho, A., Walker, J. R. & Zhu, X. D. Cdk-dependent phosphorylation regulates TRF1 recruitment to PML bodies and promotes C-circle production in ALT cells. *J. Cell. Sci.* **129**, 2559-2572, doi:10.1242/jcs.186098 (2016).
- 53 Hart, T. *et al.* High-Resolution CRISPR Screens Reveal Fitness Genes and Genotype-Specific Cancer Liabilities. *Cell* **163**, 1515-1526, doi:10.1016/j.cell.2015.11.015 (2015).
- 54 McKerlie, M., Lin, S. & Zhu, X. D. ATM regulates proteasome-dependent subnuclear localization of TRF1, which is important for telomere maintenance. *Nucleic Acids Res* **40**, 3975-3989, doi:10.1093/nar/gks035 (2012).
- 55 McKerlie, M., Walker, J. R., Mitchell, T. R., Wilson, F. R. & Zhu, X. D. Phosphorylated (pT371)TRF1 is recruited to sites of DNA damage to facilitate homologous recombination and checkpoint activation. *Nucleic Acids Res* **41**, 10268-10282, doi:10.1093/nar/gkt775 (2013).
- 56 Wu, Y., Xiao, S. & Zhu, X. D. MRE11-RAD50-NBS1 and ATM function as co-mediators of TRF1 in telomere length control. *Nat Struct Mol Biol* **14**, 832-840 (2007).

- 57 Wu, Y., Mitchell, T. R. & Zhu, X. D. Human XPF controls TRF2 and telomere length maintenance through distinctive mechanisms. *Mech Ageing Dev* **129**, 602-610 (2008).
- 58 Mitchell, T. R., Glenfield, K., Jeyanthan, K. & Zhu, X. D. Arginine methylation regulates telomere length and stability. *Mol Cell Biol* **29**, 4918-4934, doi:10.1128/MCB.00009-09 (2009).
- 59 Zhu, X. D., Kuster, B., Mann, M., Petrini, J. H. & Lange, T. Cell-cycle-regulated association of RAD50/MRE11/NBS1 with TRF2 and human telomeres. *Nat Genet* **25**, 347-352 (2000).
- 60 Ran, F. A. *et al.* Genome engineering using the CRISPR-Cas9 system. *Nat Protoc* **8**, 2281-2308, doi:10.1038/nprot.2013.143 (2013).
- 61 Berkovich, E., Monnat, R. J., Jr. & Kastan, M. B. Assessment of protein dynamics and DNA repair following generation of DNA double-strand breaks at defined genomic sites. *Nat Protoc* **3**, 915-922, doi:10.1038/nprot.2008.54 (2008).
- 62 McKerlie, M. & Zhu, X. D. Cyclin B-dependent kinase 1 regulates human TRF1 to modulate the resolution of sister telomeres. *Nat Commun* **2:371** doi: **10.1038/ncomms1372** (2011).

Chapter 5

Discussion

5.1 Overview of findings

The findings presented in this thesis have revealed novel and important functions of CSB in telomere maintenance as well as DNA DSB repair. Furthermore, I have demonstrated for the first time that CSB is a chromatin remodeler *in vivo*.

5.1.1 Role of CSB at telomeres

I have shown that CSB is important for proper telomere maintenance. CSB-deficient fibroblasts derived from CS patients or HeLa cells depleted of CSB with shRNA show an accumulation of telomere doublets. Telomere doublets are thought to arise from problems with replication at the telomere. Certain regions in the genome termed fragile sites are challenging to replication, especially in conditions of limited nucleotide pools or inhibition of DNA polymerases (Durkin & Glover, 2007). Treatment with the DNA polymerase inhibitor aphidicolin induces gaps in the chromosome (Glover *et al*, 1984). Telomeres have been identified as fragile sites where treatment with aphidicolin results in the accumulation of telomere doublets (Sfeir *et al*, 2009). While CSB has not been reported to play a role in DNA replication, these results suggest that CSB might play a role in promoting efficient replication at telomeres.

I have also shown that CSB-deficient cells or shCSB expressing HeLa cells have reduced levels of TERRA. Previously CSB has been reported to promote both RNAPI and RNAPII mediated transcription (Balajee *et al*, 1997; Bradsher *et al*, 2002; Van Den Boom *et al*, 2004; van Gool *et al*, 1997). TERRA is mainly transcribed by RNAPII (Azzalin *et al*, 2007). CSB is associated with RNAPII (Bradsher *et al*, 2002; van Gool *et*

al, 1997). It would be of interest to investigate if CSB may be associated with RNAPII at the telomere to promote efficient transcription. TERRA is an integral component of telomeres and promotes heterochromatin formation. Reduced levels of TERRA in CSB-deficient cells could lead to disruption in the heterochromatin structure and promote telomere dysfunction.

I have shown that CSB-deficient cells display accelerated telomere shortening and increased telomere loss. CSB-deficient cells also show increased association of TRF1 with telomeres. TRF1 is a negative regulator of telomere length maintenance (Ancelin *et al*, 2002; Broccoli *et al*, 1997; Okamoto *et al*, 2008; Smogorzewska *et al*, 2000; van Steensel & de Lange, 1997). Increased TRF1 binding at telomeres, combined with the possible disruption of the heterochromatic state of telomeres, may contribute to the telomere shortening observed in CS cells.

5.1.2 Role of CSB in DSB repair

I have shown that CSB plays a key role in regulating the choice of DNA DSB repair pathways. It was previously reported that cells derived from CS patients are sensitive to IR, camptothecin and etoposide, all of which induce DSBs (Elli *et al*, 1996; Leadon & Cooper, 1993; Squires *et al*, 2012; Tuo *et al*, 2002, 2003). Utilizing a human CSB knockout cell line, I was able to confirm that loss of CSB leads to a defect in DSB repair.

I have shown that CSB is recruited to DSBs in S and G2 phase of the cell cycle, coinciding with a role in HR. The C-terminus of CSB is essential for its recruitment to DSBs. This is similar to the requirement of the C-terminus for UV-induced chromatin

associated of CSB (Lake *et al*, 2010) and recruitment to other types of damage (Iyama & Wilson, 2016). These findings suggest that the mechanism by which CSB is recruited to DNA damage through the C-terminus of CSB is conserved across different types of DNA damage. On the other hand, I have shown that the ATPase activity of CSB is dispensable for its recruitment to DSBs, which is in contrast to its requirement for UV-induced chromatin association of CSB (Lake *et al*, 2010).

While CSB is recruited to DNA DSBs in an ATP-independent manner, CSB requires its ATPase activity to remodel the chromatin surrounding a DSB. Chromatin remodeling is known to regulate the efficiency of DSB repair (Goodarzi *et al*, 2011; Price & D'Andrea, 2013). Chromatin context plays an important role in HR during S and G2 phase. Whether CSB remodels chromatin in a chromatin context-dependent manner required future investigation.

The role of CSB in the repair of DNA damage seems to be linked to transcription. Over the last several years, the relationship between DSB repair and transcription has come to light (Marnef *et al*, 2017). Collisions between the transcriptional and replication machineries can cause replication fork stalling which leads to the activation of the DNA damage response and is repaired via homologous recombination (Branzei & Foiani, 2010; Helmrich *et al*, 2013). In addition, transcription-dependent R loops are known to be sources of genome instability (Aguilera & García-Muse, 2012). Highly transcribed regions of the genome are associated with high mutagenesis and recombination rate (Aguilera, 2002; Nickoloff & Reynolds, 1990; Nickoloff, 1992). It is unclear whether the increase in DSB production seen in active genes is a by-product of transcription or if it is

necessary for the release of RNAPII, however it is clear that DSB repair is altered in active genes. DNA damage including DSBs is also repaired faster in these regions compared to the rest of the genome (Bohr *et al*, 1985; Chaurasia *et al*, 2012; Mellon *et al*, 1986). This supports the existence of a “transcription-coupled DSB repair” pathway. CSB is essential for the transcription-coupled repair of UV-induced DNA lesions (Fousteri *et al*, 2006), and we have shown that CSB regulates DSB repair and is recruited to DSBs in a transcription dependent manner, therefore CSB may play a role in transcription-coupled DSB repair.

The N-terminus of CSB has previously been implicated in regulating the DNA-dependent ATPase activity and chromatin remodeling activity of CSB *in vitro* (Cho *et al*, 2013; Lake *et al*, 2010; Wang *et al*, 2014). It has been proposed that the N-terminus binds to the ATPase domain of CSB, repressing its *in vitro* ATPase activity (Lake *et al*, 2010). In contrast, the N-terminus seems to be essential for promoting the remodeling activity of CSB *in vitro* (Cho *et al*, 2013; Wang *et al*, 2014). We have shown that the N-terminus interacts with the ATPase domain and this interaction is influenced by the phosphorylation state of S10 and S158. Phosphorylation on either of these two sites is important for the ability of CSB to promote chromatin remodeling at DSBs. CSB phosphorylation on S10 is damage induced whereas phosphorylation on S158 is regulated in a cell cycle-dependent manner. Both of these phosphorylation events function together to regulate the interaction between the N-terminus and the ATPase domain of CSB. Our results suggest that the activation of CSB at DSBs requires both a DNA damage signal and a cell-cycle specific signal. These findings support a model where CSB specifically

promotes displacement of histones during S and G2 phase, limiting unwanted CSB-mediated chromatin remodeling at DSBs in undamaged or damaged cells in G1 phase.

In addition to CSB, a number of other ATP-dependent chromatin remodeling factors have been implicated in DSB repair (Jeggo & Downs, 2014). Whether and how each of these complexes collaborate or cooperate to remodel chromatin, remain poorly understood. Conceivably, it is possible that each of these remodelers operate in a tightly regulated and spatiotemporal fashion, with individual complexes being required in only certain context such as chromatin type, cell type, cell cycle, etc., or during precise times during the DNA damage response.

5.2 Implications and Significance

CSB is a multifunctional protein and regulates many different processes in the cells including UV repair, transcription, mitochondria maintenance, telomere maintenance and DSB repair. The fact that CSB affects so many different processes in the cells may provide an explanation to the multi-system nature of CS. Gaining a clearer understanding of how CSB performs these functions will be essential going forward to understanding the variation of symptoms observed in this disease.

It is well established that telomere shortening is associated with normal aging (Harley *et al*, 1990). Many diseases that display features of premature aging are correlated with significantly shorter telomeres compared to age-matched controls (Armanios & Blackburn, 2013; Garcia *et al*, 2007; Vulliamy *et al*, 2001). Some of these diseases are the result of mutations in core genes involved in telomere maintenance.

Others are the result of mutations in genes with a characterized role in DNA repair rather than telomere maintenance. Such diseases are more likely to accumulate DNA damage at telomeres and result in dysfunctional telomeres. The finding that only five dysfunctional telomeres is sufficient to trigger cellular senescence in human fibroblasts (Kaul *et al*, 2011) and not all dysfunctional telomeres are short in length, suggests that telomere structure rather than telomere length *per se* may regulate the induction of senescence (Karlseder, 2002; Kaul *et al*, 2011).

Once telomeres become uncapped, p53 mediates growth arrest, senescence and apoptosis in stem/progenitor cells (Sahin & DePinho, 2010; Wong *et al*, 2003). Functional telomeres are required not only for proper stem cell proliferation (Huang *et al*, 2011), but also for stable stem cell differentiation as in telomerase deficient mice stem cell differentiation becomes unstable (Pucci *et al*, 2013). This mechanism may explain the compromised function of highly proliferative organs, however it does not sufficiently explain the decline in more quiescent tissues such as heart, liver and brain. Work done in telomerase deficient mice has shown that short telomeres can also induce defects in mitochondria biogenesis and function (Sahin *et al*, 2011). This mitochondrial defect combined with the telomere-induced apoptosis help explain the multi-system nature of the defects induced by telomere dysfunction.

The work done by myself and Taylor Mitchell strongly supports an undiscovered role for CSB in telomere maintenance. The increased telomere shortening observed in CSB-deficient cells may contribute to the progressive and degenerative nature of CS syndrome. In addition, the shortening may also contribute to the mitochondrial defect

observed in CS cells (Aamann *et al*, 2010; Chatre *et al*, 2015; Cleaver *et al*, 2014; Osenbroch *et al*, 2009; Pascucci *et al*, 2012; Scheibye-Knudsen *et al*, 2012). Several symptoms of CS coincide with the symptoms of mitochondrial diseases including neurological defects, a complex phenotype and large variation in age of onset (Haas *et al*, 2007; Schapira, 2006; Scheibye-Knudsen *et al*, 2013).

DNA DSB repair has also been associated with aging. Normal DSB repair response declines as we age while DSBs and chromosome rearrangements increase over time. Evidence for the importance of DSB repair in aging comes from the fact that mutations in multiple genes involved in DSB repair result in premature aging phenotypes. This includes Werner syndrome (WS), ataxia-telangiectasia (AT) and Nijmegen breakage syndrome (NBS) in which the proteins WRN, ATM and NBS1 are mutated respectively. The contribution of DSBs to aging is likely to differ across tissues. When damage is induced in neuronal stem cells, they undergo premature senescence or terminally differentiate (Schneider *et al*, 2013). A defect in DSB repair would then lead to a decrease in the proliferative potential of neuronal stem cells and over time contribute to neurodegeneration. Syndromes such as AT display neurodegeneration, demonstrating the importance of proper DSB repair for neuronal health (Paula-Barbosa *et al*, 1983; Verhagen *et al*, 2012; Vinters *et al*, 1985). We have reported that CSB plays a key role in regulating DSB repair, suggesting that the neurodegeneration observed in CS patients may in part arise from a defect in DSB repair. Further research is necessary to determine the potential contribution of this defect in neurodegeneration.

CS is a unique syndrome in that it is a premature aging disease that does not show any predisposition towards cancer. Whether the lack of cancer predisposition seen in CS patients might be due to their short life-span or increased apoptosis remains to be determined. It has been reported that CSB is overexpressed in a panel of tumor samples compared to normal cells and that depletion of CSB leads to increased sensitivity of tumor samples to chemotherapeutic agents compared to normal cells (Caputo *et al*, 2013). The work presented in this thesis reveal that CSB plays an important role in maintaining telomere and genomic integrity, disruption of which is associated with cancer and aging. .

5.3 Future Directions

Is the ATPase activity of CSB required for its function in telomere maintenance?

The work presented in this thesis reveal that CSB regulates telomerase-dependent telomere length maintenance, telomere structure and TERRA transcription, however the mechanism by which CSB regulates these functions remains uncharacterized. I have shown that CSB is a chromatin remodeler *in vivo*. It will be of interest to determine in CSB regulates telomere length, structure and TERRA transcription vis its ATP-dependent chromatin remodeling activity. Furthermore, it will also be of interest to determine if any particular regions/residues are important for telomere maintenance.

Does CSB play a role in the repair of DNA damage induced at telomeres?

CSB is essential for TCR of UV-induced DNA damage and promotes repair of oxidative damage. Compared to the rest of the genome, telomeric DNA is highly susceptible to both UV and oxidative damage (Lu & Liu, 2010; Rochette & Brash, 2010; Wang *et al*,

2010). Damaged telomeric DNA can lead to a defect in telomere length maintenance, and both NER and BER promote removal of DNA damage from telomeres (Jia *et al*, 2015). For example, knockout of OGG1 in mice results in defects in telomere length maintenance and structure (Wang *et al*, 2010), and knockout of XPC in mice results in increased UV-induced telomere shortening (Stout & Blasco, 2013). In addition, oxidative damage affects the ability of TRF1 and TRF2 to recognize telomeric DNA (Opresko *et al*, 2005), and affects the efficiency that telomerase can elongate telomeric substrates (Aeby *et al*, 2016; Fouquerel *et al*, 2016). It would be of interest to address if CSB promotes the repair of such DNA damage at telomeres. Accumulation of UV-induced or oxidative DNA damage at telomeres in CSB-deficient cells could lead to the defect in telomere length maintenance and dysfunction telomeres that we have reported.

Is CSB recruited to DSBs induced in specific genomic loci?

I have shown that CSB is recruited to DSBs and this recruitment is sensitive to transcriptional inhibition. This suggests that CSB is recruited to DSBs in a manner that is dependent upon active transcription within the cell, however we have not investigated if the recruitment of CSB to DSBs is regulated by transcriptional activity of a given genomic locus. Previous reports have demonstrated that DSBs induced in active genes differ in the recruitment of DSB repair factors compared to inactive genes (Aymard *et al*, 2014; Chakraborty *et al*, 2016). It would be of interest to investigate if CSB recruitment to DSBs in chromatin context-dependent.

Does CSB regulate transcriptional silencing or recovery at DSBs?

CSB is essential for proper TC-NER, where RNAPII stalls upon encountering UV-induced DNA damage. In the absence of CSB, repair is not completed and transcription does not recover. Similar to UV-induced damage, when a DSB occurs within a coding gene, transcription of the gene is inhibited in a DNA-PK dependent manner that results in the exclusion of RNAPII from the gene (Pankotai *et al*, 2012). In addition, generation of multiple DSBs upstream of a reporter gene leads to transcriptional silencing of the reporter gene (Shanbhag *et al*, 2010). This silencing is dependent upon ATM signalling, ubiquitylation of H2A lysine 119 that recruits the PBAF (Polybromo BRG1 associated factor) complex, and histone deacetylation by the NuRD complex (Chou *et al*, 2010; Gong *et al*, 2015; Kakarougkas *et al*, 2014; Ui *et al*, 2015). ATM is also required for silencing of transcription of rDNA after induction of DSBs (Harding *et al*, 2015; Kruhlak *et al*, 2009). CSB promotes the activation of ATM after the induction of DSBs, therefore it will be of interest to investigate if CSB regulates transcriptional silencing and recovery at DSBs.

5.4 References

- Aamann MD, Sorensen MM, Hvitby C, Berquist BR, Muftuoglu M, Tian J, de Souza-Pinto NC, Scheibye-Knudsen M, Wilson DM, Stevnsner T & Bohr VA (2010) Cockayne syndrome group B protein promotes mitochondrial DNA stability by supporting the DNA repair association with the mitochondrial membrane. *FASEB J.* **24**: 2334–2346
- Aeby E, Ahmed W, Redon S, Simanis V & Lingner J (2016) Peroxiredoxin 1 Protects Telomeres from Oxidative Damage and Preserves Telomeric DNA for Extension by Telomerase. *Cell Rep.* **17**: 3107–3114
- Aguilera A (2002) The connection between transcription and genomic instability. *EMBO J.* **21**: 195–201

- Aguilera A & García-Muse T (2012) R Loops: From Transcription Byproducts to Threats to Genome Stability. *Mol. Cell* **46**: 115–124
- Ancelin K, Brunori M, Bauwens S, Koering C-E, Brun C, Ricoul M, Pommier J-P, Sabatier L & Gilson E (2002) Targeting Assay To Study the cis Functions of Human Telomeric Proteins: Evidence for Inhibition of Telomerase by TRF1 and for Activation of Telomere Degradation by TRF2. *Mol. Cell. Biol.* **22**: 3474–3487
- Armanios M & Blackburn EH (2013) The telomere syndromes. *Nat. Rev. Genet.* **14**: 235–235
- Aymard F, Bugler B, Schmidt CK, Guillou E, Caron P, Briois S, Iacovoni JS, Daburon V, Miller KM, Jackson SP & Legube G (2014) Transcriptionally active chromatin recruits homologous recombination at DNA double-strand breaks. *Nat. Struct. Mol. Biol.* **21**: 366–374
- Azzalin CM, Reichenbach P, Khoriatuli L, Giulotto E & Lingner J (2007) Telomeric repeat containing RNA and RNA surveillance factors at mammalian chromosome ends. *Science* **318**: 798–801
- Balajee AS, May A, Dianov GL, Friedberg EC & Bohr VA (1997) Reduced RNA polymerase II transcription in intact and permeabilized Cockayne syndrome group B cells. *Proc. Natl. Acad. Sci. U. S. A.* **94**: 4306–11
- Bohr VA, Smith CA, Okumoto DS & Hanawalt PC (1985) DNA repair in an active gene: Removal of pyrimidine dimers from the DHFR gene of CHO cells is much more efficient than in the genome overall. *Cell* **40**: 359–369
- Van Den Boom V, Citterio E, Hoogstraten D, Zotter A, Egly JM, Van Cappellen WA, Hoeijmakers JHJ, Houtsmuller AB & Vermeulen W (2004) DNA damage stabilizes interaction of CSB with the transcription elongation machinery. *J. Cell Biol.* **166**: 27–36
- Bradsher J, Auriol J, De Santis LP, Iben S, Vonesch JL, Grummt I & Egly JM (2002) CSB is a component of RNA pol I transcription. *Mol. Cell* **10**: 819–829
- Branzei D & Foiani M (2010) Maintaining genome stability at the replication fork. *Nat. Rev. Mol. Cell Biol.* **11**: 208–219
- Broccoli D, Smogorzewska A, Chong L & de Lange T (1997) Human telomeres contain two distinct Myb-related proteins, TRF1 and TRF2. *Nat. Genet.* **17**: 231–5
- Caputo M, Frontini M, Velez-Cruz R, Nicolai S, Prantera G & Proietti-De-Santis L (2013) The CSB repair factor is overexpressed in cancer cells, increases apoptotic resistance, and promotes tumor growth. *DNA Repair (Amst)*. **12**: 293–299
- Chakraborty A, Tapryal N, Venkova T, Horikoshi N, Pandita RK, Sarker AH, Sarker PS, Pandita TK & Hazra TK (2016) Classical non-homologous end-joining pathway utilizes nascent RNA for error-free double-strand break repair of transcribed genes. *Nat. Commun.* **7**: 13049
- Chatre L, Biard DSF, Sarasin A & Ricchetti M (2015) Reversal of mitochondrial defects with CSB-dependent serine protease inhibitors in patient cells of the progeroid Cockayne syndrome. *Proc. Natl. Acad. Sci.* **112**: E2910–E2919
- Chaurasia P, Sen R, Pandita TK & Bhaumik SR (2012) Preferential repair of DNA double-strand break at the active gene in vivo. *J. Biol. Chem.* **287**: 36414–36422

- Cho I, Tsai PF, Lake RJ, Basheer A & Fan HY (2013) ATP-Dependent Chromatin Remodeling by Cockayne Syndrome Protein B and NAP1-Like Histone Chaperones Is Required for Efficient Transcription-Coupled DNA Repair. *PLoS Genet.* **9**:
- Chou DM, Adamson B, Dephore NE, Tan X, Nottke AC, Hurov KE, Gygi SP, Colaiacovo MP & Elledge SJ (2010) A chromatin localization screen reveals poly (ADP ribose)-regulated recruitment of the repressive polycomb and NuRD complexes to sites of DNA damage. *Proc. Natl. Acad. Sci.* **107**: 18475–18480
- Cleaver JE, Brennan-Minnella AM, Swanson R a, Fong K, Chen J, Chou K, Chen Y, Revet I & Bezrookove V (2014) Mitochondrial reactive oxygen species are scavenged by Cockayne syndrome B protein in human fibroblasts without nuclear DNA damage. *Proc. Natl. Acad. Sci. U. S. A.* **111**: 13487–92
- Durkin SG & Glover TW (2007) Chromosome Fragile Sites. *Annu. Rev. Genet.* **41**: 169–192
- Elli R, Chessa L, Antonelli A, Petrinelli P, Ambra R & Marcucci L (1996) Effects of topoisomerase II inhibition in lymphoblasts from patients with progeroid and ‘chromosome instability’ syndromes. *Cancer Genet. Cytogenet.* **87**: 112–116
- Fouquierel E, Lormand J, Bose A, Lee H-T, Kim GS, Li J, Sobol RW, Freudenthal BD, Myong S & Opresko PL (2016) Oxidative guanine base damage regulates human telomerase activity. *Nat. Struct. Mol. Biol.* **23**: 1–11
- Fousteri M, Vermeulen W, van Zeeland AA & Mullenders LHF (2006) Cockayne Syndrome A and B Proteins Differentially Regulate Recruitment of Chromatin Remodeling and Repair Factors to Stalled RNA Polymerase II In Vivo. *Mol. Cell* **23**: 471–482
- Garcia CK, Wright WE & Shay JW (2007) Human diseases of telomerase dysfunction: Insights into tissue aging. *Nucleic Acids Res.* **35**: 7406–7416
- Glover TW, Berger C, Coyle J & Echo B (1984) DNA polymerase alpha inhibition by aphidicolin induces gaps and breaks at common fragile sites in human chromosomes. *Hum. Genet.* **67**: 136–142
- Gong F, Chiu LY, Cox B, Aymard F, Clouaire T, Leung JW, Cammarata M, Perez M, Agarwal P, Brodbelt JS, Legube G & Miller KM (2015) Screen identifies bromodomain protein ZMYND8 in chromatin recognition of transcription-associated DNA damage that promotes homologous recombination. *Genes Dev.* **29**: 197–211
- Goodarzi AA, Kurka T & Jeggo PA (2011) KAP-1 phosphorylation regulates CHD3 nucleosome remodeling during the DNA double-strand break response. *Nat. Struct. Mol. Biol.* **18**: 831–839
- van Gool AJ, Citterio E, Rademakers S, van Os R, Vermeulen W, Constantinou A, Egly JM, Bootsma D & Hoeijmakers JH (1997) The Cockayne syndrome B protein, involved in transcription- coupled DNA repair, resides in an RNA polymerase II-containing complex. *EMBO J.* **16**: 5955–5965
- Haas RH, Parikh S, Falk MJ, Saneto RP, Wolf NI, Darin N & Cohen BH (2007) Mitochondrial disease: a practical approach for primary care physicians. *Pediatrics* **120**: 1326–1333
- Harding SM, Boiarsky JA & Greenberg RA (2015) ATM Dependent Silencing Links

- Nucleolar Chromatin Reorganization to DNA Damage Recognition. *Cell Rep.* **13**: 251–259
- Harley CB, Futcher AB & Greider CW (1990) Telomeres shorten during ageing of human fibroblasts. *Nature* **345**: 458–460
- Helmrich A, Ballarino M, Nudler E & Tora L (2013) Transcription-replication encounters, consequences and genomic instability. *Nat. Struct. Mol. Biol.* **20**: 412–418
- Huang J, Wang F, Okuka M, Liu N, Ji G, Ye X, Zuo B, Li M, Liang P, Ge WW, Tsibris JC, Keefe DL & Liu L (2011) Association of telomere length with authentic pluripotency of ES/iPS cells. *Cell Res.* **21**: 779–792
- Iyama T & Wilson DM (2016) Elements That Regulate the DNA Damage Response of Proteins Defective in Cockayne Syndrome. *J. Mol. Biol.* **428**: 62–78
- Jeggo PA & Downs JA (2014) Roles of chromatin remodellers in DNA double strand break repair. *Exp. Cell Res.* **329**: 69–77
- Jia P, Her C & Chai W (2015) DNA excision repair at telomeres. *DNA Repair (Amst)*. **36**: 137–145
- Kakarougkas A, Ismail A, Chambers AL, Riballo E, Herbert AD, K?nzell J, L??brich M, Jeggo PA & Downs JA (2014) Requirement for PBAF in Transcriptional Repression and Repair at DNA Breaks in Actively Transcribed Regions of Chromatin. *Mol. Cell* **55**: 723–732
- Karlseder J (2002) Senescence Induced by Altered Telomere State, Not Telomere Loss. *Science (80-.)*. **295**: 2446–2449
- Kaul Z, Cesare AJ, Huschtscha LI, Neumann AA & Reddel RR (2011) Five dysfunctional telomeres predict onset of senescence in human cells. *EMBO Rep.* **13**: 52–59
- Kruhlak M, Crouch EE, Orlov M, Monta?o C, Gorski SA, Nussenzweig A, Misteli T, Phair RD & Casellas R (2009) The ATM repair pathway inhibits RNA polymerase I transcription in response to chromosome breaks. *Nature* **459**: 736–736
- Lake RJ, Geyko A, Hemashettar G, Zhao Y & Fan HY (2010) UV-Induced Association of the CSB Remodeling Protein with Chromatin Requires ATP-Dependent Relief of N-Terminal Autorepression. *Mol. Cell* **37**: 235–246
- Leadon S a & Cooper PK (1993) Preferential repair of ionizing radiation-induced damage in the transcribed strand of an active human gene is defective in Cockayne syndrome. *Proc. Natl. Acad. Sci. U. S. A.* **90**: 10499–10503
- Lu J & Liu Y (2010) Deletion of Ogg1 DNA glycosylase results in telomere base damage and length alteration in yeast. *EMBO J.* **29**: 398–409
- Marnef A, Cohen S & Legube G (2017) Transcription-Coupled DNA Double-Strand Break Repair: Active Genes Need Special Care. *J. Mol. Biol.* **429**: 1277–1288
- Mellon I, Bohr VA, Smith CA & Hanawalt PC (1986) Preferential DNA repair of an active gene in human cells. *Proc. Natl. Acad. Sci. U. S. A.* **83**: 8878–8882
- Nickoloff JA (1992) Transcription enhances intrachromosomal homologous recombination in mammalian cells. *Mol. Cell. Biol.* **12**: 5311–8
- Nickoloff JA & Reynolds RJ (1990) Transcription stimulates homologous recombination in mammalian cells. *Mol. Cell. Biol.* **10**: 4837–45

- Okamoto K, Iwano T, Tachibana M & Shinkai Y (2008) Distinct roles of TRF1 in the regulation of telomere structure and lengthening. *J. Biol. Chem.* **283**: 23981–23988
- Opresko PL, Fan J, Danzy S, Wilson DM & Bohr VA (2005) Oxidative damage in telomeric DNA disrupts recognition by TRF1 and TRF2. *Nucleic Acids Res.* **33**: 1230–1239
- Osenbroch PO, Auk-Emblem P, Halsne R, Strand J, Forstrøm RJ, Van Der Pluijm I & Eide L (2009) Accumulation of mitochondrial DNA damage and bioenergetic dysfunction in CSB defective cells. *FEBS J.* **276**: 2811–2821
- Pankotai T, Bonhomme C, Chen D & Soutoglou E (2012) DNAPKcs-dependent arrest of RNA polymerase II transcription in the presence of DNA breaks. *Nat. Struct. Mol. Biol.* **19**: 276–282
- Pascucci B, Lemma T, Iorio E, Giovannini S, Vaz B, Iavarone I, Calcagnile A, Narciso L, Degan P, Podo F, Roginskya V, Janjic BM, Van Houten B, Stefanini M, Dogliotti E & D’Errico M (2012) An altered redox balance mediates the hypersensitivity of Cockayne syndrome primary fibroblasts to oxidative stress. *Aging Cell* **11**: 520–529
- Paula-Barbosa MM, Ruela C, Tavares MA, Pontes C, Saraiva A & Cruz C (1983) Cerebellar cortex ultrastructure in ataxia-telangiectasia. *Ann. Neurol.* **13**: 297–302
- Price BD & D’Andrea AD (2013) Chromatin remodeling at DNA double-strand breaks. *Cell* **152**: 1344–1354
- Pucci F, Gardano L & Harrington L (2013) Short telomeres in ESCs lead to unstable differentiation. *Cell Stem Cell* **12**: 479–486
- Rochette PJ & Brash DE (2010) Human telomeres are hypersensitive to UV-induced DNA damage and refractory to repair. *PLoS Genet.* **6**:
- Sahin E, Colla S, Liesa M, Moslehi J, Müller FL, Guo M, Cooper M, Kotton D, Fabian AJ, Walkey C, Maser RS, Tonon G, Foerster F, Xiong R, Wang YA, Shukla SA, Jaskelioff M, Martin ES, Heffernan TP, Protopopov A, et al (2011) Telomere dysfunction induces metabolic and mitochondrial compromise. *Nature* **470**: 359–365
- Sahin E & DePinho RA (2010) Linking functional decline of telomeres, mitochondria and stem cells during ageing. *Nature* **464**: 520–528
- Schapira AH V (2006) Mitochondrial disease. *Lancet* **368**: 70–82
- Scheibye-Knudsen M, Croteau DL & Bohr VA (2013) Mitochondrial deficiency in Cockayne syndrome. *Mech. Ageing Dev.* **134**: 275–283
- Scheibye-Knudsen M, Ramamoorthy M, Sykora P, Maynard S, Lin P-C, Minor RK, Wilson DM, Cooper M, Spencer R, de Cabo R, Croteau DL & Bohr VA (2012) Cockayne syndrome group B protein prevents the accumulation of damaged mitochondria by promoting mitochondrial autophagy. *J. Exp. Med.* **209**: 855–69
- Schneider L, Pellegatta S, Favaro R, Pisati F, Roncaglia P, Testa G, Nicolis SK, Finocchiaro G & D’Adda Di Fagagna F (2013) DNA damage in mammalian neural stem cells leads to astrocytic differentiation mediated by BMP2 signaling through JAK-STAT. *Stem Cell Reports* **1**: 123–138
- Sfeir A, Kosiyatrakul ST, Hockemeyer D, MacRae SL, Karlseder J, Schildkraut CL & de Lange T (2009) Mammalian Telomeres Resemble Fragile Sites and Require TRF1 for Efficient Replication. *Cell* **138**: 90–103

- Shanbhag NM, Rafalska-Metcalf IU, Balane-Bolivar C, Janicki SM & Greenberg RA (2010) ATM-Dependent chromatin changes silence transcription in cis to dna double-strand breaks. *Cell* **141**: 970–981
- Smogorzewska A, van Steensel B, Bianchi A, Oelmann S, Schaefer MR, Schnapp G & de Lange T (2000) Control of human telomere length by TRF1 and TRF2. *Mol Cell Biol* **20**: 1659–1668
- Squires S, Ryan AJ, Strutt HL & Johnson RT (2012) Hypersensitivity of Cockayne's Syndrome Cells to Camptothecin Is Associated with the Generation of Abnormally High Levels of Double Strand Breaks in Nascent. *DNA Repair (Amst)*. **53**: 2012–2019
- van Steensel B & de Lange T (1997) Control of telomere length by the human telomeric protein TRF1. *Nature* **385**: 740–3
- Stout GJ & Blasco MA (2013) Telomere length and telomerase activity impact the UV sensitivity syndrome xeroderma pigmentosum C. *Cancer Res.* **73**: 1844–1854
- Tuo J, Jaruga P, Rodriguez H, Bohr V & Dizdaroglu M (2003) Primary fibroblasts of Cockayne syndrome patients are defective in cellular repair of 8-hydroxyguanine and 8-hydroxyadenine resulting from oxidative stress. *FASEB J.* **17**: 668–674
- Tuo J, Jaruga P, Rodriguez H, Dizdaroglu M & Bohr VA (2002) The cockayne syndrome group B gene product is involved in cellular repair of 8-hydroxyadenine in DNA. *J. Biol. Chem.* **277**: 30832–30837
- Ui A, Nagaura Y & Yasui A (2015) Transcriptional elongation factor ENL phosphorylated by ATM recruits polycomb and switches off transcription for DSB repair. *Mol. Cell* **58**: 468–482
- Verhagen MMM, Martin JJ, van Deuren M, Ceuterick-de Groote C, Weemaes CMR, Kremer BHPH, Taylor MAR, Willemsen MAAP & Lammens M (2012) Neuropathology in classical and variant ataxia-telangiectasia. *Neuropathology* **32**: 234–244
- Vinters H V, Gatti RA & Rakic P (1985) Sequence of cellular events in cerebellar ontogeny relevant to expression of neuronal abnormalities in ataxia-telangiectasia. *Kroc Found. Ser.* **19**: 233–55
- Vulliamy T, Marrone A, Goldman F, Dearlove A, Bessler M, Mason PJ & Dokal I (2001) The RNA component of telomerase is mutated in autosomal dominant dyskeratosis congenita. *Nature* **413**: 432–435
- Wang L, Limbo O, Fei J, Chen L, Kim B, Luo J, Chong J, Conaway RC, Conaway JW, Ranish J a, Kadonaga JT, Russell P & Wang D (2014) Regulation of the Rhp26ERCC6/CSB chromatin remodeler by a novel conserved leucine latch motif. *Proc. Natl. Acad. Sci. U. S. A.* **111**: 18566–71
- Wang Z, Rhee DB, Lu J, Bohr CT, Zhou F, Vallabhaneni H, de Souza-Pinto NC & Liu Y (2010) Characterization of oxidative guanine damage and repair in mammalian telomeres. *PLoS Genet.* **6**: e1000951
- Wong K-K, Maser RS, Bachoo RM, Menon J, Carrasco DR, Gu Y, Alt FW & DePinho RA (2003) Telomere dysfunction and Atm deficiency compromises organ homeostasis and accelerates ageing. *Nature* **421**: 643–648